SYNTHESIS AND CHARACTERIZATION OF NEW RUTHENIUM(II), RHODIUM(III) AND IRIDIUM(III) COMPLEXES CONTAINING TRIDENTATE AND TETRADENTATE N-BASES

A THESIS SUBMITTED IN PARTIAL
FULFILMENT OF THE REQUIREMENTS
FOR THE DEGREE OF DOCTOR OF PHILOSOPHY

BY

THIRUMALA PRASAD KOTA

DEPARTMENT OF CHEMISTRY
SCHOOL OF PHYSICAL SCIENCES
NORTH-EASTERN HILL UNIVERSITY
SHILLONG – 793022

MARCH, 2010

Synthesis and characterization of new Ruthenium(II), Rhodium(III) and Iridium(III) complexes containing tridentate and tetradentate N-bases

A Thesis submitted in partial

fulfilment of the requirements for the degree of

Doctor of Philosophy

By

Thirumala Prasad Kota

Department of Chemistry

School of Physical Sciences

North-Eastern Hill University

Shillong-793022

March-2010

.....This work is dedicated to my beloved parents

Asato ma sat gamaya

Tamaso ma jyothir gamaya

Mrithyor ma amritam gamaya

DECLARATION

I, Mr. Thirumala Prasad Kota hereby declare that the thesis entitled “Synthesis and characterization of new Ruthenium(II), Rhodium(III) and Iridium(III) complexes containing tridentate and tetradentate N-bases” is the result of work originally carried out by me under the supervision of Professor. K. Mohan Rao, Department of Chemistry, School of Physical Sciences, North-Eastern Hill University, Shillong, for the award of Doctor of Philosophy in Chemistry. The contents of this thesis did not form basis of the award of any previous degree to me or to anybody else to the best of my knowledge. I have not submitted the thesis for any research degree in any other university or institution.

This is being submitted to the North-Eastern Hill University, Shillong for the degree of Doctor of Philosophy in Chemistry.

Place: Shillong

Date: Thirumala Prasad Kota

DEPARTMENT OF CHEMISTRY

NORTH-EASTERN HILL UNIVERSITY, NEHU PERMANENT CAMPUS, UMSHING

SHILLONG- 793022, INDIA

CERTIFICATE

This is to certify that the thesis entitled "Synthesis and characterization of new Ruthenium(II), Rhodium(III) and Iridium(III) complexes containing tridentate and tetradentate N-bases" is the original work done by Mr. Thirumala Prasad Kota for the degree of doctor of philosophy under my supervision in the Department of Chemistry, School of Physical Sciences, North-Eastern Hill University, Shillong. The work embodied in the thesis does not form basis of the award of any previous degree or any other similar title and that it represents entirely an independent work on the part of the candidate.

(Professor K. Mohan Rao)
Supervisor

(Professor B. Myrboh)
Head
Department of Chemistry
North-Eastern Hill University
Shillong-793022

Place: Shillong

Date:

ACKNOWLEDGEMENTS

I express my profound gratitude to my research supervisor, Professor K. Mohan Rao for his invaluable guidance, encouragement, numerous discussions and constructive suggestions through out the course of this investigation. Throughout the duration of my Ph.D he has provided me a perfect balance between the guidance and autonomy: he has always been generous in his support during the most trying circumstances. His enthusiasm for chemistry is inspiring and I hope that at least some small part of his knowledge has rubbed off on me. I am privileged to have him as supervisor, his baffling affection for Macs notwithstanding.

I would like to express my gratitude to Prof. B. Myrboh, Head department of chemistry, Prof. R. K. Poddar, Dean, School of physical sciences for their constant encouragement, support and providing me all facilities required throughout my research. . My sincere gratitude to Prof. B. Syama Sundar, principal, Pharmacy College, ANU, Guntur, for his constant encouragement, support and who help me in joining in research.

Thanks to Prof. R.H. Duncan Lyngdoh, Dr. A.K. Chandra and their groups for helping me in theoretical studies. I wish to extend my gratitude towards Prof. K. Ismail, Prof. R A Lal, Dr. G Bez, Dr. D P S Negi and Dr. S. Mitra for their constant encouragement. I would be failing in my duty if I do not thank other teachers of Department of Chemistry, NEHU, for their kind cooperation

My thanks are due to Dr. Bruno Therrien, University of Neuchatel, Neuchatel, Switzerland, Babulal Das, Indian Institute of Technology, Guwahati, India and Steven Geib, University of Pittsburgh, USA, for single crystal X- ray diffraction studies. I am thankful to the Head of the institutions of the SAIF-NEHU Shillong and IISc- Bangalore for the services rendered in sample analyses.

It gives me a great pleasure to express my deep sense of gratitude and indebtedness to Mr. Bah Dkhar, bah Andy, madam Florency, bah Warjri, Dr. D Dey, Dr. Wandon, Miss Lana, Mr. Thomas and all the other scientific and non-scientific staff of NEHU for their help and rendered in sample analyses for carrying out the research work.

My special Thanks are due to my labmates Mr. Gajendra Gupta, Mr. Anna Venkateswara Rao, Miss. Saphidabha Lyngdoh Nongbri, Miss Sairem Gloria and Miss. Smita Basu for providing a friendly work atmosphere and always being there unconditionally and for all those extra miles they walked with me.

I acknowledge Dr. S. Jeeva, Dr. K. Pachhunga and Mr. Joseph for their help during the initial stages of my staying and research tenure. I am much obliged to Venkat, for his encouragement

and he had been always with me, whenever I needed his help and making my life in NEHU memorable. I sincerely appreciate the friendship and encouragement of Radhika.

Finally I take the opportunity to thank all my friends, Dr. M. Siva, Dr. Krishna Mohan, Dr. Naga Rosaiah, Dr. Rameswara Rao, Chandra Mouli Reddy, Sahoo, Bala Raju, Nabo, Santosh, Giri, Prabhakar, Kalyani, Stella, Salma, Mantu, Hormi, Tovishe, Hussain, Ramana, Siam, karlos, Rakshak, Prof K.M.Rao family, Dr. C.S. Rao family, Hanuman family, Dr. Venugopal family and other family members from whom I have received unfailing support, tremendous patience and encouragement during many years of studies that they have shown to me in their own special way.

I express my heartily gratitude to my parents, brother and sister for their love, affection, and encouragement. Finally, I do like to thank all my teachers and almighty God for their unlimited blessings throughout my life.

k. Thirumala prasad

Preface

One of the most interesting and important areas in which contemporary inorganic chemists could contribute profitably is organometallic chemistry, a broad interdisciplinary field whose sphere of interest includes all compounds wherein metal usually in a low valence state is bonded through carbon of an organic molecule, radical or ion. Since the publication of the synthesis of Zeise salt (1848), and Victor Grignards' organomagnesium halides (1900), there have been spasmodic references to the syntheses of such novel compounds as ferrocene, ruthenocene *etc*. But from the middle of the twentieth century and particularly after the syntheses of the cyclopentadienyl, its analogue's and arene transition metal complexes are came a vast blossoming of Organic-Transition Metal Chemistry which has led into the development of a large number of new areas like homogeneous catalysis, *etc*.

Organic and organometallic chemists have extensively investigated Arene metal complexes for over four decades. The organometallic complexes of η^6- and η^5- half-sandwich complexes of ruthrnium, rhodium and iridium have attracted considerable current interest especially from the catalytic prospective, is the design of Ru=O functional groups and analogues capable of reversibly accepting multiple electrons and protons within a relatively small potential range. This capacity to modify the environment in order to induce electronic as well as steric effects gives scope for the design and fabrication of tailored catalysts for specific reactions. The arene ruthenium or Cp* rhodium or iridium dimers appear to be good starting materials for access to reactive arene metal hydrides and have been used for carbon-hydrogen bond activation. Recently, from classic organometallic arene ruthenium has grown an area making significant contributions to the chemistry of cyclophanes and metal grids. These compounds are potential precursors of organometallic polymers that show interesting electrical properties and conductivity. The η^6-arene ruthenium complexes are also the subject of intensive studies due to their interesting coordination chemistry and catalytic properties. Apart from these some of the monodentate ruthenium(II) arene complexes of the type $[(\eta^6\text{-arene})Ru(en)X]PF_6$, where *en* is ethylenediamine and X is chloride or iodide, constitute a group that is believed to exert an antitumor action *via* mechanisms different from those of other ruthenium(III) complexes such as NAMI-A or KP1019. Keeping in mind the importance of these type of complexes, one part of this research work is based on the synthesis and characterization

of new complexes arising from a very versatile starting material $[(\eta^6\text{-arene})Ru(\mu\text{-}Cl)Cl]_2$ (arene = benzene, *p*-cymene and hexamethylbenzene). Apart from these, another materials with similar isoelectronic metal d^6 systems namely $[(\eta^5\text{-}C_5Me_5)M(\mu\text{-}Cl)Cl]_2$ (C_5Me_5 = pentamethyl cyclopentadienyl; M = Rh or Ir) are also chosen as a starting materials.

The primary objective of the thesis is to explore the chemistry of arene ruthenium and pentamethylcyclopentadienyl rhodium or iridium complexes and main objective is to synthesize or frame the ligand, in which it can coordinate to two metal centers and preparation of mono and dinuclear complexes by using nitrogen bases. Final aim is to place the reader in a synthetic methodology for these classes of complexes.

The sequence of chapters reflects preparation of a wide range of half sandwich arene ruthenium and pentamethylcyclopentadienyl rhodium or iridium complexes and their characterization with help of analytical and spectroscopic data. The solid state structure of representative complexes were also studied using single crystal X-ray crystallography.

This thesis carries syntheses of arene ruthenium, and pentamethyl-cyclopentadienyl rhodium and iridium complexes of polypyridyl, polypyrazolyl, thiazolyl and Schiff base ligands.

Graphical Abstracts

Chapter 1: General Introduction (pages 1-21)

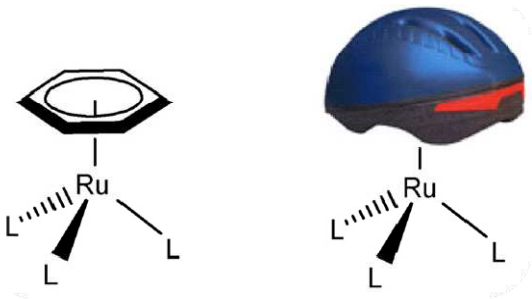

This chapter provides the motivation for the research presented in this thesis and is intended to situate the reader in the field of study, Coordination Chemistry and Organometallic Chemistry. General aspects and recent advances in the half-sandwich platinum group metal complexes are discussed. Platinum group metal complexes find applications in most of the areas where coordination and organometallic chemistry present.

Chapter 2: Mono and dinuclear half-sandwich platinum group metal complexes bearing pyrazolyl-pyrimidine ligands: Syntheses and structural studies (pages 22-50)

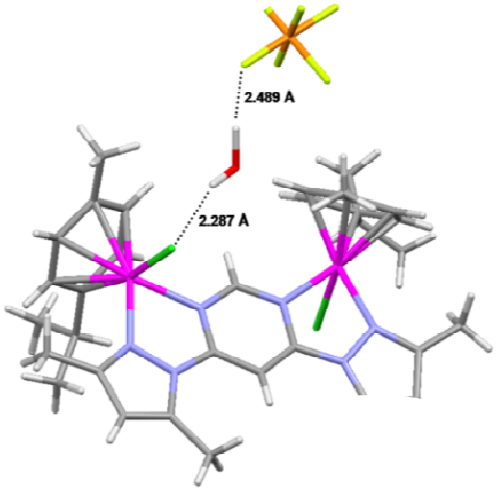

In this chapter, we focus on the synthetic methodology applied for the development of homogeneous and immobilized half-sandwich ruthenium, rhodium and iridium complexes bearing bis(pyrazolyl)pyrimidine, as a specific *N*,*N*-bidentate bridging ligand

Chapter 3: Spectral, structural and DFT studies of platinum group metal 3,6-bis(2-pyridyl)-4-phenylpyridazine complexes and their ligand bonding modes (pages 51-81)

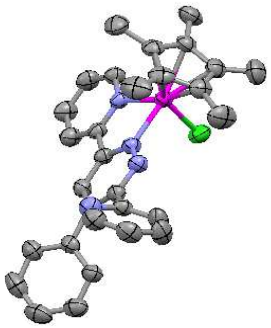

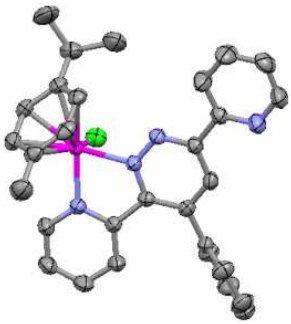

New mononuclear half-sandwich platinum group metal (Ru, Rh and Ir) complexes were obtained by the reaction of arene or pentamethylcyclopentadienyl metal (Ru, Rh and Ir) complexes with 3,6-bis(2-pyridyl)-4-phenylpyridazine (L^{ph}), yielding two sets of complexes. In one set (*type-A*), the metal bonds to the N1 and N2 atoms of the (L^{ph}) ligand, and in the other (*type-B*), the metal bonds to the N3 and N4 atoms. The structures of these complexes were confirmed through X-ray crystallography and density functional theory calculations.

Chapter 4: Cationic half-sandwich complexes (Rh, Ir, Ru) containing 2-substituted-1,8-naphthyridine chelating ligands: Syntheses, X-ray structure analyses and spectroscopic studies (pages 82-103)

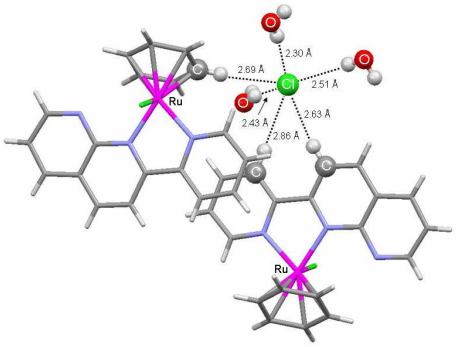

In this chapter, we describe the synthesis of twelve η^5-C_5Me_5 rhodium, iridium and η^6-C_6H_6, η^6-*p*-$^{i}PrC_6H_4Me$ ruthenium complexes incorporating 2-substituted-1,8-naphthyridine ligands; 2-(2-pyridyl)-1,8-naphthyridine (pyNp), 2-(2-thiazolyl)-1,8-naphthyridine (tzNp) and 2-(2-furyl)-1,8-naphthyridine (fuNp).

Chapter 5: Half-sandwich mono and dinuclear complexes of platinum group metals bearing pyrazolyl-pyridine analogues: Synthesis and spectral characterization (pages 104-125)

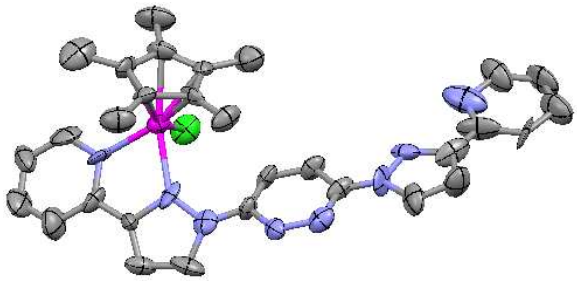

The chelating ligands *pp-Cl and bppp* were synthesized and their reactions with arene ruthenium, Cp* rhodium and Cp* iridium dimers resulted in the formation of mono and dinuclear complexes. However reactions with the *bppm* ligand which is having Pyrimidine Bridge between pyrazolyl-pyridine units resulted only in the formation of mononuclear complexes.

Chapter 6

Part A: Mono and dinuclear complexes of half-sandwich platinum group metals (Ru, Rh and Ir) bearing a flexible pyridyl-thiazole multidentate donor ligand (pages 126-150)

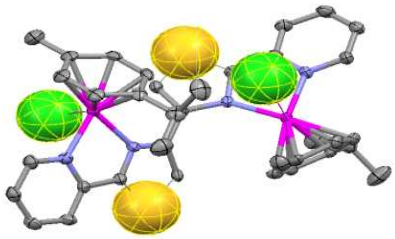

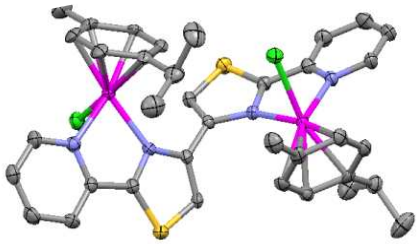

In this chapter, we have synthesized new mononuclear and dinuclear complexes with arene ruthenium, rhodium and iridium complexes with polypyridyl ligand as thiazolyl rings backbone. All these new complexes were characterized by elemental analyses, ^{1}H-NMR, UV-Visible and mass spectrometry as well as X-crystallographic analyses for some representatives

Part B: New series of platinum group metal complexes bearing η5- and η6-Cyclichydrocarbons and Schiff base derived from 2-acetylthiazole: syntheses and structural studies. (Pages 151-168)

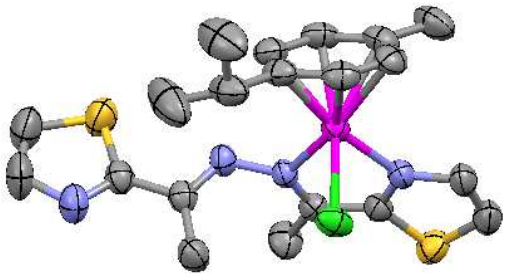

In this chapter we focus on the synthetic methodology applied for the development of homogeneous and immobilized half- sandwich ruthenium, rhodium and iridium complexes bearing Schiff base (*ata*) as a specific N, N-bidentate bridging ligand has shown below.

Chapter 7: Syntheses and characterization of mono and dinuclear complexes of platinum group metals bearing benzene-linked bis(pyrazolyl)methane ligands. (Pages 169-190)

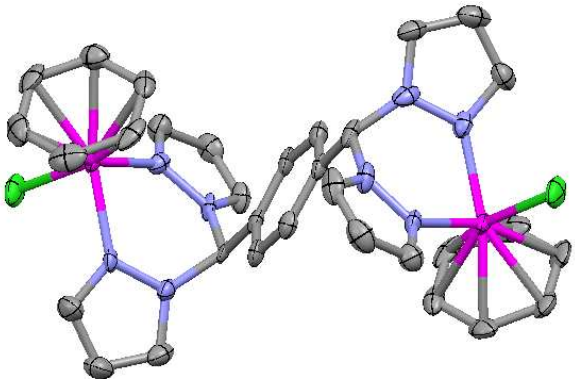

In this chapter, we have synthesized homogeneous and immobilized half-sandwich rhodium, iridium and ruthenium complexes bearing bis(pyrazolyl)methanes bridged by benzene-linker, as bidentate or tetradentate bridging ligands (L). The Cp* rhodium and iridium complexes with ligands L give both mono and dinuclear complexes, while only dinuclear complexes are obtained with arene ruthenium complexes.

CONTENTS

Chapter 3

Spectral, structural and DFT studies of platinum group metal 3,6-bis(2-pyridyl)-4-phenylpyridazine complexes and their ligand bonding modes

Chapter 4

Cationic half-sandwich complexes (Rh, Ir, Ru) containing 2-substituted-1,8-naphthyridine chelating ligands: Syntheses, X-ray structure analyses and spectroscopic studies

List of abbreviations

ata	2-acetylthiazole azine
bdmpzpm	4,6-bis(3,5-dimethylpyrazolyl)pyrimidine
bmpzmb	1,4-bis{bis(3-methylpyrazolyl)methyl}benzene
bmpzpm	4,6-bis(3-methylpyrazolyl)pyrimidine
bppm	3,6-bis(3-pyridylpyrazolyl)pyrimidine
bppp	3,6-bis(3-pyridylpyrazolyl)pyridazine
bptz	4,4'-bis(2-pyridyl-2-thiazole)
bpzmb	1,4-bis{bis(pyrazolyl)-methyl}benzene
bpzpm	4,6-bis(pyrazolyl)pyrimidine
Cp	η^5-Cyclopentadienyl,
Cp*	Pentamethylcyclopentadienyl
d	Doublet (NMR)
dd	Doublet of doublets (NMR)
DFT	Density function theory
DMSO	Dimethylsulfoxside
dppn	3,6-bis(2-pyridyl)pyridazine
dppn-ph	3,6-bis(2-pyridyl)4-phenylpyridazine
dt	Doublet of triplets (NMR)
fuNp	2-(2-furyl)-1,8-naphthyridine (fuNp).
GOF	Goodness of fit
sept	septet (NMR)
HMB	Hexamethylbenzene
IR	Infrared
J	Coupling constant in Hertz
m	Multiplet (NMR spectroscopy)
NH_4PF_6	Ammonium hexafluorophosphate
pp-cl	3-chloro-6-(3-pyridyl-1-pyrazolyl)pyridazine
pyNp	2-(2-pyridyl)-1,8-naphthyridine (pyNp)
q	Quartet (NMR)
t	Triplet
T	Temperature
tt	Triplet of triplets
tzNp	2-(2-thiazolyl)-1,8-naphthyridine (tzNp)
V	Crystal cell volume
VIS	Visible part of spectrum
Z	Molecules per elementary cell

Chapter 1

General Introduction

This chapter provides the motivation for the research presented in this thesis and is intended to situate the reader in the field of Coordination Chemistry and Organometallic Chemistry. The general aspects and recent advances of the half-sandwich platinum group metal complexes are discussed in this chapter. Platinum group metal complexes find applications in most of the areas where coordination and organometallic chemistry present. The last section of this chapter provides the information for the starting materials and physical techniques which are used in this study.

1.1 Organometallic and coordination chemistry

Organometallic compounds are defined as materials which possess direct, more or less polar bonds between metal and carbon atoms.[1] Zeise synthesized in 1827 the first organometallic compound, $K[PtCl_3(CH_2{=}CH_2)]$, since then the organometallic chemistry has grown enormously although most of its applications have only been developed in recent decades. Some of the key points in the fast expansion of organometallic chemistry are the selectivity of organometallic complexes in organic synthesis (discovered with Grignard reagents at the end of the 19th century),[2,3] and the interesting role that metals play in biological systems (*e.g.* enzymes, haemoglobin, *etc.*).[4]

Since Werner's pioneering work, coordination chemistry has maturated in a continuous way, being bioinorganic and bio-metallic chemistry and the growing interest in materials its latest driving forces. Now days, coordination compounds are involved in an unbelievable wide range of applications that can be divided in the following areas: (i) use of coordination complexes in all types of catalyses: (ii) applications related to the optical properties of coordination complexes, which cover fields as diverse as solar cells, non linear optics, display devices and pigments, dyes and optical data storage devices; (iii) hydrometallurgical extraction; (iv) medicinal and biomedical applications of coordination complexes, including both image and therapy and (v) use of coordination complexes as precursors to semiconductor films and nanoparticles. If nothing else, such an extensive list of applications can be employed, as suggested by Professor Ward in the last edition of *Comprehensive Coordination Chemistry*[5] as a suitable answer to the eternally irritating question that everyone involved in the field get asked at parties when we reveal what we do for a living. "But what's it for?"

1.2 η^6–arene ruthenium chemistry and half- sandwich piano stool complexes

The first arene ruthenium complex was obtained from the reaction of $RuCl_3.nH_2O$ with 1,3-cyclohexadiene (scheme 1.1) and reported by Winkhaus and Singer in 1967 as a polymeric material, $[(\eta^6\text{-}C_6H_6)RuCl_2]_n$.[6] Later studies by Zelonka and Baird[7] and by Bennett and Smith[8] showed this complex is to be a dimer, $[(\eta^6\text{-}C_6H_6)RuCl_2]_2$. Since these early reports, the chemistry of arene ruthenium complexes has been steadily developed.[9,10,11]

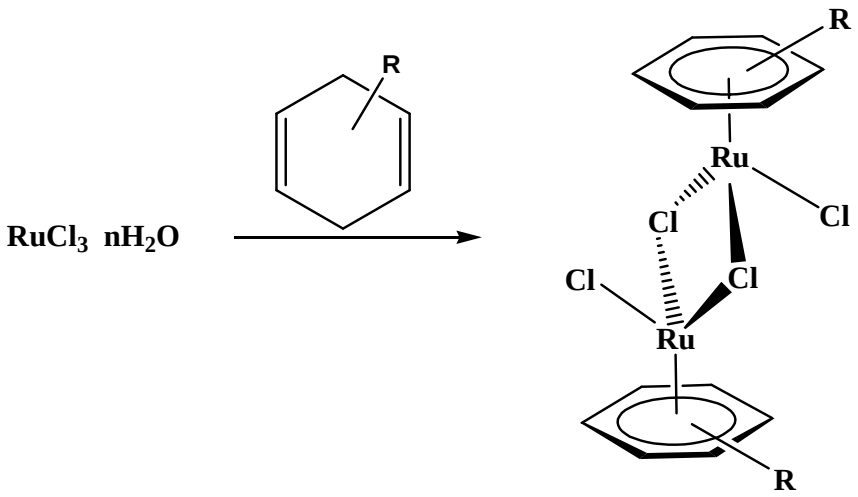

Scheme 1.1

Within this large family of η^6-arene ruthenium complexes, piano-stool complexes are undeniably the most studied ones. They have found applications as catalysis, supramolecular assemblies, molecular devices and have shown antiviral, antibiotic, and anticancer activities. These piano stool complexes are resulted by the reaction of the dimeric complexes with coordinating solvents such as CH_3CN, DMSO and some of the monodentate ligands such as CO, pyridine, triphenylphosphine etc. (Scheme 1.2) due to the presence of more labile chloro bridges in dimeric complexes. These three-legged piano-stool complexes possess a pseudo-octahedral geometry at the ruthenium(II) center, the arene ligand occupying three coordinating sites (the seat) where as other coordination sites occupied by with other three ligands (the legs) (figure 1.1). Therefore, the octahedral geometry can be viewed as pseudo- tetrahedral, thus limiting the number of possible isomers.

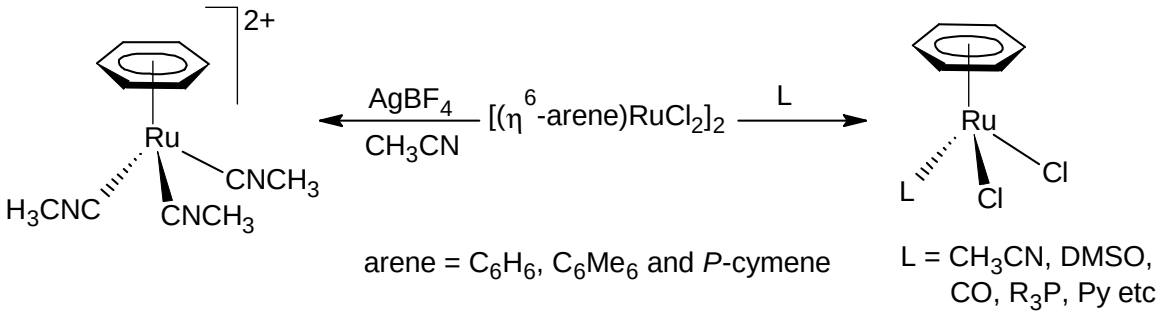

Scheme 1.2

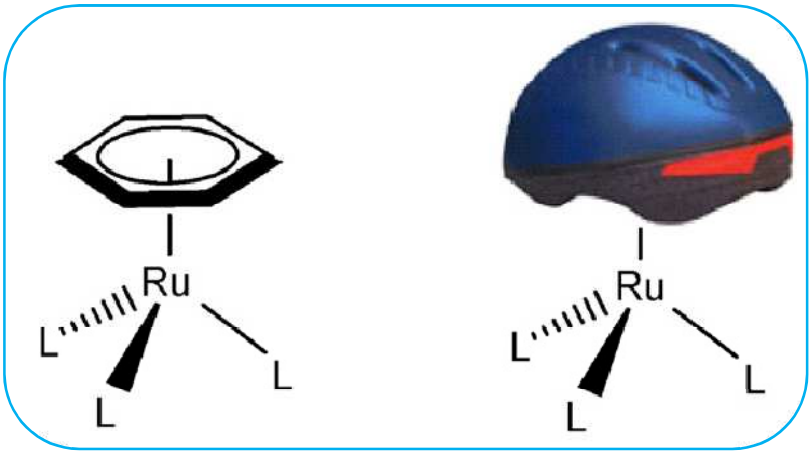

Figure 1.1: 3-remaining coordination sites for ligands L

The arene ligands are relatively inert towards substitution reactions and consequently are often considered as spectator ligands. However, the arene moiety which is strongly coordinated to the ruthenium atom can be customised by simply attaching different substituents (Scheme 1.3). These functionalised substituents can be modified to tune the properties of the arene-ruthenium complexes. The three remaining coordination sites opposite to the arene ligand can be used to introduce a wide variety of ligands such as N-, O-, S- or P- donor atoms. The resulting complexes are neutral, mono- or dicationic, and often these ligands are labile. This tendency to exchange ligands in solution is crucial in self-assemblies[12] and catalytic processes.[13]

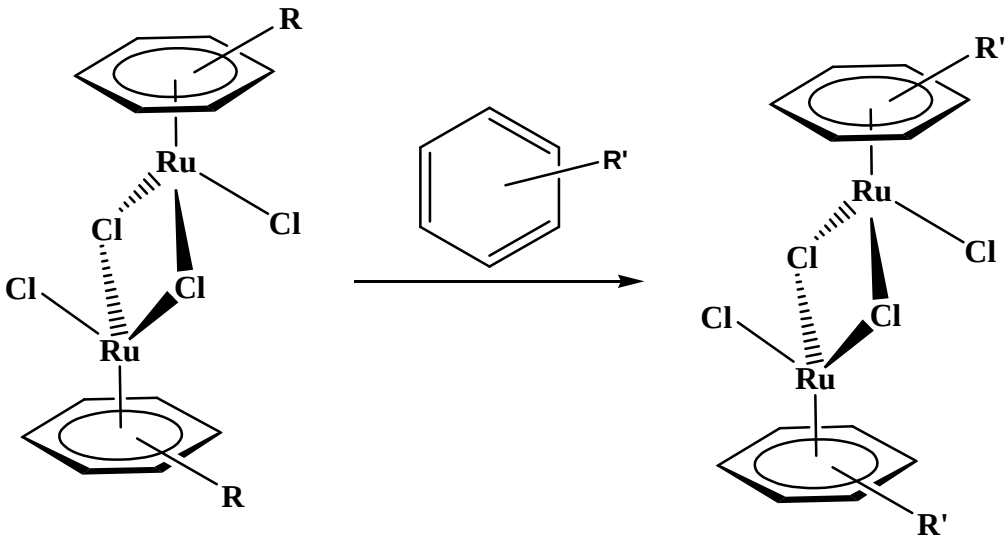

Scheme 1.3

Interest in the reactions of arene-ruthenium(II) has led to a large number of publications between the mid 1980 to 2008. Severe page constraints on this chapter is not

possible to provide a fully survey of this area. However, it is hoped that the discussion that follows will give some important entry into the literature. More recently, Gimeno *et al*., found that catalytic efficiency of compounds [{(η^6-arene)Ru(μ-Cl)Cl}$_2$] is strongly dependent on the arene ligand. The rate order observed, *i.e.* C_6H_6 (TOF = 500 h^{-1}) > *p*-cymene (TOF – 333 h^{-1}) > C_6Me_6 (TOF = 125 h^{-1}), indicates clearly that the less sterically demanding and electron-rich arene exhibit the higher performance, also found that these arene ruthenium complexes are much more active than the classical ruthenium(II) catalysts [$RuCl_2(PPh_3)_3$] and [(η^5-C_9H_7)Ru(PPh_3)$_2$Cl].[14] Furthermore, Finke *et.al*., reported that arene-ruthenium monometallic complexes are only heterogeneous catalysts and pentamethylcyclopentadienyl-rhodium compounds are homogeneous catalysts.[15]

1.2.1. Applications of η^6–areneruthenium chemistry

1.2.1.1 Biological applications

The monodentate ruthenium(II) arene complexes of the type [(η^6-arene)Ru(II)(en)X][PF_6], where *en* is ethylenediamine and X is chloride or iodide (see Chart 1.1), constitute a group that is believed to exert an antitumor action *via* mechanisms different from those of other ruthenium(III) complexes such as NAMI-A or KP1019.[16-19] The chlorido or iodido ligand is readily lost to yield the more reactive aqua species.[20] DNA appears to be a target for these compounds, which bind preferentially to the guanine residues and also interact “non-covalently” *via* both arene intercalation and minor groove binding.[21,22] [(η^6-toluene)Ru(II)(pta)Cl_2] (RAPTA-T), where *pta* is 1,3,5-triaza-7-phosphaadamantane (see chart 1.1), is the parent compound from which a group of water-soluble selective DNA-binding antimetastatic drugs was synthesized.[23, 24] The RAPTA compounds exhibit pH dependent DNA binding, almost no toxicity towards cancer cells *in vitro* and no toxicity at all towards healthy cells, also *in vitro*. However, RAPTA-T was found to inhibit lung metastases in mice bearing a mammary carcinoma, again with only mild effects on the primary tumours. The mechanism of action of the RAPTA compounds is only starting to be investigated.[25,26]

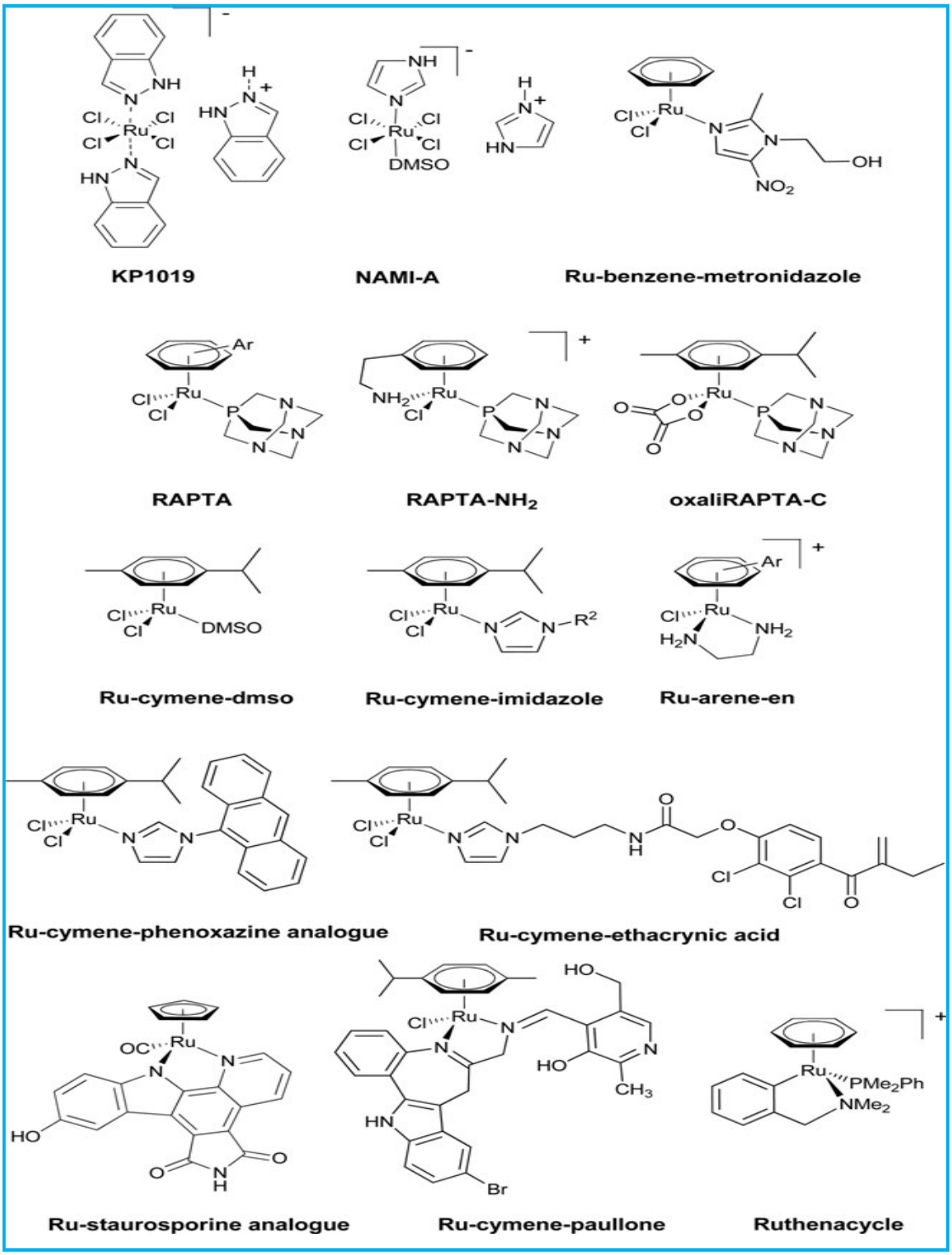

Chart 1.1: Structures of ruthenium-based anticancer drug candidates.

1.2.1.2 Catalytic applications

(a) Homogeneous catalysis:

A catalytic system in which the substrates for the reaction and the catalyst are mixed together in one phase, most often the liquid phase, is known as homogenous

catalysis. Ligand effects are crucial in homogeneous catalysis by metal complexes.[27] The catalytic properties of a given transition metal can be tuned through the nature of ligands bonded to the metal centre. Therefore, one metal can give a variety of products from a single substrate simply by changing the ligands around it. As example, Figure 1.2 shows the different products that can be obtained from styrene with various ruthenium catalysts

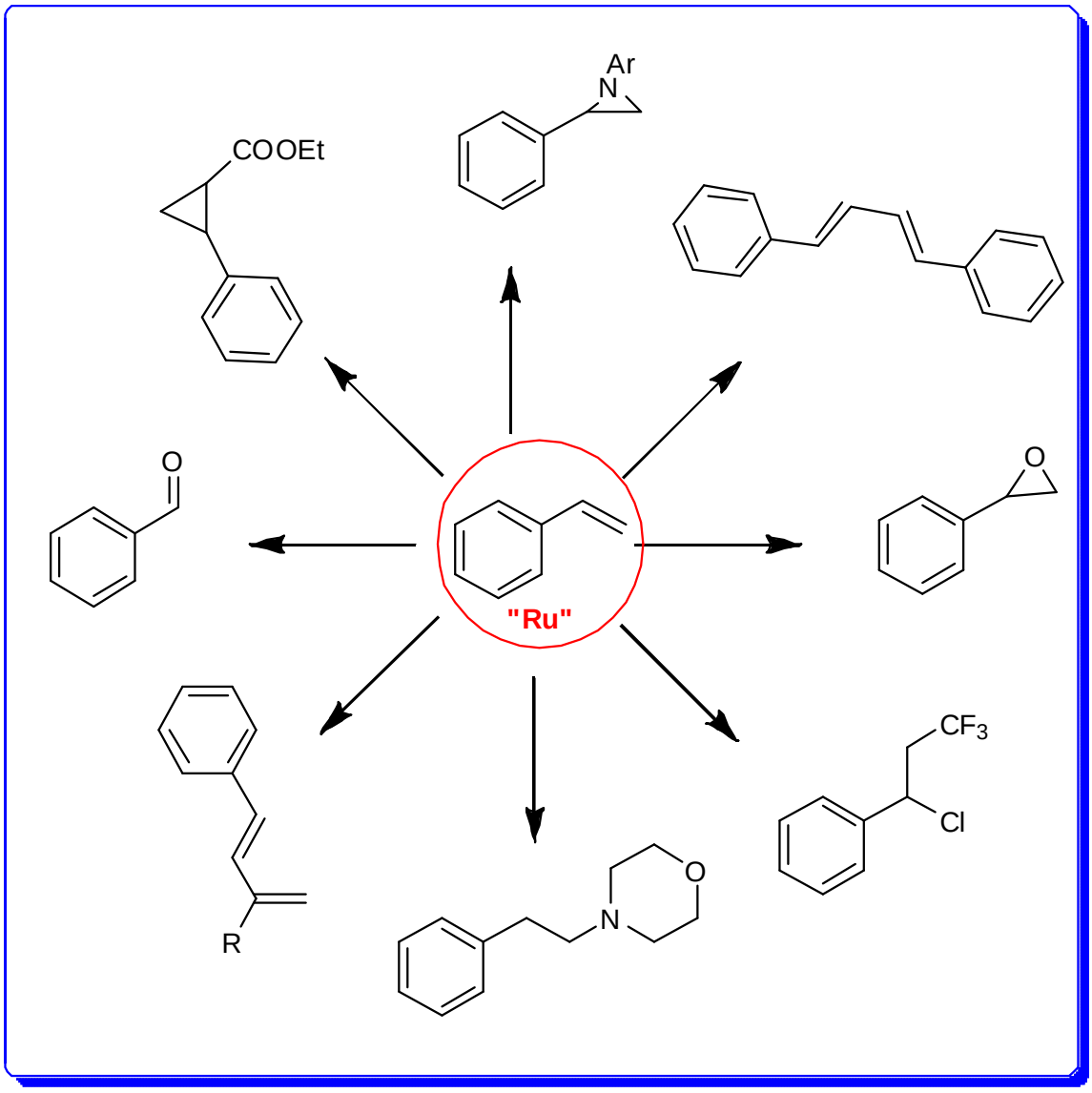

Figure 1.2: Ruthenium catalyzed reactions of styrene

(b) Water oxidation by ruthenium dimers

In the past decade, mankind has begun to appreciate more fully the delicate balance between his existence and his environment. This awareness has taken several forms. One form is the realization that current energy resources will not be sufficient to provide for rapidly expanding population and emerging economies. Most important in

this regard is the finite limitation of fossil fuel resources. These resources were accumulated over millions of years and thus are not renewable in any realistic sense. Another major emerging concern is the effect that our current utilization of natural resources, such as petroleum, is having on the atmosphere and general environment of our planet.[28,29,30]

In this respect the eventual movement to a hydrogen-based economy is particularly promising. Hydrogen is generally considered the best fuel for the future due to its ease of application in fuel cells and clean burning properties. This fuel could be used to replace oil as the source of electricity, heat and transportation to give us a *hydrogen economy*.[31]

In view of this; producing hydrogen from water would offer several benefits over current methods, including steam reforming of natural gas, which produces carbon dioxide along with the hydrogen. Heat derived from fossil-fuel combustion is currently used to drive the steam reforming process, resulting in even more carbon dioxide as a byproduct, all of which contributes to global warming. Making hydrogen by splitting water would not add carbon dioxide to the atmosphere.

In view of all these things, designing and syntheses of water oxidation catalytic complexes has been receiving continuous attention for the last few decades. Especially the ruthenium complexes have been showing most promising feature for the catalytic activities. For nearly 15 years **1** (blue dimer) (see figure 1.3) was the only ruthenium complex known to catalyze water to oxygen. Following that, many groups are working on this theme, but only few research groups have been succeeded with the prospect; they are Llobet and co-workers synthesized[32,33] complex **2** (figure 1.3) and a more substantial structural change has come from the laboratory of Thummel[34] with the synthesis of complex **3** (see figure 1.2). However, the stability of the complex is only modestly improved and turnover increases to 20 with k_{∞} rising by a factor of six to 1.4 x 10^{-2}. s^{-1}, in later the rate increases to k_{∞} = 7.7 x10^{-2} s^{-1}.[35]

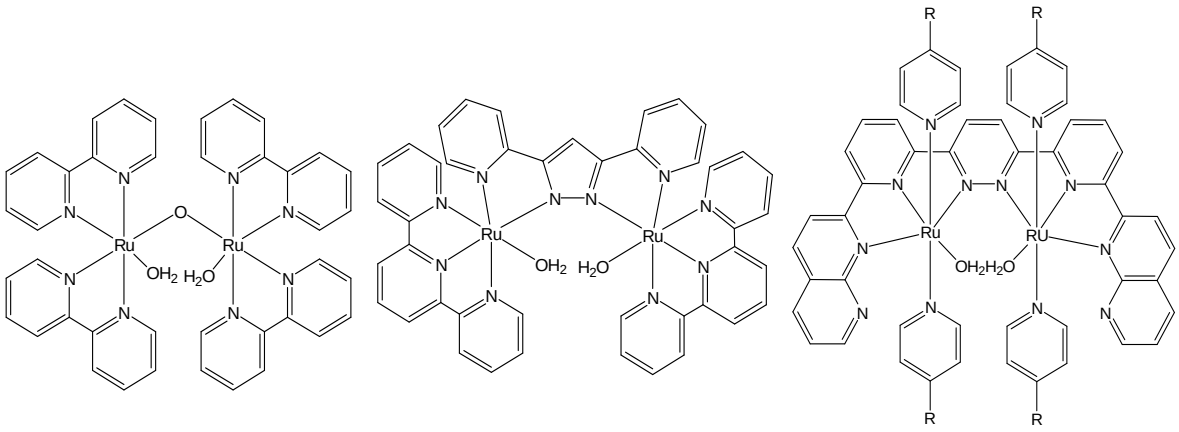

1 **2** **3**

Figure1.3: Some of the compounds which shown catalytic activity to oxidize water

1.3 Arene-ruthenium polypyridyl compounds

Reactions of dimeric complex $[\{(\eta^6\text{-arene})RuCl_2\}_2]$ (arene = C_6H_6, *p*-cymene and C_6Me_6) with various mono, bi and polydentate nitrogen bases gave neutral and cationic substitution complexes of formulation $[(\eta^6\text{-arene})RuCl(L)]^+$ or dinuclear complexes of formulation $[\{(\eta^6\text{-arene})RuCl\}_2(\mu\text{-}L)]^{2+}$ (L = polypyridyl ligands, L_1 to L_{15}) (Chart 1.2) by cleavage of chloride bridges.[36,37] In the case of polydentate nitrogen bases co-ordinates as a bidentate manner.[38,39] Reactions with 1,10-phenanthroline (L_1) or with its 5-nitro or 5-amino derivatives to give quantitatively the cationic chloro complexes $[(\eta^6\text{-arene})Ru(N\cap N)Cl]Cl$ containing the corresponding N,N-donor as chelating ligand.[40] All these complexes $[(\eta^6\text{-}C_6Me_6)Ru(L_1)Cl]^+$ have shown the catalytic property for the hydrogenation of acetophenone with formic acid in aqueous solution to give phenylethanol and carbon dioxide.[40] Reactions with two equivalents of 5,6-diphenyl-3-(pyridine-2-yl)-1,2,4-triazine (L_2),[41] 4,6-bis(2-pyridyl)pyridazine (L_3),[42] 4,6-bis(2-pyridyl)4-phenylpyridazine (L_4),[42] 4,6-bis(pyrazolyl)pyridazine (L_5)[42] in the presence of KPF_6 to form the cationic mononuclear arene ruthenium complexes where as some of the polypyridyl ligands yielded both mono and dinuclear complexes based on their molar ratios, for example 2,2'-bipyrimidine (L_6),[43] 3,5-bis(2-pyridyl)pyrazole (L_7),[44] 2,3-bis(2-pyridyl)pyrazine (L_8),[44,46] 2,4,6,-tris(2-pyridyl)1,3,5-triazine (L_9),[44] pyridine-2-carbaldehyde azine (L_{10})[47] *etc*. Interestingly few ligands yielded only dinuclear complexes upon reaction of arene ruthenium dimers, for example p-phenylene-

bis(picoline)-aldamine (L_{11}), p-biphenylene-bis(picoline)-aldamine (L_{12})[47] and .3,6-bis(2-pyridyl)bithiazole (L_{13}), 3,6-bis(2-pyridyl)1,2,4,5-tetrazine(L_{14}) (Chart 1.2).[44]

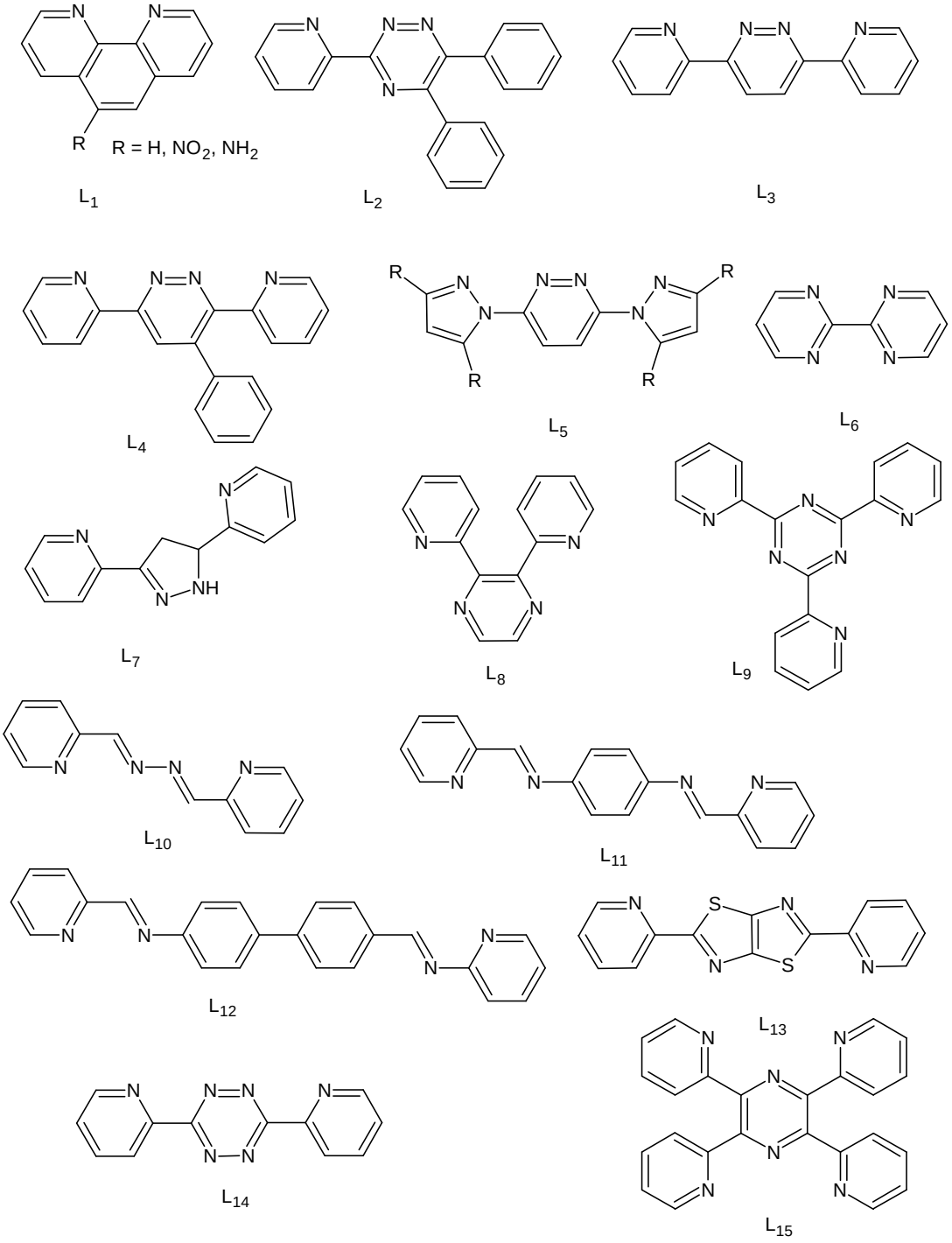

Chart 1.2

Bruno *et al* reported[48] a hexa-nuclear metal grid $[(\eta^6\text{-}p\text{-}^{i}PrC_6H_4Me)_6Ru_6(\mu_3\text{-tpt-}\kappa N)_2(\mu\text{-}C_2O_4\text{-}\kappa O)_3]^{6+}$ with the reaction of *tpt* ligand (figure 1.4) as well as a tetra nuclear arene ruthenium complexes with porphyrin ligand (figure 1.5).[49,50]

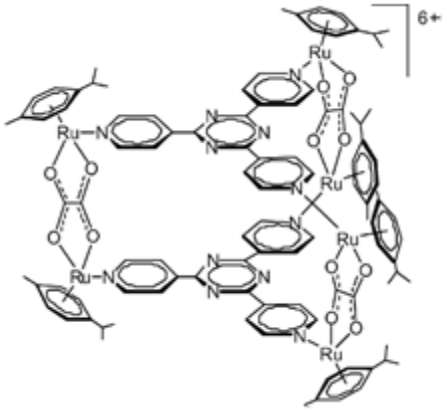

Figure 1.4

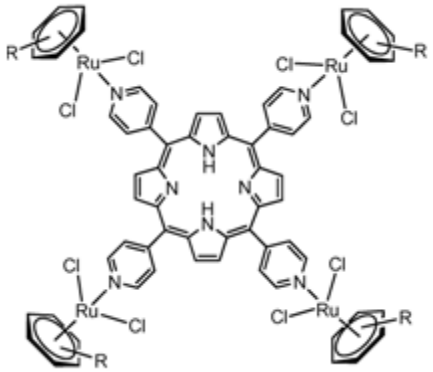

Figure 1.5

1.4 η^5-Pentamethylcyclopentadienyl (Cp*) rhodium(III) and iridium(III) chemistry

The discovery of $[(\eta^5\text{-Cp*})MCl_2]_2$ (M = Rh and Ir) (scheme 1.4) by Maitlis[51,52] has provided a relevant milestone on the development of organometallic chemistry and homogeneous catalysis for nearly four decades, resulting in major advances in the understanding of these areas. The η^5-pentamethylcyclopentadienyl group is an excellent protecting ligand towards rhodium and iridium, whilst substitution of the chloride ligands occurs very easily, with a marked tendency to form mononuclear complexes.

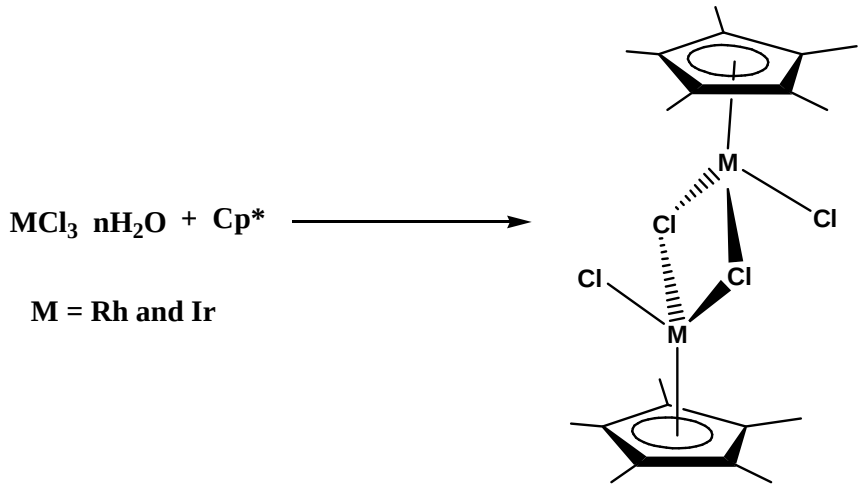

Scheme 1.4

1.4.1 Application of pentamethylcyclopentadienyl rhodium and iridium complexes

Ir(III) and Rh(III) metal centres are reactive and have the potential to catalyse a range of other transformations not reliant on oxidative addition. Recent work by Crabtree

et al. has utilised an Ir(III) hydride complex to catalyse the intramolecular hydroamination and hydroalkoxylation of alkynes.[53] $[Cp^*IrCl_2]_2$ is effective as a catalyst for the hydroborylation of styryl sulfonamides,[54] the *N*-alkylation of amines with alcohols[55] and also the transfer hydrogenation of ketones[56] and quinolines.[57] Rh(III) complexes are known to be effective in catalysing carbon-carbon bond formation,[58] and $[Cp^*RhCl_2]_2$ has been shown to effect transfer dehydrochlorination of aryl chlorides.[59] For example the complex $[(Cp^*)RhCl(N\text{-}N)]^+$ (N-N = 2,2'-bipyridine), was shown to occur as a crucial intermediate[60] in hydride transfer catalysis schemes intended at H_2 production[60] or NADH regeneration (Scheme 1.5). Related compounds could be generated from photolysis of olefin-containing precursors.[61] Treatment of hydroquinone with $[Cp^*M(solvent)_3][OTf]_2$ (M = Rh, Ir) in acetone afforded the π-bonded complexes $\{[Cp^*M(\eta^5\text{-semiquinone})][OTf]_n\}$ (M = Rh, Ir).[62]

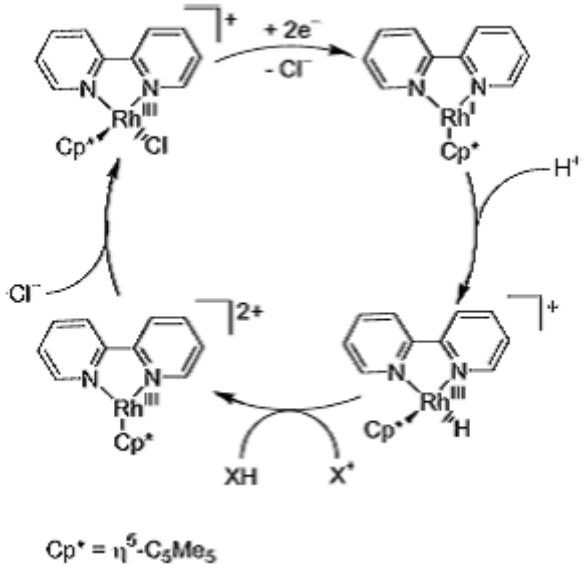

Scheme 1.5

1.5 Rhodium and iridium polypyridyl compounds

The chemistry of rhodium(III) and iridium(III) is very similar to the chemistry of arene ruthenium(II) since all these metals are with isoelectronic (d^6) configuration. As is typical within the d^6 configuration, many of the organometallic reactions studied with arene ruthenium(II) are often equally valid for Cp* rhodium(III) and iridium(III). Pentamethylcyclopentadienyl (Cp*) is ubiquitous as a ligand in organometallic complexes. Many complexes incorporating this ligand are important as active catalysts, largely due to the electron-rich nature of the Cp*group and also the ability of Cp* to

completely block one face of the complex, imparting steric bulk and structural rigidity. Rh(III) and Ir(III) complexes incorporating both the Cp* ligand and bidentate sp^2-nitrogen donor ligands have been synthesised previously.[63-70] In particular, the complex $[Cp^*Ir(bipy)(H_2O)]SO_4$ (bipy = 2,2'-bipyridine) was found to be active as a catalyst for the hydration of phenylacetylene in water,[71] and the complex $[Cp^*Rh(^iPr\text{-}pymox)]^{2+}$ (pymox = pyridyloxazoline) was found to promote the enantioselective Diels–Alder reaction of methacrolein with cyclopentadiene.[66]

The reactions of Cp* Rh and Ir complexes with N donor ligands with a series of bidentate ligands with sp^2 N-donors such as bis(pyrazolyl)-methane (L_{16}), bis(1-methylimidazolyl)methane (L_{17}), bis(3,5-dimethylpyrazolyl)methane (L_{18}), bis(1-methylimidazolyl)ketone (L_{19}), bis(2,4,6-trimethylphenylimino)-acenapthene (L_{20}) (Chart 1.3) resulted a series of complexes of the formulations [Cp*MCl(N–N)][X] (M = Rh and Ir), where N–N (L_{16}-L_{21})[72] (Chart 1.3).

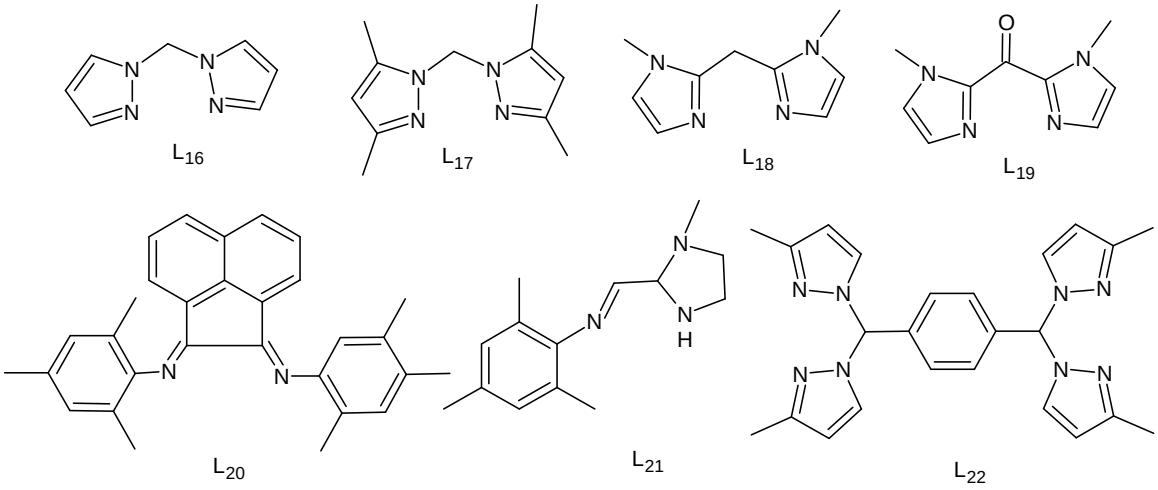

Chart 1.3

1.6 Materials and physical measurements

1.6.1 Materials

All solvents were dried and distilled prior to use. The chemicals which were used in the present research were purchased from Aldrich, Fluka, Mercury and Rankem Companies and were used as received. The metal chlorides $RuCl_3$, $RhCl_3$ and $IrCl_3$ were purchased from Arora Matthey *Ltd*. $[(\eta^6\text{-}C_6H_6)Ru(\mu\text{-}Cl)Cl]_2$, $[(\eta^6\text{-}p\text{-}^iPrC_6H_4Me)Ru(\mu\text{-}Cl)Cl]_2$, $[(\eta^6\text{-}C_6Me_6)Ru(\mu\text{-}Cl)Cl]_2$[73-75] $[(Cp^*)M(\mu\text{-}Cl)Cl]_2$ (M = Rh, Ir),[76-78] $[(Cp)Ru(PPh_3)_2Cl]$,[82] $[(Cp^*)Ru(PPh_3)_2Cl]$ and $[(\eta^5\text{-}C_9H_7)Ru(PPh_3)_2Cl]$[78,80,81] were prepared according to literature methods. The synthetic procedure for the ligands which

were used in the present research was mentioned on proceeding chapters and their structures are shown in Chart 1.4.

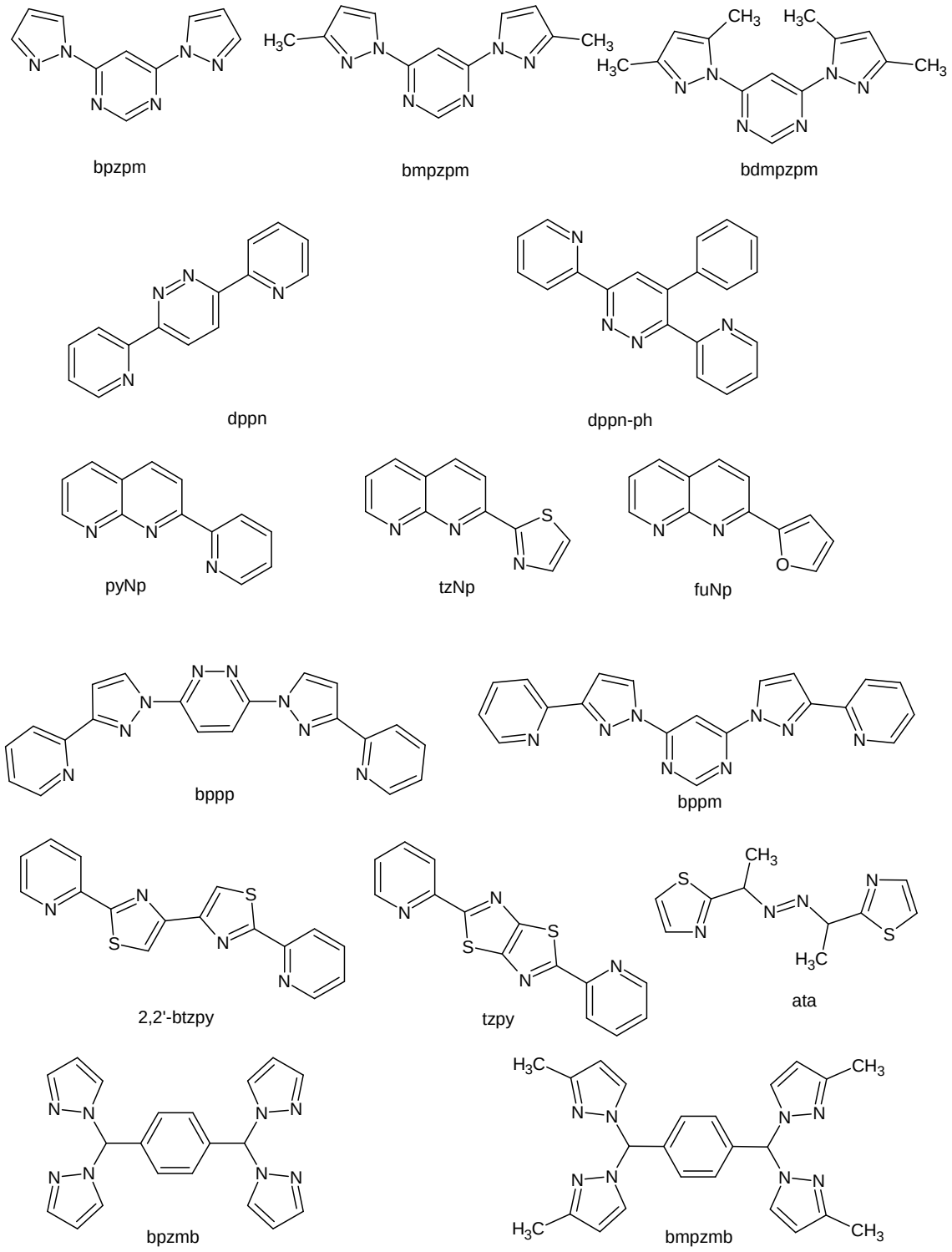

Chart 1.4: Ligands used in the present study: polypyridyl and polypyrazolyl bridging and terminal ligands.

1.6.2 Synthesis of the starting materials

1.6.2.1 Synthesis of [{(η^6-p-cymene)$RuCl_2$}$_2$]

The [{(η^6-*p*-cymene)$RuCl_2$}$_2$] was prepared according to well established synthetic procedure.[73] A solution of hydrated ruthenium trichloride (approximating $RuCl_3$ $3H_2O$, containing 38-39% Ru) (1 g, 3.85 mmol) in 80 ml ethanol is treated with 5 ml of α-phellandrene and heated under reflux in a 150 ml round-bottomed flask for 4 hours. The solution is allowed to cool to room temperature, and the red-brown, microcrystalline product is filtered off. Additional product is obtained by evaporating the orange-yellow filtrate under reduced pressure to approximately half-volume and cooling over night to 4 ºC. After drying in *vacuo* the yield is 1.10 g (81%).

^{1}H NMR (400 MHz, $CDCl_3$): δ =5.48 (d, 2H, ^3J = 6.4 Hz, $Ar_{p\text{-}cy}$), 5.34 (d, 2H, ^3J = 6.4 Hz, $Ar_{p\text{-}cy}$), 2.95 (sept, 1H, ^3J = 6.2 Hz, $CH(CH_3)_2$), 2.15 (s, 3H, $Ar_{p\text{-}cy}$-Me), 1.28 (d, 6H, ^3J = 6.4 Hz, $CH(CH_3)_2$.

1.6.2.2 Synthesis of [{(η^6-C_6H_6)$RuCl_2$}$_2$]

Preparation of [{(η^6-C_6H_6)$RuCl_2$}$_2$] followed *Bennett* method.[73] Hydrated $RuCl_3$ (2 g) in 100 ml of ethanol was heated under reflux with 10 ml of cyclohexadiene (either 1,3- or 1,4-) for 4 hours. The brown precipitate was filtered off, washed with methanol, and dried in vacuo (1.83g, 95%). ^{1}H NMR (400 MHz, $CDCl_3$): δ = 6.07 (s, 6H, C_6H_6)

1.6.2.3 Synthesis of [{(η^6-C_6Me_6)$RuCl_2$}$_2$][75]

To the dimer [{(η^6-*p*-cymene)$RuCl_2$}$_2$] (200 mg, 0.33 mmol) taken in sealed glass vial of 5 ml capacity, a three fold excess of hexamethylbenzene (0.98 mmol) was added and mixed properly. The reaction was carried out fixing the microwave at 170^0 c and a pressure of 5 bar. With the 200 W microwave system, this temperature was reached within a few minutes, and the reaction completed in 10 min. Excess hexamethylbenzene was recovered by washing with hexane through a silica gel column using hexane as eluent. The orange red band [{(η^6-*p*-cymene)$RuCl_2$}$_2$] was collected by passing a mixture of methanol- acetone in 1:1 ratioo. The solvent was removed on a rotary evaporator. The resulting solid was washed with hexane and diethylether and dried in vacuum. Yield (175 mg, 96%), ^{1}H NMR (400 MHz, $CDCl_3$): δ = 2.07 (s, 18H, C_6Me_6)

1.6.2.4 Synthesis of [{(η^5-Cp)$RhCl_2$}$_2$] and [{(η^5-Cp*)$IrCl_2$}$_2$]*

The [{(η^5-Cp*)MCl_2}$_2$] (M = Rh and Ir) was prepared according to well established synthetic procedure.[78] A solution of hydrated metal trichloride (1 g) in 80 ml methanol is treated with 0.8 ml of pentamethylcylopentadiene and heated under reflux in a 100 ml round-bottomed flask for 48 hours. The solution is allowed to cool to room temperature, and the red-brown, microcrystalline product is filtered off. The crystalline product was filtered and washed with cold methanol, diethyl ether and after drying in *vacuo* the yield is 1.1 g (78%).

^{1}H NMR (400 MHz, $CDCl_3$): δ =1.62 (s, 15H, C_5Me_5)

1.6.2.5 Synthesis of [(η^5-C_5H_5)$Ru(PPh_3)_2Cl$]

The compound hydrated ruthenium trichloride (1 g, 4.82 mmol) in dry ethanol (20 ml) was added rapidly to the refluxing solution of triphenylphosphine (5 g) in ethanol 100 ml, followed immediately afterward by a solution of freshly distilled cyclopentadiene (10 ml) in ethanol (20 ml). The mixture was then refluxed until the color change from dark brown to orange was completed (60 min to 90 min), and then cooled in a refrigerator overnight. The orange crystalline product was filtered, washed with cold ethanol, water, ethanol and petroleum ether and dried to give pure product (2.50 g, 86%).

^{1}H NMR (400 MHz, $CDCl_3$): δ =4.52 (s, 5H, C_5H_5),

^{13}P {^{1}H} NMR (162 MHz, $CDCl_3$): δ =46

1.6.2.6 Synthesis of [(η^5-C_5Me_5)$Ru(PPh_3)_2Cl$]

The compound $RuCl_3$ $3H_2O$ (1 g, 4.82 mmol) and C_5Me_5 (131 ml, 9.64 mmol) were dissolved in ethanol (60 ml) and refluxed for 90 min after which a solution of PPh_3 (5 g, 20 mmol) and NaOEt (92 mg of Na in 4 ml ethanol) in ethanol (40 ml) was added dropwise. The solution was then refluxed for 18 hours. The orange yellow precipitate was collected and washed with ethanol and hexane to give pure product (2.6 g, 70%).

^{1}H NMR (400 MHz, $CDCl_3$): δ =1.62 (s, 55H, C_5Me_5)

^{13}P {^{1}H} NMR (162 MHz, $CDCl_3$): δ =48

1.6.3 Physical measurements

Infrared spectra were recorded as KBr pellets on a Perkin-Elmer 983 FT-IR spectrophotometer in the 4000 - 400 cm^{-1}. Elemental analyses of the complexes were performed on a Perkin-Elmer-2400 CHN/S analyzer. NMR spectra were recorded on

Bruker AMX-400 MHz FT-NMR spectrometer using TMS as the internal standard. Mass spectra were obtained from Waters ZQ 4000 mass spectrometer by ESI method. Absorption spectra were obtained at room temperature using a Perkin-Elmer Lambda 25 UV/Visible spectrophotometer.

1.7 Crystallographic data collection and structure analyses

Single crystal X-ray diffraction measurements were carried out on a Bruker Smart Apex CCD diffractometer. The crystals were mounted on a Stoe Image Plate Diffraction system equipped with a ϕ circle goniometer, using Mo-Kα graphite monochromated radiation (λ = 0.71073 Å) with ϕ range 0–200º. The structures were solved by direct methods using the program SHELXS–97.[82] Refinement and all further calculations were carried out using SHELXL–97.[83] The H-atoms were included in calculated positions and treated as riding atoms using the SHELXL default parameters. The non-H atoms were refined anisotropically, using weighted full-matrix least-square on F^2. The structures were drawn with the softwares ORTEP[84] and MERCURY.[85, 86]

The crystal data for the representative complexes can be obtained free of charge *via* www.ccdc.cam.ac.uk/data_request/cif, by e-mailing data_request@ccdc.cam.ac.uk or contacting The Cambridge Crystallographic Data Centre, 12, Union Road, Cambridge CB2 1EZ, UK; fax: +44 1223 336033. The CCDC numbers of the crystal structures are mentioned in corresponding chapters with a heading under supplementary material.

References

1 Ch. Elschenbroich, A. Salzer, Organometallics, VCH, Germany, (1992).

2 E. I. Negishi, *Organometallics in Organic Synthesis*, Wiley, New York, (1980).

3 M. Beller, C. Bolm, *Transitions Metals for Organic Synthesis*, Wiley-VCH, Weinheim, (1998).

4 R. H. Crabtree, The Organometallic Chemistry of the Transition Metals, Wiley, New York, (1988).

5 Jon A Mc Cleverty, Thomas J. Meyer, Comprehensive Coordination Chemistry II, from biology to nanotechnology; Oxford: Elsevier pergamon, (2004).

6 G. Winkhaus, H. Singer, J. Organomet. Chem. 7 (1967) 487.

7 R. A. Zelonka, M. C. Baird, Can. J. Chem. 50 (1972) 3063.

8 M. A. Bennett, A. K. Smith, J. Chem. Soc., Dalton Trans. (1974) 233.

9 H. L. Bozec, D. Touchard, Pierre H. Dixneuf, Adv. Organomet. Chem. 29 (1989) 163.

10 M. A. Bennett, In Comprehensive Organometallic Chemistry II; G. Winkinson, Ed., Pergamon: Oxford, England, 7 (1982) 549.

11 B. Therrien, Coord. Chem. Rev. 253 (2009) 493.

12 J. Canivet, G. Süss-Fink, Green Chem. 9 (2007) 391.

13 J. Canivet, G. Süss-Fink, P. Štěpnička, Eur. J. Inorg. Chem. (2007) 4736.

14 V. Carierno, P. Crochet, S. E. G. –Garrido, J. Gimeno, Dalton Trans. (2004) 3635.

15 C. M. Hagen, J. A. Widegren, P. M. Maitlis, R. G. Finke, J. Am. Chem. Soc., 127 (2005) 4423.

16 R. E. Morris, R. E. Aird, P. D. Murdoch, H.M. Chen, J. Cummings, N. D. Hughes, S. Parsons, A. Parkin, G. Boyd, D. I. Jodrell, P. J. Sadler, J. Med. Chem. 44(2001**)** 3616.

17 R. E. Aird, J. Cummings, A. A. Ritchie, M. Muir, R. E. Morris, H. Chen, P. J. Sadler, D. I. Jodrell, Br. J. Cancer 86 (2002) 1652.

18 O. Nováková, H. M. Chen, O. Vrána, A. Rodger, P. J. Sadler, V. Brabec, Biochemistry 42 (2003**)** 11544.

19 O. Nováková, J. Kaspárková, V. Bursova, C. Hofr, M. Vojtiskova, H. M. Chen, P. J. Sadler, V. Brabec, Chem. Biol.12 (2005**)** 121.

20 F. Wang, H. M. Chen, S. Parsons, L. D. H. Oswald, J. E. Davidson, P.J. Sadler, Chem.-Eur. J. 9 (2003) 5810.

21 H. M. Chen, J. A. Parkinson, S. Parsons, R. A. Coxall, R. O. Gould, P. J. Sadler, J. Am. Chem. Soc.124 (2002) 3064.

22 F. Y. Wang, J. Bella, J. A. Parkinson, P. J. Sadler, J. Biol. Inorg. Chem.10 (2005**)** 147.

23 C. S. Allardyce, P. J. Dyson, D. J. Ellis, S. L. Heath, Chem. Commun. (2001) 1396.

24 W. H. Ang, E. Daldini, C. Scolaro, R. Scopelliti, L. J. Jeannerat, P. J. Dyson, Inorg. Chem. 45 (2006) 9006.

25 P. J. Dyson, G. Sava, Dalton Trans. (2006) 1929.

26 M. Auzias, B. Therrien, G. Süss-Fink, P. P. Štěpnička, W. H. Ang, P. J. Dyson, Inorg. Chem. 47 (2008) 578.

27 Homogeneous catalysis, Understanding the art: Van Leeuwen, P.W.N.M. Kluwer Academic publishers, Amsterdam (2004).

28 *The Hydrogen Economy*; The National Academies Press: Washington,DC, (2004).

29 B. Sorenson, *Hydrogen and Fuel Cells*; Elsevier: Oxford, U.K. (2005).

30 C. –J. Winter, J. Nitsch, Eds. *Hydrogen Asian Energy Carrier*; Springer-Verlag: Berlin, Germany, (1988).

31 J. J. Romm, *The Hype About Hydrogen*; Island Press: Washington, (2004).

32 I. Romero, M. Rodriguez, C. Sens, J. Mola, K. M. Rao, L. Franca's, E. Mass-marza, L. Escriche, A. Llobet, Inorg. Chem. 47 (2008) 1824.

33 C. Sens, I. Romero, M. Rodriguez, A. Llobet, T. Parella, J. Benet-Buchholz, J. Am. Chem. Soc. 126 (2004) 7798.

34 R. Zong, D. Wang, R. Hammitt, R. P. Thummel, J. Org. Chem. 71 (2006) 167.

35 Z. Deng, H. W. Tseng, R. Zong, D. Wang, R. P. Thummel, Inorg. Chem.47 (2008) 1835.

36 C. D. Nunes, M. Pillinger, A. Hazell, J. Jepsen, T. M. Santos, J. Madureira, A. D. Lopes, I. S. Goncalves, Polyhedron 22 (2003) 2799.

37 J. M. Malecki, J. O. Dzuegielewski, M. Jaworksa, R. Kruszynki, T. J. Bartczak. Polyhedron 23 (2003) 885.

38 R. Lalrempuia, K. M. Rao, Polyhedron, 23 (2003) 3155.

39 K. S. Singh, Y. A. Mozharivskyj, K. M. Rao Z. Anorg. Allg. Chem. 632 (2006) 172.

40 J. Canivet, L. K.-Brelot, G. Süss-Fink, J. Organomet. Chem. 690 (2005) 3202

41 B. Therrien, C. S.-Mohamed, G. Süss-Fink, Inorganica Chimica Acta 361 (2008) 2601.

42 K. T. Prasad, G. Gupta, A. K. Chandra, M. P. Pavan, K. M. Rao, J. Organomet. Chem. 695 (2010) 707.

43 P. Govindaswamy, J. Canivet, B. Therrien, G. Süss-Fink, P. Štêpnicka, J. Ludvík, J. Organomet. Chem. 692 (2007) 3664

44 G.Gupta, G. P. A.Yap, B. Therrien, K. M. Rao, polyhedron 28 (2009) 844.

45 A. Singh, N. Singh, D. S. Pandey, J. Organomet. Chem. 642 (2002) 48.

46 A. Singh, S. K. Singh, M. Trivedi, D. S. Pandey, J. Organomet. Chem. 690 (2005) 4243.

47 A. Singh, M. Chandra, A. N. Sahay, D. S. Pandey, K. K. Pandey, S. M. Mobin, M. C. Puerta, P. Valerga, J. Organomet. Chem. 689 (2004) 1821.

48 P. Govindaswamy, D. Linder, J. Lacour, G. Süss-Fink, B. Therrien, Dalton Trans. (2007) 4457

49 F. Schmitt, P. Govindaswamy, G. Süss-Fink, W. H. Ang, P. J. Dyson, L. Juillerat-Jeanneret, B. Therrien, J. Med. Chem., 51 (2008) 1811.

50 M. Auzias, B. Therrien, G. Süss-Fink, P. Stepnicka, W. H. Ang, P. J. Dyson, Inorg. Chem. 47 (2008) 578.

51 P. M. Maitlis, Accounts Chem. Res. 11 (1978) 301.

52 P. M. Maitlis, Chem. Soc. Rev. 10 (1981) 1.

53 X. Li, A. R. Chianese, T. Vogel, R. H. Crabtree, Org. Lett. 24 (2005) 5437.

54 N. A. Wynberg, L. J. Leger, M. L. Contad, C. M. Vogels, A. Decken, S. J. Duffy, S. A. Wescott, Can. J. Chem. Eng. 83 (2005) 666.

55 K.-I. Fujita, Z. Li, N. Ozeki, R. Yamaguchi, Tetrahedron Lett. 44 2003) 2687.

56 M. Furegati, A. J. Rippert, Tetrahedron: Asymmetery (2005) 3947.

57 K.-I. Fujita, C. Kitasuji, S. Furukawa, R. Yamagushi, Tetrahedron Lett. 45 (2004) 3215.

58 For a recent review of rhodium-catalysed C–C bond formation;K. Fagnou, M. Lautens, Chem. Rev. 103 (2003) 169.

59 K.-I. Fujita, M. Owaki, R. Yamaguchi, Chem. Commun. (2002) 2964.

60 M. Sieger, W. Kaim, D. J. Stufkens, T. L. Snoeck, H. Stoll, S. Zalis, Dalton Trans. (2004) 3815

61 D. Godard, S. B. Duckett, S. Parsons, R. N. Perutz, Chem. Comm., (2003) 2332.

62 J. Moussa, C. G. –Duhayon, P. Herson, H. Amouri, M. N. Rager, A. Jutand, Organometallics 23 (2004) 6231.

63 S. Greulicj, A. Klein, A. Knödler, W. Kaim, Organometallics 21 (2002) 765.

64 Y. Himeda, N. Onozawa-Komatsuaki, H. Sugihara, H. Arakawa, K. Kasuga, Organometallics 23 (2004) 1480.

65 P. Govindaswamy, Y. A. Mozharivskyj, K. M. Rao, Polyhedron 24 (2005) 1710.

66 D. L. Davies, J. Fawcett, S. A. Garrat, D. R. Russel, Dalton Trans. (2004) 3629.

67 B. J. Wik, C. Rømming, M. Tilset, J. Mol. Catal. A (2002) 23.

68 E. Carmona, A. Cingolani, F. Marcheti, C. Pettinari, R. Pettinari, B. W. Skelton, A. H. White, Organometallics 22 (2003) 2820.

69 P. Govindaswamy, K. M. Rao, J. Coord. Chem. 59 (2006) 663.

70 S. Berger, F. Baumann, T. Scheiring, W. Kaim, Z. Anorg. Allg. Chem. 627 (2001) 620.

71 S. Ogo, K. Uehara, T. Abura, Y. Watanabe, S. Fukuzumi, J. Am. Chem. Soc. 126 (2004) 16520.

72 D. F. Kennedy, B. A. Messerle, M. K. Smith, Eur. J. Inorg. Chem. (2007) 80

73 M. A. Bennett, T. N. Huang, T. W. Matheson, A. K. Smith, Inorg. Synth. 21 (1982) 74.

74 M. A. Bennett, T. W. Matheson, G. B. Robertson, A. K. Smith, P. A. Tucker, Inorg. Chem. 19 (1980) 1014.

75 S. L. Nongbri, B. Das, K. M. Rao, J. Organomet. Chem. 694 (2009) 3881.

76 J. W. Kang, K. Moseley, P. M. Maitlis, J. Am. Chem. Soc. 91 (1969) 5970.

77 R. G. Ball, W. A. G. Graham, D. M. Heinekey, J. K. Hoyano, A. D. McMaster, B. M. Mattson, S. T. Michel, Inorg. Chem. 29 (1990) 2023.

78 C. White, A. Yates, P. M. Maitlis, Inorg. Synth. 29 (1992) 228.

79 M. I. Bruce, N. J. Windsor, Aust. J. Chem. 30 (1977) 1601.

80 M. I. Bruce, B. C. Hall, N. N. Zaitseva, B. W. Skelton, A. H. White, J. Chem. Soc., Dalton Trans. (1998) 1793.

81 G. Consiglio, F. Morandini, Chem. Rev. 87 (1987) 761.

82 G. M. Sheldrick, Acta Cryst. A46 (1990) 467.

83 G. M. Sheldrick, SHELXL-97, University of Göttingen, Göttingen, Germany. 1999.

84 L. J. Farrugia, J. Appl. Cryst. 30 (1997) 565.

85 I. J. Bruno, J. C. Cole, P. R. Edgington, M. Kessler, C. F. Macrae, P. McCabe, J. Pearson, R. Taylor, Acta Cryst. B58 (2002) 389.

86 H. van der Poel, G. van Koten, K. Vrieze, Inorg. Chem. 19 (1980) 1145.

Chapter 2

Mono and dinuclear half-sandwich platinum group metal complexes bearing pyrazolyl-pyrimidine ligands: Syntheses and structural studies*

In the present chapter, we focus on the synthetic methodology applied for the development of homogeneous and immobilized half-sandwich ruthenium, rhodium and iridium complexes bearing bis(pyrazolyl)pyrimidine as a specific *N,N*-bidentate bridging ligands

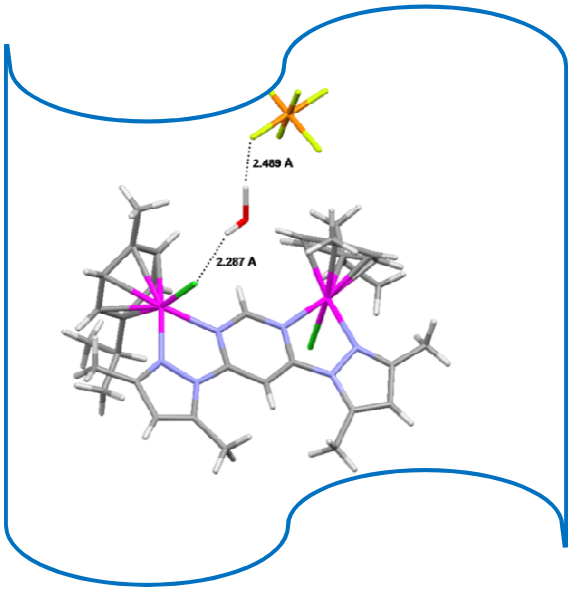

---

*The work presented in this chapter has been published: K. T. Prasad, B. Therrien, S. Geib and K. Mohan Rao, J. Organomet. Chem. 695 (2010) 495-604.

2.1 Introduction

During the last few decades there has been great interest in the chemistry of transition metals associated with polydentate ligands with sp^2-hybridized nitrogen atoms, for instance, polypyrazolylborates[1,2] and polypyridines.[2-6] In many cases, the charge transfer properties of these compounds justify this interest. Especially these nitrogen donor ligands have shown to be effective catalysts for oxidation reactions[7-15] and for ring-opening metathesis polymerization[16] and recent studies of arene ruthenium complexes have shown that they are found to inhibit cancer cell growth,[17-22] as non-linear optical (NLO) materials[23,24]. For a majority of the complexes studied, the metal centers are linked by a bridging ligand and the nature of the bridge has a fundamental influence on the electronic interaction between the metals and therefore on the characteristics of the material.

The ligand 4,6-bis(pyrazolyl)pyrimidine (L1) and its analogues, 4,6-bis(3-methyl-pyrazolyl)pyrimidine (L2) and 4,6-bis(3,5-dimethyl-pyrazolyl)pyrimidine (L3) are the subject of this investigation. They have a structural similarity to 3,6-bis(pyrazolyl)pyridazine (**A**) and 4,5-bis(pyrazolyl)quinoxaline (**B**), both of which have been previously studied.[25,26] In our previous work, we demonstrated that the ligand **A** does not yield dinuclear compounds with two half-sandwich platinum group metal atoms, due to the steric nature of the ligand, it resulted only in the formation of mononuclear complexes.[25] However it is true in the case of more sterically free ligand **B** also, because it also yielded mononuclear complexes, since the pyrazole rings of the ligand tilted with respect to the central quinoxaline ring because of the steric collide between the R' groups of the pyrazole rings. In the case of ligand **A**, the pyrazolyl rings are bonded *para* to each other, where as in the case of ligand **B**, they are bonded *ortho* to each other on the central six membered rings. But sterically less demanding ligand L (L1 to L3) can coordinate to two half-sandwich platinum group metal centers, since the pyrazolyl rings of the ligand are bonded *meta* to each other, leading to reduced steric interaction, which enhances the stability of the dinuclear complexes.

In recent years, we have been carrying out arene ruthenium complexation reactions with a variety of nitrogen-based ligands[27-32] including pyridyl-pyridazine and pyrazolyl-pyridazine ligands. Ruthenium complexes of these types of nitrogen-based ligands have a capacity to function as catalysts for the oxidation of water to oxygen.[33-35] Although extensive studies have been made on ruthenium complexes containing

polypyridyl ligands, complexes containing pyrazolyl-pyrimidine ligands have not yet been investigated.

In the present chapter, we focus on the synthetic methodology applied for the development of homogeneous and immobilized half-sandwich ruthenium, rhodium and iridium complexes bearing bis(pyrazolyl)pyrimidine, as a specific *N*,*N*-bidentate bridging ligands (L) (Scheme 2.1).

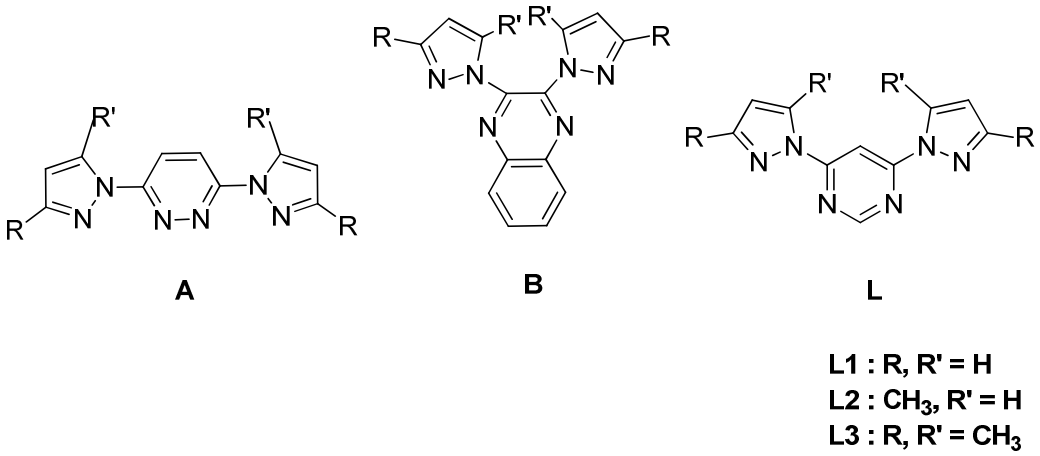

Scheme 2.1

2.2 Experimental

2.2.1 Preparation of ligands (L1 to L3)

2.2.1.1 4,6-bis(pyrazolyl)pyrimidine (L1)[36]

A solution of pyrazole (1.20 g, 17.6 mmol) in 50 ml of THF was added a suspension of NaH (550 mg, 22.0 mmol) under a nitrogen atmosphere at 0°C and the mixture was stirred until evolution of hydrogen gas ceased (30 - 45 minutes). The solution of 4,6-dichloropyrimidine (1.30 g, 8.50 mmol) in 10 ml of THF was added to the above solution and the whole was stirred at room temperature (25 ^{0}C) overnight. The solvent was evaporated off; the residue was diluted with water and extracted with dichloromethane. The extract was dried (Na_2SO_4) and concentrated. The residue was chromatographed on silica gel ($CHCl_3$ – MeOH). The first elute gave a pure color less compound.

Yield: 1.38 g, 75%; Elemental Anal (%) Calc. for $C_{10}H_8N_6$: C 56.60; H 3.80; N 39.60; found: C 56.43; H 3.88; N 39.32; ^{1}H NMR (400 MHz, $CDCl_3$): δ = 8.71 (s, 1H), 8.45 (d,

2H, ^{3}J = 2.4 Hz), 8.29 (s, 1H), 6.67 (d, 2H, ^{3}J = 2.4 Hz), 6.39 (dd, 2H); ESI-MS (m/z): 241.11 $[M+H]^+$; IR (KBr, cm^{-1}): 2924m, 1597s, 1464m, 1382m, 1211m, 1044s, 777s.

2.2.1.2 4,6-bis(3-methy-1-pyrazolyl)pyrimidine (L2)[37]

To a solution of 3-methylpyrazole (1.20 g, 14.7 mmol) in 50 ml of THF was added fine pieces of potassium (0.600 g, 15.3 mmol), the mixture was refluxed at 50°C until the potassium was completely dissolved. Then 4,6-dichloropyrimidine (1.094 g, 7.35 mmol) was added to the reaction mixture(pale-brown solution), which was refluxed for 5 h. Then 80 ml of water was added and the solution refrigerated overnight. The colorless solid was filtered and washed with water (2 X 10 ml) and dried under P_2O_5. The pure compound was obtained after recrystallization from chloroform/hexane.

Yield: 0.72 g, 57.8%; Elemental Anal (%) Calc. for $C_{12}H_{12}N_6$: C 59.99; H 5.03; N 34.98; found: C 59.63; H 5.18; N 34.72; ^{1}H NMR (400 MHz, $CDCl_3$): δ = 8.71 (s, 1H), 8.45 (d, 2H, ^{3}J = 2.4 Hz), 8.29 (s, 1H), 6.29 (d, 2H, ^{3}J = 2.4 Hz), 2.39 (s, 6H, CH_3); ESI-MS (m/z): 241.11 $[M+H]^+$; IR (KBr, cm^{-1}): 2924m, 1597s, 1464m, 1382m, 1211m, 1044s, 777s.

2.2.1.2 4,6-bis(3,5-dimethyl-pyrazolyl)pyrimidine (L3)[37]

The L3 ligand was synthesized in a similar manner using 3,5-dimethylpyrazole (1.50 g, 15.6 mmol), potassium (0.60 g, 15.0 mmol) and 4,6-dichloropyrimidine (1.10 g, 7.35 mmol). However, after refluxing the THF solution for 5 hours, the mixture was evaporated to dryness. The product was extracted three times with 30 ml of toluene. The solvent was removed, and the white solid obtained was dissolved in dichloromethane layering the resulting solution with hexane led to the precipitation of traces of pyrazole. L3 was obtained after filtration and evaporation to dryness of the resulting solution. The solid was recrystallized from chloroform/hexane.

Yield: 1.5 g, 55%; Elemental Anal (%) Calc. for $C_{14}H_{16}N_6$: C 62.67; H 6.01; N 31.32; found: C 62.68; H 6.05; N 31.28; ^{1}H NMR (400 MHz, $CDCl_3$): δ = 8.74 (s, 1H), 8.37 (s, 1H), 6.01 (s, 2H,), 2.67 (s, 6H, CH_3), 2.29 (s, 6H, CH_3); ESI-MS (m/z): 269.14 $[M+H]^+$); IR (KBr, cm^{-1}): 3446w, 2925m, 1593s, 1484s, 1385m, 1266m, 1019s, 771m.

2.2.2 General procedure for the preparation of the mononuclear complexes **1 - 6**

A mixture of $[(\eta^6\text{-}C_6H_6)Ru(\mu\text{-}Cl)Cl]_2$ (arene = C_6H_6 and *p*-^{i}PrC_6H_4Me) (0.07 mmol), ligand L (L1, L2 or L3) (0.15 mmol) and 2.5 equivalents of NH_4PF_6 in dry methanol (15 ml) was stirred at room temperature for 8 hours resulting in the precipitation of a dark

yellow solid. The precipitate was separated by filtration, washed with cold methanol, diethyl ether and dried *in vacuo*.

2.2.2.1 [(η^6-C_6H_6)Ru(L1)Cl]PF_6 ([**1**]PF_6)

Yield: 66 mg, 82.5%; Elemental Anal (%) Calc. for $C_{16}H_{14}N_6RuClPF_6$ (571.97): C 33.61; H 2.47; N 14.70; found: C 33.73; H 2.65; N 13.98; ^{1}H NMR (400 MHz, $CDCl_3$): δ = 9.56 (d, 1H, ^3J = 2.4 Hz), 8.75 (d, 1H, ^3J = 2.4 Hz), 8.66 (d, 1H, ^3J = 7.6 Hz), 8.63 (d, 1H, ^3J = 7.6 Hz), 8.29 (s, 1H), 8.02 (s, 1H), 6.96 (dd, 1H, ^3J = 2.0 Hz), 6.67 (dd, 1H, ^3J = 1.6 Hz), 6.07 (s, 6H, C_6H_6); ESI-MS (m/z): 427.2 $[M\text{-}PF_6]^+$, 392.1 $[M\text{-}PF_6\text{-}Cl]^+$, 314.1 $[M\text{-}PF_6\text{-}Cl\text{-}C_6H_6]^+$; IR (KBr, cm^{-1}): 844s $\nu_{(P\text{-}F)}$, 1522m, 1558m, 1608s ($\nu_{C=N}$ L1), 2925m, 3446w; UV–Vis {acetonitrile, λ_{max} nm ($\varepsilon 10^{-5} M^{-1}$ cm^{-1})}: 246(0.16), 324(0.17), 381(0.25), 464(0.04).

*2.2.2.2 [(η^6-C_6H_6)Ru(L2)Cl]PF_6 ([**2**]PF_6)*

Yield: 62 mg, 74.6%; Elemental Anal (%) Calc. for $C_{18}H_{18}N_6RuClPF_6$ (599.86): C 39.91; H 3.35; N 15.51; found: C 40.22; H 3.08; N 14.92; ^{1}H NMR (400 MHz, CD_3CN, 25°C, TMS): δ = 9.15 (s, 1H), 8.54 (d, 1H, ^3J = 8.4 Hz), 8.09 (s, 1H), 7.50 (d, 1H, ^3J = 4.6 Hz), 7.21 (d, 1H, ^3J = 4.6 Hz), 6.92 (d, 1H, ^3J = 2.8 Hz), 6.24 (s, 6H, C_6H_6), 2.83 (s, 3H, CH_3), 2.76 (s, 3H, CH_3); ESI-MS (m/z): 455.2 $[M\text{-}PF_6]^+$, 419.2 $[M\text{-}PF_6\text{-}Cl]^+$, 341.1 $[M\text{-}PF_6\text{-}Cl\text{-}C_6H_6]^+$; IR (KBr, cm^{-1}): 845s $\nu_{(P\text{-}F)}$, 1592m, 1558m, 1522m ($\nu_{C=N}$ L2), 2925m, 3434w; UV–Vis {acetonitrile, λ_{max} nm ($\varepsilon 10^{-5} M^{-1}$ cm^{-1})}: 319(0.23), 345(0.18), 456(0.04).

*2.2.2.3 [(η^6-C_6H_6)Ru(L3)Cl]PF_6 ([**3**]PF_6)*

Yield: 65 mg, 86.3%; Elemental Anal (%) Calc. for $C_{20}H_{22}N_6RuClPF_6$ (628.03): C 42.16; H 3.89; N 14.75; found: C 41.90; H 4.05; N 14.33; ^{1}H NMR (400 MHz, CD_3CN): δ = 9.44 (s, 1H), 8.17 (s, 1H), 7.39 (s, 1H), 6.53 (s, 1H), 6.10 (s, 6H, C_6H_6), 2.82 (s, 3H, CH_3), 2.76 (s, 3H, CH_3), 2.75 (s, 3H, CH_3), 2.29 (s, 3H, CH_3); ESI-MS (m/z): 483.3 $[M\text{-}PF_6]^+$, 448.2 $[M\text{-}PF_6\text{-}Cl]^+$, 413.3 $[M\text{-}PF_6\text{-}Cl\text{-}C_6H_6]^+$; IR (KBr, cm^{-1}): 845s $\nu_{(P\text{-}F)}$, 1601m, 1560m, 1525m ($\nu_{C=N}$ L3), 2925m, 3482w; UV–Vis {acetonitrile, λ_{max} nm ($\varepsilon 10^{-5} M^{-1}$ cm^{-1})}: 273(0.15), 309(0.15), 354(0.25), 452(0.06).

*2.2.2.4 [(η^6-p-^{i}PrC$_6$H$_4$Me)Ru(L1)Cl]PF_6 ([**4**]PF_6)*

Yield: 65 mg, 75.5%; Elemental Anal (%) Calc. for $C_{20}H_{22}N_6RuClPF_6$ (628.03): C 38.26; H 3.53; N 13.38; found: C 37.92; H 3.77; N 12.95; ^{1}H NMR (400 MHz, $CDCl_3$): δ = 9.48

(d, 1H, ^3J = 2.4 Hz), 8.77 (d, 1H, ^3J = 2.4 Hz, 1H), 8.67 (d, 1H, ^3J = 4.6 Hz), 8.61 (d, 1H, ^3J = 6.4 Hz), 8.29 (s, 1H), 7.97 (s, 1H), 6.96 (dd, 1H, ^3J = 2.0 Hz), 6.69 (dd, 1H, ^3J = 2.0 Hz), 6.04 (d, 1H, $^3J_{H,H}$ = 6.4 Hz, $Ar_{p\text{-}cy}$), 6.07 (d, 1H, ^3J = 6.4 Hz, $Ar_{p\text{-}cy}$), 5.99 (d, 1H, ^3J = 6.0 Hz, $Ar_{p\text{-}cy}$), 5.86 (d, 1H, ^3J = 6.0 Hz, $Ar_{p\text{-}cy}$), 2.74 (sept, 1H, ^3J = 6.2 Hz, $CH(CH_3)_2$), 2.18 (s, 3H, $Ar_{p\text{-}cy}$-Me), 1.14 (d, 3H, ^3J = 6.4 Hz, $CH(CH_3)_2$), 1.10 (d, 3H, ^3J = 7.6 Hz, $CH(CH_3)_2$); ESI-MS (m/z): 483.2 $[M\text{-}PF_6]^+$, 447.2 $[M\text{-}PF_6\text{-}Cl]^+$, 312.1 $[M\text{-}PF_6\text{-}Cl\text{-}p\text{-}{}^iPrC_6H_4Me]^+$; IR (KBr, cm^{-1}) 844s $\nu_{(P\text{-}F)}$, 1605m, 1557m, 1523m ($\nu_{C=N}$ L1), 3058m, 3489w; UV–Vis {acetonitrile, λ_{max} nm ($\varepsilon 10^{-5} M^{-1}\ cm^{-1}$)}: 286(0.65), 333(0.21), 436(0.02).

*2.2.2.5 [(η^6-p-^{i}PrC$_6$H$_4$Me)Ru(L2)Cl]PF$_6$ ([**5**]PF$_6$)*

Yield: 68 mg, 73.4%; Elemental Anal (%) Calc. for $C_{22}H_{26}N_6RuClPF_6$ (651.06): C 43.28; H 4.29; N 13.77; found: C 43.78; H 3.94; N 13.92; ^{1}H NMR (400 MHz, $CDCl_3$): δ = 9.25 (s, 1H), 8.48 (d, 1H, ^3J = 2.4 Hz), 7.89 (s, 1H), 7.78 (d, 1H, ^3J = 2.8 Hz), 6.70 (d, 1H, ^3J = 9.6 Hz), 6.39 (d, 1H, ^3J = 2.8 Hz), 5.98 (d, 2H, ^3J = 6.0 Hz, $Ar_{p\text{-}cy}$), 5.90 (d, 1H, ^3J = 6.0 Hz, $Ar_{p\text{-}cy}$), 5.86 (d, 1H, ^3J = 6.0 Hz, $Ar_{p\text{-}cy}$), 2.81 (s, 3H, CH_3), 2.75 (sept, 1H, $CH(CH_3)_2$), 2.38 (s, 3H, CH_3), 2.18 (s, 3H, $Ar_{p\text{-}cy}$-Me), 1.42 (d, 3H, ^3J = 3.2 Hz, $CH(CH_3)_2$), 1.17 (d, 3H, ^3J = 3.2 Hz, $CH(CH_3)_2$); ESI-MS (m/z): 513.2 $[M\text{-}PF_6]^+$, 478.6 $[M\text{-}PF_6\text{-}Cl]^+$, 344.2 $[M\text{-}PF_6\text{-}Cl\text{-}p\text{-}{}^iPrC_6H_4Me]^+$; IR (KBr, cm^{-1}): 843s $\nu_{(P\text{-}F)}$, 1606m, 1560m, 1524m ($\nu_{C=N}$ L2), 2995m, 3447w; UV–Vis {acetonitrile, λ_{max} nm ($\varepsilon 10^{-5} M^{-1}\ cm^{-1}$)}: 294(0.36), 349(0.82), 470(0.02).

*2.2.2.6 [(η^6-p-^{i}PrC$_6$H$_4$Me)Ru(L3)Cl]PF$_6$ ([**6**]PF$_6$)*

Yield: 77 mg, 82.7%; Elemental Anal (%) Calc. for $C_{24}H_{30}N_6RuClPF_6$ (684.09): C 46.06; H 4.83; N 13.43; found: C 46.73; H 4.25; N 13.07; ^{1}H NMR (400 MHz, $CDCl_3$): δ = 9.44 (s, 1H), 8.11 (s, 1H), 7.32 (s, 1H), 7.05 (s, 1H), 5.96 (d, 1H, ^3J = 4.0 Hz, $Ar_{p\text{-}cy}$), 5.92 (d, 1H, ^3J = 3.2 Hz, $Ar_{p\text{-}cy}$), 5.84 (d, 1H, ^3J = 6.4 Hz, $Ar_{p\text{-}cy}$), 5.77 (d, 1H, ^3J = 6.4 Hz, $Ar_{p\text{-}cy}$), 2.81 (s, 3H, CH_3), 2.79 (s, 3H, CH_3), 2.81 (s, 3H, CH_3), 2.78 (s, 3H, CH_3), 2.49 (sept, 1H, $CH(CH_3)_2$), 2.17 (s, 3H, $Ar_{p\text{-}cy}$-Me), 1.09 (d, 3H, ^3J = 3.2 Hz, $CH(CH_3)_2$), 1.06 (d, 3H, ^3J = 3.2 Hz, $CH(CH_3)_2$); ESI-MS (m/z): 538.8 $[M\text{-}PF_6]^+$, 503.5 $[M\text{-}PF_6\text{-}Cl]^+$, 369.2 $[M\text{-}PF_6\text{-}Cl\text{-}p\text{-}{}^iPrC_6H_4Me]^+$; IR (KBr, cm^{-1}): 843s $\nu_{(P\text{-}F)}$, 1608m, 1560m, 1527m ($\nu_{C=N}$ L3), 3050m, 3447w; UV–Vis {acetonitrile, λ_{max} nm ($\varepsilon 10^{-5} M^{-1}\ cm^{-1}$)}: 287(0.38), 346(0.74), 477(0.08).

2.2.3 General procedure for the preparation of the mononuclear complexes **7** –**12**

A mixture of $[(\eta^5\text{-}C_5Me_5)M(\mu\text{-}Cl)Cl]_2$ (M= Rh and Ir) (0.08 mmol), ligand L (L1, L2 and L3) (0.17 mmol) and 2.5 equivalents of NH_4PF_6 in dry methanol (20 ml) was refluxed at 50^{o}C temperature for 4 to 6 hours, resulting yellow color precipitation. The precipitate was separated by filtration, washed with cold methanol, diethyl ether and dried *in vacuo*.

2.2.3.1 [(Cp)Rh(L1)Cl]PF_6 ([**7**]PF_6)*

Yield: 73 mg, 77.8%; Elemental Anal (%) Calc. for $C_{20}H_{23}N_6RhClPF_6$ (630.04): C 38.08; H 3.68; N 13.98; found: C 38.13; H 3.75; N 13.91; ^{1}H NMR (400MHz, CD_3CN): δ = 9.01 (s, 1H), 8.84 (d, 1H, ^3J = 3.2 Hz), 8.66 (d, 1H, ^3J = 2.4 Hz), 8.33 (d, 1H, ^3J = 1.6 Hz), 8.31 (d, 1H, ^3J = 1.6 Hz), 7.98 (s, 1H), 7.02 (dd, 1H, ^3J = 1.6 Hz), 6.71 (dd, 1H, ^3J = 1.6 Hz), 1.75 (s, 15H, C_5Me_5); ESI-MS (m/z): 485.2 $[M\text{- }PF_6]^+$, 450.6 $[M\text{-}PF_6\text{-}Cl]^+$, 315.2 [M-$PF_6$-Cl-Cp*]; IR (KBr, cm^{-1}): 844s $\nu_{(P\text{-}F)}$, 1606m, 1560m, 1524m ($\nu_{C=N}$ L1), 2999m, 3448w; UV–Vis {acetonitrile, λ_{max} nm ($\varepsilon 10^{-5} M^{-1}$ cm^{-1})}: 268(0.78), 286(0.76), 357(0. 4), 444(0.09).

2.2.3.2 [(Cp)Rh(L2)Cl]PF_6 ([**8**]PF_6)*

Yield: 65 mg, 62.5%; Elemental Anal (%) Calc. for $C_{22}H_{27}N_6RhClPF_6$ (658.07): C 35.32; H 3.64; N 11.23; found: C 35.26; H 3.69; N 11.21; ^{1}H NMR (400 MHz, CD_3CN): δ = 8.78 (s, 1H), 8.43 (d, 1H, ^3J = 6.4 Hz), 8.09 (s, 1H), 6.76 (d, 1H, ^3J = 4.6 Hz), 6.40 (d, 1H, ^3J = 4.6 Hz), 6.32 (d, 1H, ^3J = 2.8 Hz), 2.70 (s, 3H, CH_3), 2.43 (s, 3H, CH_3), 1.77 (s, 15H, C_5Me_5); ESI-MS (m/z): 513.8 $[M\text{- }PF_6]^+$, 478.12 $[M\text{-}PF_6\text{-}Cl]^+$, 343.2 [M-$PF_6$-Cl-Cp*]; IR (KBr, cm^{-1}): 845s $\nu_{(P\text{-}F)}$, 1598m, 1559m, 1521m ($\nu_{C=N}$ L2), 2995m, 3447w; UV–Vis {acetonitrile, λ_{max} nm ($\varepsilon 10^{-5} M^{-1}$ cm^{-1})}: 266(0.54), 301(0.45), 343(0.57), 452(0.07).

2.2.3.3 [(Cp)Rh(L3)Cl]PF_6 ([**9**]PF_6)*

Yield: 78 mg, 72%; Elemental Anal (%) Calc. for $C_{24}H_{31}N_6RhClPF_6$ (686.87): C 41.97; H 4.55; N 12.24; found: C 41.86; H 4.65; N 12.18; ^{1}H NMR (400 MHz, CD_3CN): δ = 9.05 (s, 1H), 8.67 (s, 1H), 7.40 (s, 1H), 6.66 (s, 1H), 2.82 (s, 3H, CH_3), 2.76 (s, 3H, CH_3), 2.75 (s, 3H, CH_3), 2.29 (s, 3H, CH_3), 2.01 (s, 15H, C_5Me_5); ESI-MS (m/z): 541.81 $[M\text{- }PF_6]^+$, 506.6 $[M\text{-}PF_6\text{-}Cl]^+$, 371.2 [M-$PF_6$-Cl-Cp*]; IR (KBr, cm^{-1}): 843s $\nu_{(P\text{-}F)}$, 1601m, 1557m, 1524m ($\nu_{C=N}$ L3), 3050m, 3434w; UV–Vis {acetonitrile, λ_{max} nm ($\varepsilon 10^{-5} M^{-1}$ cm^{-1})}: 261(0.09), 314(0.61), 441(0.05).

2.2.3.3 [(Cp)Ir(L1)Cl]PF_6 ([**10**]PF_6)*

Yield: 66 mg, 58.4%; Elemental Anal (%) Calc. for $C_{20}H_{23}N_6IrClPF_6$ (720.09): C 33.61; H 2.47; N 14.70; found: C 33.73; H 2.65; N 13.98; ^{1}H NMR (400 MHz, CD_3CN): δ = 8.99 (s, 1H), 8.84 (d, 1H, ^3J = 3.2 Hz), 8.66 (d, 1H, ^3J = 2.4 Hz), 8.39 (d, 1H, $^3J_{H,H}$ = 1.6 Hz), 8.32 (d, 1H, $^3J_{H,H}$ = 1.6 Hz), 7.98 (s, 1H), 7.01 (dd, 1H, $^3J_{H,H}$ = 1.6 Hz), 6.70 (dd, 1H, $^3J_{H,H}$ = 2.0 Hz), 2.01 (s, 15H, C_5Me_5); ESI-MS (m/z): 575.2 [M- PF_6]$^+$, 535.6 [M-PF_6-Cl]$^+$, 400.2 [M-PF_6-Cl-Cp*]; IR (KBr, cm^{-1}): 845s $\nu_{(P-F)}$, 1592m, 1558m, 1522m ($\nu_{C=N}$ L1) 2924m, 3439w; UV–Vis {acetonitrile, λ_{max} nm ($\varepsilon 10^{-5}M^{-1}$ cm^{-1})}: 279(0.53), 340(0.89), 402(0.20).

2.2.3.4 [(Cp)Ir(L2)Cl]PF_6 ([**11**]PF_6)*

Yield: 70 mg, 57.8%; Elemental Anal (%) Calc. for $C_{22}H_{27}N_6IrClPF_6$ (748.13): C 35.32; H 3.64; N 11.23; found: C 35.25; H 3.68; N 11.22; ^{1}H NMR (400 MHz, CD_3CN): δ = 8.78 (s, 1H), 8.43 (d, 1H, ^3J = 6.4 Hz), 8.09 (s, 1H), 6.76 (d, 1H, ^3J = 4.6 Hz), 6.40 (d, 1H, ^3J = 4.6 Hz), 6.32 (d, 1H, ^3J = 2.8 Hz), 2.70 (s, 3H, CH_3), 2.43 (s, 3H, CH_3), 1.77 (s, 15H, C_5Me_5); ESI-MS (m/z): 603.1 [M- PF_6]$^+$, 568.2 [M-PF_6-Cl]$^+$, 433.2 [M-PF_6-Cl-Cp*]; IR (KBr, cm^{-1}): 845s $\nu_{(P-F)}$, 1598m, 1559m, 1521m ($\nu_{C=N}$ L2), 2995m, 3446w; UV–Vis {acetonitrile, λ_{max} nm ($\varepsilon 10^{-5}M^{-1}$ cm^{-1})}: 267(0.54), 298(0.82), 429(0.08)

2.2.5.6 [(Cp)Ir(L3)Cl]PF_6 ([**12**]PF_6)*

Yield: 78 mg, 64.4%; Elemental Anal (%) Calc. for $C_{24}H_{31}N_6IrClPF_6$ (776.96): C 37.14; H 4.03; N 10.83; found: C 37.06; H 4.05; N 10.33; ^{1}H NMR (400 MHz, CD_3CN): δ = 8.90 (s, 1H), 8.21 (s, 1H), 6.67 (s, 1H), 6.20 (s, 1H), 2.83 (s, 3H, CH_3), 2.76 (s, 3H, CH_3), 2.64 (s, 3H, CH_3), 2.30 (s, 3H, CH_3), 2.15 (s, 15H, C_5Me_5); ESI-MS (m/z): 631.2 [M-PF_6]$^+$, 596.6 [M-PF_6-Cl]$^+$, 461.2 [M-PF_6-Cl-Cp*]; IR (KBr, cm^{-1}): 843s $\nu_{(P-F)}$, 1606m, 1560m, 1524m ($\nu_{C=N}$ L2), 3050m, 3446w; UV–Vis {acetonitrile, λ_{max} nm ($\varepsilon 10^{-5}M^{-1}$ cm^{-1})}: 268(0.50), 301(0.41), 361(0.51) and 464(0.04).

2.2.4 General procedure for the preparation of the dinuclear complexes 13–18

A mixture of [(η^6-arene)Ru(μ-Cl)Cl]$_2$ (arene = C_6H_6 and η^6-*p*-^{i}PrC_6H_4Me) (0.1 mmol), ligand L (L1, L2 and L3) (0.1 mmol) and 2.5 equivalents of NH_4PF_6 in dry methanol (15 ml) was stirred at room temperature for 14 hours resulting orange color precipitation. The precipitate was filtered, washed with cold methanol, diethyl ether and dried *in vacuo*.

*2.2.4.1 [{(η^6-C_6H_6)RuCl}$_2$(L1)](PF$_6$)$_2$ ([**13**](PF$_6$)$_2$)*

Yield: 72 mg, 77.4%; Elemental Anal (%) Calc. for $C_{22}H_{20}N_6Ru_2Cl_2P_2F_{12}$ (931.41): C 28.37; H 2.16; N 9.02; found: C 38.21; H 2.45; N 8.98; ^{1}H NMR (400 MHz, CD_3CN): δ = 9.68 (d, 2H, ^3J = 2.8 Hz), 8.79 (s, 1H), 8.71 (d, 2H, ^3J = 7.2 Hz), 8.32 (s, 1H), 7.01 (dd, 2H, ^3J = 2.0 Hz), 6.15 (s, 12H, C_6H_6);. ESI-MS (m/z): 786.1 $[M^{2+}+PF_6^-]^+$, 427.2 $[M-PF_6]^+$; IR (KBr, cm^{-1}): 845s $\nu_{(P-F)}$, 1598m, 1559m, 1521m ($\nu_{C=N}$ L1), 2995m, 3447w; UV–Vis {acetonitrile, λ_{max} nm ($\varepsilon 10^{-5}$M^{-1} cm^{-1})}: 259(0.21), 318(0.23), 380(0.08).

*2.2.4.2 [{(η^6-C_6H_6)RuCl}$_2$(L2)](PF$_6$)$_2$ ([**14**](PF$_6$)$_2$)*

Yield: 71 mg, 74.7%; Elemental Anal (%) Calc. for $C_{24}H_{24}N_6Ru_2Cl_2P_2F_{12}$ (959.46): C 30.04; H 2.52; N 8.76; found: C 29.95; H 2.58; N 8.61; ^{1}H NMR (400 MHz, CD_3CN): δ = 9.46 (s, 1H), 8.58 (d, 2H, ^3J = 8.4 Hz), 8.15 (s, 1H), 7.25 (d, 2H, ^3J = 4.6 Hz), 6.24 (s, 12H, C_6H_6), 2.83 (s, 3H,CH_3), 2.81 (s, 3H, CH_3); ESI-MS (m/z):814.2 $[M^{2+}+PF_6^-]^+$, 455.2 $[M-PF_6]^+$; IR (KBr, cm^{-1}): 843s $\nu_{(P-F)}$, 1601m, 1557m, 1524m ($\nu_{C=N}$ L2), 3010m, 3449w; UV–Vis {acetonitrile, λ_{max} nm ($\varepsilon 10^{-5}$M^{-1} cm^{-1})}: 262(0.29), 310(0.75), 374(0.12).

*2.2.4.3 [{(η^6-C_6H_6)RuCl}$_2$(L3)](PF$_6$)$_2$ ([**15**](PF$_6$)$_2$)*

Yield: 81 mg, 82.6 %; Elemental Anal (%) Calc. for $C_{24}H_{28}N_6Ru_2Cl_2P_2F_{12}$ (987.52): C 31.62; H 2.86; N 8.51; found: C 31.50; H 2.95; N 8.33; ^{1}H NMR (400 MHz, CD_3CN): δ = 10.02 (s, 1H), 7.68 (s, 1H), 6.72 (s, 2H), 6.21 (s, 12H, C_6H_6), 2.81 (s, 6H, CH_3), 2.69 (s, 6H, CH_3); ESI-MS (m/z): 842.4 $[M^{2+}+PF_6^-]^+$, 483.3 $[M- PF_6]^+$; IR (KBr, cm^{-1}): 843s $\nu_{(P-F)}$, 1606m, 1560m, 1524m ($\nu_{C=N}$ L3), 3050m, 3451w; UV–Vis {acetonitrile, λ_{max} nm ($\varepsilon 10^{-5}$M^{-1} cm^{-1})}: 271(0.18), 315(0.81), 380(0.11).

*2.2.4.4 [{(η^6-p-^{i}PrC$_6$H$_4$Me)RuCl}$_2$(L1)](PF$_6$)$_2$ ([**16**](PF$_6$)$_2$)*

Yield: 87 mg, 83.6%; Elemental Anal (%) Calc. for $C_{30}H_{36}N_6Ru_2Cl_2P_2F_{12}$ (1043.62): C 34.53; H 3.48; N 8.05; found: C 34.42; H 3.47; N 7.96; ^{1}H NMR (400 MHz, $CDCl_3$): δ = 9.65 (d, 2H, ^3J = 2.4 Hz), 8.71 (d, 2H, ^3J = 4.6 Hz), 8.68 (s, 1H), 7.28 (s, 1H), 7.06 (dd, 2H, ^3J = 2.4 Hz), 6.08 (d, 2H, ^3J = 6.4 Hz, Ar_{p-cy}), 6.06 (d, 2H, ^3J = 6.4 Hz, Ar_{p-cy}), 5.99 (d, 2H, ^3J = 6.0 Hz, Ar_{p-cy}), 5.93 (d, 2H, ^3J = 6.0 Hz, Ar_{p-cy}), 2.74 -2.69 (sept, 2H, ^3J = 6.2 Hz, $CH(CH_3)_2$), 2.18 (s, 6H, Ar_{p-cy}-Me), 1.14 (d, 6H, ^3J = 6.8 Hz, $CH(CH_3)_2$), 1.04 (d, 6H, ^3J = 7.6 Hz, $CH(CH_3)_2$); ESI-MS (m/z): 898.2 $[M^{2+}+PF_6^-]^+$, 483.3 $[M- PF_6]^+$; IR (KBr, cm^{-1}): 844s $\nu_{(P-F)}$, 1599m, 1560m, 1525m ($\nu_{C=N}$ L1), 2995m, 3447w; UV–Vis {acetonitrile, λ_{max} nm ($\varepsilon 10^{-5}$M^{-1} cm^{-1})}: 260(0.29), 310(0.58), 378(0.13).

*2.2.4.5 [{(η^6-p-^{i}PrC$_6$H$_4$Me)RuCl}$_2$(L2)](PF$_6$)$_2$ ([**17**](PF$_6$)$_2$)*

Yield: 77 mg, 71.9%; Elemental Anal (%) Calc. for $C_{32}H_{40}N_6Ru_2Cl_2P_2F_{12}$ (1071.67): C 35.86; H 3.76; N 7.84; found: C 43.78; H 3.94; N 13.92; ^{1}H NMR (400 MHz, $CDCl_3$): δ = 9.38 (s, 1H), 8.51 (d, 2H, ^3J = 2.8 Hz), 7.89 (s, 1H), 6.75 (d, 2H, ^3J = 9.6 Hz), 6.01 (d, 2H, ^3J = 6.0 Hz, $Ar_{p\text{-}cy}$), 5.99 (d, 2H, ^3J = 6.04 Hz, $Ar_{p\text{-}cy}$), 5.96 (d, 2H, ^3J = 6.0 Hz, $Ar_{p\text{-}cy}$), 5.96 (d, 2H, ^3J = 6.04 Hz, $Ar_{p\text{-}cy}$), 2.81 (s, 6H, CH_3), 2.75 (sept, 2H, $CH(CH_3)_2$), 2.26 (s, 6H, $Ar_{p\text{-}cy}$-Me), 1.19 (d, 6H, ^3J = 3.2 Hz, $CH(CH_3)_2$), 1.17 (d, 6H, ^3J = 3.2 Hz, $CH(CH_3)_2$); ESI-MS (m/z): 926.2 $[M^{2+}+PF_6^-]^+$, 513.2 $[M\text{-}PF_6]^+$; IR (KBr, cm^{-1}): 843s $\nu_{(P\text{-}F)}$, 1601m, 1557m, 1524m ($\nu_{C=N}$ L2), 3011m, 3451w; UV–Vis {acetonitrile, λ_{max} nm ($\varepsilon 10^{-5}M^{-1}$ cm^{-1})}: 271(0.18), 315(0.81), 380(0.11).

*2.2.4.6 [{(η^6-p-^{i}PrC$_6$H$_4$Me)RuCl}$_2$(L3)](PF$_6$)$_2$ ([**18**](PF$_6$)$_2$)*

Yield: 90 mg, 82.5%; Elemental Anal (%) Calc. for $C_{34}H_{44}N_6Ru_2Cl_2P_2F_{12}$ (1099.73): C 37.13; H 4.03; N 7.64; found: C 37.05; H 4.07; N 7.64; ^{1}H NMR (400 MHz, $CDCl_3$): δ = 9.91 (s, 1H), 7.67 (s, 1H), 6.68 (s, 2H), 6.11 (d, 2H, ^3J = 6.4 Hz, $Ar_{p\text{-}cy}$), 6.08 (d, 2H, ^3J = 6.2 Hz, $Ar_{p\text{-}cy}$), 5.95 (d, 2H, ^3J = 6.0 Hz, $Ar_{p\text{-}cy}$), 5.89 (d, 2H, ^3J = 6.4 Hz, $Ar_{p\text{-}cy}$), 2.80 (s, 6H, CH_3), 2.76 (s, 6H, CH_3), 2.66 (sept, 2H, $CH(CH_3)_2$), 2.28 (s, 6H, $Ar_{p\text{-}cy}$-Me), 1.09 (d, 6H, ^3J = 3.2 Hz, $CH(CH_3)_2$), 1.06 (d, 6H, ^3J = 3.2 Hz, $CH(CH_3)_2$); ESI-MS (m/z): 954.73 $[M^{2+}+PF_6^-]^+$, 538.8 $[M\text{-}PF_6]^+$; IR (KBr, cm^{-1}): 843s $\nu_{(P\text{-}F)}$, 1608m, 1562m, 1524m ($\nu_{C=N}$ L3), 3041m, 3447w; UV–Vis {acetonitrile, λ_{max} nm ($\varepsilon 10^{-5}M^{-1}$ cm^{-1})}: 263(0.29), 310(0.75), 376(0.12).

2.2.5 General procedure for the preparation of the dinuclear complexes **19** – **24**

A mixture of [(Cp*)M(μ-Cl)Cl]$_2$ (M = Rh and Ir) (0.08 mmol), ligand L (L1, L2 and L3) (0.08 mmol) and 2.5 equivalents of NH_4PF_6 in dry methanol (20 ml) was refluxed at 50^{o}C for 12 hours, resulting a orange color precipitation. The precipitate was separated by filtration, washed with cold methanol, diethyl ether and dried *in vacuo*.

2.2.5.1 [{(Cp)RhCl}$_2$(L1)](PF$_6$)$_2$ ([**19**](PF$_6$)$_2$)*

Yield: 66 mg, 79.5%; Elemental Anal (%) Calc. for $C_{30}H_{38}N_6Rh_2Cl_2P_2F_{12}$ (1049.31): C 34.34; H 3.65; N 8.01; found: C 34.23; H 3.75; N 7.91; ^{1}H NMR (400 MHz, CD_3CN): δ = 9.18 (s, 1H), 8.84 (d, 2H, ^3J = 3.2 Hz), 8.36 (d, 2H, ^3J = 1.6 Hz), 8.01 (s, 1H), 6.92 (dd, 2H, ^3J = 1.6 Hz), 1.81 (s, 30H, C_5Me_5); ESI-MS (m/z): 904.3 $[M^{2+}+PF_6^-]^+$, 485.2 [M-

$PF_6]^+$; IR (KBr, cm^{-1}): 845s $\nu_{(P-F)}$, 1592m, 1558m, 1522m ($\nu_{C=N}$ L1), 2995m, 3447w; UV–Vis {acetonitrile, λ_{max} nm ($\varepsilon 10^{-5} M^{-1}$ cm^{-1})}: 271(0.18), 315(0.81), 380(0.11).

2.2.5.2 [{(Cp)RhCl}$_2$(L2)](PF$_6$)$_2$ ([**20**](PF$_6$)$_2$)*

Yield: 60 mg, 70.5%; Elemental Anal (%) Calc. for $C_{32}H_{42}N_6Rh_2Cl_2P_2F_{12}$ (1077.36): C 35.67; H 3.93; N 7.80; found: C 35.26; H 3.99; N 7.61; ^{1}H NMR (400 MHz, CD_3CN): δ = 9.05 (s, 1H), 8.46 (d, 2H, ^3J = 6.0 Hz), 8.12 (s, 1H), 6.79 (d, 2H, ^3J = 4.6 Hz), 2.76 (s, 3H, CH_3), 2.73 (s, 3H, CH_3), 1.77 (s, 30H, C_5Me_5); ESI-MS (m/z):513.8 [M- PF_6], 932.1 $[M^{2+}+PF_6^-]^+$, 513.8 [M- $PF_6]^+$; IR (KBr, cm^{-1}): 845s $\nu_{(P-F)}$, 1598m, 1559m, 1521m ($\nu_{C=N}$ L2), 2998m, 3449w; UV–Vis {acetonitrile, λ_{max} nm ($\varepsilon 10^{-5} M^{-1}$ cm^{-1})}: 259(0.11), 315(0.51), 380(0.08).

2.2.5.3 [{(Cp)RhCl}$_2$(L3)](PF$_6$)$_2$ ([**21**](PF$_6$)$_2$)*

Yield: 67 mg, 77.1%; Elemental Anal (%) Calc. for $C_{34}H_{46}N_6Rh_2Cl_2P_2F_{12}$ (1105.41): C 36.94; H 4.19; N 7.60; found: C 36.86; H 4.15; N 7.58; ^{1}H NMR (400 MHz, CD_3CN): δ = 9.09 (s, 1H), 7.36 (s, 1H), 6.79 (s, 2H), 2.84 (s, 6H, CH_3), 2.79 (s, 6H, CH_3), 1.88 (s, 30H, C_5Me_5); ESI-MS (m/z): 960.2 $[M^{2+}+PF_6^-]^+$, 541.81 [M- $PF_6]^+$; IR (KBr, cm^{-1}): 843s $\nu_{(P-F)}$, 1601m, 1557m, 1524m ($\nu_{C=N}$ L3), 3010m, 3442w; UV–Vis {acetonitrile, λ_{max} nm ($\varepsilon 10^{-5} M^{-1}$ cm^{-1})}: 269(0.18), 315(0.48), 371(0.10).

2.2.5.4 [(Cp)IrCl}$_2$(L1)](PF$_6$)$_2$ ([**22**](PF$_6$)$_2$)*

Yield: 72 mg, 75.7%; Elemental Anal (%) Calc. for $C_{30}H_{38}N_6Ir_2Cl_2P_2F_{12}$ (1227.93): C 29.34; H 3.12; N 6.84; found: C 29.23; H 3.15; N 6.71; ^{1}H NMR (400 MHz, CD_3CN): δ = 9.01 (s, 1H), 8.84 (d, 2H, ^3J = 3.2 Hz), 8.41 (d, 2H, ^3J = 2.4 Hz), 8.03 (s, 1H), 6.95 (dd, 2H, ^3J = 1.6 Hz), 1.79 (s, 30H, C_5Me_5); ESI-MS (m/z): 1082.2 $[M^{2+}+PF_6^-]^+$, 575.2 [M-$PF_6]^+$; IR (KBr, cm^{-1}): 845s $\nu_{(P-F)}$, 1598m, 1559m, 1521m ($\nu_{C=N}$ L1), 2995m, 3447w; UV–Vis {acetonitrile, λ_{max} nm ($\varepsilon 10^{-5} M^{-1}$ cm^{-1})}: 260(0.19), 310(0.67), 368(0.11).

2.2.5.5 [{(Cp)IrCl}$_2$(L2)](PF$_6$)$_2$ ([**23**](PF$_6$)$_2$)*

Yield: 60 mg, 61%; Elemental Anal (%) Calc. for $C_{32}H_{42}N_6Ir_2Cl_2P_2F_{12}$ (1255.98): C 30.60; H 3.37; N 6.69; found: C 30.45; H 3.48; N 6.51; ^{1}H NMR (400 MHz, CD_3CN): δ = 9.01 (s, 1H), 8.48 (d, 2H, ^3J = 6.4 Hz), 8.15 (s, 1H), 6.71 (d, 2H, ^3J = 4.6 Hz), 2.63 (s, 6H, CH_3), 1.75 (s, 30H, C_5Me_5); ESI-MS (m/z):1111.1 $[M^{2+}+PF_6^-]^+$, 603.1 [M- $PF_6]^+$; IR

(KBr, cm^{-1}): 844s $\nu_{(P-F)}$, 1599m, 1560m, 1525m ($\nu_{C=N}$ L2), 3002m, 3441w; UV–Vis {acetonitrile, λ_{max} nm ($\varepsilon 10^{-5} M^{-1} cm^{-1}$)}: 265(0.16), 315(0.56), 371(0.09).

2.2.5.6 [{(Cp)IrCl}$_2$(L3)](PF$_6$)$_2$ ([**24**](PF$_6$)$_2$)*

Yield: 74 mg, 74%; Elemental Anal (%) Calc. for $C_{34}H_{46}N_6Ir_2Cl_2P_2F_{12}$ (1284.04): C 31.80; H 3.61; N 6.54; found: C 31.76; H 3.78; N 6.33; ^{1}H NMR (400 MHz, CD_3CN): δ = 9.04 (s, 1H), 7.31 (s, 1H), 6.68 (s, 2H), 2.83 (s, 6H, CH_3), 2.79 (s, 6H, CH_3), 1.82 (s, 30H, C_5Me_5); ESI-MS (m/z): 1139.5 [M^{2+}+PF_6^-]$^+$, 631.2 [M- PF_6]$^+$; IR (KBr, cm^{-1}): 843s $\nu_{(P-F)}$, 1608m, 1562m, 1524m ($\nu_{C=N}$ L3), 3016m, 3450w; UV–Vis {acetonitrile, λ_{max} nm ($\varepsilon 10^{-5} M^{-1} cm^{-1}$)}: 268(0.19), 321(0.61), 376(0.13).

2.3 Results and discussion

2.3.1 Syntheses of ligands and complexes

Ligands L2 and L3 were prepared from the corresponding pyrazolato anion and 4,6-dichloropyrimidine. Reaction of half equivalent of dinuclear arene ruthenium complexes [(η^6-arene)Ru(μ-Cl)Cl]$_2$ (arene = C_6H_6, *p*-^{i}PrC_6H_4Me) with one equivalent of 4,6-disubstituted pyrimidine ligands *viz*. 4,6-bis(pyrazolyl)pyrimidine (L1), 4,6-bis(3-methyl-pyrazolyl)pyrimidine (L2) or 4,6-bis(3,5-dimethyl-pyrazolyl)pyrimidine (L3) in methanol generates the mononuclear complexes [(η^6-C_6H_6)Ru(L)Cl]$^+$ (L = L1, **1**; L2, **2**; L3, **3**), [(η^6-*p*-^{i}PrC_6H_4Me)Ru(L)Cl]$^+$ (L= L1, **4**; L2, **5**; L3, **6**), respectively (Scheme 2.2). The homologous complexes with two coordinated arene ruthenium fragments, [{(η^6-C_6H_6)RuCl}$_2$(L)](PF$_6$)$_2$ (L = L1, **13**; L2, **14**; L3, **15**) and [{(η^6-*p*-^{i}PrC_6H_4Me)RuCl}$_2$(L)](PF$_6$)$_2$ (L = L1, **16**; L2, **17**; L3, **18**), were prepared when a 1:1 molar ratio was used and over prolonged reaction times (Scheme 2.2). All these cationic ruthenium complexes were isolated as their hexafluorophosphate salts.

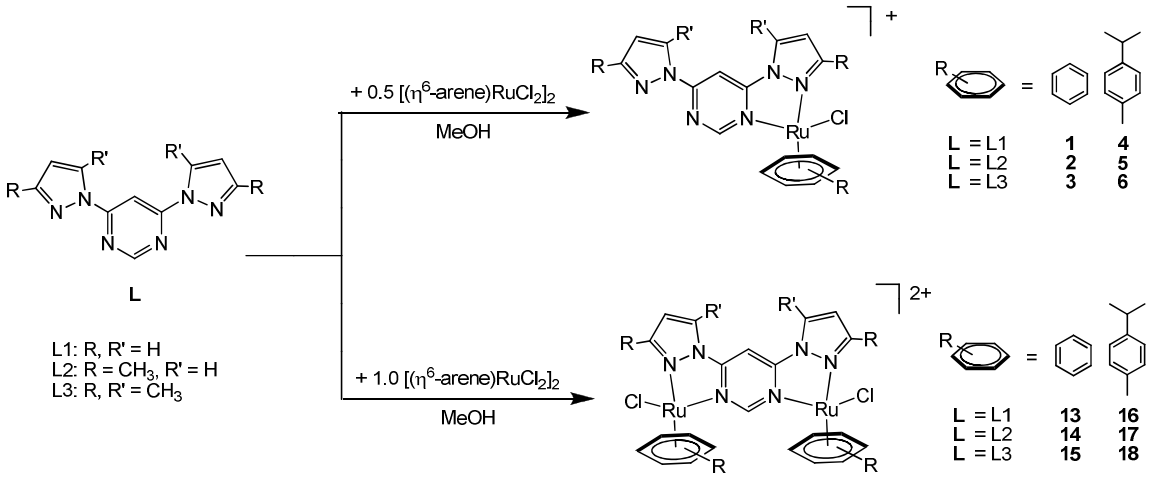

Scheme 2.2

Similarly, the reaction of half equivalent of the dimeric chloro-bridged complexes $[(Cp^*)M(\mu\text{-}Cl)Cl]_2$ (M = Rh, Ir) with 4,6-disubstituted-pyrimidine ligands (L) in methanol generates the mononuclear cationic complexes of the type $[(Cp^*)Rh(L)Cl]^+$ (L = L1, **7**; L2, **8**; L3, **9**), $[(Cp^*)Ir(L)Cl]^+$ (L= L1, **10**; L2, **11**; L3, **12**), respectively (Scheme 2.3). The homologous complexes with two coordinated Cp*Rh or Cp*Ir fragments, $[\{(Cp^*)RhCl\}_2(L)](PF_6)_2$ (L = L1, **19**; L2, **20**; L3, **21**) and $[\{(Cp^*)IrCl\}_2(L)](PF_6)_2$ (L = L1, **22**; L2, **23**; L3, **24**), were prepared when a 1:1 molar ratio was used and at prolonged reaction times (Scheme 2.3). All these cationic rhodium or iridium complexes were isolated as their hexafluorophosphate salts.

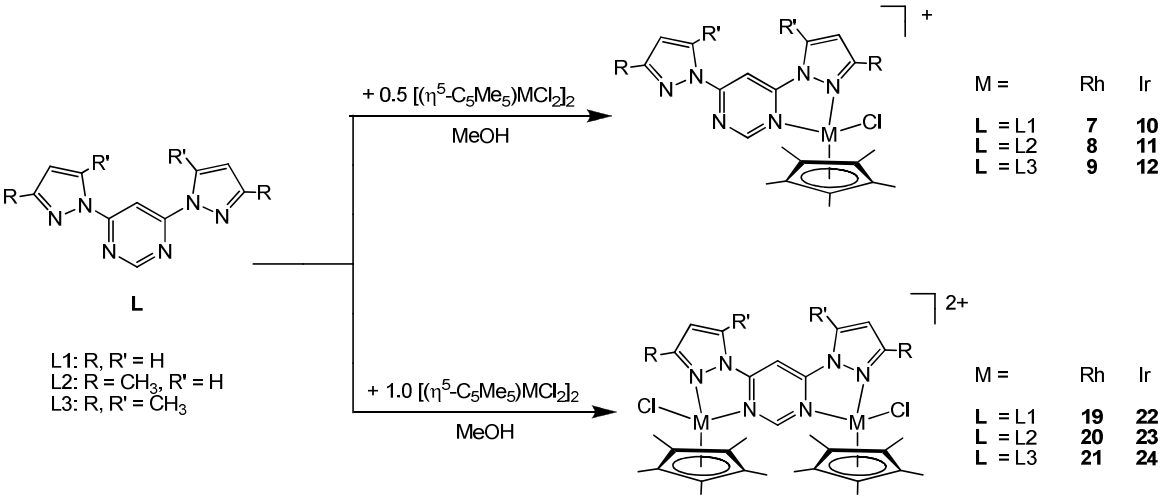

Scheme 2.3

When the mononuclear complexes [**1**]PF_6 **–** [**12**]PF_6 were further reacted with half mole of arene ruthenium or Cp*Rh or Ir dimers in acetonitrile solution, no reaction took

place and isolated as starting compounds. Also attempts to synthesize hetero-nuclear complexes by reaction of the mononuclear complexes with other metal atoms led to no reaction.

All these complexes are orange yellow in color, non-hygroscopic, air stable solids. They are soluble in acetonitrile but partially soluble in dichloromethane, chloroform and acetone.

2.3.2 Characterization of mononuclear complexes **1 – 12**

All these mononuclear complexes were characterized by IR, ^{1}H NMR, mass and elemental Analysis. The infrared spectra of the complexes [**1**]PF_6 – [**12**]PF_6 exhibit a strong band in the region 844-850 cm^{-1}, a typical $\nu_{P\text{-}F}$ stretching band for the PF_6 anions. Moreover, all complexes show absorption bands around 1600 – 1610 cm^{-1}, 1550 – 1558 cm^{-1} and 1522-1528 cm^{-1} corresponding to $\nu_{C=N}$ vibrations of pyrazole and pyrimidine moieties[38] besides these absorptions 2990-3050 and 3400-3450 were observed. For instance the IR spectrum of complex **2** was presented in figure 2.1.

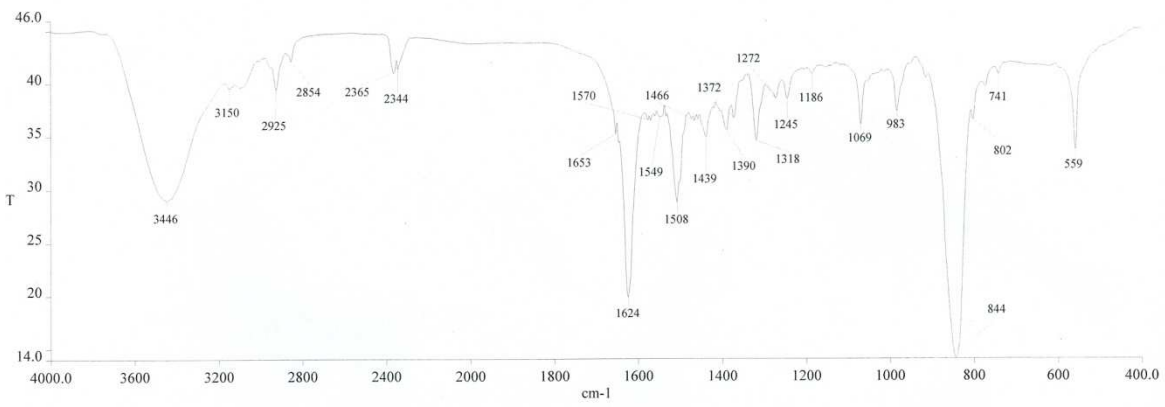

Figure 2.1: IR spectrum of complex [(η^6-C_6H_6)Ru(L2)Cl] PF_6 ([**2**]PF_6)

The mass spectra of these complexes exhibited, as expected, the corresponding molecular ion peaks m/z at 427, 455, 483, 483, 511, 538, 485, 513, 541, 575, 603 and 631. For instance complex [**1**]PF_6 shown four fragments, a molecular ion peak at 427 $[M]^+$, 391 $[M\text{-}Cl]^+$, 313 $[M\text{-}Cl\text{-arene}]^+$ and 213 [L+1]. For example the mass spectrum of the complex **4** was depicted in figure 2.2.

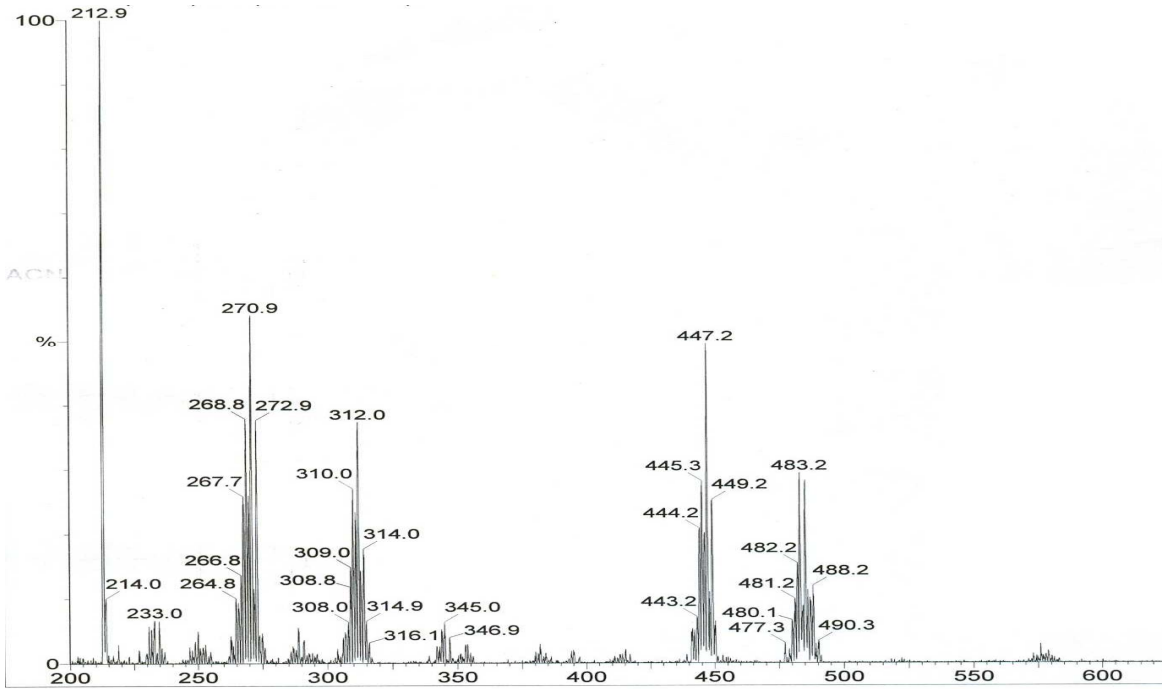

Figure 2.2: Mass spectrum of complex $[(\eta^6\text{-}p\text{-}^{i}PrC_6H_4Me)Ru(L1)Cl]PF_6$ ([**4**]PF_6)

The ^{1}H NMR spectra of the free ligands L1 to L3 exhibit a characteristic set of five resonances for the protons of pyrazole and pyrimidine rings, since the pyrazole rings are in symmetrical position. Upon coordination with the metal atom, each mononuclear complex has shown seven to eight set of resonances for the ligand L1 to L3 protons in the region δ = 9.56 to 6.78, δ = 9.41 to 2.43, and δ = 9.34 to 2.17, respectively. It indicates the formation of mononuclear complexes. The resonances of the coordinated pyrazole and pyrimidine rings protons shifted to higher frequency as a consequence of their coordination to the ruthenium or rhodium or iridium atom. However, arene- ruthenium complexes [**1**]PF_6–[**6**]PF_6, the resonances of ligand protons significantly shifted to down field compared to Cp*Rh or Cp*Ir complexes, [**7**]PF_6 – [**12**]PF_6. Besides these ligand resonances, complexes [**1**]PF_6 – [**3**]PF_6 exhibit a singlet for the benzene ring protons at δ= 6.20 to 5.93, complexes [**4**]PF_6 to [**6**]PF_6 exhibit a septet at δ = 2.70 for the protons of the isopropyl group and a singlet at δ = 2.17 for the methyl protons of the *p*-cymene ring. The ring protons and methyl protons of the isopropyl group of the *p*-cymene ligand have shown an unusual pattern of resonances. For instance, the methyl protons of the isopropyl group displays two doublets at *ca.* δ = 1.18 to 1.07, instead of one doublet as in the starting complex. The aromatic protons of the *p*-cymene ligand display four doublets, instead of two doublets as in the starting precursor. This unusual pattern is due to the

diastereotopic methyl protons of the isopropyl group and aromatic protons of the *p*-cymene ligand since the ruthenium atom is stereogenic due to the coordination of four different ligand atoms.[39,40] Complexes [**1**]PF_6 to [**12**]PF_6 exhibit a singlet at δ = 1.71 to 1.55 for the five methyl groups of the Cp* ligand. The chemical shift of the co-ligands arene or Cp* ring protons are shifted to down field compared to the starting precursors. For instance the ^{1}H NMR spectra of complexes 5 and 7 were depicted below (figure 2.3 and 2.4).

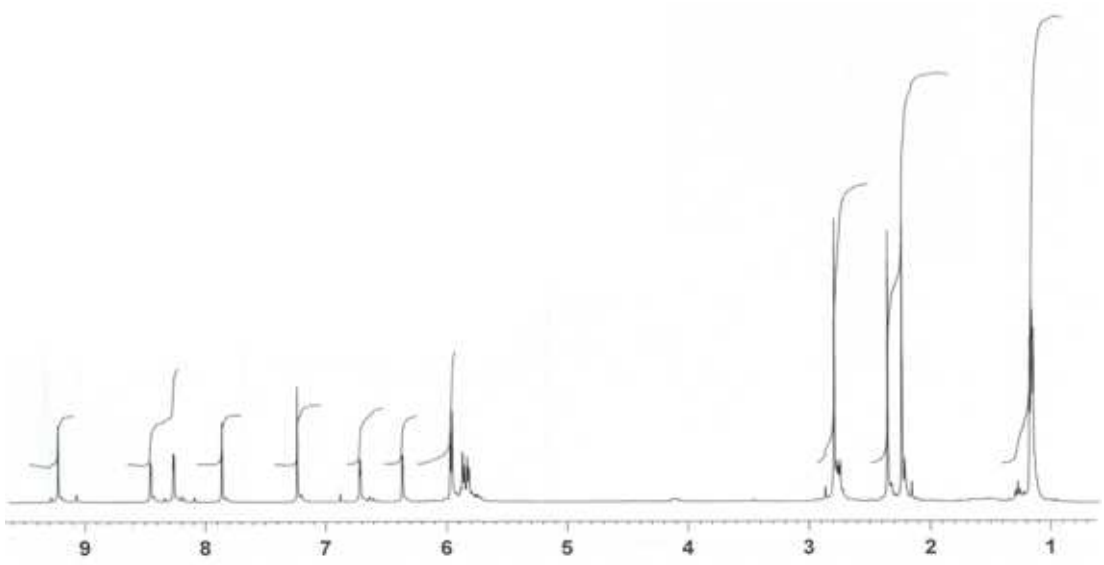

Figure 2.3: ^{1}H NMR spectrum of complex [(η^6-*p*-^{i}PrC_6H_4Me)Ru(L2)Cl]PF_6 ([**5**]PF_6)

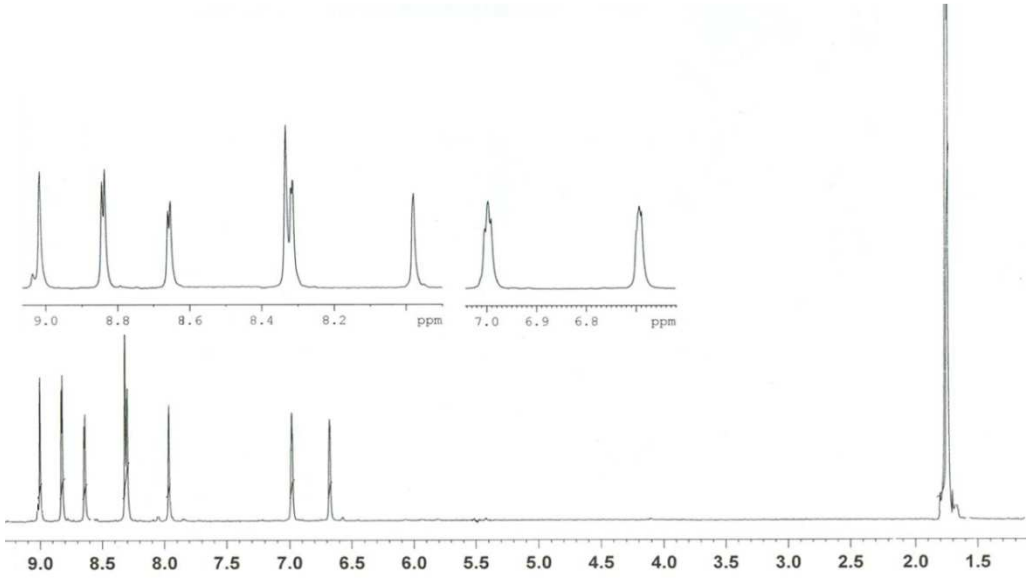

Figure 2.4: ^{1}H NMR spectrum of complex [(Cp*)Rh(L1)Cl]PF_6 ([**7**]PF_6)

2.3.3 Molecular structure of selected mononuclear complexes

The molecular structure of the $[(\eta^6\text{-}C_6H_6)Ru(L3)Cl]PF_6$ ([**3**]PF_6), $[(\eta^6\text{-}p\text{-}^iPrC_6H_4Me)Ru(L3)Cl]PF_6$ ([**6**]PF_6) as well as the Cp* rhodium complex $[(Cp^*)Rh(L1)Cl]PF_6$ ([**7**]PF_6) have been established by single crystal X-ray structure analysis. These cationic complexes show a typical piano-stool geometry with the metal center being coordinated by an aromatic ligand, a terminal chloro ligand and a chelating 4,6-disubstituted-pyrimidine ligand. The metal atom possesses an octahedral arrangement with two *cis*-nitrogen atoms of the pyrazolyl-pyrimidine ligand acting as a bidentate chelating ligand in a five-membered ring chelating fashion involving one nitrogen atom of the pyrazolyl moiety and the nitrogen atom of the pyrimidine group. The structures are shown in Figures 2.5, 2.6 and 2.7. Crystallographic details are summarized in Table 2.1 and selected bond lengths and angles for [**3**]PF_6, [**6**]PF_6 and [**7**]PF_6 are presented in Table 2.2.

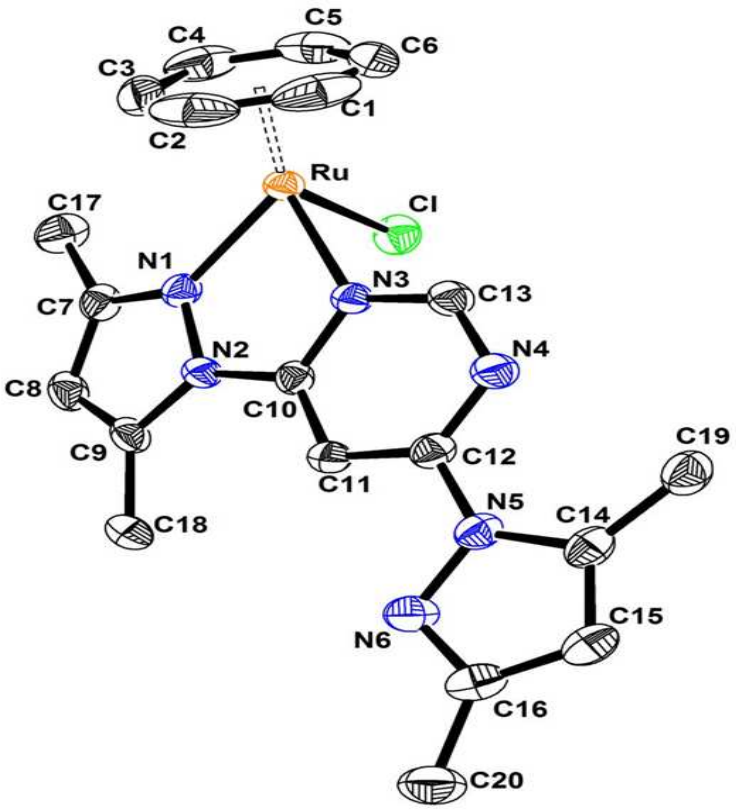

Figure 2.5: Molecular structure of $[(\eta^6\text{-}C_6H_6)Ru(L3)Cl]PF_6$ ([**3**]PF_6) at 50% probability level. Hydrogen atoms, water molecule and hexafluorophosphate anion have been omitted for clarity.

In the mononuclear complexes [**3**]PF_6 and [**7**]PF_6 the N1-metal distance (2.076 and 2.106 Å) of the pyrazolyl moiety is slightly shorter than the corresponding pyrimidinyl, N3-metal distance (2.092, and 2.138 Å), in contrast to complex [**6**]PF_6 in which the N1-metal (2.102 Å) distance is slightly longer than the corresponding N3-metal distance (2.093(2) Å). The Rh-N bond distance (2.106(3) and 2.138(3) Å) in **7** is slightly longer than the corresponding distances of ruthenium complex **3** (2.076(3) and 2.092(2) Å) and complex **6** (2.102 and 2.093), while the M-Cl [2.402(7), 2.388(8) and 2.400(6)] bond lengths show no significant differences in all the cations and similar reported values.[41, 42] The N-M-N bond angles [75.33(7) in **3** and 75.56°(9) in **6**] are similar to that of complexes [(η^6-*p*-^{i}PrC_6H_4Me)RuCl(2,3-bis(α-pyridyl)quinoxaline)]$^+$ [76.2 (2)°].[43] The distances between the ruthenium atom and the centroid of the C_6 aromatic ring in **3** and **6** are comparable (1.69 and 1.68 Å) but quite shorter than the distance between the rhodium atom and the C_5 aromatic ring observed in **7** (1.77 Å). The M-N1 bond distances [2.076(9) to 2.102(2) Å] are comparable to those in [(η^6-C_6H_6)RuCl(2-(1-imidazol-2-yl)pyridine)]$^+$ and [(Cp*)Ir(2-(2'-pyridyl)-imidazole)Cl]$^+$.[44]

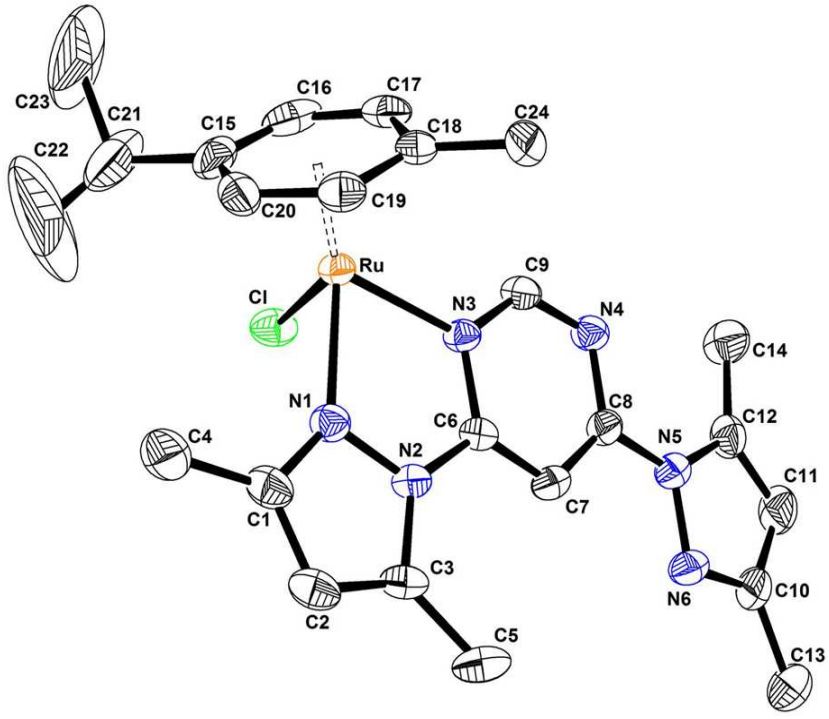

Figure 2.6: Molecular structure of [(η^6-*p*-^{i}PrC_6H_4Me)Ru(L3)Cl]PF_6 ([**6**]PF_6) at 50% probability level. Hydrogen atoms and hexafluorophosphate anion have been omitted for clarity.

As amplified in Figures 2.5 to 2.7, all cations possess metal-centered chirality as the metal atom is coordinated to four different ligator atoms. However, since none of the ligands contain chiral centers, they are all obtained as a racemic mixture and they all crystallize in the centrosymmetric space group $P\bar{1}$.

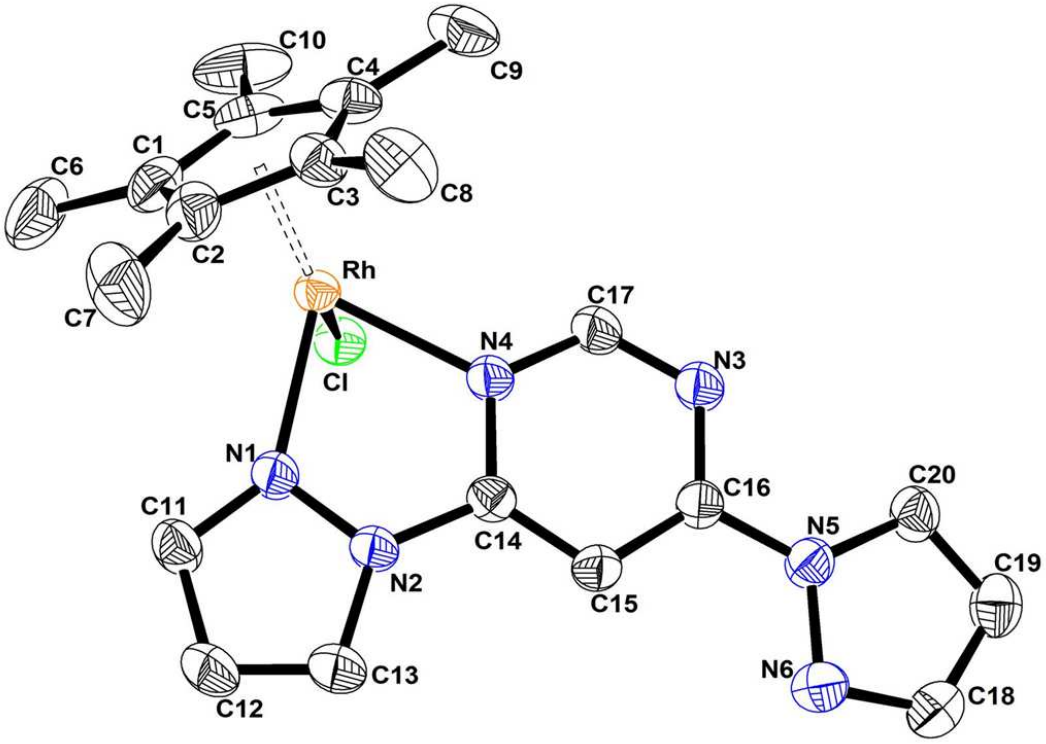

Figure 2.7: Molecular structure of [(Cp*)Rh(L1)Cl]PF_6 ([7]PF_6) at 50% probability level. Hydrogen atoms and anion have been omitted for clarity.

In the crystal packing of [3]$PF_6 \cdot H_2O$, the hexafluorophosphate anion sits on side of the cationic complex and interacts with an hydrogen atom of the C_6H_6 ligand (see figure 2.8). The hexafluorophosphate anion interacts with C_6H_6 ligand through C–H···F contacts: the C···F distances being 3.22 and 3.26 Å with C–H···F angles of 148.9 and 138.3°, respectively. In addition to this the oxygen atom interacts with one of the hydrogen atoms of ligand L1through C-H···O contact: the C···O distance being 3.10 Å and C-H···O angle is 149.06 °.

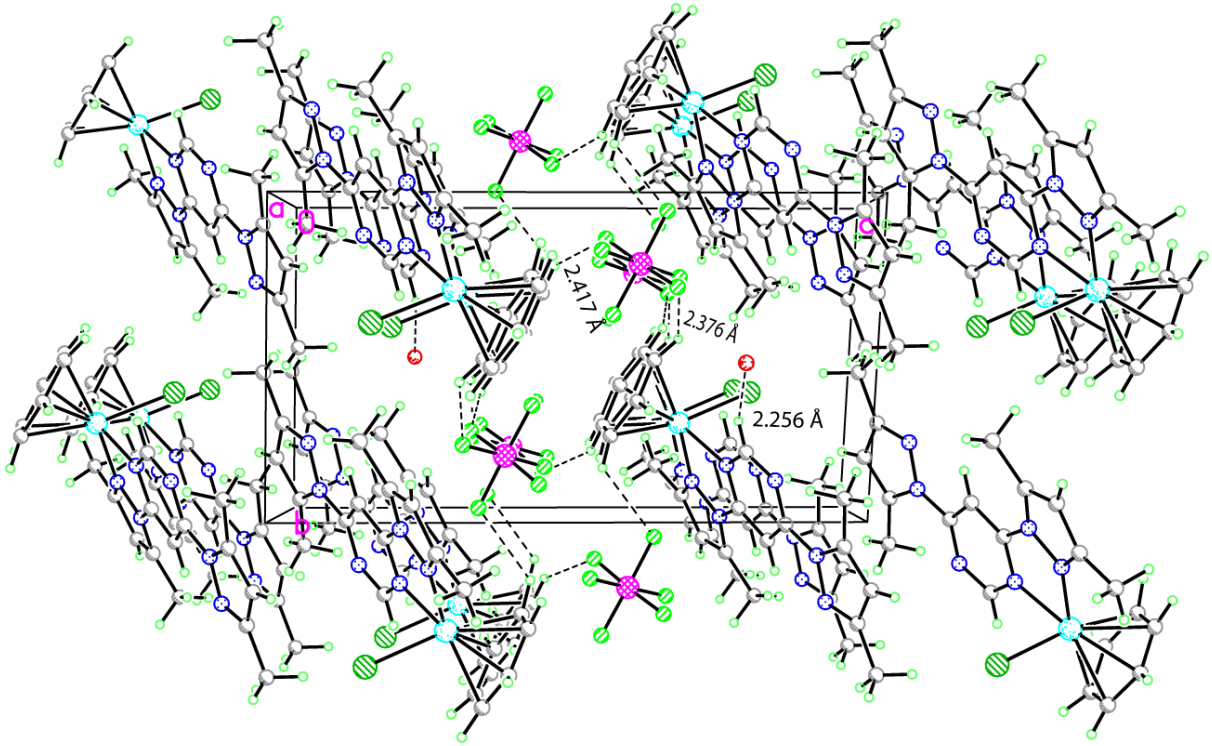

Figure 2.8: Network of $[(\eta^6\text{-}C_6H_6)Ru(L3)Cl]PF_6$ ([**3**]PF_6)·H_2O showing the intermolecular interactions involving the hexafluorophosphate anion and water molecule

2.3.4 Characterization of the dinuclear complexes

The infrared spectra of the dinuclear complexes [**13**]$(PF_6)_2$ – [**24**]$(PF_6)_2$ exhibit a similar trend as for the mononuclear complexes [**1**]PF_6 – [**12**]PF_6. The mass spectra of these complexes exhibited two main peaks; a minor peak with an approximately 50% intensity attributed to $[M - PF_6]^+$ at m/z 786, 814, 842, 898, 926, 954, 904, 932, 960 , 1082, 1110 and 1138, respectively, and a major peak which corresponds to the loss of an $[(arene/Cp^*)MCl]^+$ fragment, thus giving the corresponding mononuclear cations $[\mathbf{1} - PF_6]^+$ – $[\mathbf{12} - PF_6]^+$ at m/z = 427, 455, 483, 483, 511, 538, 485, 513, 541, 575, 603 and 631.

The ^{1}H NMR spectra of the dinuclear complexes [**13**]$(PF_6)_2$ – [**24**]$(PF_6)_2$, exhibit five distinct resonances, which are assigned to pyrazole or substituted pyrazoles and pyrimidine ring protons of the ligand L1 or L2 or L3, indicating the formation of dinuclear complexes. The number of distinct resonances of these complexes is similar to the number of distinct resonances of free ligands, indicating that the pyrazole rings of the ligands remain symmetrical even after formation of the complexes. These results indicate the formation of dinuclear complexes. The resonances of the coordinated pyrazole and

pyrimidine protons shifted to considerable down filed as compared to mononuclear complexes, a consequence of their coordination to two ruthenium, rhodium or iridium atoms. For instance the ^{1}H NMR spectrum of complex **21** was depicted in figure 2.9.

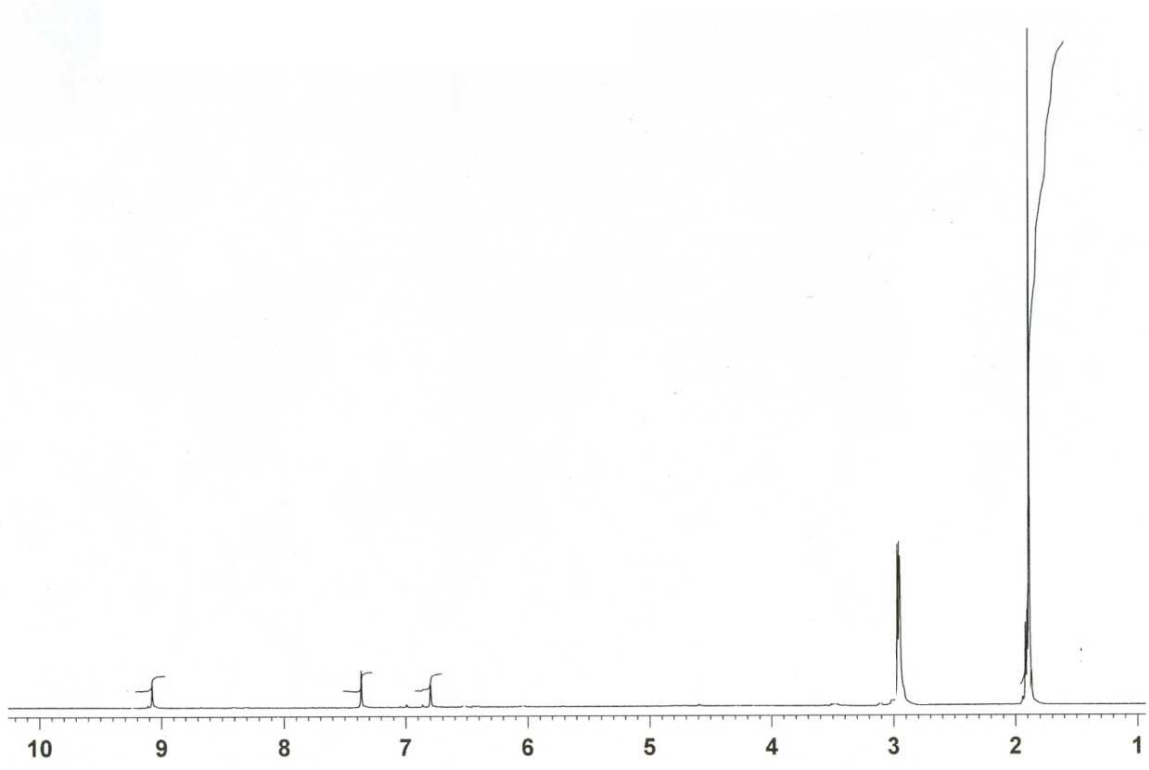

Figure 2.9: ^{1}H NMR spectrum of complex [{(Cp*)RhCl}$_2$(L3)](PF$_6$)$_2$ ([**21**](PF$_6$)$_2$)

However, in the arene ruthenium complexes [13](PF$_6$)$_2$ – [18](PF$_6$)$_2$, the resonances of the ligand protons significantly shifted to down field compared to Cp*Rh or Ir complexes, [**19**](PF$_6$)$_2$ – [**24**](PF$_6$)$_2$. Besides these resonances complexes [**13**](PF$_6$)$_2$ – [**15**](PF$_6$)$_2$ exhibit a singlet for both benzene ring protons at δ = 6.24 and 6.15 ppm, complexes [**16**](PF$_6$)$_2$ – [**18**](PF$_6$)$_2$ exhibit a similar trend like the mononuclear complexes [**4**]PF$_6$ **–** [**4**]PF$_6$. A septet at δ = 2.70 for the protons of the isopropyl group, a singlet at δ = 2.17 for the methyl protons of *p*-cymene ring, four doublets *ca.* δ = 6.09 to 5.93 for the ring protons of the *p*-cymene ligand and finally methyl protons of the isopropyl group displays two doublets at *ca.* δ = 1.18 and 1.07. Complexes [**19**](PF$_6$)$_2$ – [**24**](PF$_6$)$_2$ exhibit *a* singlet in the region δ = 1.88 to 1.77 for the five methyl groups of the Cp* ligand. The chemical shift of the arene co-ligands or Cp* ring protons are shifted to higher frequency compared to the starting precursors as well as compared to the mononuclear complexes.

2.3.5 Molecular structure of the dinuclear complex [**18**](PF$_6$)$_2$

The molecular structure of [{(η^6-*p*-^{i}PrC$_6$H$_4$Me)RuCl}$_2$(L3)]$^{2+}$ ([**18**](PF$_6$)$_2$) has been established by single-crystal X-ray structure analysis. Selected bond lengths and angles are presented in Table 2.2. The dinuclear complex [**18**](PF$_6$)$_2$ shows a typical piano-stool geometry for the ruthenium atoms with the metal centers being coordinated by the aromatic ligand, a terminal chloride and a chelating N,N-ligand (Figure. 2.10). The compound [**18**](PF$_6$)$_2$ contains two Ru(II) metal centers which are bonded to a η^6-^{i}*p*-PrC$_6$H$_4$Me ligand and bridged by the L3 ligand through its nitrogen atoms. Interestingly, the dinuclear complex [**18**](PF$_6$)$_2$ reveals a *trans* conformation of the two chloro ligands (Figure. 2.10). The distance between the ruthenium atoms and the corresponding centroid of the η^6-*p*-^{i}PrC$_6$H$_4$Me ring is 1.68 and 1.67 Å. These distances are comparable to those in the related complex cation [(η^6-*p*-^{i}PrC$_6$H$_4$Me)Ru(2-acetylthiazoleazine)Cl]$^+$.[45]

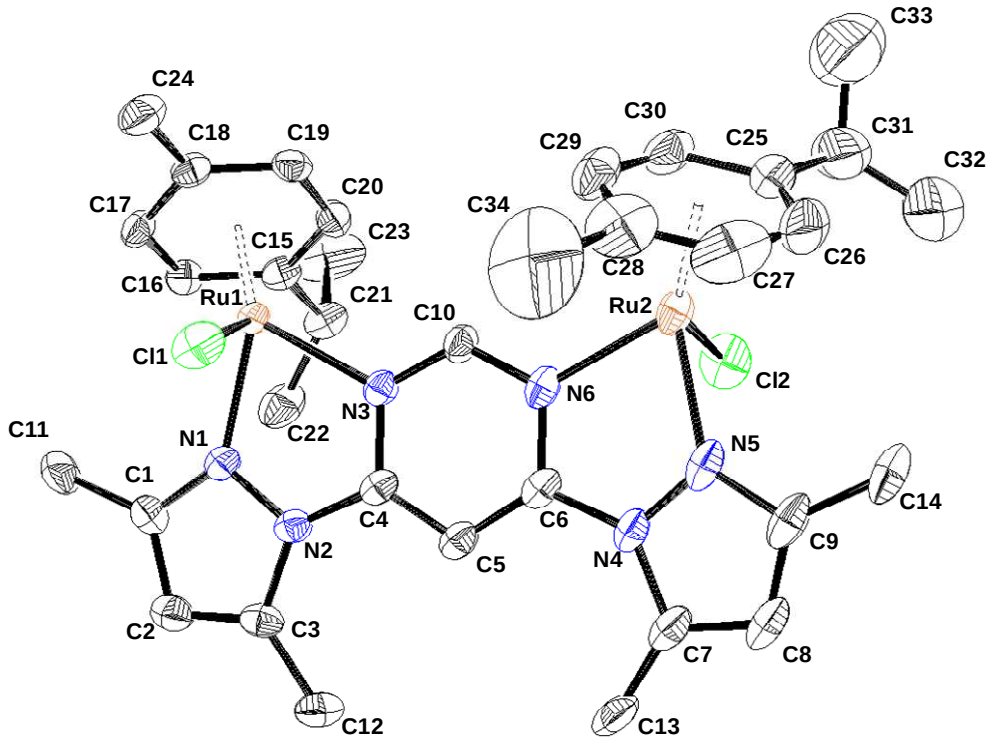

Figure 2.10: Molecular structure of [{(η^6-*p*-^{i}PrC$_6$H$_4$Me)RuCl}$_2$(L3)]$^{2+}$ [18](PF$_6$)$_2$·H$_2$O at 50% probability level. Hydrogen atoms, water molecule and hexafluorophosphate anions have been omitted for clarity.

The Ru-N bond distances ranging from 2.072(3) to 2.092(3) Å are shorter than in the mononuclear complex [**6**]PF$_6$ [2.102(3) and 2.093(3) Å], interestingly the Ru to N1 or N5 (pyrazole) distances are shorter than the Ru-N3 or N6 (pyrimidine) distances in the

dinuclear complex [**18**]$(PF_6)_2$, where as it is opposite in mononuclear complex [**6**]PF_6, while the ruthenium-chlorine bond distances are comparable. In complex [1**8**]$(PF_6)_2$, the isopropyl group of the *p*-cymene ligand at Ru1 center located opposite to the halide ligand in order to reduce steric interactions, while at Ru2 the isopropyl group is located on same side to the halide ligand.

Complex [**18**]$(PF_6)_2$ crystallizes with one molecule of water per asymmetric unit, forming an hydrogen-bonded network to the chloride atom and the fluorine atom of the hexafluorophosphate anion (Figure 2.11). The water molecule interacts with chloride ligand through O–H···Cl contacts: the O···Cl distance being 3.26 Å with an O–H···Cl angle of 156.3°. In addition to this, the water molecule interacts with one of the fluoride atoms of the hexafluorophosphate anion through F···H-O contacts: the F···O distance being 3.51 Å and the F···H-O angle 154.09°.

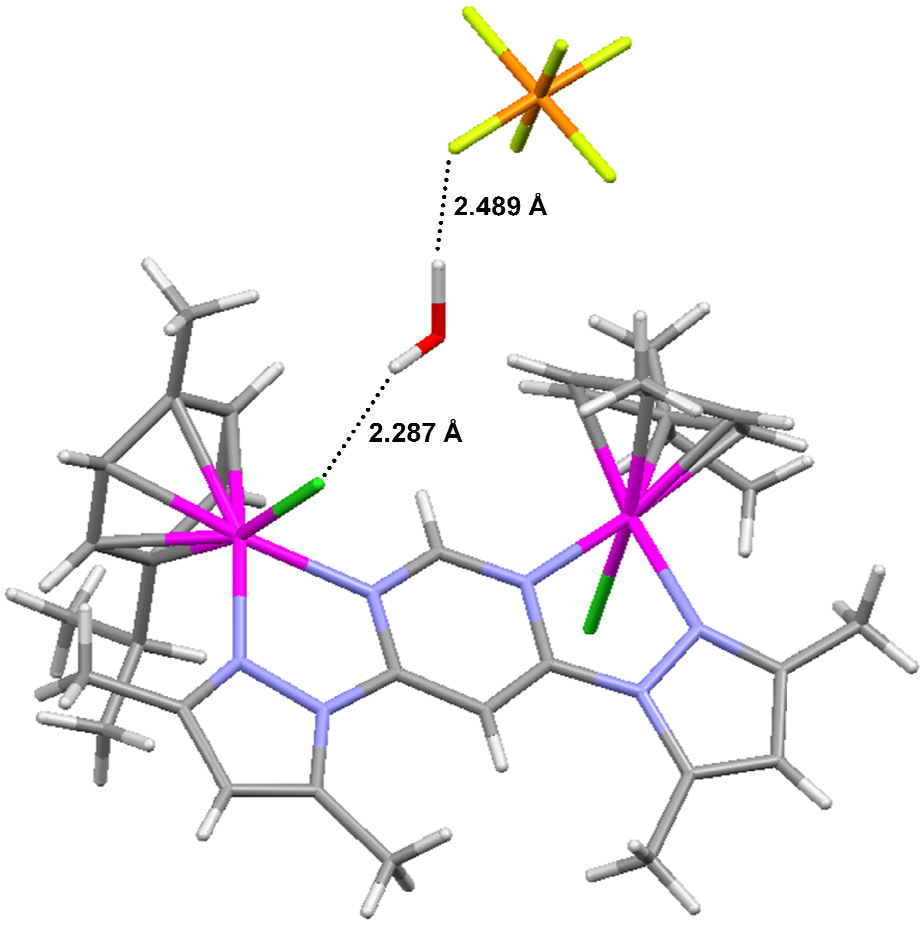

Figure 2.11: Hydrogen bond network in $[\{(\eta^6\text{-}p\text{-}^{i}PrC_6H_4Me)RuCl\}_2(L3)]^{2+}$ [**18**]$(PF_6)_2 \cdot H_2O$ showing the intermolecular interactions involving an hexafluorophosphate anion, a water molecule and cation

Table 2.1: Details of the data collection and results of the structure refinement parameters for complexes [**3**]$PF_6 \cdot H_2O$, [**6**]PF_6, [**7**]PF_6 and [**18**]$(PF_6)_2 \cdot H_2O$

Complex	[**3**]$PF_6 \cdot H_2O$	[**6**]PF_6	[**7**]PF_6	[**18**]$(PF_6)_2 \cdot H_2O$
Chemical formula	$C_{20}H_{22}ClF_6N_6OPRu$	$C_{24}H_{30}ClF_6N_6PRu$	$C_{20}H_{23}ClF_6N_6PRh$	$C_{34}H_{46}Cl_2F_{12}N_6OP_2Ru_2$
Formula weight	628.03	684.03	630.77	1117.75
Crystal system	Triclinic	Triclinic	Triclinic	Monoclinic
Space group	*P*-1	*P*-1	P-1	*P* $2_1/a$
Crystal color and shape	orange blade	red block	red block	orange block
Crystal size (mm^3)	0.25 x 0.12 x 0.12	0.28 x 0.28 x 0.18	0.50 x 0.26 x 0.15	0.21x0.18x0.13
a (Å)	8.4350(11)	8.4928(10)	7.5841(6)	17.1745(13)
b (Å)	9.1359(12)	12.1384(14)	11.2581(10)	13.5980(8)
c (Å)	16.328(2)	14.1361(16)	14.7304(12)	17.6465(11)
α (°)	91.340(2)	99.418(2)	74.056(2)	90.00
β (°)	92.071(2)	90.677(2)	88.015(2)	90.062(8)
γ (°)	105.129(2)	104.611(2)	88.408(2)	90.00
V ($Å^3$)	1213.2(3)	1389.0(3)	1208.39(17)	4121.1(5)
Z	2	2	2	4
T (K)	203(2)	203(2)	203(2) K	173(2)
D_x (g /cm^3)	1.763	1.636	1.734	1.802
μ (mm^{-1})	0.895	0.785	0.952	1.033
Scan range (°)	$2.31 < \theta < 28.31$	$1.76 < \theta < 32.38$	$1.88 < \theta < 32.33$	$1.91 < \theta < 26.08$
Unique reflections	12483	17438	14825	8096
Reflections used [$I>2\sigma(I)$]	5998	9027	7813	5203
R_{int}	0.0260	0.0383	0.0244	0.0644
Final *R* indices [$I>2\sigma(I)$]	0.0385, wR_2 0.1160	0.0513, wR_2 0.1368	0.0428, wR2 = 0.1387	0.0379, wR2 = 0.0791
R indices (all data)	0.0415, wR_2 0.1203	0.0615, wR_2 0.1471	0.0463, wR2 = 0.1437	0.0700, wR2 = 0.0862
Goodness-of-fit	1.186	1.121	1.178	0.849
Max, Min $\Delta\rho$ (e $Å^{-3}$)	1.183, -0.564	1.128, -0.754	1.214, -1.051	0.949, -0.807

Table 2.2: Selected bond lengths and angles for complexes [**3**]$PF_6 \cdot H_2O$, [**6**]PF_6, [**7**]PF_6 and [**18**]$(PF_6)_2 \cdot H_2O$.

	[**3**]PF_6	[**6**]PF_6	[**7**]PF_6	[**18**]$(PF_6)_2$
Distances (Å)				
M1-Cl1	2.402(7)	2.388(8)	2.40(6)	2.393(1)
M2-Cl2	-	-	-	2.391(1)
M1-N1	2.076(2)	2.102(2)	2.106(2)	2.072(3)
M1-N3	2.092(2)	2.093(2)	2.138(2)	2.092(3)
M2-N4	-	-	-	2.092(3)
M2-N6	-	-	-	2.076(3)
M1-centroid[a]	1.690	1.685	1.770	1.685
M2-centroid[a]	-	-	-	1.678
Angles (º)				
N1-M1-N3	75.33(7)	75.56(9)	75.34(8)	75.70(1)
N4-M2-N6	-	-	-	75.0(1)
N1-M1-Cl1	84.76(6)	87.51(7)	90.43(7)	82.86(3)
N4-M2-Cl2	-	-	-	84.26(9)
N3-M1-Cl1	84.09(6)	84.27(7)	84.73(6)	83.31(9)
N6-M2-Cl2	-	-	-	81.70(9)

[a]Calculated centroid-to-metal distances (η^6-C_6 or η^5-C_5 coordinated aromatic ring).

2.3.6 UV-visible spectroscopy

Electronic absorption spectra of the mononuclear complexes [**1**]PF_6 – [**12**]PF_6 as well as the dinuclear complexes [**13**]$(PF_6)_2$ – [**24**]$(PF_6)_2$ were acquired in acetonitrile, at 10^{-5} M concentration in the range 250-550 nm. Electronic spectra of representative complexes are depicted in Figure 2.12. The spectra of these complexes are characterized by two main features, *viz*., an intense ligand–localized or intra-ligand $\pi \rightarrow \pi^*$ transition in the ultraviolet region and metal-to-ligand charge transfer (MLCT) $d\pi(M) \rightarrow \pi^*$ (L1 - ligand) bands in the visible region.[46] Since the low spin d^6 configuration of the mononuclear complexes provides filled orbitals of suitable symmetry at the Ru(II), Rh(III) and Ir(III) centers, these can interact with low lying π^* orbitals of the ligands. All

these mononuclear complexes [**1**]PF_6 – [**12**]PF_6 show two medium intensity bands in the region 261-310 nm, an intense band in the region 340-380 nm in UV region and a low energy absorption band in the visible region 450 – 470 nm. Where as the dinuclear complexes [**13**]$(PF_6)_2$ – [**24**]$(PF_6)_2$ shown similar number of bands in higher frequency region, for instance a medium intensity band in the region 260 – 275 nm, a high intensity band in the region 318 – 322 nm and a broad band in the region 356 – 418 nm. The medium intensity bands in UV region is assigned to π – π*, a high intensity band in UV region is assigned to inter and intra-ligand π – π*/ n – π* transitions,[47, 48] while the low energy absorption band in the visible region is assigned to metal-to-ligand charge transfer (MLCT) (t_{2g} – π*).

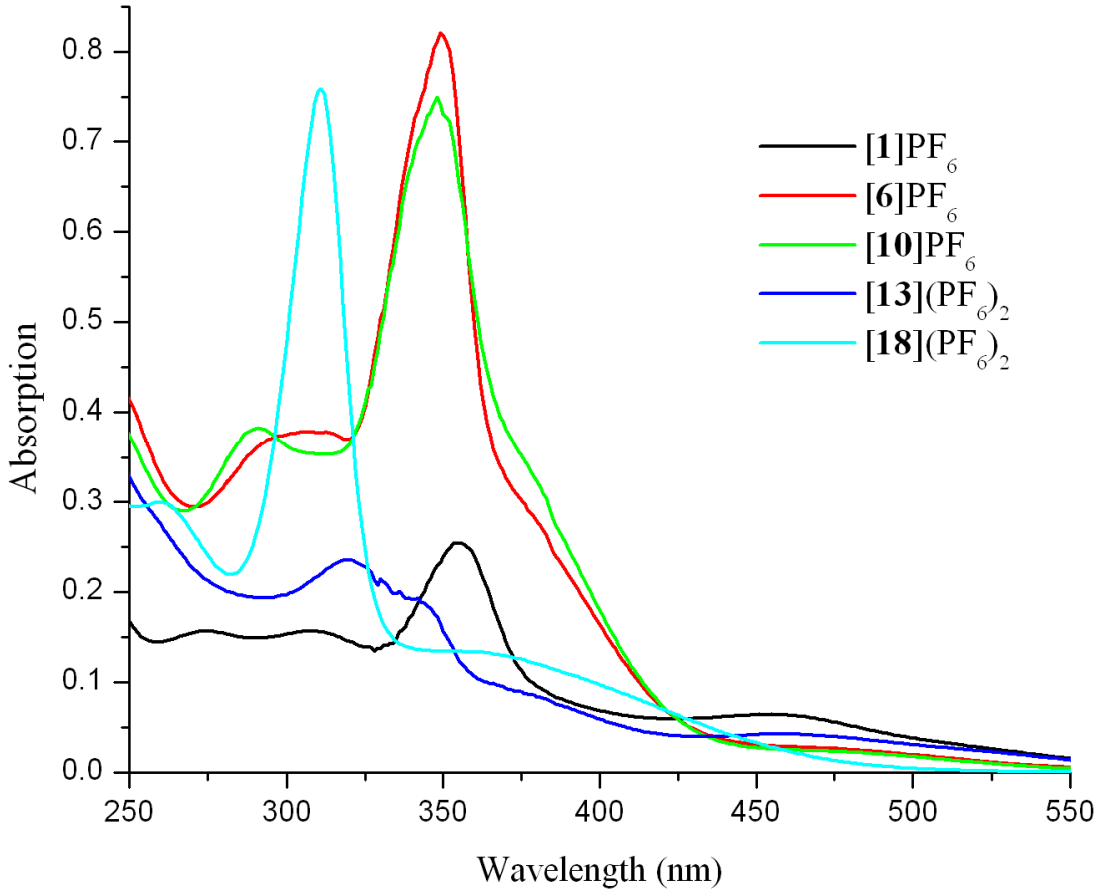

Figure 2.12: UV-Visible electronic spectra of selected complexes in acetonitrile at 298 K.

2.4 Conclusions

We have described and characterized new mono and dinuclear ruthenium, rhodium and iridium complexes with the ligands L1, L2 and L3, in good yield, which are remarkably stable in air as well as in solution. In both, mono and dinuclear complexes,

the metal atom are bonded with the N-atom of the pyrazole moiety and the N-atom of the pyrimidine moiety. But our effort to make heteronuclear complexes by using second binding site of the mononuclear complexes was unsuccessful, since coordination of the first metallic center does not induce the bonding in the second position in a kind of chemical symbiosis driven by the ligand or the metal center.

2.5 Supplementary material

CCDC-**742491** [**3**]$PF_6 \cdot H_2O$, CCDC-**742492** [**6**]PF_6, CCDC-**742493** [**7**]PF_6 and CCDC-**751116** [**18**]$(PF_6)_2 \cdot H_2O$ contain the supplementary crystallographic data for this chapter.

References

1 S. Trofimenko, Chem. Rev. 93 (1993) 943.

2 M. D. Ward, Annu. Rep. Prog. Chem., Sect. A: Inorg. Chem. 91 (1994) 317.

3 A. Juris, S. Barigelletti, S. Campagna, V. Balzani, P. Belser, A. von Zelewsky, Coord. Chem. Rev. (1988) 27.

4 J. A. Bailey, M. G. Hill, R. E. Marsh, V. M. Miskowski, W. P. Schaefer, H. B. Gray, Inorg. Chem. 34 (1995) 4591.

5 M. G. Hill, J. A. Bailey, V. M. Miskowski, H. B. Gray, Inorg. Chem. 35 (1996) 4585.

6 A. Gelling, K. G. Orrell, A. G. Osborne, V. Sÿik, J. Chem. Soc., Dalton Trans. (1998) 937.

7 M. Navarro, W. F. D. Giovani, J. R. Romero, Synth. Commun. 20 (1990) 399.

8 N. Grover, H. H. Thorp, J. Am. Chem. Soc. 113 (1991) 7030.

9 X. Hua, M. Shang, A.G. Lappin, Inorg. Chem. 36 (1997) 3735.

10 C. M. Che, C. Ho, T.C. Lau, J. Chem. Soc., Dalton Trans. (1991) 901.

11 S. J. Raven, T. J. Meyer, Inorg. Chem. 27 (1988) 4478.

12 C. M. Che, W.T. Tang, W.O. Lee, K.Y. Wong, T.C. Lau, J. Chem. Soc., Dalton Trans. (1992) 1551.

13 A. Dovletoglou, S. A. Adeyemi, M.N. Lynn, D.J. Hodgson, T.J. Meyer, J. Am. Chem. Soc. 112 (1990) 8989.

14 C. M. Che, V.W.W. Yam, Adv. Inorg. Chem. 39 (1992) 233.

15 R. A. Binstead, M. E. Mc Guire, A. Dovletoglou, W. K. Seok, L. E. Roecker, T. J. Meyer, J. Am. Chem. Soc. 114 (1992) 173.

16 A. W. Stumpf, E. Saive, A. Demonceau, A.F. Noels, J. Chem. Soc., Chem. Commun. (1995) 1127.

17 O. Zava, S. M. Zakeeruddin, C. Danelon, H. Vogel, M. Grätzel, P. J. Dyson, Chem. Bio. Chem. 10 (2009) 1796.

18 P. C. A. Bruijnincx, P. J. Sadler, Adv. Inorg. Chem. 61 (2009) 1.

19 F. Schmitt, P. Govindaswamy, O. Zava, G. Süss-Fink, L. Juillerat-Jeanneret, B. Therrien, J. Biol. Inorg. Chem. 14 (2009) 101.

20 B. Therrien, G. Süss-Fink, P. Govindaswamy, A. K. Renfrew, P. J. Dyson, Angew. Chem. Int. Ed. 47 (2008) 3773.

21 P. Govender, N. C. Antonels, J. Mattsson, A. K. Renfrew, P. J. Dyson, J. R. Moss, B. Therrien, G. S. Smith, J. Organomet. Chem. 694 (2009) 3470.

22 N. P. E. Barry, N. H. Abd Karim, R. Vilar, B. Therrien, Dalton Trans. (2009) DOI:10.1039/b913642h

23 L. Rigamonti, F. Demartin, A. Forni, S. Righetto and A. Pasini, Inorg. Chem. 45 (2006) 10976.

24 J. Gradinaru, A. Forni, V. Druta, F. Tessore, S. Zecchin, S. Quici and N. Garbalau, Inorg. Chem. 46 (2007) 884.

25 G. Gupta, K. T. Prasad, B. Das, G. L. P. Yap, K. M. Rao, J. Organomet. Chem. 694 (2009) 2618.

26 L. Soriano, F. A. Jalón, B. R. Manzano, M. Maestro, Inorg. Chim. Acta 362 (2009) 4486.

27 K. Sarjit Singh, Y. A. Mozharivskyj, K. M. Rao, Z. Anorg. Allg. Chem. 632 (2005) 172.

28 K. Sarjit Singh, Y. A. Mozharivskyj, C. Thöne, K. M. Rao, J. Organomet. Chem. 690 (2005) 3720.

29 G. Gupta, G. P. A. Yap, B. Therrien, K. M. Rao, Polyhedron, 28 (2009) 844.

30 P. Govindaswamy, Y. A. Mozharivskyj, K. M. Rao, J. Organomet. Chem. 689 (2004) 3265.

31 P. Govindaswamy, P. J. Carroll, Y. A. Mozharivskyj, K. M. Rao, J. Organomet. Chem. 690 (2005) 885.

32 P. Govindaswamy, Y. A. Mozharivskyj, K. M. Rao, Polyhedron 23 (2004) 3115.

33 J. K. Hurst, Coord. Chem. Rev. 249 (2005) 313.

34 C. Sens, I. Romero, M. Rodriguez, A. Llobet, T. Parella, J. B. Buchholz, J. Am. Chem. Soc. 126 (2004) 7798.

35 I. Romero, M. Rodriguez, C. Sens, J. Mola, K. M. Rao, L Francas, E. M. Marza, L. Escriche, A. Llobet, Inorg. Chem. 47 (2008) 1824-1834.

36 M. Ikeda, K. Maruyama, Y. Nobuhara, T. Yamada, S. Okabe, Chem. Pharm. Bull. 45 (1997) 549.

37 R. Uson, L. A. Oro, M. Esteban, Polyhedron 3 (1984) 213.

38 H. van der Poel, G. van Koten, K. Vrieze, Inorg. Chem. 19 (1980) 1145.

39 P. Govindaswamy, B. Therrien, G. Süss-Fink, P. Štěpnička, Ludvík, J. Organomet. Chem. 692 (2007) 1661.

40 K. T. Prasad, B. Therrien, K. M. Rao, J. Organomet. Chem. 693 (2008) 3049.

41 K. T. Prasad, B. Therrien, K. M. Rao, J. Organomet. Chem. 695 (2010) 226 -234.

42 B. Therrien, C. Saïd-Mohamed, G. Süss-Fink, Inorg. Chim. Acta. 361 (2008) 2601.

43 R. Lalrempuia, K. M. Rao, Polyhedron, 22 (2003) 3155.

44 K. Pachhunga, B. Therrien, K. A. Kreisel, G. P. A. Yap, M. R. Kollipara, Polyhedron. 26 (2007) 3638.

45 K. T. Prasad, G. Gupta, A. V. Rao, B. Das, K. M. Rao, Polyhedron 28 (2009) 2649.

46 E. Binamira-Soriaga, N. L. Keder, W. C. Kaska, Inorg. Chem. 29 (1990) 3167.

47 C. S. Araújo, M. G. B. Drew, V. Félix, L. Jack, J. Madureira, M. Newell, S. Roche, T. M. Santos, J. A. Thomas, L. Yellowlees, Inorg.Chem. 41 (2002) 2250.

48 H. Deng, J. Li, K.C. Zheng, Y. Yang, H. Chao, L. N. Ji, Inorg. Chim. Acta, 358 (2005) 3430.

Chapter 3

Spectral, structural and DFT studies of platinum group metal 3,6-bis(2-pyridyl)-4-phenylpyridazine complexes and their ligand bonding modes

---

New mononuclear half-sandwich platinum group metal (Ru, Rh and Ir) complexes were obtained by the reaction of arene or Cp or Cp* metal (Ru, Rh and Ir) complexes with 3,6-bis(2-pyridyl)-4-phenylpyridazine (L^{ph}), yielding two sets of complexes. In one set (*type-A*), the metal bonds to the N1 and N2 atoms of the (L^{ph}) ligand, and in the other (*type-B*), the metal bonds to the N3 and N4 atoms. The structures of these complexes were confirmed through X-ray crystallography and density functional theory calculations.

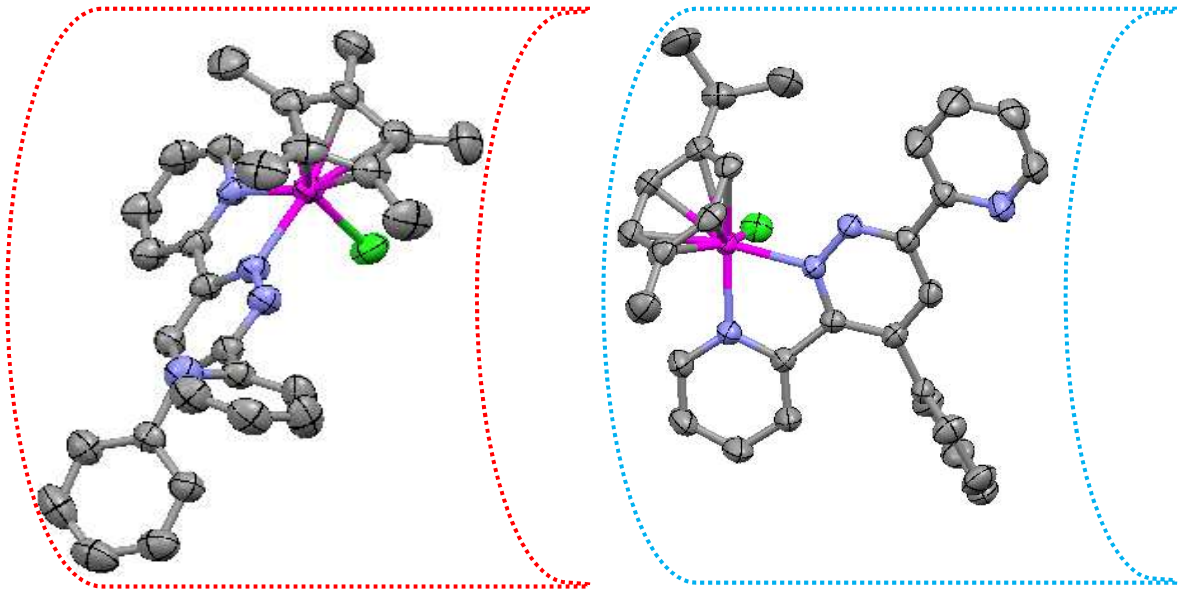

---

*The work presented in this chapter has been published: **K. T. Prasad**, B. Therrien and K. Mohan Rao, J. Organomet. Chem. 695 (2010) 707-716.

3.1 Introduction

Polypyridyl complexes of platinum group metals are being continuously investigated because of their multiple applications in fields of science including photophysics and photochemistry,[1-6] supramolecular chemistry,[7] catalysis[8 -11] and bioinorganic chemistry.[12-15] The organometallic complexes of η^6-arene ruthenium[16,17] and η^5-half-sandwich complexes of rhodium and iridium have attracted considerable current interest as potential anticancer agents (Dyson *et al.*).[12-15,18,19] Another important aspect, especially from the catalytic prospective, is the design of Ru=O functional groups and analogues capable of reversibly accepting multiple electrons and protons within a relatively small potential range.[20-22] This capacity to modify the environment in order to induce electronic as well as steric effects gives scope for the design and fabrication of tailored catalysts for specific reactions.

The properties of metal complexes largely depend on how the nature of the bridging ligand mediates metal–metal interactions. This role of bridging ligands is strongly influenced by factors such as the acceptor and donor properties of coordination sites, the length and rigidity of the spacers, the presence or absence of conjugated bonds, the orientation of substituents and the scope for manipulating ligand charge. In this regard, bridging polypyridyl ligands (*viz*. 2,2'-bipyrimidine (bpym), 2,3-bis(2-pyridyl)pyrazine (bppz), 3,5-bis(2-pyridyl)-1,2,4,5-tetrazine (bptz), 3,6-bis(2-pyridyl)pyridazine (bppn), and 2,4,6-tris(2-pyridyl)-1,3,5-triazine ligands) have received much attention.[23-25] The wider family of such ligands with 4- or 4,5-substituted pyridazine moieties (*viz*., 3,6-bis(2-pyridyl)-4-phenylpyridazine (L^{ph}) (figure 3.1) has been relatively less studied. More recently, Constable and co-workers published a few reports on silver(I) complexes[26-29] incorporating such ligands.

Symmetrical 3,5-bis(2-pyridyl)-1,2,4,5-tetrazine (bptz) and to a lesser extent 3,6-bis(2-pyridyl)pyridazine (bppn) frequently bind *via* any two of the four nitrogen atoms present (N1 and N2 or N3 and N4) on the pyridine and tetrazine/pyridazine moieties, employing a bidentate κ^2 bonding mode to coordinate with d^6 metal centers.[30,31] A phenyl substituent introduces an element of asymmetry in the 3,6-bis(2-pyridyl)pyridazine (L) ligand moiety, as shown by the 3,6-bis(2-pyridyl)-4-phenylpyridazine (L^{ph}) ligand. This can bind to a metal *via* atoms N1 and N2 (*type-A*) or atoms N3 and N4 (*type-B*) (see figure 3.2) in a bidentate κ^2 bonding mode. The ligand is a four electron donor since the

phenyl substituent creates differences in the electronic environment on the two available binding sites. Apart from the above two possibilities (*type-A or type-B*) (figure 3.2), a combination of the two types (*type-A* + *type-B*) for the same compound is also possible, but not treated in this research.

The reaction of 3,6-bis(2-pyridyl)-4-phenylpyridazine (L^{ph}) with $[(\eta^6\text{-arene})Ru(\mu\text{-}Cl)Cl]_2$ (arene = C_6H_6 and *p*-$^{i}PrC_6H_4Me$), $[(\eta^5\text{-}C_5Me_5)Ir(\mu\text{-}Cl)Cl]_2$ and $[(\eta^5\text{-}Cp)Ru(PPh_3)_2Cl]$ (Cp = C_5H_5, C_5Me_5 and C_9H_7) led to the formation of *type-A* mononuclear complexes. Use of $[(\eta^6\text{-}C_6Me_6)Ru(\mu\text{-}Cl)Cl]_2$ and $[(\eta^5\text{-}C_5Me_5)Rh(\mu\text{-}Cl)Cl]_2$ led to the formation of *type-B* complexes. The third possibility (combination of *type-A* and *type-B*) was not borne out in this work. The nature of the bonding modes for the above complexes was elucidated here through NMR and X-ray crystallography. In addition to these studies, we have performed DFT calculations on the complexes **2**, **3**, **4**, **5** and **6** in order to better understand the nature of the bonding modes in the ruthenium, rhodium and iridium complexes with L^{ph}.

To the best of our knowledge, there are yet no reports on half-sandwich platinum group metal complexes with the L^{ph} ligand. The successful formation here of such mononuclear complexes gives promising scope for the development of *metallo-ligands* or *synthons* based on organometallic systems. Another important factor is the presence of a phenyl ring on the ligand backbone. In the absence of this feature (*viz,*. with the 3,6-bis(2-pyridyl)pyridazine ligand), we were unable to obtain stable and acceptable yields of both mononuclear as well as dinuclear complexes. Due to this, some research groups had suspended further work on such systems, notably those striving to prepare water oxidation catalysts using this ligand.[32]

We here report the synthesis of eight new platinum group metal complexes having arenes, Cp* and 3,6-bis(2-pyridyl)-4-phenylpyridazine (L^{ph}) as ligands, all characterized by IR, NMR, mass spectrometry and UV/visible spectroscopy. The complexes and free ligands were also subjected to density functional theory (DFT) calculations. Molecular structures of three representative complexes (derived from X-ray cryatal data) are presented as well.

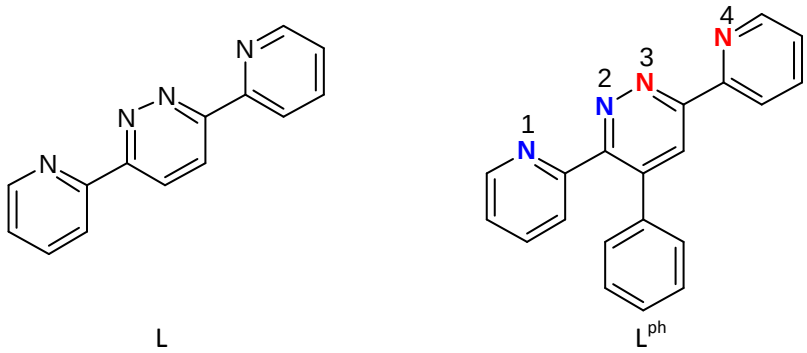

Figure 3.1: Unsubstituted 3,6-bis(2-pyridyl)pyridazine (L) and substituted 3,6-bis(2-pyridyl)-4-phenylpyridazine (L^{ph}).

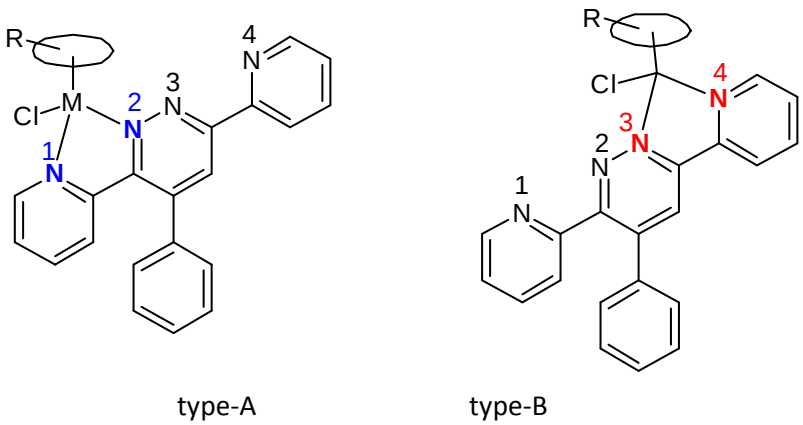

Figure 3.2: The two types of complexes [^{R}⬭M(L^{ph})X]$^{+}$ (M=Ru, Rh and Ir).

3.2 Experimental

3.2.1 Preparation of ligand 3,6-bis(2--pyridyl)-4-phenylpyridazine (L^{ph})[33]

One gram of 3,6-bis(2-pyridyl)1,2,4,5-tetrazine was added to a solution of 0.50 g of phenylacetylene in 25 ml. of toluene. The resulting mixture was refluxed overnight. After this time the red color of the tetrazine had disappeared. The solid residue which remained after removal of the solvent was recrystallized from ethanol to give 0.90 g. (68%) of color less needles, m. p. 177.5-178.5° C.

Anal. Calc. for $C_{20}H_{14}N_4$ C, 77.40; H, 4.55. Found: C, 77.24; H, 4.66: ^{1}H NMR (CD_3CN, δ): 8.81 (d, 1H), 8.74 (d, 1H), 8.67 (s, 1H), 8.49 (d, 1H), 7.93 (t, 2H), 7.83 (t, 2H), 7.42 (t, 1H), 7.34 -7.26 (m, 5H).

3.2.2 General procedure for preparation of mononuclear complexes **1 –3**

A mixture of $[(\eta^6\text{-arene})Ru(\mu\text{-}Cl)Cl]_2$ (arene = C_6H_6, *p*-$^{i}PrC_6H_4Me$ and C_6Me_6) (0.07 mmol), ligand L^{ph} (0.15 mmol) and 2.5 equivalents of NH_4PF_6 in dry methanol (15 ml) was stirred at room temperature for 6 hours. The precipitate was separated by filtration, washed with cold methanol, diethyl ether and dried under vacuum.

*3.2.2.1 $[(\eta^6\text{-}C_6H_6)Ru(L^{ph})Cl]PF_6$ [**1**]*

Orange-yellow solid, Yield 80 mg (89%): $C_{26}H_{20}ClN_4RuPF_6$ (669.5) Calc.: C 46.61, H 3.01, N 8.36; Found: C 46.68, H 3.18, N 8.48: ^{1}H NMR (400 MHz, CD_3CN, 25°C): δ = 9.57 (d, 1H, J_{H-H} = 5.58 Hz), 8.86 (d, 1H, J_{H-H} = 8 Hz), 8.64 (s, 1H), 8.49 (d, 1H), 8.28 (td, 1H), 8.08 (td, 2H), 7.71 (td, 1H), 7.53-7.51 (m, 5H), 7.25 (d, 1H), 6.18 (s, 6H, C_6H_6) ppm; ESI-MS (m/z): 525.1 (100%) $[M\text{-}PF_6]^+$, 489.1 (10%) $[M\text{-}PF_6\text{-}Cl]^+$; IR (KBr, cm^{-1}): $\nu_{(P\text{-}F)}$ 844s; 558m.

*3.2.2.2 $[(\eta^6\text{-}p\text{-}^{i}PrC_6H_4Me)Ru(L^{ph})Cl]PF_6$ [**2**]*

Dark orange solid, Yield 80 mg (89%): $C_{30}H_{28}ClN_4RuPF_6$ (726.05) Calc.: C 49.63, H 3.89, N 7.72; Found: C 50.08, H 3.78, N 7.95: ^{1}H NMR (400 MHz, CD_3CN, 25°C): δ = 9.42 (d, 1H, J_{H-H} = 5.60 Hz), 8.78 (dd, 2H, J_{H-H} = 8 Hz), 8.67 (s, 1H), 8.15(dt, 1H), 7.75 (td, 1H), 7.58-7.63 (m, 5H),7.43 (td, 2H), 7.20 (d, 1H, J_{H-H} = 8Hz), 6.04 (d, 1H), 6.01 (d, 1H), 5.85 (d, 1H), 5.81 (d, 1H), 2.82 (sept, 1H, $CH(CH_3)_2$), 2.28 (s, 3H, CH_3), 1.18 (d, 3H, $CH(CH_3)_2$), 1.14 (d, 3H, $CH(CH_3)_2$) ppm; ESI-MS (m/z): 580.8 (100%) $[M\text{-}PF_6]^+$, 544.7 (20%) $[M\text{-}PF_6\text{-}Cl]^+$; IR (KBr, cm^{-1}): $\nu_{(P\text{-}F)}$ 842s; 558m.

*3.2.2.3 $[(\eta^6\text{-}C_6Me_6)Ru(L^{ph})Cl]PF_6$ [**3**]*

Orange-yellow solid, yield 80 mg (89%): $C_{32}H_{32}ClN_4RuPF_6$ (754.1) Calc.: C 50.97, H 4.28, N 7.43; Found: C 51.08, H 4.31, N 7.29. ^{1}H NMR (400 MHz, CD_3CN, 25°C): δ = 8.91 (d, 1H, J_{H-H} = 5.58 Hz), 8.82 (d, 1H, J_{H-H} = 8 Hz), 8.67 (s, 1H), 8.59 (d, 1H, J_{H-H} =8 Hz), 8.04 (td, 1H), 7.67-7.61 (m, 7H), 7.53 (td, 2H), 2.18 (s, 18H, $C_6(Me)_6$) ppm; ESI-MS (m/z): 608.9 (100%) $[M\text{-}PF_6]^+$, 573.6 (30%) $[M\text{-}PF_6\text{-}Cl]^+$; IR (KBr, cm^{-1}): $\nu_{(P\text{-}F)}$ 845s; 558m.

3.2.3 General procedure for preparation of mononuclear complexes **4** and **5**

A mixture of $[(\eta^5\text{-}C_5Me_5)M(\mu\text{-}Cl)Cl]_2$ (M = Rh, Ir) (0.07 mmol), ligand L^{ph} (0.18 mmol) and 2.5 equivalents of NH_4PF_6 in dry methanol (15 ml) was refluxed for 4 hours.

The reaction mixture was cooled overnight at room temperature, during which time the crystalline compound was formed. It was separated by filtration, washed with cold methanol, diethyl ether and dried under vacuum.

*3.2.3.1 [(η^5-C_5Me_5)Rh(L^{ph})Cl]PF_6 [**4**]*

Dark yellow color, yield 80 mg (77%): $C_{30}H_{29}ClN_4RhPF_6$ (728.9) Calc.: C 49.43, H 4.01, N 7.69; Found: C 50.10, H 3.99, N 7.65. ^{1}H NMR (400 MHz, $CDCl_3$, 25°C): δ = 8.91 (d, 1H, J_{H-H} =8 Hz), 8.59 (d, 1H), 8.41 (s, 1H), 8.39 (d, 1H), 8.19 (td,1H), 7.81 (m, 2H), 7.68 (d, 1H), 7.66 -7.61 (m, 5H), 7.40 (d, 1H), 1.77 (s, 15H, C_5Me_5) ppm; ESI-MS (m/z): 583.1 (100%) $[M-PF_6]^+$, 558.1 (23%) $[M-PF_6-Cl]^+$; IR (KBr, cm^{-1}): $\nu_{(P-F)}$ 845s; 558m.

*3.2.3.2 [(η^5-C_5Me_5)Ir(L^{ph})Cl]PF_6 [**5**]*

Dark yellow color, yield 70 mg (83%): $C_{30}H_{29}ClN_4IrPF_6$ (818.2) Calc.: C 44.04, H 3.57, N 6.85; Found: C 44.10, H 3.59, N 6.79; ^{1}H NMR (400 MHz, $CDCl_3$, 25°C): δ = 9.30 (d, 1H, J_{H-H} = 8 Hz), 8.88 (dd, 2H, J_{H-H} = 6.8 Hz), 8.71 (s, 1H), 8.45 (td, 1H), 8.22 (td, 2H), 7.84 (td, 1H), 7.75 to 7.67 (m, 5H), 7.53 (d, 1H), 1.68 (s, 15H, C_5Me_5) ppm; ESI-MS (m/z): 673.3 (100%) $[M-PF_6]^+$, 638.1 (32%) $[M-PF_6-Cl]^+$; IR (KBr, cm^{-1}): $\nu_{(P-F)}$ 845s; 558m.

3.2.4 General procedure for preparation of mononuclear complexes **6** to **8**

A mixture of [(Cp)Ru(PPh_3)$_2$Cl] (Cp = C_5H_5, C_5Me_5, C_9H_7) (0.07 mmol), ligand L^{ph} (0.08 mmol) and 1.5 equivalents of NH_4PF_6 in dry ethanol (15 ml) was refluxed for 14 hours. The color changed from a dark yellow to a dark red color. The reaction mixture was cooled over-night at room temperature during which time the crystalline compound was formed. Some of the crystals were found suitable for X-ray crystal study. The product was separated by filtration, washed with cold ethanol, diethyl ether and dried under *vacuo*.

*3.2.4.1 [(η^5-C_5H_5)Ru(L^{ph})(PPh_3)]PF_6 [**6**]*

Orange color, yield 60 mg (63%): $C_{43}H_{34}ClN_4RuP_2F_6$ (888.2) Calc.: C 58.14, H 3.86, N 6.31; Found: C 58.11, H 3.90, N 6.59. ^{1}H NMR (400 MHz, $CDCl_3$, δ) 9.50 (d, 1H), 8.75 (d, 1H), 8.72 (d, 1H), 8.21 (s, 1H), 8.14 (td,1H), 7.57 (td, 1H), 7.37 (td, 1H),

7.30-7.20 (m, 20H),7.14 (td, 1H) 6.78 (d, 1H), 4.83 (s, 5H, C_5H_5) ppm; $^{31}P\{^1H\}$ = 46.12 ppm.; ESI-MS (m/z): 743.5 (100%) $[M\text{-}PF_6]^+$; IR (KBr, cm^{-1}): $\nu_{(P\text{-}F)}$ 842s; 527m.

*3.2.4.2 [(η^5-C_5Me_5)Ru(L^{ph})(PPh_3)]PF_6 [**7**]*

Orange color, yield 68 mg (60%): $C_{48}H_{44}ClN_4RuP_2F_6$ (958.38) Calc.: C 60.16, H 4.63, N 5.85; Found: C 60.11, H 4.69, N 5.74. ^1H NMR (400MHz, $CDCl_3$, 25°C): δ = 9.07 (d, 1H), 8.89 (d, 1H), 8.81 (td, 1H), 8.25 (s, 1H), 8.17 (td, 1H), 7.51-7.12 (m, 23H), 6.76 (d, 1H), 4.90 (s, 5H, C_5Me_5) ppm; $^{31}P\{^1H\}$ = 45.25 ppm; ESI-MS (m/z): 818.1 (100%) $[M\text{-}PF_6]^+$; IR (KBr, cm^{-1}): $\nu_{(P\text{-}F)}$ 844s; 527m.

*2.2.4.3 [(η^5-C_9H_7)Ru(L^{ph})(PPh_3)]PF_6 [**8**]*

Yellowish brown color, yield 70 mg (83%): $C_{47}H_{36}ClN_4RuP_2F_6$ (938.3) Calc.: C 60.16, H 3.87, N 5.97; Found: C 60.11, H 3.89, N 5.99. ^1H NMR (400 MHz, $CDCl_3$, 25°C): δ = 9.68 (d, 1H), 8.76 (d, 1H), 8.69 (d, 1H), 8.20 (s, 1H), 8.12 (td, 2H), 7.94 (td, 2H) 7.63 (td, 1H), 7.22-7.55 (m, 24H, 4Ph), 4.87(t, 1H), 4.71 (d, 2H) ppm; $^{31}P\{^1H\}$ = 48.42 ppm; ESI-MS (m/z): 789.4 (100%) $[M\text{-}PF_6]^+$; IR (KBr, cm^{-1}): $\nu_{(P\text{-}F)}$ 841s; 548m.

3.3 Results and Discussion

3.3.1 Syntheses

The dinuclear arene-ruthenium complexes $[(\eta^6\text{-arene})Ru(\mu\text{-}Cl)Cl]_2$ (arene = C_6H_6, *p*-^{i}PrC_6H_4Me and C_6Me_6) react with two equivalents of 3,6-bis(2-pyridyl)-4-phenylpyridazine (L^{ph}) in methanol, being stirred at room temperature in the presence of NH_4PF_6 to form the mononuclear areneruthenium complex cations $[(\eta^6\text{-}C_6H_6)Ru(L^{ph})Cl]^+$ (**1**), $[(\eta^6\text{-}p\text{-}^i PrC_6H_4Me)\ Ru(L^{ph})Cl]^+$ (**2**), and $[(\eta^6\text{-}C_6Me_6)Ru(L^{ph})Cl]^+$ (**3**) (Scheme 3.1) and isolated as their hexafluoro-phosphate salts. The metal atom bonds to the L^{Ph} ligand through the N1 and N2 atoms in the *type-A* complexes **1** and **2**, while in the *type-B* complex **3** the metal bonds through the N3 and N4 atoms of the ligand.

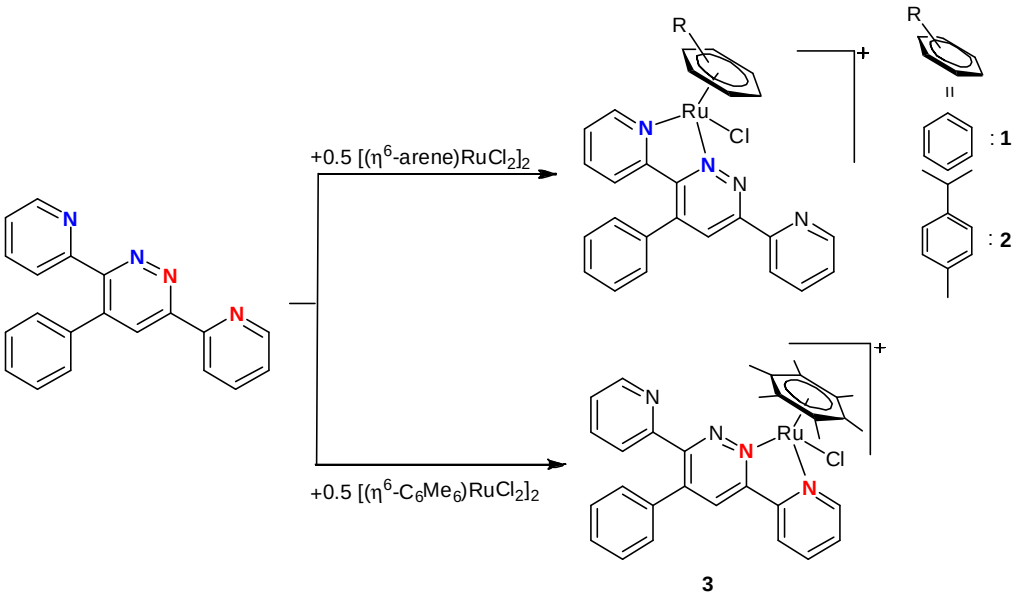

Scheme 3.1

Similarly, reacting the dimeric chloro-bridged complexes $[(\eta^5\text{-}C_5Me_5)M(\mu\text{-}Cl)Cl]_2$ (M = Rh, Ir) with the same L^{ph} ligand at 50° C leads to the formation of the mononuclear cationic complexes $[(\eta^5\text{-}C_5Me_5)Rh(L^{ph})Cl]^+$ (**4**) and $[(\eta^5\text{-}C_5Me_5)Ir(L^{ph})Cl]^+$ (**5**) (Scheme 3.2), isolated as their hexafluorophosphate salts. The metal atom bonded to the L^{Ph} ligand through the N3 and N4 atoms in the *type-B* complex **4**, while in the *type-A* complex **5** the metal bonded *via* the N1 and N2 atoms of the ligand.

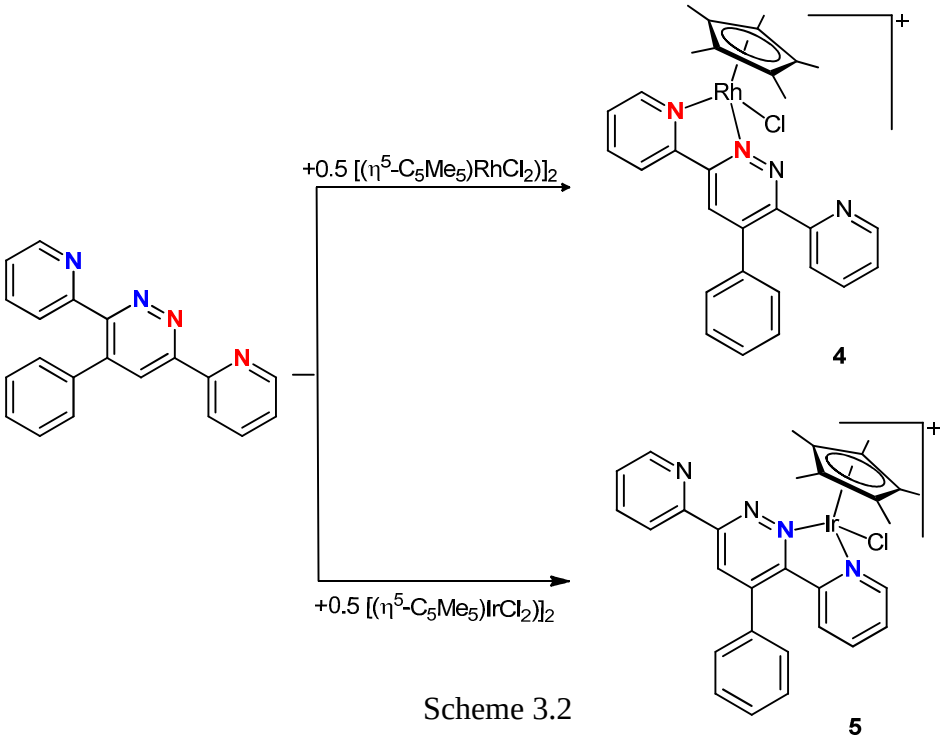

Scheme 3.2

The complexes $[(\eta^5\text{-}C_5H_5)Ru(PPh_3)_2Cl]$, $[(\eta^5\text{-}C_5Me_5)Ru(PPh_3)_2Cl]$ and $[(\eta^5\text{-}C_9H_7)Ru(PPh_3)_2Cl]$ reacted with the same L^{ph} ligand in ethanol at 60°C to form the mononuclear complex cations $[(\eta^5\text{-}C_5H_5)Ru(L^{ph})PPh_3]^+$ (**6**), $[(\eta^5\text{-}C_5Me_5)Ru(L^{ph})PPh_3]^+$ (**7**) and $[(\eta^5\text{-}C_9H_7)Ru(L^{ph})PPh_3]^+$ (**8**) (Scheme 3.3), isolated as their hexafluorophosphate salts. In all these *type-A* complexes the metal is bonded through the N1 and N2 atoms of the ligand.

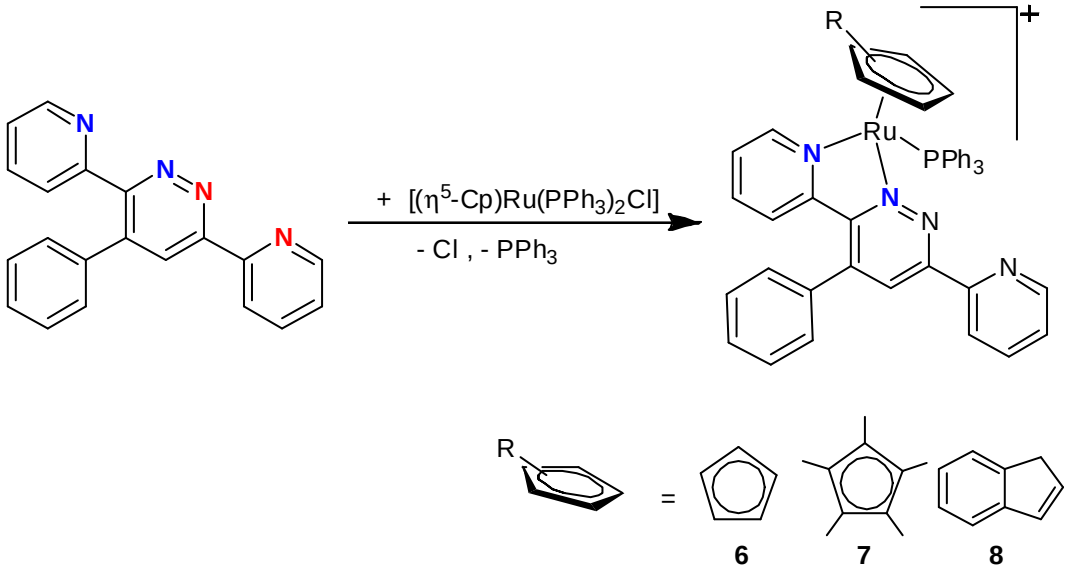

Scheme 3.3

Complexes **1**, **2** and **3** are orange-yellow, **4** and **5** are dark yellow, while **6**, **7** and **8** are orange-brown in color. All are non-hygroscopic, air-stable solids soluble in acetonitrile and partially soluble in dichloromethane, chloroform, methanol and acetone. All complexes have been characterized on the basis of elemental analyses, ^{1}H NMR, IR, UV-visible spectroscopy and mass spectrometry.

The infrared spectra of complexes **1 - 8** exhibit a strong band in the region 844–850 cm^{-1}, a typical $\nu_{P\text{-}F}$ stretching band for the PF_6 anions. Besides this, peaks were observed which correspond to the phenyl, pyridyl and pyridazine rings (C=C and C=N moieties). The mass spectra display peaks with *m/z* at 580, 525, 573, 554, 638, 743, 818 and 789, corresponding to the molecular ion M^+ peaks for complexes **1** to **8** respectively. For instance the mass spectra of the complexes 2 and 8 have been depicted in figure 3.3 and 3.4 respectively.

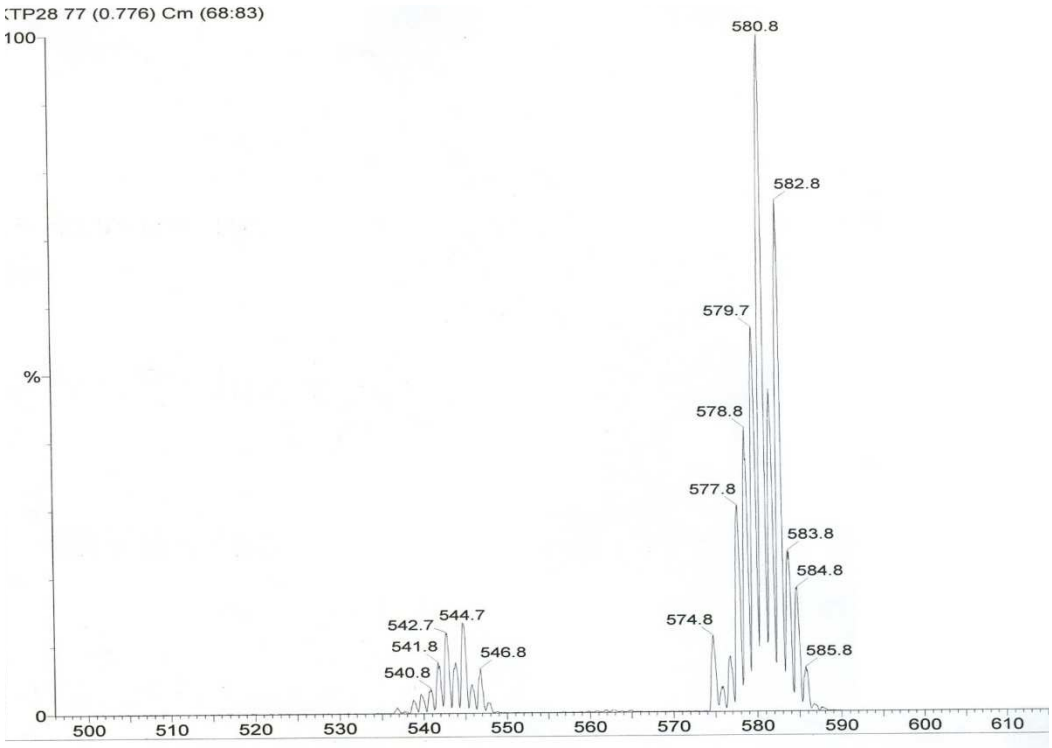

Figure 3.3: Mass spectrum of complex $[(\eta^6\text{-}p\text{-}^{i}PrC_6H_4Me)Ru(L^{ph})Cl]PF_6$ [**2**]

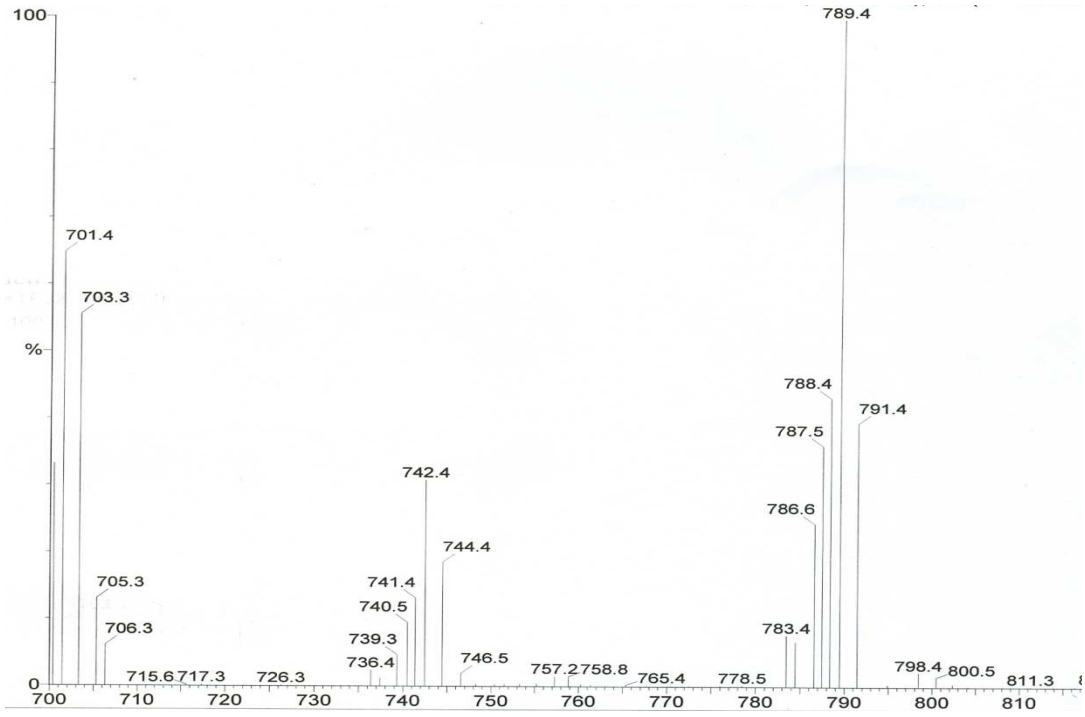

Figure 3.4: Mass spectrum of complex $[(\eta^5\text{-}C_9H_7)Ru(L^{ph})(PPh_3)]PF_6$ [**8**]

3.3.2 NMR studies

The ^{1}H NMR spectrum of the free (unbound) ligand L^{ph} exhibits resonances at δ 8.80 (d, 6-H), 8.74 (d, 6'-H), 8.67 (s, 9-H), 8.49 (d, 3-H) 7.94 (td, 3',4-H), 7.80 (td, 4'-H), 7.44 (m, Ph-H), 7.34 (dd, 5-H), 7.28 (dd, 5'-H) in $CDCl_3$. Upon coordination with metal atoms, the ^{1}H NMR spectrum of the L^{ph} ligand protons exhibits two different sets of resonances for the two different types of complexes. The *type-A* complexes **1**, **2**, **5**, **6**, **7** and **8** show one type of spectral resonance (see figure 3.5), while the *type-B* complexes **3** and **4** show a different set of resonances (see figure 3.6) for the aromatic regions of the ligand.

Type-A: The ^{1}H NMR spectra of the Ru(II)L^{ph} and Ir(III)L^{ph} complexes **1**, **2** and **5** to **8** exhibit ten sets of resonances at ~ δ 9.54 (d, 6-H), 8.76 (d, 6'-H), 8.72 (d, 3-H), 8.21 (s, 9-H), 8.18 (td, 4-H), 7.57 (td, 4'-H), 7.37 (td, 5-H), 7.30 (m, ph-H), 7.15 (td, 5'-H) and 6.79 (d, 3'-H) ppm for the protons of the L^{ph} ligand in CD_3CN-d_3. The resonances of the protons 6, 6', 3 and 4 of ligand L^{ph} are shifted downfield by δ ~ 0.75, 0.10, 0.32 and 0.31 respectively with respect to the free ligand. As an example, the NMR spectrum of the *type-A* complex **6** is presented in figure 3.5.

Type-B: The ^{1}H NMR spectra of the Ru(II) and Rh(III) complexes $[(\eta^6\text{-}C_6Me_6)Ru(L^{ph})Cl]^+$ (**3**) and $[(\eta^5\text{-}C_5Me_5)Rh(L^{ph})Cl]^+$ (**4**) exhibit eight sets of resonances at δ = 8.91 (d, 6'-H), 8.82 (d, 6-H), 8.67 (s, 9-H), 8.59 (d, 3'-H), 8.04 (td, 4'-H), 7.67-7.61 (m, 5 & ph-H), 7.53 (td, 4& 5'-H) and δ = 8.91 (d, 6'-H), 8.59 (d, 6-H), 8.41 (s, 9-H), 8.39 (d, 3'-H), 8.19 (td, 4'-H), 7.81 (m, 4& 5'-H), 7.68 (d, 3-H), 7.66 -7.61 (m, 5 & ph-H) ppm in $CDCl_3$ (figure 3.6a, b). The resonances of protons 6', 9, 3' and 4' of the ligand are shifted downfield by δ ≈ 0.17, 0.01, 0.55 and 0.21 ppm respectively (with respect to the corresponding free L^{ph} protons) due to the inductive effect of the metal. The significant downfield shift of proton 9 of ligand L^{ph} reveals the formation of *type-B* complexes as compared to the previous type.

We choose to distinguish the two types of complex on the basis of NMR, and present the spectra of the type-B complexes **3** and **4** are depicted herein (figure 3.6 a, b). This furnishes the evidence for the formation of complex **3** with the *type-B* bonding mode in ruthenium complexes having the hexamethylbenzene co-ligand. This is not the case with ruthenium complexes having the η^6-*p*-^{i}PrC_6H_4Me and η^6-C_6H_6 co-ligands, where Ru-L^{Ph} bonding occurs in *type-A* fashion. Similar results for other complexes (based on

reactivity studies) were observed earlier in our research group, where complexes containing the hexamethylbenzene co-ligand contrast clearly with those containing the η^6-*p*-$^{i}PrC_6H_4Me$ and η^6-C_6H_6 ligands.[34, 35]

Furthermore, the aromatic regions of L^{ph} ligand signals of complex **2** exhibit a singlet at δ = 2.28 for the methyl protons, a septet at δ = 2.82 for the CH proton of the isopropyl group, two doublets for the diastereotopic methyl protons of the isopropyl group, and likewise four doublets for the diastereotopic CH protons of the *p*-cymene ligand. Complexes **1** and **3** exhibit a singlet for the protons of the benzene ring and protons of the hexamethylbenzene at δ 6.18 and 2.18 respectively. Complexes **4** and **5** exhibit a singlet for the methyl protons of the pentamethylcyclopentadienyl ligand at δ 1.77 and 1.68 respectively. Complexes **6** and **7** exhibit a singlet at δ 4.91 and 2.03 for the protons of the cyclopentadienyl ligand and the methyl protons of pentamethylcyclopentadienyl ligand respectively. Complex **8** exhibits three characteristic sets of signals (multiplet, triplet and doublet) for the protons of the indenyl ligand. The protons of the triphenylphosphine ligand exhibit a multiplet at δ 7.22 - 7.55. The $^{31}P\{^{1}H\}$ NMR spectra of complexes **6**, **7**, and **8** show chemical shifts at δ 46.12, 49.21, and 48.42 respectively, which indicate that each metal atom is bonded with a single triphenylphosphine ligand.

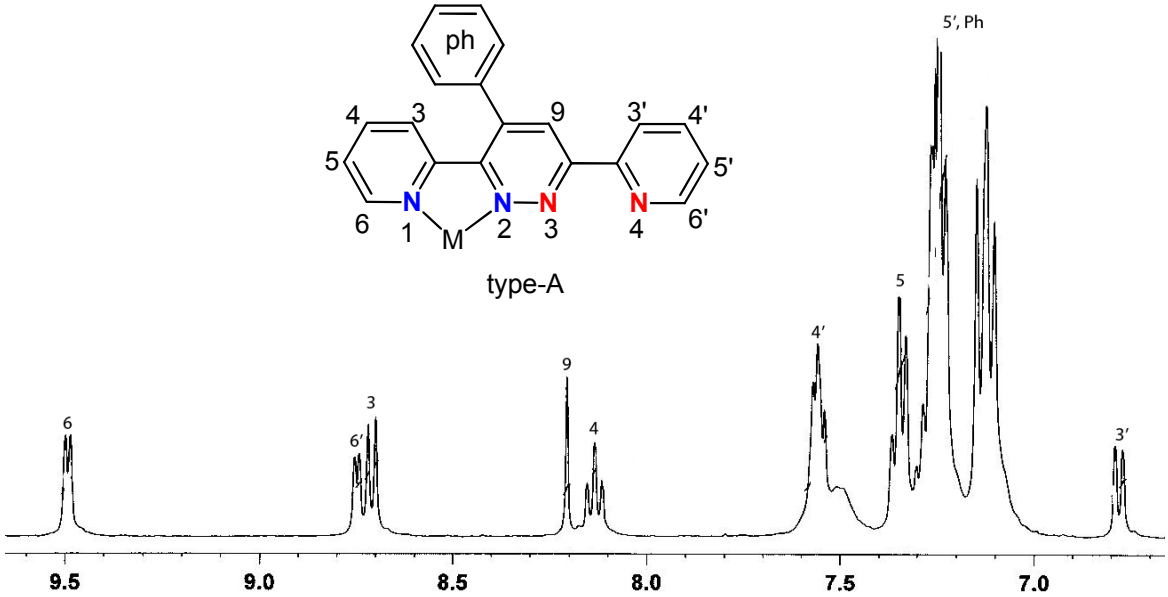

Figure 3.5: Aromatic region of the ^{1}H-NMR spectrum of complex **6** (*type-A*) in $CDCl_3$

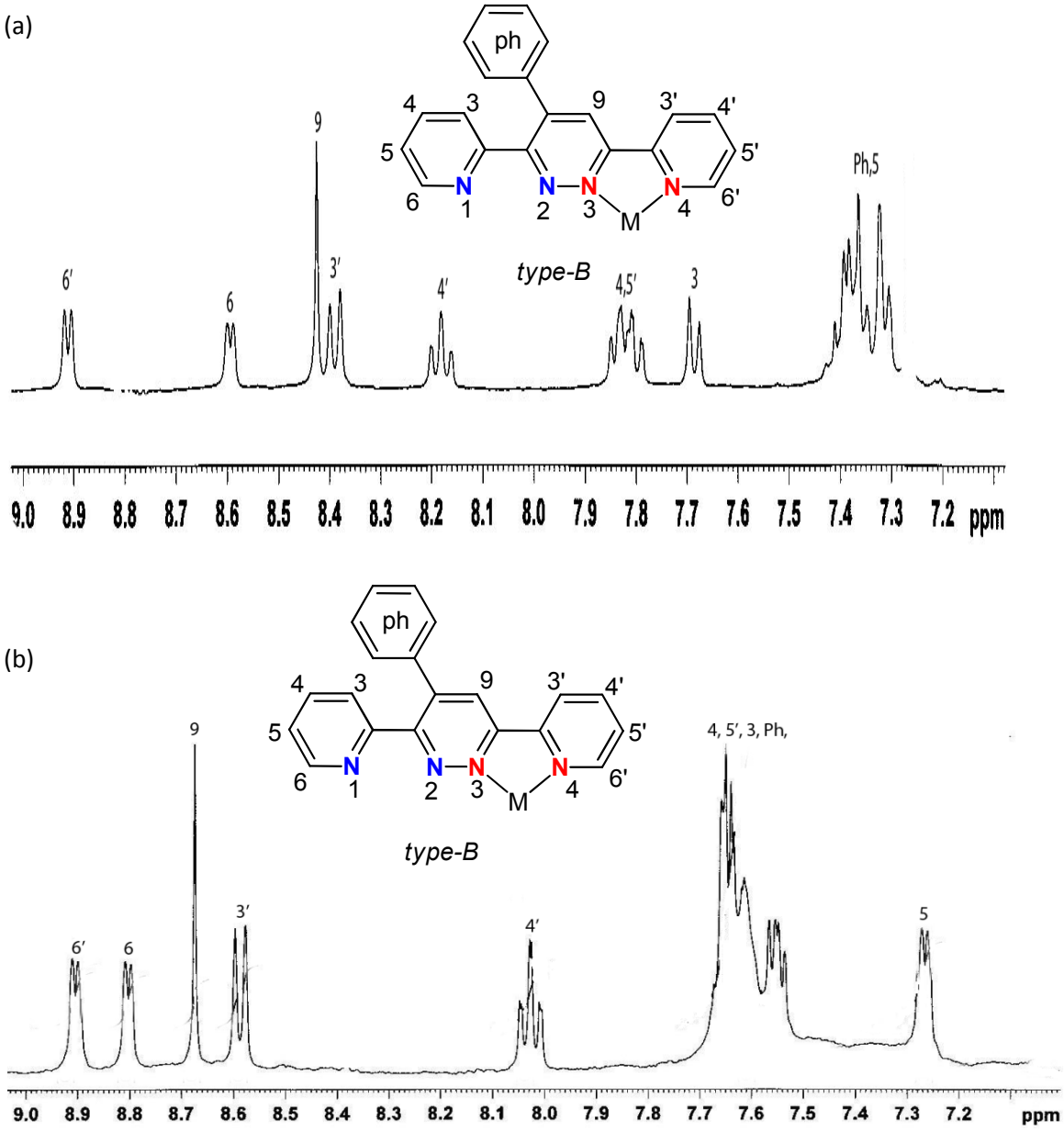

Figure 3.6: Aromatic regions of the ^{1}H-NMR spectra of (a) complex **4** (*type-B*)**;** (b) complex **3** (*type-B*) in $CDCl_3$.

3.3.3 Molecular structures

The molecular structures of $[(\eta^6\text{-}p\text{-}^{i}PrC_6H_4Me)Ru(L^{ph})Cl]^+$ **(2),** $[(\eta^5\text{-}C_5Me_5)Rh(L^{ph})Cl]^+$ (**4**) and $[(\eta^5\text{-}C_5H_5)Ru(L^{ph})(PPh_3)]^+$ (**6**) have been established by single-crystal X-ray analysis of their hexafluorophosphate salts (tables 3.1 and 3.2). The complexes show a typical piano-stool geometry with the metal centre coordinated to the arene ligand, to the chelating L^{ph} ligand, and to a terminal chloride in complexes **2** and **4** and triphenylphosphine in complex **6**. The metal atom is in an octahedral arrangement

with the two *cis*-nitrogen atoms of the L^{ph} ligand acting as a bidentate chelating ligand through the two neighboring pyridyl and pyridazinyl nitrogen atoms. In principle, in mononuclear complexes, tetradentate ligands such as L or L^{ph} can coordinate to the metal centre either through the N1 and N2 atoms (*type-A*) or the N3 and N4 atoms (*type-B*). It is fascinating to observe here that the crystal structures of complexes **2** and **6** are found to be N1, N2-coordinated (*type-A*), while the complex **4** is found to be N3, N4-coordinated (*type-B*) in a five-membered ring chelating fashion involving the nitrogen atom of the pyridine moiety and one nitrogen atom of the pyridazinyl moiety. This could be due to the steric interactions of arene ligands, electronic factors, the nature of the co-ligands, the oxidation state of the metal atom and the symmetry of the ligand. The nature of these bonding modes is studied here by density functional theory (see later). The solid state molecular structures of complexes **2**, **4** and **6** are shown in figures 3.7, 3.8 and 3.9 respectively, with the bond lengths and angles presented in table 3.1.

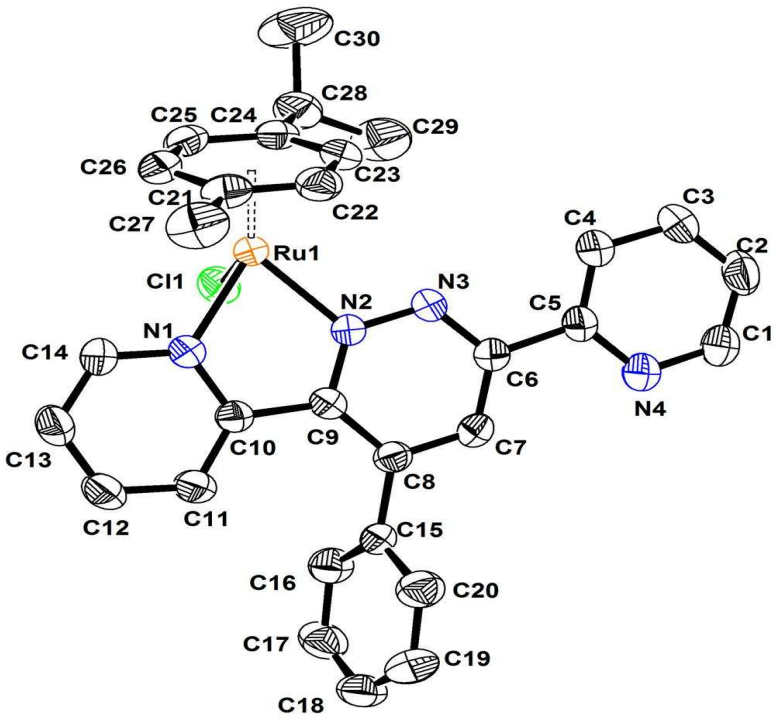

Figure 3.7: Molecular structure of a complex **2** at 35% probability level. Hydrogen atoms, chloroform molecule and hexafluorophosphate anion have been omitted for clarity.

In the mononuclear complexes **2, 4** and **6** the nitrogen-metal distances (2.073, 2.120 and 2.086 Å) associated with the pyridyl ligand are slightly longer than the

corresponding pyridazinyl ligand nitrogen-metal distance (2.045, 2.084 and 2.076 Å). These are comparable to those in the previously studied complexes [(η^6-*p*-^{i}PrC$_6$H$_4$Me)RuCl(2,3-bis(2-pyridyl)pyrazine)]BF$_4$,[36] [Rh$_2$(L-H)(NBD)(η^1-C$_7$H$_7$)(CH$_3$OH)(CH$_3$CN)](BF$_4$)$_2$,[37] and [(η^6-*p*-^{i}PrC$_6$H$_4$Me)Ru(2-(2-pyridyl)-1,8-naphthyridine)Cl]PF$_6$.[38] The Rh-N distances (2.120(3) and 2.084(3) Å) in **4** are slightly longer than the corresponding distances in complex **2** (2.073(3) and 2.045(2) Å) and complex **6** (2.076 and 2.086). The M-Cl bond lengths [2.387(10) and 2.384(13)] show no significant differences between values for the cations studied here and other reported values.[39]. The N-M-N bond angles [76.1(11)° in **2** and 76.0(13)° in **4** are similar in value to that [76.2(2)˚] observed in the complex [(η^6*p*-^{i}PrC$_6$H$_4$Me)RuCl(2,3-bis(α-pyridyl)quinoxaline)]$^+$.[40]

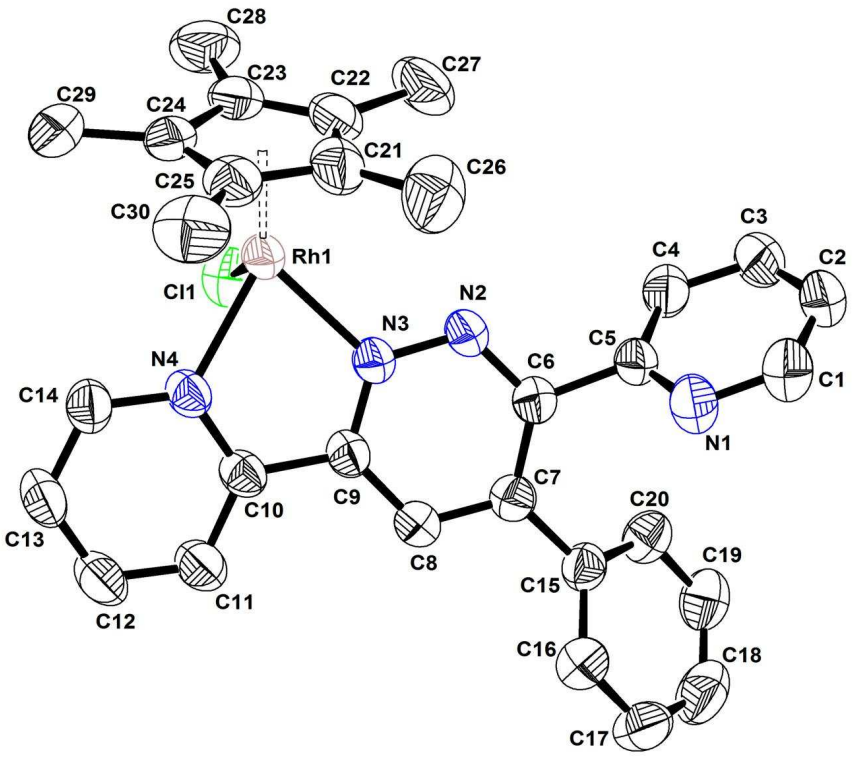

Figure 3.8: Molecular structure of complex **4** at 35% probability level. Hydrogen atoms and hexafluorophosphate anion have been omitted for clarity

In complex **2**, the distance between the ruthenium atom and the centroid of the η^6-*p*-^{i}PrC$_6$H$_4$Me ring is 1.693 Å. In complex **4**, the distance between the rhodium atom and the centroid of the η^5-C$_5$Me$_5$ ring is 1.789 Å, while the distance between the ruthenium atom and the η^5-C$_5$H$_5$ ring is 1.843 Å. These bond distances are comparable to those in

the related complex cations $[(\eta^6\text{-}p\text{-}^{i}PrC_6H_4Me)Ru(pyNp)Cl]PF_6$, $[(\eta^5\text{-}C_5Me_5)Ir(pyNp)\text{-}Cl]PF_6$ (PyNp=2-(2-pyridyl)-1,8-naphthyridine) (1.68 and 1.79 Å),[46] $[(\eta 5\text{-}C_5Me_5)RhCl\text{-}(C_5H_4N–2CH=N–C_6H_4\text{-}p\text{-}Cl)]^+$ [41] and $[Ru(\eta^5\text{-}C_5H_5)(PPh_3)(\kappa^2\text{-}paa)]^+$ and $[Ru(\eta^5\text{-}C_5H_5)\text{-}(\kappa^1\text{-}dppm)(\kappa^2\text{-}paa)]^+$ [42].

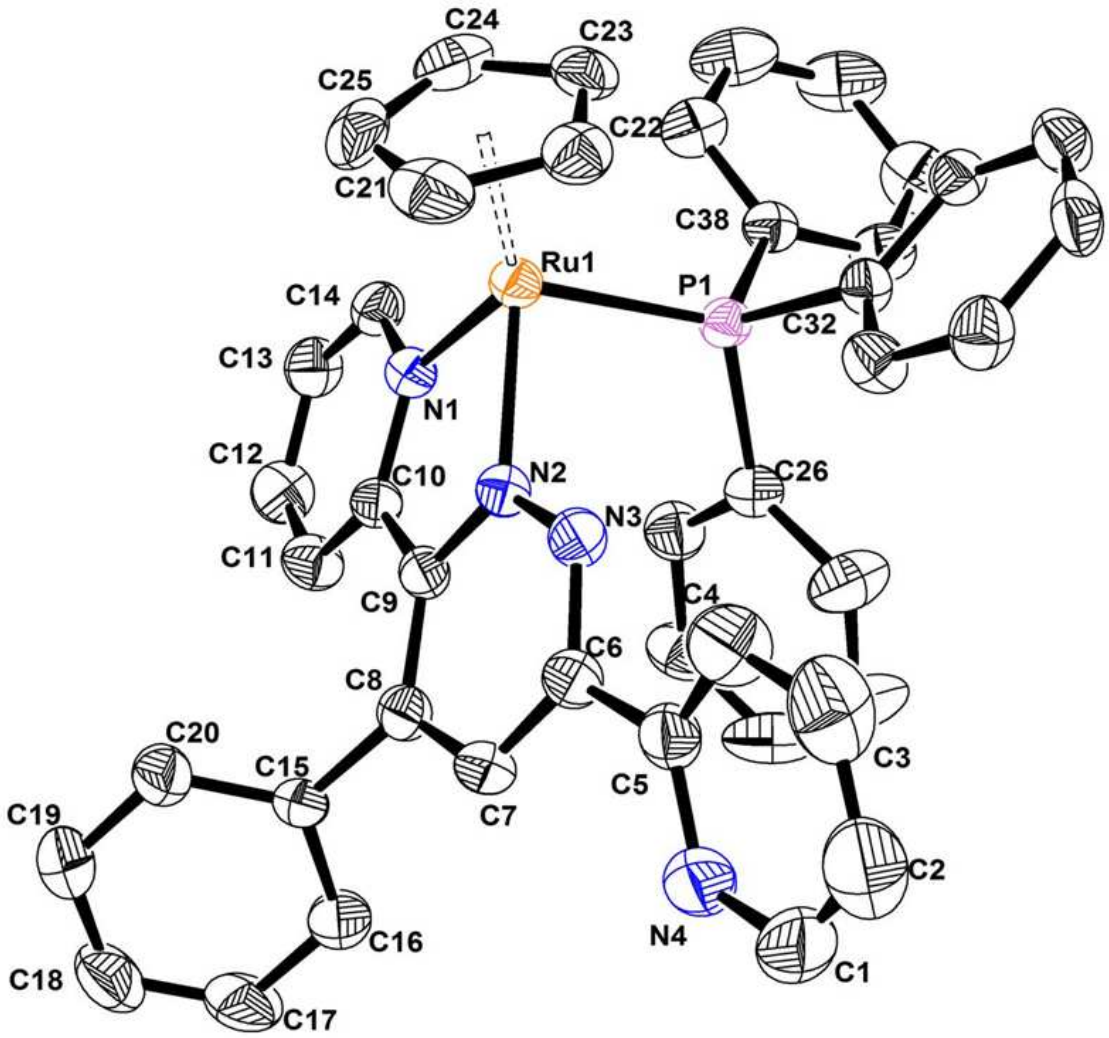

Figure 3.9: Molecular structure of complex **6** at 35% probability level. Hydrogen atoms and hexafluorophosphate anion have been omitted for clarity.

Table 3.1: Selected bond lengths (Å) and bonf angles (º) for complexes **2**, **6** and **4**.

	Complex **2**	Complex **6**	Complex **4**	
		Bond distances		
Ru-N1	2.073(3)	2.086(3)	Rh-N4	2.120(3)
Ru-N2	2.045(3)	2.076(3)	Rh-N3	2.084(3)
Ru-Cl1	2.387(10)	2.308(10)	Rh-Cl1	2.384(13)
Ru-centroid (arene)	1.693	1.843	Rh-centroid (Cp^* ring)	1.789
C9-C10	1.483(5)	1.466(5)	C9-C10	1.471(5)
C5-C6	1.479(5)	1.490(6)	C5-C6	1.500(5)
N2-N3	1.334(4)	1.340(4)	N3-N4	1.330(4)
		Bond angles		
N1-Ru-N2	76.11(11)	76.11(2)	N2-Rh-N3	76.00(13)
N1-Ru-Cl1	83.91(9)	95.75(9)	N4-Rh-Cl1	83.50(10)
N2-Ru-Cl1	84.95(8)	89.97(9)	N3-Rh-Cl1	88.73(10)
Ru1-N2-C9	119.83	118.9(3)	Rh1-N3-C9	117.99
Ru1-N2-N3	117.16	117.9(2)	Rh1-N3-N2	120.35
Ru1-N1-C10	117.61	116.7(2)	Rh1-N4-C10	116.03

Table 3.2: Crystallographic and structure refinement parameters for complexes **2**, **4** and **6**

Complex	**2**.$CHCl_3$	4	6
Chemical formula	$C_{31}H_{29}Cl_4N_4RuPF_6$	$C_{30}H_{29}ClN_4RhPF_6$	C_{43} H_{34} F_6 N_4 P_2 Ru
Crystal system	Triclinic	Monoclinic	Monoclinic
Space group	*P*-1 (no. 2)	*P* $2_1/n$ (no. 14)	P2(1)/c
Crystal color and shape	orange block	red block	red block
Crystal size (mm3)	0.23 x 0.17 x 0.16	0.28 x 0.23 x 0.18	0.50 x 0.26 x 0.15
a (Å)	10.4283(19)	9.244(3)	10.1059(2)
b (Å)	11.247(2)	14.147(5)	20.6495(4)
c (Å)	15.491(3)	23.425(8)	18.8735(4)
α (°)	85.104(3)		
β (°)	81.287(3)	95.900(6)	94.3950(10)
γ (°)	71.700(3)		
V ($Å^3$)	1703.8(5)	3047.4(18)	3926.97(14)
Z	2	4	4
T (K)	173(2)	173(2)	293(2) K
D_x (g /cm^3)	1.648	1.589	1.495
μ (mm^{-1})	0.883	0.765	0.546
Scan range (°)	$2.28 < \theta < 25.95$	$2.26< \theta < 25.60$	$1.46< \theta <28.29$
Unique reflections	6597	5963	9046
Reflections used [I>2σ(I)]	5719	4684	5505
R_{int}	0.0260	0.0426	0.0376
Final R indices [I>2σ(I)][c]	0.0452, wR_2 0.1264	0.0496, wR_2 0.1267	0.0568, wR2 = 0.1560
R indices (all data)	0.0518, wR_2 0.1323	0.0642, wR_2 0.1355	0.1004, wR2 = 0.1778
Goodness-of-fit	1.005	1.068	1.048
Max, Min Δρ (e $Å^{-3}$)	0.864, -0.710	0.807, -0.543	0.953, -0.797

[c]Structures were refined on F_0^2: $wR_2 = [\Sigma [w(F_0^2 - F_c^2)^2] / \Sigma w(F_0^2)^2]^{1/2}$, where $w^{-1} = [\Sigma (F_0^2) + (aP)^2 + bP]$ and $P = [\max(F_0^2, 0) + 2F_c^2]/3$

3.3.4 Theoretical calculations

All calculations on the molecular species studied were carried out using the B3LYP DFT method and different basis sets. All species were subjected to full geometry optimization.

3.3.4.1 L and L^{ph} ligand structures

We have performed DFT calculations using the B3LYP/6-31+G** strategy to determine the effect of the phenyl substituent on the nitrogen atoms of the central pyridazine and pyridine rings. Firstly, both the ligands L and L^{ph} in their free state were optimized in the low-energy *anti* orientation (figure 3.10; a, c). Since these ligands occur in the *syn* conformer in complexes **2**, **4** and **6**, they were also optimized in the higher energy *syn* orientation (figure 3.10; b, d). The *anti* conformer of L is planar but the *syn* conformer is non-planar with the N-C-C-N dihedral being 83.8° (table 3.3). On the other hand, both *anti* and *syn* orientations of L^{ph} are non-planar, due to the effect of the phenyl substituent on the central pyridazine ring. The dihedral angles N1-C2-C3-N2 and N3-C6-C7-N4 are respectively found to be 141.3°and 179.2° for *anti* L^{Ph}, and -62.9°and -47.2° for *syn* L^{Ph} (table 3.3). These values are very close to the experimental values.[26] In terms of energy, *anti* L is 14.33 kcal / mol more stable than *syn* L while *anti* L^{ph} is 9.68 kcal/mol (table 3.4) more stable than *syn* L^{ph}. The coordinated L^{ph} ligand in complexes **2** and **4** is in the *syn* conformation.

Table: 3.3. Select bond lengths and dihedral angles for *syn* and *anti* L^{ph} conformations.

	N2-N3	C2-C3	C4-C8	C6-C7	N1-C2-C3-N2	N3-C6-C7-N4
syn-L^{ph}	1.324	1.498	1.487	1.489	-62.9°	-47.2°
anti-L^{ph}	1.323	1.492	1.489	1.489	141.3°	179.2°

Table: 3.4: Total energies (in atomic units) of ligands L and Lph with syn and anti conformations and the energy difference between the two conformations

Ligands	Syn	anti	Difference (kcal/mol)
L	-758.511886	-758.534796	-14.37
L^{ph}	-989.579921	-989.595354	-9.68

The electronic charges on the nitrogen atoms in the *anti* L^{ph} conformation reveal that atoms N3 and N4 have more negative charge than atoms N1 and N2 (see figure 3.10; c). This suggests that presence of the phenyl group affects the electronic charges on the four nitrogen atoms as well as the dihedral angles of the pyridine and pyridazine rings, so that the N3-N4 (*type-B*) binding site is more electron rich than the N1-N2 (*type-A*) bonding site.

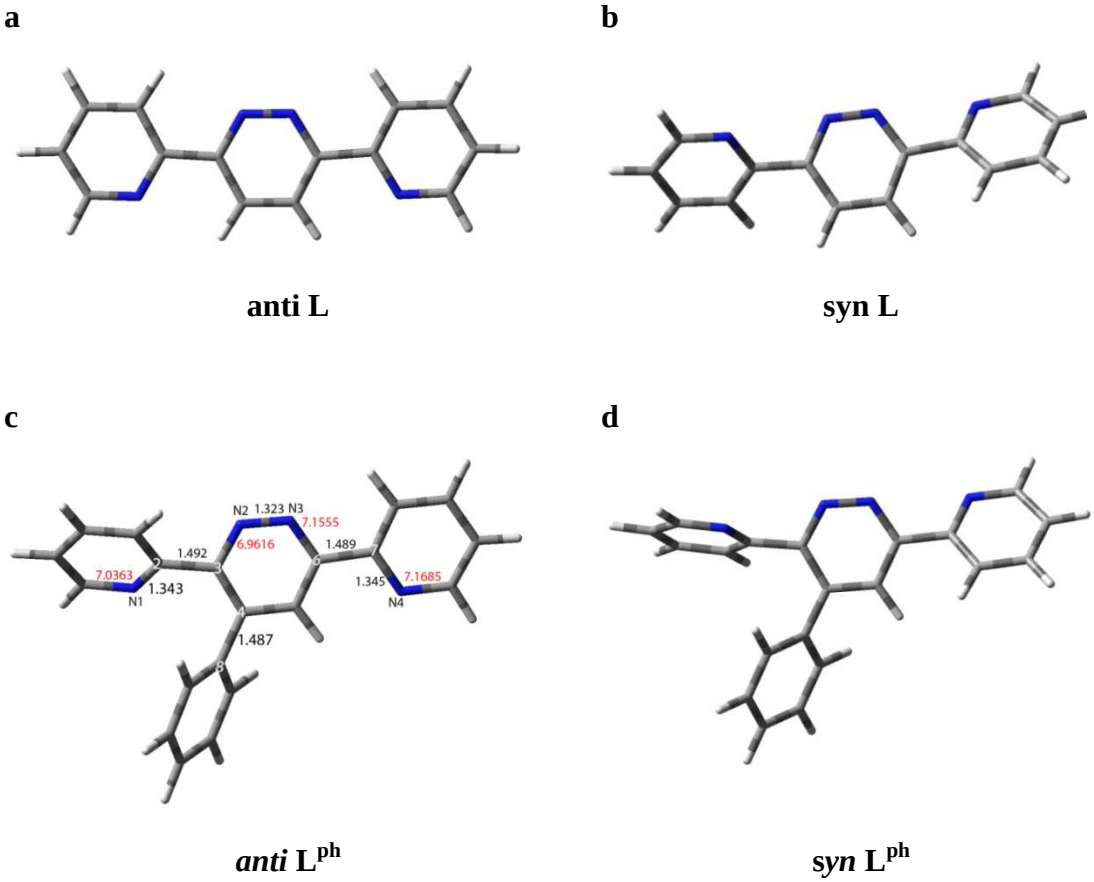

Figure 3.10: B3LYP/6-31+G** geometry optimization for (a) L in the *anti* orientation, (b) L in the *syn* orientation, (c) L^{ph} in the *anti* orientation and (d) L^{ph} in the *syn* orientation. Values with red color indicate the electronic charges corresponding to N atoms.

3.3.4.2 Structures of complexes

In order to gain further insight into the bonding modes in the ruthenium, rhodium and iridium complexes, we have carried out a detailed investigation using density functional theory. The key findings are described in the following sections.

B3LYP/LanL2DZ calculations with full geometry optimization were undertaken for the cationic species **2**, **4** and **6** in both *type-A* and *type-B* bonding modes as depicted in figure 3.11, where the crystal structure geometries provided the starting input for

optimization. The other species **3** and **5** were subjected to calculation using appropriate modifications of the geometries of **2**, **4** and **6**. The calculated geometrical parameters of the above complexes (table 3.5) are found to be in close agreement with the experimental values obtained from X-ray crystallographic study (table 3.1). From table 3.5 we can see that the positions of binding have discernible effects on the stability and geometrical structure of the complexes. Comparing the computed results of the parent complexes **2**, **3**, **4**, **5**, **6** with the experimental data (see table 3.1), we find that the computed coordination bond lengths (Ru-N) are shorter than the corresponding experimental value by 1 - 3 %, the largest differences being found for the metal-arene carbon distances.[43] Computed coordinated bond angles are wider by 2 % than those found experimentally. At the same time, the computed mean bond lengths C-C(N) of the ligand skeletons of these complexes are close to the general bond lengths. We thereby deduce that the structures obtained from these DFT calculations are reliable.

2A

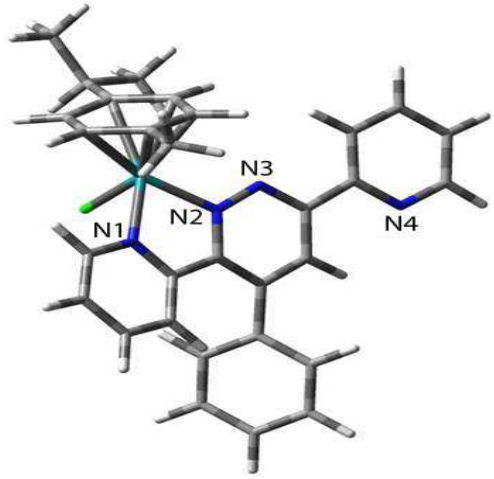

2B

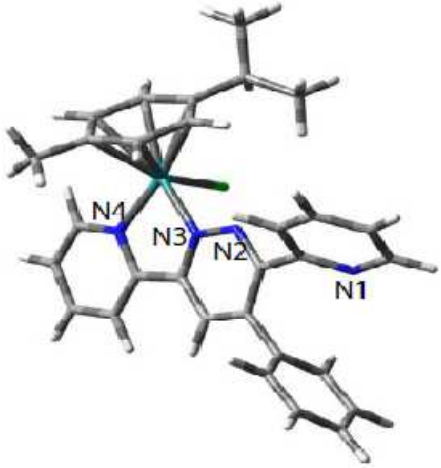

3A

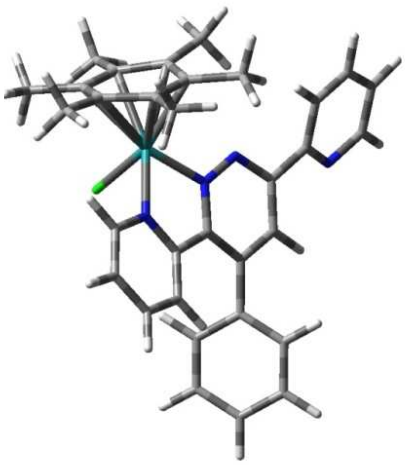

3B

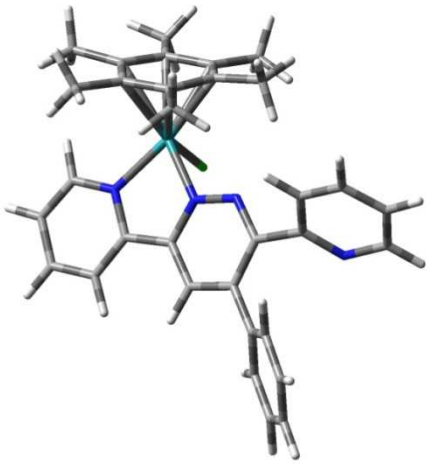

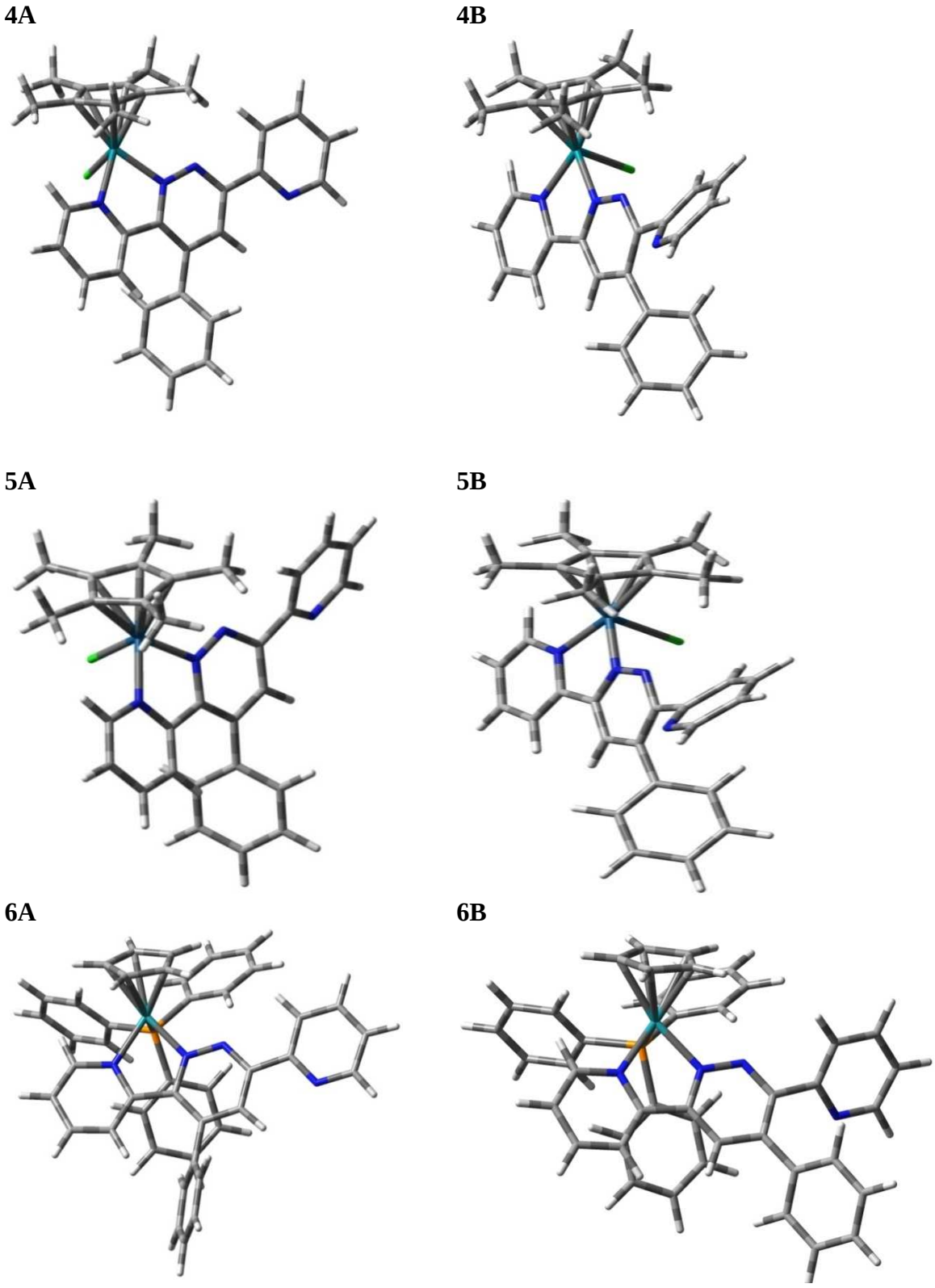

Figure 3.11: B3LYP/LanL2DZ optimized structures of complexes 2A, 3A, 4A, 5A and 6A in *type-A* binding mode and 2B, 3B, 4B, 5B and 6B in *type-B* binding mode.

The 3,6-bis(2-pyridyl)-4-phenylpyridazine (L^{ph}) ligand has two bidentate binding sites, *viz*., the N1 and N2 atoms (type-A) and the N3 and N4 atoms (type-B). In principle, the metal atom should prefer the *type-A* mode (atoms N1 and N2), since the substituents of the pyridazine ring (phenyl and pyridine rings) are *meta* with respect to N2, and the dihedral angle N1-C2-C3-N2 for the *anti* conformer of L^{ph} (141.3°) is found to be less than the dihedral angle N3-C6-C7-N4 (179.2°). On the other hand, for the *type-B* bonding mode (at atoms N3 and N4), the substituents of the central pyridazine ring (phenyl and pyridine rings) are respectively *para* and *meta* with respect to N3. The dihedral angle N3-C6-C7-N4 (179.2°) is found to be noticeably greater than the dihedral angle N1-C2-C3-N2 (141.3°) (see table 3.5). These results suggest that the metal atom prefers to bind through the N1 and N2 atoms (*type-A*) rather than through the N3 and N4 atoms (*type-B*).

On the other hand, the Mulliken atomic charges on the N3 and N4 atoms of ligand L^{ph} are more negative than for the N1 and N2 atoms (see figure 3.10 c). This means that atoms N3 and N4 should be better electron donors towards the metal center than atoms N1 and N2, implying that formation of *type-B* complexes is more favorable than *type-A* complexes. Interestingly, experimental results reveal that complexes **3** and **4** favor the *type-B* bonding mode while all the other complexes favor the *type-A* mode. Possible reasons could be the size of the metal atom, oxidation state of the complex, symmetry of the ligand and nature of the substituents on the metal atom.

The molecular structure of complex $[(\eta^6\text{-}p\text{-}^{i}PrC_6H_4Me)Ru(L^{ph})Cl]^+$ (**2**) shows κ^2 type coordination in the *type-A* bonding mode (see figure 3.7). This geometry was optimized for both *type-A* and *type-B* bonding modes. The results reveal that the *type-A* bonding mode is 1.25 kcal/mol more stable than *type-B*. Replacing $p\text{-}^{i}PrC_6H_4Me$ of **2** with the more electron-rich hexamethylbenzene (C_6Me_6) ligand gives the complex $[(\eta^6\text{-}C_6Me_6)Ru(L^{ph})Cl]^+$ (**3**). The geometry of this complex was built up by modification of complex **2** in both conformations, being optimized at the B3LYP level with a LanL2DZ basis set (figure 3.11. 3A and 3B). The results reveal that the *type-B* structure is 0.96 kcal/mol more stable than the *type-A* structure. These trends suggest that the nature of the co-ligands impacts on the bonding mode of the L^{ph} ligand. Since the energy difference between *type-A* and *type-B* (see table 3.6) structures is quite low, packing and other environmental factors may affect preference of one form over the other. The molecular structure of $[(\eta^5\text{-}C_5Me_5)Rh(L^{ph})Cl]PF_6$ (**4**) shows a κ^2 type of coordination with the *type-*

B bonding mode (see figure 3.8). The geometry was optimized for both *type-A* and *type-B* bonding modes (figure 3.11; 4A and 4B), where the results predict the *type-A* structure as 0.95 kcal/mol less stable than the *type-B* structure. Replacing rhodium in [(η^5-C_5Me_5)Rh(L^{ph})Cl]PF_6 (**4**) with the larger atom iridium gives [(η^5-C_5Me_5)Ir(L^{ph})Cl]PF_6 **5**, where the energy of the *type-A* structure is 0.35 kcal/mol lower in energy than the *type-B* structure (figure 3.11; 5A and 5B). This suggests that size of the metal atom also has a significant effect on the preferred choice of bonding mode.

In order to study the effect of steric interactions on the choice of bonding mode, we replaced the *p*-$^{i}PrC_6H_4Me$ and chloride ligands in complex **2** with the less electron-rich (but sterically free) cyclopentadienyl ligand and the bulky triphenylphosphine ligand respectively, giving the complex **6**. Calculated energies of the optimized geometries (figure 3.11; 6A and 6B) reveal that the *type-A* structure of 6 is 1.96 kcal/mol more stable than the *type-B* structure. This suggests that steric factors do not have much impact on the choice of bonding mode (see table 3.6).

In conclusion, the calculated energies of the optimized geometries of complexes **2**, **3**, **4**, **5** and **6** reveal that the preferred choice of binding mode neither depends on the steric nature of the co-ligands nor on the oxidation state of the complex. However, the optimized geometries of **4** and **5** reveal that size of the metal atom does have a significant impact on choice of binding mode, where the rhodium complex **4** favors the *type-B* bonding mode while the iridium complex **5** favors the *type-A* bonding mode (substituents or co-ligands and oxidation state being the same). In addition to the effect of the size of the metal atom, the nature of the co-ligand also has an impact on the choice of bonding mode because complexes with less electron-rich donor co-ligands favor the *type-A* bonding mode (**1**and **2** and **5** to **8**) while complexes having more electron-rich donor co-ligands favor the *type-B* bonding mode (**3** and **4**). These DFT results thus elucidate the effects of the size of the metal atom, the nature of the co-ligands and various electronic factors on the nature of bonding mode.

Table 3.5: Selected bond lengths (Å) and angles (º) for complexes **2**, **3**, **4**, **5** and **6** from the optimized geometries in *type-A* and *type-B*[d].

Atoms	2A	2B	3A	3B	4A	4B	5A	5B	6A	6B
Bond distances										
Ru-N1(N4)	2.056	2.068	2.058	2.071	2.099	2.116	2.091	2.076	2.070	2.083
Ru-N2(N3)	2.036	2.025	2.022	2.026	2.059	2.061	2.042	2.039	2.042	2.048
Ru-Cl1	2.334	2.453	2.462	2.460	2.463	2.459	2.479	2.480	2.447	2.447
N2-N3	1.344	1.348	1.344	1.346	1.295	1.341	1.348	1.344	1.357	1.358
M-C21	2.393	2.391	2.426	2.411	2.272	2.278	2.257	2.256	2.313	2.308
M-C22	2.354	2.354	2.403	2.399	2.297	2.299	2.258	2.247	2.309	2.309
M-C23	2.368	2.358	2.380	2.371	2.235	2.229	2.339	2.302	2.326	2.319
M-C24	2.369	2.362	2.313	2.309	2.282	2.273	2.303	2.262	2.319	2.313
M-C25	2.316	2.305	2.321	2.322	2.278	2.273	2.2080	2.281	2.309	2.308
M-C26	2.356	2.347	2.420	2.409	-	-	-	-	-	-
C2-C3	1.475	1.466	1.471	1.463	1.481	1.472	1.466	1.475	1.475	1.464
C5-C7	1.488	1.496	1.489	1.496	1.487	1.495	1.496	1.488	1.486	1.493
C4-C8	1.491	1.486	1.490	1.486	1.490	1.486	1.485	1.491	1.496	1.485
Bond angles										
N1-Ru-N2	77.7	76.9	77.4	77.8	77.0	77.3	77.2	77.0	77.08	77.4
N1-Ru-Cl1	84.1	83.4	83.5	83.3	85.5	84.0	83.0	84.2	94.98	95.4
N2-Ru-Cl1	85.6	85.4	85.7	86.6	85.2	85.9	85.0	84.6	90.12	89.8
Torsion angles										
N1-C2(7)-C3(6)-N2	6.9	58.2	7.4	-0.6	9.2	-46.6	-47.1	7.3	3.7	-134.1
N4-C7(2)-C6(3)-N3	33.2	-0.8	30.7	53.8	30.0	1.2	1.1	30.3	-175.1	1.1

[d]Labels were given on the basis of figure 3.11; 2A and 9.2B.

Table 3.6: Total energies (in atomic units) of complexes **2**, **3**, **4**, **5** and **6** (1 atomic unit = 27.21 eV) and the energy difference ΔE between the two conformers.

Compound	L^{ph} (type-A)	L^{ph} (type-B)	ΔE^{e} (kcal/mole)	Favored geometry
2	-1487.548062	-1487.546073	-1.25	type-A
3	-1566.175211	-1566.176748	+0.96	type-B
4	-1503.778281	-1503.779793	+0.95	type-B
5	-1498.974271	-1498.973714	-0.35	type-A
6	-1977.973671	-1977.970548	-1.96	type-A

[e] $\Delta E = E_{type\text{-}A} - E_{type\text{-}B}$

3.3.5 UV/visible spectroscopy

Electronic absorption spectral data of complexes **1** to **8** at 10^{-5} M concentration in the range 290-600 nm are summarized in table 3.7. The spectra of these complexes are characterized by two main features, *viz*., an intense ligand–localized or intra-ligand $\pi \rightarrow \pi^*$ transition in the ultraviolet region and metal toligand charge transfer (MLCT) $d\pi(M) \rightarrow \pi^*$ (L^{ph} ligand) bands in the visible region.[44] Since the low spin d^6 configuration of the mononuclear complexes provides filled orbitals of proper symmetry at the Ru(II), Rh(III) and Ir(III) centers, these can interact with low lying π^* orbitals of the ligands. All these complexes show an intense band in the region 290-320 nm and a low energy absorption band in the visible region 420 – 445 nm. In addition to these two absorption bands, an additional low intensity band at 350 nm and a shoulder type band at 280 nm for complexes **4** and **5** respectively are observed. The high intensity band in the UV region is assigned to inter- and intra-ligand π–π^* transitions,[45,46] while the low energy absorption band in the visible region is assigned to metal to ligand charge transfer (MLCT) ($t_{2g} \rightarrow \pi^*$). Spectra of these complexes are presented in figure 3.12.

Table 3.7: UV/visible spectral data for selected complexes in acetonitrile at 298 K.

Complex No.	Complex	λ_{max} (nm) / ε 10^{-5} M^{-1} cm^{-1}
1	$[(\eta^6\text{-}C_6H_6)Ru(L^{ph})Cl]^+$	306 (0.47) 412
2	$[(\eta^6\text{-}p\text{-}^iPrC_6H_4Me)Ru(L^{ph})Cl]^+$	320 (0.65) 420
3	$[(\eta^6\text{-}C_6Me_6)Ru(L^{ph})Cl]^+$	317 (0.61) 412
4	$[(\eta^5\text{-}C_5Me_5)Rh(L^{ph})Cl]^+$	299 (0.49) 349 (0.15) 420
5	$[(\eta^5\text{-}C_5Me_5)Ir(L^{ph})Cl]^+$	300 (0.51) 380 470
6	$[(\eta^5\text{-}C_5H_5)Ru(L^{ph})PPh_3]^+$	290 (0.61) 435(0.15)
7	$[(\eta^5\text{-}C_9H_7)Ru(L^{ph})PPh_3]^+$	294 (0.36) 445

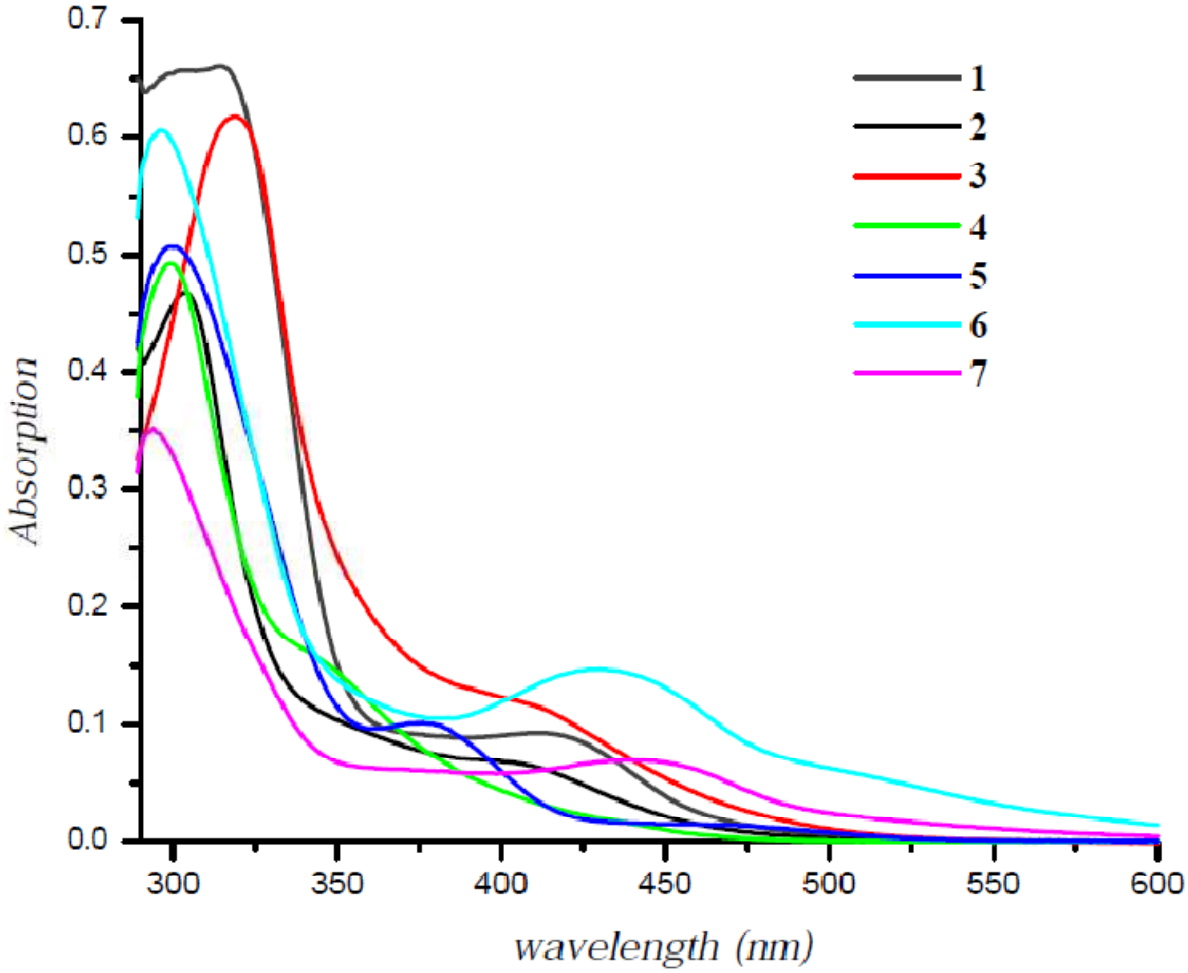

Figure 3.12: UV/Visible electronic spectra of complexes in acetonitrile at 298K.

3.3.6 Theoretical calculations:

Density functional theory (DFT)[47] calculations were undertaken for the ligands L and L^{ph} as well as for the complexes $[(\eta^6\text{-}p\text{-}^{i}PrC_6H_4Me)Ru(L^{ph})Cl]^+$, $[(\eta^5\text{-}C_5Me_5)Rh(L^{ph})Cl]^+$, $[(\eta^5\text{-}C_5Me_5)Ir(L^{ph})Cl]^+$, $[\eta^5\text{-}C_5H_5)Ru(L^{ph})(PPh_3)]^+$ in both the binding modes (*type-A* and *type-B*). Full geometry optimization was carried out with the use of the B3LYP [Becke three-parameter exchange functional (B3) and the Lee-Yang-Parr correlation functional (LYP)] method[48,49] together with the 6-31+G** and LanL2DZ[50-52] basis sets for ligands and for complexes respectively. Staring atomic coordinates for the cationic complexes (**2**, **4** and **6)** were taken from the single-crystal X-ray structures. All computations were performed with the GAUSSIAN 03 package.[53] Frequency calculations were performed to determine whether the optimized geometries were minima on the potential energy surface.

3.4 Supplementary material

Files CCDC-**739572** (**2**.CHCl3), CCDC-**739570** (**4)** and CCDC-**739571** (**6)** contain the supplementary crystallographic data for this chapter.

References

1 M. H. Keefe, K. D. Benkstein, J. T. Hupp, Coord. Chem. Rev.205 (2008) 201-228.

2 D. S. Tyson, C. R. Luman, X. Zhou, F. N. Castellano, Inorg. Chem. 40 (2001) 4063-4071.

3 J. F. Endicott, H. B. Schlegel, Md. J. Uddin, D. S. Seniveratne, Coord. Chem. Rev. 229 (2002) 95-106.

4 W. R. Browne, R. Hage, J. G. Vos, Coord. Chem. Rev. 250 (2006) 1653-1668.

5 M. T. Indelli, C. Chiorboli, F. Scandola, Topics in Current Chemistry 80 (2007) 215.

6 M. Yanagida, L. P. Singh, K. Sayama, K. Hara, R. Katoh, A. Islam, H. Sugihara, H. Arakawa, M. K. Nazeeruddin and M. Grätzel, J. Chem. Soc., Dalton Trans. 16 (2000) 2817-2822.

7 P. R. Ashton, R. Ballardini, V. Balzani, A. Credi, K. R. Dress, E. Ishow, C. J. Clevelaan, O. Kosian, J. A. Preece, N. Spencer, J. F. Stoddart, M. Venturi, S. Wenger, Chem. Eur. J. 6 (2008) 3558-3574.

8 F. Hanasaka, K. -I. Fujita, R. Yamaguchi, Organometallics 24 (2005) 3422-3433.

9 R. Noyori, S. Hashigushi, Acc. Chem. Res. 30 (1997) 97-102, and reference therein.

10 U. J. Jauregui-Haja, M. Dessoudeix, P. Kalck, M. Wilhelm, H. Delmas, Catl. Today. 66 (2001) 297

11 C. A. Sandoval, T. Ohkuma, N. Utsumi, K. Tsutsumi, K. Murata, R. Noyori, Chem. Asian J. 1-2 (2006) 102-110.

12 P. J. Dyson, G. Sava, Dalton Trans. (2006) 1929-1933.

13 A. F. A. Peacock, A. Habtemariam, R. Fernandez, V. Walland, F. P. A. Fabbiani, S. Parsons, R. E. Aird, D. I. Jodrell, P. J. Sadler, J. Am. Chem. Soc. 128 (2006) 1739-1748.

14 A. Habtemariam, M. Melchart, R. Fernandez, S. Parsons, I. D. H. Oswald, A. Parkin, F. P. A. Fabbiani, J. E. Davidson, A. Dawson, R. E. Aird, D. I. Jodrell, P. J. Sadler, J. Med. Chem. 49 (2006) 6858-6868.

15 C. Scolaro, A. Bergamo, L. Brescacin, R. Delfino, M. Cocchietto, G. Laurenczy, T. J. Geldbach, G. Sava, P. J. Dyson, J. Med. Chem. 48 (2005) 4161-4171.

16 E. Hilllard, A. Vessieres, F. Le Bideau, D. Plazuk, D. Spera, M. Huche, G. Jaouen, Chem. Med. Chem. 1 (2006) 551-559.

17 M. Auzias, B. Therrien, G. Süss-Fink, P. P. Štěpnička, W. H. Ang, P. J. Dyson, Inorg. Chem. 47 (2008) 578-583.

18 M. A. Scharwitz, I. Ott, Y. Geldmacher, R. Gust, W. S. Sheldrick, J. Organomet. Chem. 693 (2008) 2299-2309.

19 S. K. Singh, S. Joshi, A. R. Singh, J. K. Saxena, D. S. Pandey, Inorg. Chem. 46 (2007) 10869-10876.

20 M. Haga, M. M. Ali, H. Maegawa, K. Nozaki, A. Yoshimura, T. Ohno, Coord. Chem. Rev. 94 (1994) 99-118.

21 M. Haga, M. M. Ali, R. Arakava, Angew. Chem. Int., Ed. Engl. 35 (1996) 76-78.

22 S. Baitalik, U. Florke, K. Nag, Inorg. Chem. 38 (1999) 3296-3308.

23 P. Ceroni, F. Paolucci, S. Roffia, S. Serroni, S. Campagna, A. J. Bard, Inorg. Chem. 37 (1998) 2829-2832.

24 C. Metcalfe, S. Spey, J. A. Thomas, Dalton trans. (2002) 4732-4739.

25 P. A. Anderson, F. R. Keene, T. J. Meyer, J. A. Moss, G. F. Strouse, J. A. Treadway, Dalton trans. (2002) 3820-3831.

26 E. C. Constable, C. E. Housecroft, M. Neuburger, S. Reymann, S. Schaffner, Eur. J. Org. Chem. (2008) 1597-1607.

27 E. C. Constable, C. E. Housecroft, M. Neuburger, S. Reymann, S. Schaffner, Eur. J. Inorg. Chem. (2008) 3540-3548.

28 E. C. Constable, C. E. Housecroft, B. M. Kariuki, N. Kelly, C. B. Smith, Inorg. Chem. Commun. 5 (2002) 199-202.

29 E. C. Constable, C. E. Housecroft, B. M. Kariuki, M. Neuburger, C. B. Smith, Aust. J. Chem., 56 (2003) 653-655.

30 N. Singh, D. S. Pandey, J. Organomet. Chem. 689 (2004) 1821-1834.

31 S. Ghumaan, B. Sarkar, S. Patra, K. Parimal, J. V. Slageren, J. Fiedler, W. Kaim and G. K. Lahiri, J. Chem. Soc., Dalton. Trans. (2005) 706-712.

32 Z. Deng, H-W. Tseng, R. Zong, D. Wang, R. P. Thummel, Inorg. Chem. 4**7** (2008) 1835-1848.

33 W. A. Butte, F. Case, J. Org. Chem. 26 (1961) 4690-4692.

34 P. Govindaswamy, Y. A. Mozharivskyj, K. M. Rao, J. Organomet. Chem. 689 (2004) 3265-3274.

35 P. Govindaswamy, P. J. Carroll, Y. A. Mozharivskyj, K. M. Rao, J. Organomet. Chem. 690 (2005) 885-894.

36 A. Singh, N. Singh, D. S. Pandey, J. Orgnomet. Chem. 642 (2002) 48-57.

37 R. Dorta, L. Konstantinovski, L. J. W. Shimon, Y. Ben-David, D. Milstein, Eur. J. Inorg. Chem. (2003) 70-76.

38 K. T. Prasad, B. Therrien, K. M. Rao, J. Organomet. Chem. 693 (2008) 3049-3056.

39 B. Therrien, C. Said-Mohamed, G. Suss-Fink, Inorg. Chim. Acta 361 (2008) 2601-2608.

40 R. Lalrempuia, K. M. Rao, Polyhedron 22 (2003) 3155-3160.

41 P. Govindaswamy, Y. A. Mozharivskyj, K. M. Rao, Polyhedron 24 (2005) 1710-1716.

42 K. Pachhunga, B. Therrien, K. A. Kreisel, G. P. A. Yap, K. M. Rao, Polyhedron 26 (2007) 3638-3634.

43 J. G. Małecki, R. Kruszynski, M. Jaworska, P. Lodowski, Z. Mazurak, J. Organomet. Chem. 693 (2008) 1096-1108.

44 E. Binamira-Soriaga, N. L. Keder, W. C. Kaska, Inorg. Chem. 29 (1990) 3167-3171.

45 C. S. Arau´jo, M. G. B. Drew, V. Fe´lix, L. Jack, J. Madureira, M. Newell, S. Roche, T. M. Santos, J. A. Thomas, L. Yellowlees, Inorg. Chem. 41 (2002) 2250-2259.

46 H. Deng, J. Li, K. C. Zheng, Y. Yang, H. Chao, L. N. Ji, Inorg. Chim. Acta 358 (2005) 3430-3440.

47 R. G. Parr, W. Yang, Density Functional Theory of Atoms and Molecules; Oxford University Press: New York, 1989.

48 A. D. Becke, J. Chem. Phys. 98 (1993) 5648-5652.

49 C. Lee, W. Yang, R. G. Parr, Phys. Rev. B 37 (1988) 785-789.

50 A. D. Becke, J. Chem. Phys. 98 (1993) 1372.

51 A. Gorling, Phys. Rev. A. 54 (1996) 3912-3915.

52 L. Tan, S. Zhang, X. Liu, Y. Chen, X. Liu, J. Organomet. Chem. 693 (2008) 3387-3395.

53 *Gaussian 03,* M. J. Frisch *et al Revision E.01*, Gaussian, Inc., Pittsburgh PA, 2004.

Chapter 4

Cationic half-sandwich complexes (Rh, Ir, Ru) containing 2-substituted-1,8-naphthyridine chelating ligands: Syntheses, X-ray structure analyses and spectroscopic studies

---

Herein, we describe the synthesis of twelve η^5-C_5Me_5 rhodium, iridium and η^6-C_6H_6, η^6-*p*-$^{i}PrC_6H_4Me$ ruthenium complexes incorporating 2-substituted-1,8-naphthyridine ligands; 2-(2-pyridyl)-1,8-naphthyridine (pyNp), 2-(2-thiazolyl)-1,8-naphthyridine (tzNp) and 2-(2-furyl)-1,8-naphthyridine (fuNp).

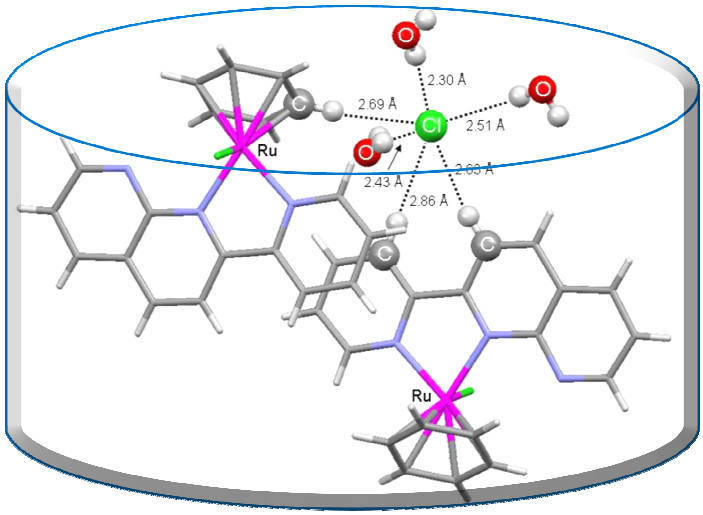

---

*The work presented in this chapter has been published: K. T. Prasad, B. Therrien and K. Mohan Rao, J. Organomet. Chem. 693 (2008) 3049-3056.

4.1 Introduction

Mononuclear complexes of platinum group metals containing heterocyclic nitrogen based ligands have received considerable attention owing to their photochemical properties,[1-9] catalytic activities,[10-19] electrochemical behaviour,[20-26] as well as in the development of new biologically active agents.[27-33] Ruthenium, rhodium and iridium unsubstituted 1,8-naphthyridine based complexes are interesting in their own right of uses as dye – sensitized solar cells and photophysical effects.[34] The reactivity of these metals with substituted 1,8-naphthyridine based ligands have also been reported. Examples with dinuclear metal-metal bonded compounds,[35-37] and mononuclear compounds[38] being known. However no reports dealing with η^5-pentamethylcyclopentadienyl or η^6-arene platinum group metal (Rh, Ir, or Ru) in connectivity with substituted 1,8-naphthyridine ligands have been reported so far.

Herein, we describe the syntheses of twelve η^5-C_5Me_5 rhodium, iridium and η^6-C_6H_6, η^6-*p*-$^{i}PrC_6H_4Me$ ruthenium complexes incorporating 2-substituted-1,8-naphthyridine ligands (Chart 4.1); 2-(2-pyridyl)-1,8-naphthyridine (pyNp), 2-(2-thiazolyl)-1,8-naphthyridine (tzNp) and 2-(2-furyl)-1,8-naphthyridine (fuNp). All complexes are characterized by IR, NMR, mass spectrometry and UV/Visible spectroscopy. The molecular structures of five representative complexes are presented as well.

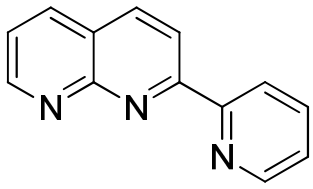

pyNp

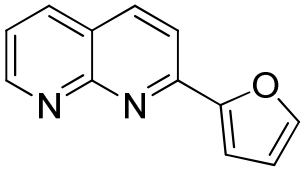

fuNp

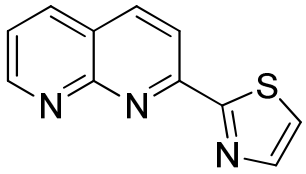

tzNp

Chart 4.1

4.2 Experimental

4.2.1 Preparation of ligands (pyNp, fuNp and tzNP).[39, 40]

4.2.1.1 Preparation of pyNp

500 mg (4.1 mmol) of 2-aminonicotinaldehyde was dissolved in 15 ml of dry ethanol. To this solution was added 0.55 ml (4.95 mmol) of 2-acetylpyridine. The solution was refluxed under nitrogen and treated with three drops of freshly prepared saturated solution of KOH in methanol. After refluxing overnight the solution was concentrated to one third of its original volume and kept in refrigerator to get yellowish crystals. The crystals were isolated by filtration and washed with cold ethanol and dried under vacuum to get pure pyNP.

Yield: 640 mg 75%. ^{1}H NMR (CD_3CN, δ): 9.09 (dd, 1H), 8.82 (d, 1H), 8.68 (m, 2H), 8.26 (d, 1H), 8.17 (d, 1H), 7.83 (td, 1H), 7.43 (q, 1H), 7.32 (m, 1H).

4.2.1.2 Preparation of tzNp

500 mg (4.1 mmol) of 2-aminonicotinaldehyde was dissolved in 15 ml of dry ethanol. To this solution was added 0.51 ml (4.95 mmol) of 2-acetylthiazole. The solution was refluxed under nitrogen and treated with three drops of freshly prepared saturated solution of KOH in methanol. After refluxing overnight the solution was concentrated to one-third of its original volume and kept in refrigerator to get yellowish crystals. The crystals were isolated by filtration and washed with cold ethanol and dried under vacuum to get pure tzNP.

Yield: 675 mg, 78%. ^{1}H NMR (CD_3CN, δ): 9.12 (d, 1H), 8.45 (d, 1H), 8.28 (d, 1H), 8.19 (dd, 1H), 7.98 (d, 1H), 7.54 (d, 1H), 7.49 (q, 1H).

4.2.1.3 Preparation of fuNp

The fuNP ligand was synthesized and isolated in a similar manner described for the synthesis of tzNP taking 50 mg (4.1 mmol) of 2-aminonicotinaldehyde and 0.50 ml (5 mmol) of 2-acetyl-furan.

Yield: 660 mg, 82%. ^{1}H NMR (CD_3CN, δ): 9.07 (dd, 1H), 8.19 (m, 2H), 7.96 (d, 1H), 7.58 (dd, 1H), 7.50 (d, 1H), 7.45 (q, 1H), 6.57 (dd, 1H)

4.2.2 Preparation of complexes **1**-**6**

*4.2.2.1 Synthesis of [(η^6-C_6H_6)Ru(pyNp)Cl]Cl ([**1**]Cl)*

A mixture of [(η^6-C_6H_6)Ru(μ-Cl)Cl]$_2$ (50 mg, 0.09 mmol) and pyNp (42 mg, 0.18 mmol) in 10 ml of acetonitrile was refluxed for 90 minutes. A colour change from light brown to dark brown was observed. The resulting solution was concentrated under vacuum (2 ml). Then 15 ml of hexane was added to induce precipitation. The yellowish brown solid was filtered off, washed with diethyl ether and dried under vacuum.

Yield 80 mg, (87%): $C_{19}H_{15}Cl_2N_3Ru$ (457.31) Calc.: C 49.90, H 3.31, N 9.19; Found: C 50.08, H 3.39, N 9.15. ^{1}H NMR ($CDCl_3$, δ): 9.56 (d, 1H, J_{H-H} = 8Hz), 9.38 (q, 1H), 8.76 (d, 1H), 8.58 (m, 2H), 8.48 (d, 1H), 7.91 (td, 1H), 7.90 (q, 1H), 7.78 (td, 1H), 6.15 (s, 6H, C_6H_6). ESI-MS (m/z): 419.8 (100%) $[M-Cl]^+$

*4.2.2.2 Synthesis of [(η^6-C_6H_6)Ru(tzNp)Cl]PF_6 ([**2**]PF_6)*

A mixture of [(η^6-C_6H_6)Ru(μ-Cl)Cl]$_2$ (50 mg, 0.09 mmol), tzNp (43 mg, 0.20 mmol) and 2.5 equivalents of NH_4PF_6 in 10 ml of acetonitrile was stirred at room temperature for 12 hours. A color change was observed from light brown to yellowish brown during the process. The reaction mixture was filtered off and washed with acetonitrile. The filtrate was reduced under vacuum (2 ml) and 15 ml of diethyl ether was then added to induce precipitation. After standing for 15 minutes, yellow precipitate settled down. The resulting precipitate was filtered, washed with diethyl ether and dried under vacuum.

Yield 85 mg (76%): $C_{17}H_{13}ClN_3F_6SPRu$ (572.85) Calc.: C 35.64, H 2.29, N 7.34, S 5.60; Found: C 35.70, H 2.35, N 7.46, S 5.51. ^{1}H NMR (CD_3CN, δ): 9.40 (q, 1H), 8.74 (d, 1H, J_{H-H} = 8.12 Hz, tz-H_1), 8.69 (d, 1H), 8.56 (dd, 1H), 8.24 (d, 1H, J_{H-H} = 4 Hz, tz-H_2), 8.19 (d, 1H), 7.9 (q, 1H), 6.20 (s, 6H, C_6H_6). ESI-MS (m/z): 425.2 (100%) $[M-PF_6]^+$, 389.4 (20%) $[M-PF_6-Cl]^+$.

*4.2.2.3 Synthesis of [(η^6-C_6H_6)Ru(fuNp)Cl]PF_6 ([**3**]PF_6)*

A mixture of [(η^6-C_6H_6)Ru(μ-Cl)Cl]$_2$ (50 mg, 0.09 mmol), fuNp (36 mg, 0.18 mmol) and 2.5 equivalents of NH_4PF_6 was used and treated following a procedure similar to that described in the synthesis of complex [**2**]PF_6. The resulting precipitate was filtered, washed with benzene and dried under vacuum.

Yield 70 mg, (63%): $C_{18}H_{14}ClF_6N_2OPRu$ (555.80) Calc.: C 38.90, H 2.54, N 6.38; Found: C 38.70, H 2.45, N 6.46 ^{1}H NMR ($CDCl_3$, δ): 9.52 (dd, 1H), 8.49 (dd, J_{H-H} = 7.12 Hz, 1H), 8.09 (dd, 1H, J_{H-H} = 8.08 Hz), 7.84 (d, 1H), 7.71 (d, 1H), 7.67 (q, 1H), 7.57 (q, 1H), 6.81 (q, 1H), 5.93 (S, 6H, C_6H_6); ESI-MS (m/z): 411.1 (100%) $[M\text{-}PF_6]^+$, 374.1 (20%) $[M\text{-}PF_6\text{-}Cl]^+$.

*4.2.2.4. Synthesis of [(η^6-p-^{i}PrC$_6$H$_4$Me)Ru(pyNp)Cl]PF$_6$ ([**4**]PF$_6$)*

A mixture of $[(\eta^6\text{-}p\text{-}^i PrC_6H_4Me)Ru(\mu\text{-}Cl)Cl]_2$ (50 mg, 0.081 mmol), pyNp (34 mg, 0.163 mmol) and 2.5 equivalents of NH_4PF_6 in 10 ml of acetonitrile were stirred at room temperature for 5 h. A white precipitate (NH_4Cl) was removed by filtration. The filtrate was concentrated to 2 ml and diethyl ether was added to induce precipitation. After standing for 15 minutes, an orange-yellowish precipitate was observed. After filtration, the solid was washed with diethyl ether and dried under vacuum.

Yield 82 mg, (81%): $C_{23}H_{23}ClF_6N_3PRu$ (622.93) Calc.: C 44.35, H 3.72, N 6.75; Found: C 44.70, H 3.65, N 6.76 ^{1}H NMR (CD_3CN, δ): 9.46 (d, 1H, J_{H-H} = 12 Hz,), 9.37 (q, 1H, J_{H-H} = 4 Hz), 8.73 (d, 1H), 8.57 (m, 2H), 8.48 (d, 1H), 8.26 (td, 1H), 7.91 (q, 1H), 7.78 (td, 1H), 6.21 (d, 1H, J_{H-H} = 5.4 Hz, $Ar_{p\text{-}cy}$), 6.13 (d, 2H, J_{H-H} = 6.2 Hz, $Ar_{p\text{-}cy}$), 5.79 (d,1H, J_{H-H} = 5.2 Hz, $Ar_{p\text{-}cy}$), 2.47 (sept, 1H, J_{H-H} = 4.4 Hz, $CH(CH_3)_2$), 2.27 (s, 3H, CH_3), 0.91 (d, 3H, $CH(CH_3)_2$), 0.83 (d, 3H, $CH(CH_3)_2$); ESI-MS (m/z): 478.3 (100%) $[M\text{-}PF_6]^+$, 440 (8%) $[M\text{-}PF_6\text{-}Cl]^+$, 306.4 (4%) $[M\text{-}PF_6\text{-}Cl\text{-}p\text{-}cy]^+$.

*4.2.2.5 Synthesis of [(η^6-p-^{i}PrC$_6$H$_4$Me)Ru(tzNp)Cl]PF$_6$ ([**5**]PF$_6$)*

A mixture of $[(\eta^6\text{-}p\text{-}^i PrC_6H_4Me)Ru(\mu\text{-}Cl)Cl]_2$ (50 mg, 0.08 mmol), tzNp (35 mg, 0.17 mmol) and 2.5 equivalents of NH_4PF_6 in 10 ml of methanol was refluxed for 3 h. A color change from brown to yellowish brown was observed. The solution was evaporated and the residue extracted with dichloromethane. The white insoluble material was filtered off. The filtrate was concentrated to 2 ml and diethyl ether was added to induce precipitation. The yellowish orange precipitate was washed with diethyl ether and dried under vacuum.

Yield 80 mg, (78%): $C_{21}H_{21}ClF_6N_3SPRu$ (628.96) Calc.: C 40.10, H 3.37, N 6.68, S 5.10; Found: C 40.43, H 3.35, N 6.76, S 5.22. ^{1}H NMR ($CDCl_3$, δ): 9.35 (q, 1H), 8.74 (d, 1H, J_{H-H} = 3.36 Hz), 8.62 (d, 1H), 8.45 (dd, 1H), 8.15 (d, 1H, J_{H-H} = 8.32 Hz), 8.06 (d, 1H), 7.86 (q, 1H), 6.31 (d, 1H, J_{H-H} = 6.2 Hz, $Ar_{p\text{-}cy}$), 6.26 (d, 1H, J_{H-H} = 6 Hz, $Ar_{p\text{-}cy}$),

6.11 (d.1H, J_{H-H} = 5.68 Hz, Ar_{p-cy}), 5.99 (d, 1H, J_{H-H} = 6 Hz, Ar_{p-cy}), 2.79 (sept, 1H, J_{H-H} = 4.14 Hz, $CH(CH_3)_2$), 2.28 (s, 3H, CH_3), 1.08 (d, 3H, $CH(CH_3)_2$), 1.02 (d, 3H, $CH(CH_3)_2$); ESI-MS (m/z): 481.9 (100%) $[M\text{-}PF_6]^+$, 445.6 (45%) $[M\text{-}PF_6\text{-}Cl]^+$.

*4.2.2.6 Synthesis of [(η^6-p-^{i}PrC$_6$H$_4$Me)Ru(fuNp)Cl]PF$_6$ ([**6**]PF$_6$)*

The reaction of [(η^6-*p*-^{i}PrC$_6$H$_4$Me)Ru(μ-Cl)Cl]$_2$ (50 mg, 0.08 mmol), fuNp (32 mg, 0.16 mmol) and 2.5 equivalents of NH_4PF_6 was carried out following a procedure similar to that described in the synthesis of [**2**]PF_6.

Yield 70 mg, (70%): $C_{22}H_{22}ClF_6N_2OPRu$ (611.91) Calc.: C 43.18, H 3.62, N 5.79; Found: C 43.23, H 3.73, N 5.46. ^{1}H NMR (CD_3CN, δ): 9.58 (dd, 1H), 9.05 (dd, 1H), 8.32 (dd, 1H, J_{H-H} = 8.12 Hz), 8.10 (d, 1H), 7.99 (d, 1H), 7.76 (d, 1H), 7.57 (q, H), 6.81 (q, 1H), 5.81 (d, 2H, J_{H-H} = 6.24 Hz, Ar_{p-cy}), 5.56 (d, 2H, J_{H-H} = 6.14 Hz, Ar_{p-cy}), 2.86 (sept, 1H, J_{H-H} = 4.04 Hz, $CH(CH_3)_2$), 2.16 (s, 3H, CH_3), 1.18 (d, 3H, $CH(CH_3)_2$), 1.07 (d, 3H, $CH(CH_3)_2$); ESI-MS (m/z): 464.9 (100%) $[M\text{-}PF_6]^+$, 429.2 (15%) $[M\text{-}PF_6\text{-}Cl]^+$.

4.2.3 Preparation of the cationic complexes **7-12**

General procedure: A mixture of [(η^5-C_5Me_5)M(μ-Cl)Cl]$_2$ (0.07 mmol), 2-substituted-1,8-naphthyridine ligand (0.14 mmol) and 2.5 equivalents of NH_4PF_6 in dry methanol (10 ml) was stirred at room temperature for 8 h. The solvent was evaporated under reduced pressure, and the residue was dissolved in dichloromethane. After filtration, the volume was reduced to 2 ml and excess diethyl ether was added to induce precipitation. The precipitate was washed with diethyl ether and dried under vacuum.

*4.2.3.1 [(η^5-C$_5$Me$_5$)Rh(pyNp)Cl]PF$_6$ ([**7**]PF$_6$)*

Orange-yellow solid, yield 70 mg (79%). $C_{23}H_{24}ClF_6N3PRh$ (625.77) Calc.: C 44.14, H 3.87, N 6.71; Found: C 44.70, H 3.75, N 6.76. ^{1}H NMR (CD_3CN, δ): 9.32 (q, 1H, J_{H-H} = 4.08 Hz), 9.03 (d, 1H, J_{H-H} = 4 Hz), 8.78 (d, 1H), 8.55 (m, 2H), 8.5 (d, 1H), 8.29 (td,1H), 7.87 (td, 2H), 1.60 (s, 15H, C_5Me_5); ESI-MS (m/z): 480.81 (100%) $[M\text{-}PF_6]^+$, 444.1 (70%) $[M\text{-}PF_6\text{-}Cl]^+$.

*4.2.3.2 [(η^5-C$_5$Me$_5$)Rh(tzNp)Cl]PF$_6$ ([**8**]PF$_6$)*

Orange solid, yield 80 mg (89%). $C_{21}H_{22}ClF_6N_3SPRh$ (628.96) Calc.: C 39.72, H 3.51, N 6.65, S 5.08; Found: C 39.43, H 3.45, N 6.76, S 5.02. ^{1}H NMR (CD_3CN, δ): 9.34 (q, 1H, J_{H-H} = 1.92 Hz), 8.76 (d, 1H, J_{H-H} = 8.4 Hz), 8.57 (dd, 1H), 8.38 (d, 3H), 8.29 (d, 1H, J_{H-H}

= 8.4 Hz), 8.23 (d, 1H), 7.87 (q, 1H), 1.71 (s, 15H, C_5Me_5); ESI-MS (m/z): 485.28 (100%) $[M\text{-}PF_6]^+$, 450.1 (9%) $[M\text{-}PF_6\text{- } Cl]^+$.

*4.2.3.3 [(η^5-C_5Me_5)Rh(fuNp)Cl]PF_6 ([**9**]PF_6)*

Orange-yellow solid, yield 68 mg (78%) $C_{22}H_{23}ClF_6N_2OPRh$ (614.75) Calc.: C 42.98, H 3.77, N 4.56; Found: C 42.23, H 3.73, N 4.34. ^{1}H NMR (CD_3CN, δ): 9.42 (dd, 1H), 9.09 (dd, 1H), 8.52 (d, 1H), 8.12 (dd, 1H), 7.79 (d, 1H), 7.76 (d, 1H), 7.67 (q, 1H), 7.52 (q, 1H), 1.55 (s, 15H, C_5Me_5); ESI-MS (m/z): 468.6 $[M\text{-}PF_6]^+$,
433.1 (7%) $[M\text{-}PF_6\text{- } Cl]^+$.

*4.2.3.4 [(η^5-C_5Me_5)Ir(pyNp)Cl]PF_6 ([**10**]PF_6)*

Orange-yellow solid, yield 80 mg (89%) $C_{23}H_{24}ClF_6N_3PIr$ (715.09) Calc.: C 38.63, H 3.38, N 5.58; Found: C 38.70, H 3.55, N 5.66. ^{1}H NMR ($CDCl_3$, δ): 9.38 (d, 1H), 9.3 (q, 1H), 8.73 (d, 1H), 8.55 (m, 2H), 8.49 (d, 1H), 8.28 (td, 1H), 7.96 (q,1H), 7.87 (td, 1H), 1.71 (s, 15H, C_5Me_5); ESI-MS (m/z): 569.1 (100%) $[M\text{-}PF_6]^+$, 533.2 (23%) $[M\text{-}PF_6\text{-}Cl]^+$.

*4.2.3.5 [(η^5-C_5Me_5)Ir(tzNp)Cl]PF_6 ([**11**]PF_6)*

Orange-yellow solid, yield 82 mg (91%). $C_{21}H_{22}ClF_6N_3SPIr$ (721.11) Calc.: C 34.98, H 3.08, N 5.83, S 4.45; Found: C 34.63, H 3.15, N 5.76, S 4.42. ^{1}H NMR (CD_3CN, δ): 9.32 (q, 1H), 8.73 (d, 1H), 8.58 (dd, 1H), 8.37 (d, 3H), 8.31 (d,1H), 8.21 (d, 1H), 7.89 (q, 1H), 1.71 (s, 15H, C_5Me_5); ESI-MS (m/z): 575.1 (100%) $[M\text{-}PF_6]^+$, 539.4 (35%) $[M\text{-}PF_6\text{-}Cl]^+$.

*4.2.3.6 [(η^5-C_5Me_5)Ir(fuNp)Cl]PF_6 ([**12**]PF_6)*

Orange-yellow solid, yield 61 mg (69%). $C_{22}H_{23}ClF_6N_2OPIr$ (704.06) Calc.: C 37.53, H 3.29, N 3.98; Found: C 37.23, H 3.23, N 4.04. ^{1}H NMR ($CDCl_3$, δ): 9.40 (dd, 1H), 9.06 (m, 1H), 8.51 (dd, 1H), 8.13 (d, 1H), 7.84 (d, 1H), 7.72 (d, 1H),7.65 (q, 1H), 7.55 (q, 1H), 1.56 (s, 15H, C_5Me_5); ESI-MS (m/z): 558.9 (100%) $[M\text{-}PF_6]^+$, 522.4 (10%) $[M\text{-}PF_6\text{- } Cl]^+$.

4.2.4 Single crystal X-ray structure analyses

In [**10**]PF_6 a positive residual electron density of 11.43 eÅ^{-3} (0.80 Å from Iridium) and electron density hole of -4.61 eÅ^{-3} (0.66 Å from Iridium) surrounded the heavy iridium atom. Crystallographic details are summarised in Table 4.1.

4.3 Results and Discussion

4.3.1 Syntheses

The dinuclear arene ruthenium complexes $[(\eta^6\text{-arene})Ru(\mu\text{-}Cl)Cl]_2$ (arene = C_6H_6, *p*-$^{i}PrC_6H_4Me$) react in acetonitrile with the 2-substituted-1,8-naphthyridine ligands - 2-(2-pyridyl)-1,8-naphthyridine (pyNp), 2-(2-thiazolyl)-1,8-naphthyridine (tzNp) and 2-(2-furyl)-1,8-naphthyridine (fuNp) to give the mononuclear cationic complexes $[(\eta^6\text{-}C_6H_6)Ru(L)Cl]^+$ {L = pyNp (**1**); tzNp (**2**); fuNp (**3**)}, $[(\eta^6\text{-}p\text{-}^{i}PrC_6H_4Me)Ru(L)Cl]^+$ {L= pyNp (**4**); tzNp (**5**); fuNp (**6**)} (Scheme 4.1). Cation **1** is isolated as its chloro salt, while the other cationic ruthenium complexes are obtained as their hexafluorophosphate salts.

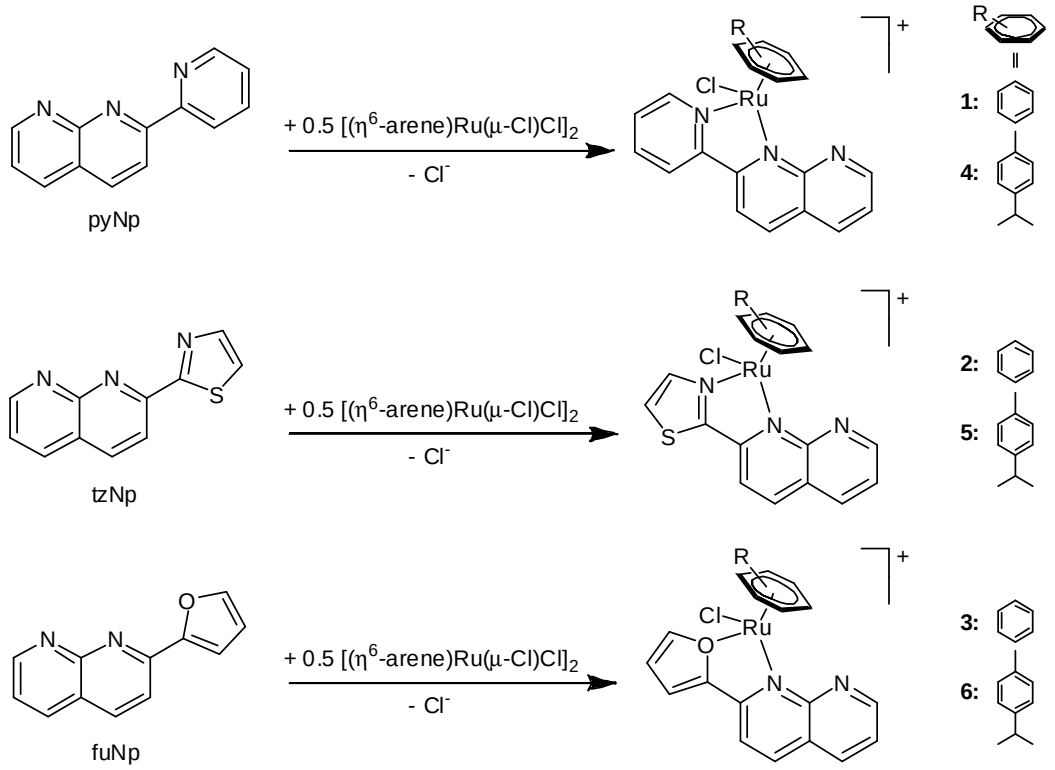

Scheme 4.1

Similarly, the reaction in methanol of the dimeric chloro-bridged complexes $[(\eta^5\text{-}C_5Me_5)M(\mu\text{-}Cl)Cl]_2$ (M = Rh, Ir) with the same 2-substituted-1,8-naphthyridine ligands leads to the formation of the mononuclear cationic complexes $[(\eta^5\text{-}C_5Me_5)Rh(L)Cl]^+$ {L = pyNp (**7**); tzNp (**8**); fuNp (**9**)} and $[(\eta^5\text{-}C_5Me_5)Ir(L)Cl]^+$ {L = pyNp (**10**); tzNp (**11**); fuNp (**12**)} (Scheme 4.2). All rhodium and iridium complexes are isolated as their hexafluorophosphate salts.

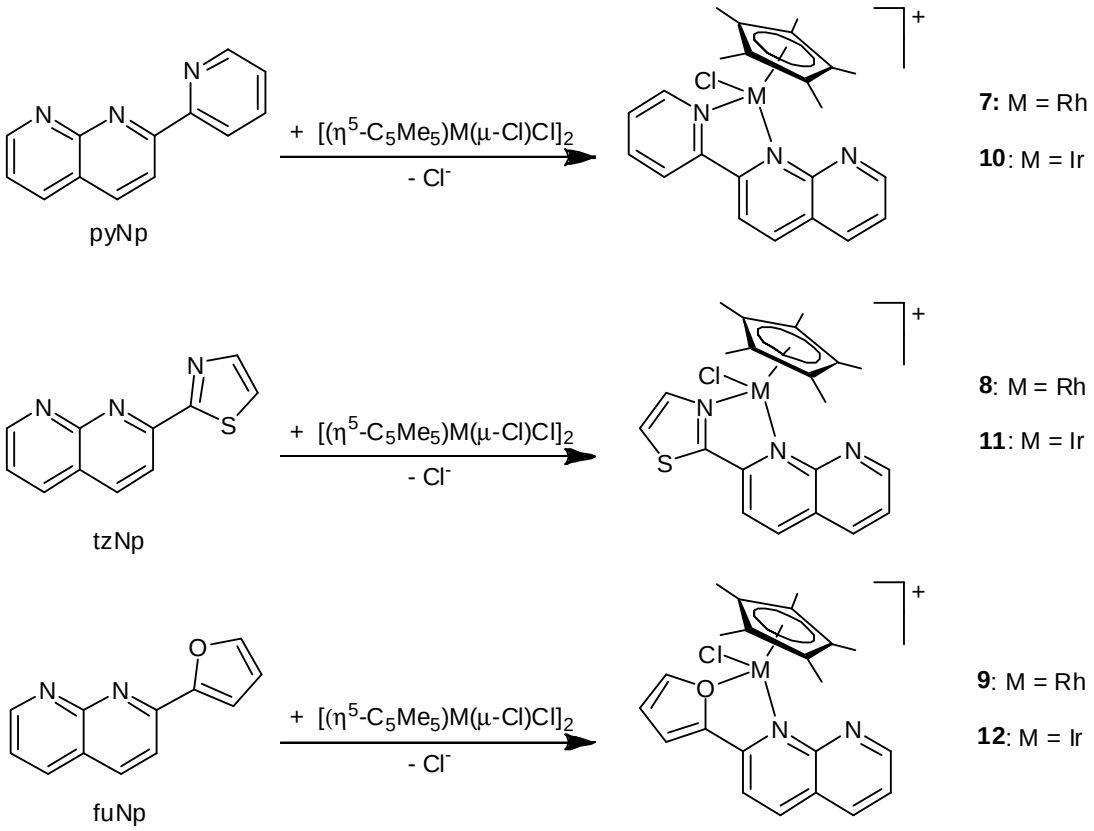

Scheme 4.2

All complexes are orange yellow in color, non-hygroscopic, air stable solids. However, the complexes with the fuNp ligand (**3, 6, 9** and **12**) are unstable in solution. They are soluble in acetonitrile but partially soluble in dichloromethane, chloroform and acetone. The reactions of pyNp and tzNp with the dinuclear rhodium and iridium precursors are instantaneous as compared to those with the ruthenium precursors. However, the reaction is comparatively slow for fuNp with these dinuclear precursors.

The infrared spectra of the complexes **2-12** exhibit a strong band in the region 844-850 cm^{-1}, a typical ν_{P-F} stretching band for the PF_6 anions. Moreover, all complexes show absorption bands at 1600-1610 cm^{-1} and 1470-1474 cm^{-1} for the $\nu_{C=C}$ and $\nu_{C=N}$ vibrations of the 1,8-naphthyridine moiety.[41] The complexes **2**, **5**, **8** and **11** show two additional absorption bands at 1450-1452 cm^{-1} and 1480-1484 cm^{-1} corresponding to the $\nu_{C=N}$ and $\nu_{C=S}$ stretching frequency of the thiazolyl group. The complexes **3**, **6**, **9** and **12** show a characteristic absorption band at 1626-1630 cm^{-1} which correspond to $\nu_{C=C}$ of the furyl group. The mass spectra of all these complexes exhibited corresponding molecular

ion peaks. For instance the mass spectra of complexes 3 and 4 have been depicted in figure 4.1 and 4.2 respectively.

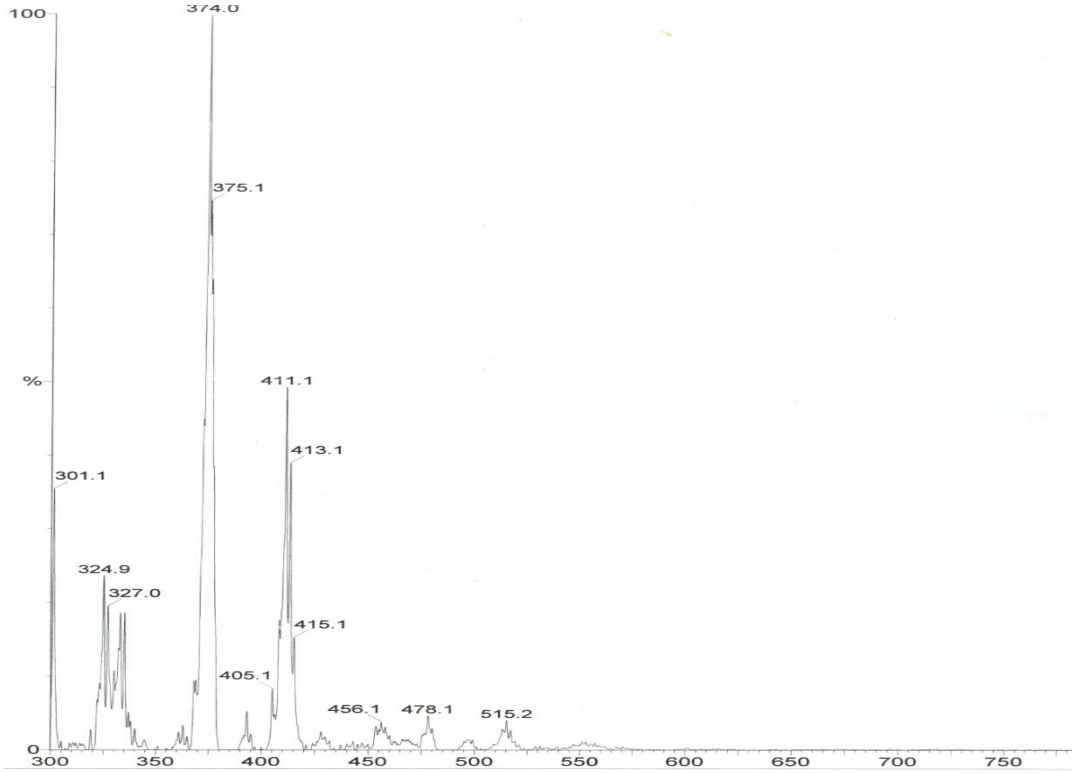

Figure 4.1: Mass spectrum of complex $[(\eta^6\text{-}C_6H_6)Ru(fuNp)Cl]PF_6$ ([**3**]PF_6)

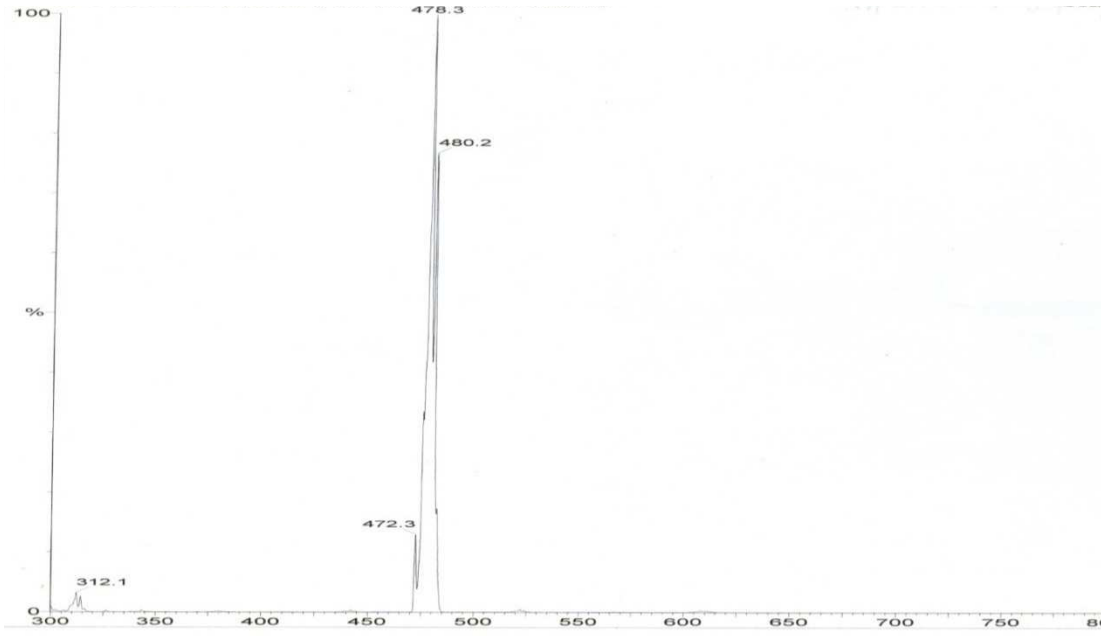

Figure 4.2: Mass spectrum of complex $[(\eta^6\text{-p-}^{i}PrC_6H_4Me)Ru(pyNp)Cl]PF_6$ ([**4**]PF_6)

4.3.2 NMR spectrometry

The ^{1}H NMR spectra of the benzene, *p*-cymene and *pentamethylcyclopentadienyl* derivatives which have pyNp, tzNp and fuNp as ligands exhibit nine resonances in the region δ = 9.56 to 7.78, seven resonances around δ = 9.41 to 7.90, and eight resonances around δ = 9.58 to 6.68 in the aromatic region, respectively. In addition to these signals, complexes ***1***, ***2*** *and* ***3*** exhibit a singlet resonance for the benzene ring protons at δ= 6.20 to 5.93. Complexes **4**, **5** and **6** exhibit an unusual pattern of resonances for the *p*-cymene ligand. For instance, the methyl protons of the isopropyl group displays two doublets at *ca.* δ = 1.18 to 1.07, instead of one doublet (see Figure 4.3 and 4.4) as in the starting complex. The aromatic protons of the *p*-cymene ligand displays three doublets for complex **4** (see Figure 4.3) and four doublets for complex **5** (see Figure 4.4) at *ca.* δ = 6.31 to 5.79, instead of two doublets as in the starting precursor. This unusual pattern is due to the diastereotopic methyl protons of the isopropyl group and aromatic protons of the *p*-cymene ligand, since the ruthenium atom is stereogenic due to the coordination of four different ligand atoms.[42] The other reason could be due to the loss of planarity of the *p*-cymene ligand, because of the steric nature of the ligand.[43]

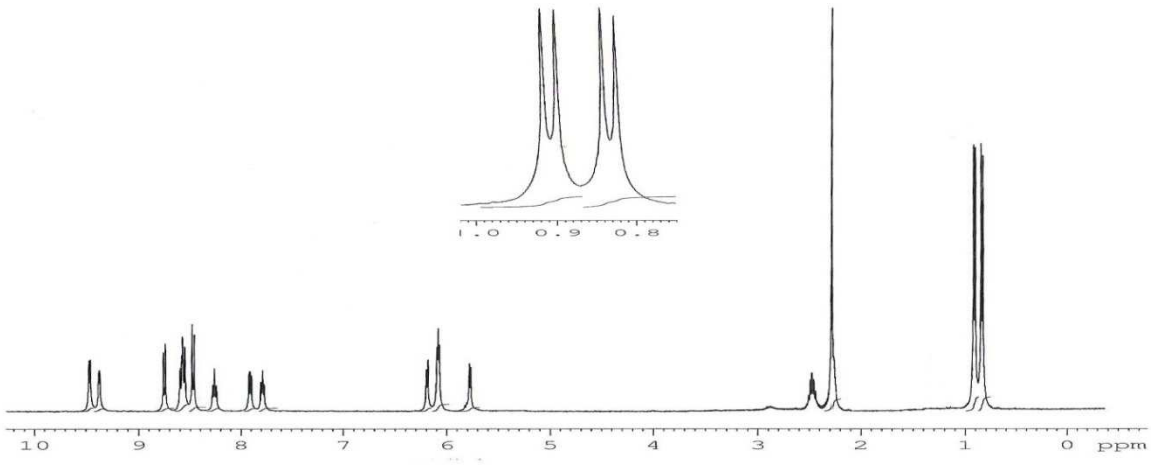

Figure 4.3: ^{1}H NMR spectrum of complex **4** in acetonitrile-d_3.

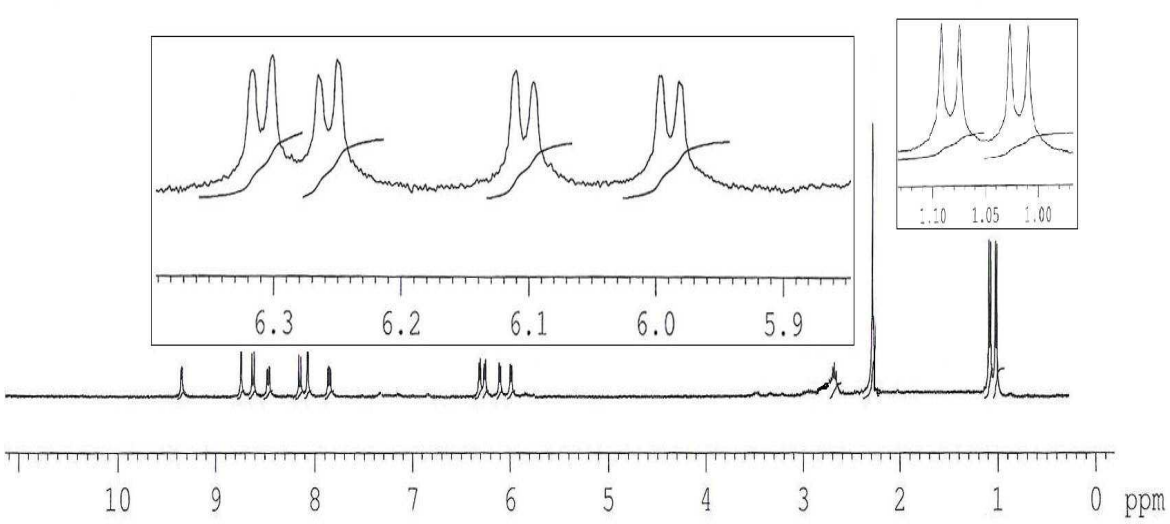

Figure 4.4: ^{1}H NMR spectrum of complex **5** in acetonitrile-d_3.

All these complexes show down field shift for all protons compared to the starting precursors, which might result from the charge transfer from metal centre to naphthyridine-based ligands such as pyNp and tzNp. Complexes **7** to **12** exhibit a *singlet resonance at* δ = 1.71 to 1.55 for the five methyl groups of the *p*entamethyl-cyclopentadienyl ligand.

4.3.3 X-ray structural study

The molecular structure of the benzene derivatives [(η^6-C_6H_6)Ru(pyNp)Cl]Cl or [**1**]Cl and [(η^6-C_6H_6)Ru(tzNp)Cl]PF_6 or [**2**]PF_6, the *p*-cymene derivatives [(η^6-*p*-$^{i}PrC_6H_4Me$)Ru(pyNp)Cl]PF_6 or [**4**]PF_6 and [(η^6-*p*-$^{i}PrC_6H_4Me$)Ru(tzNp)Cl]PF_6 or [**5**]PF_6 as well as the pentamethylcyclopentadienyl iridium complex [(η^5-C_5Me_5)Ir(pyNp)Cl]PF_6 or [**10**]PF_6 have been established by single crystal X-ray structure analysis. All cationic complexes show a typical piano-stool geometry with the metal centre being coordinated by an aromatic ligand, a terminal chloro ligand and a chelating 2-substituted-1,8-naphthyridine ligand. Formally, the 2-substituted-1,8-naphthyridine ligand can coordinate to the metal centre either through one or two nitrogen atoms of the naphthyridine moiety or through the N, O or S atoms of the 2-substituted ring. Interestingly, in this study, all metal centres were found to be coordinated to the 2-substituted-1,8-naphthyridine ligand in a five-membered ring chelating fashion involving one nitrogen atom of the naphthyridine moiety and the nitrogen atom of the 2-pyridyl or 2-thiazolyl group and the

oxygen atom of the 2-furyl group. Indeed, in [**1**]Cl, [**4**]PF_6 and [**10**]PF_6 the pyNp ligand is found as a five-membered ring *N*,*N*-chelating ligand (see Figure 4.5 to 4.6).

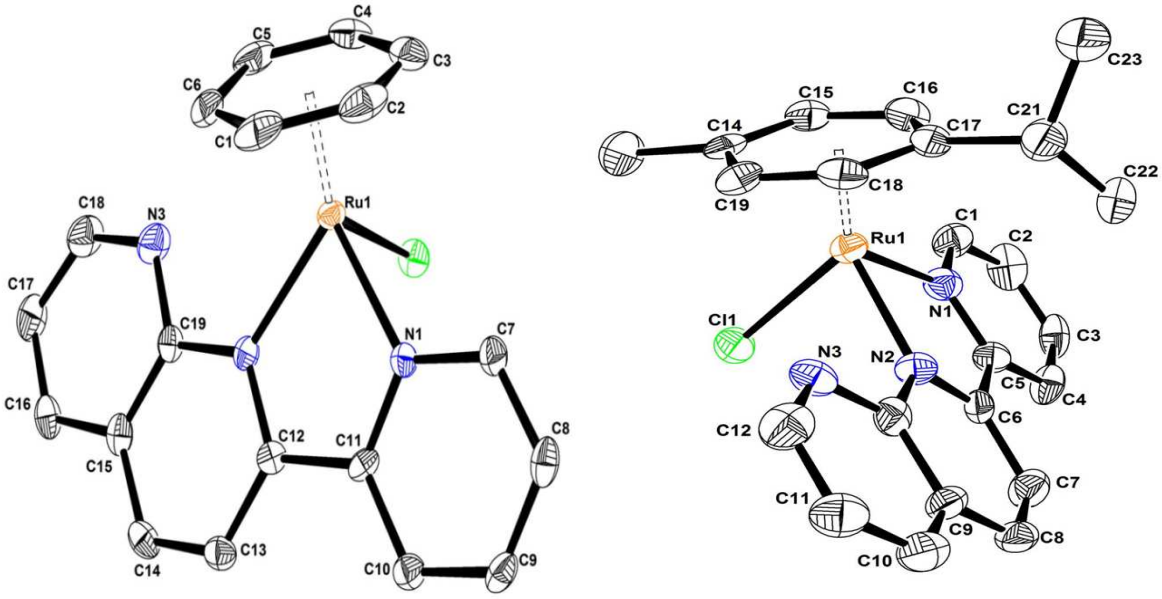

Figure 4.5: ORTEP diagram of cations **1** and **4** at 35% probability level, chloride anion and hydrogen atoms being omitted for clarity.

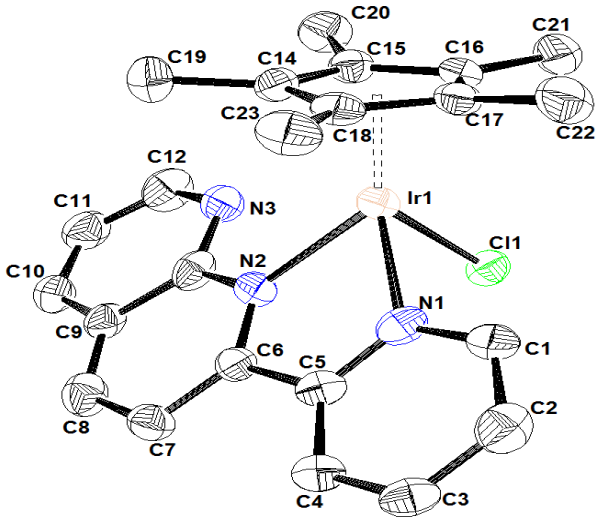

Figure 4.6: ORTEP diagram of cation **10** at 35% probability level, hexafluorophosphate anion and hydrogen atoms being omitted for clarity.

Similarly, in [**2**]PF_6 and [**5**]PF_6, the tzNp ligand is found to coordinate through the N1 atom of the naphthyridine moiety and the N3 atom of the 2-substituted thiazolyl ring to generate a five-membered ring metallo-cycle (see Figure 4.7). In these tzNp

complexes, the S atom points away from the metal centre and show no interaction with neighbouring cations. Selected bond lengths and angles for [**1**]Cl · 3 H_2O, [**2**]PF_6, [**4**]PF_6, [**5**]PF_6 and [**10**]PF_6 are presented in Table 4.2.

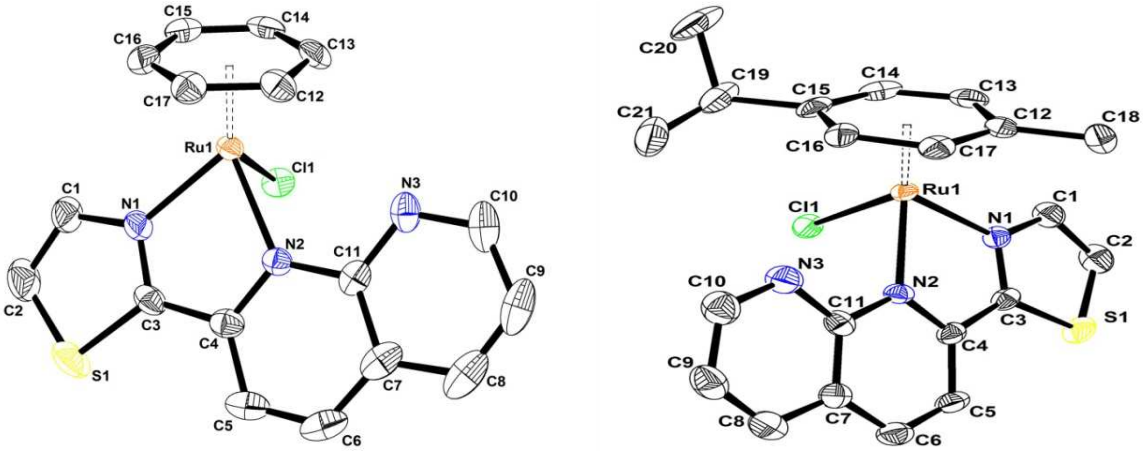

Figure 4.7: ORTEP diagram of cations 2 and 5 at 50% probability level, hexafluorophosphate anion and hydrogen atoms being omitted for clarity.

Table 4.1. Crystallographic and structure refinement parameters for complexes [**1**]Cl · 3 H_2O, [**2**]PF_6, [**4**]PF_6, [**5**]PF_6 and [**10**]PF_6.

Complex	[**1**]Cl · 3 H_2O	[**2**]PF_6	[**4**]PF_6	[**5**]PF_6	[**10**]PF_6
Chemical formula	$C_{19}H_{21}Cl_2N_3O_3Ru$	$C_{17}H_{13}ClF_6N_3PRuS$	$C_{23}H_{23}ClF_6N_3PRu$	$C_{21}H_{21}ClF_6N_3PruS$	$C_{23}H_{24}ClF_6N_3PIr$
Formula weight	511.36	572.85	622.93	628.96	715.07
Crystal system	Triclinic	Monoclinic	Monoclinic	Monoclinic	Monoclinic
Space group	*P*-1 (no. 2)	*P* $2_1/a$ (no. 14)	*P* $2_1/c$ (no. 14)	*P* $2_1/n$ (no. 14)	*P* $2_1/n$ (no. 14)
Crystal color, shape	orange block	orange rod	orange block	orange rod	yellow block
Crystal size (mm^3)	0.23 x 0.17 x 0.16	0.28 x 0.23 x 0.18	0.35 x 0.26 x 0.21	0.27 x 0.19 x 0.16	0.36 x 0.19 x 0.18
a (Å)	6.8771(9)	8.1508(7)	13.5963(11)	12.2831(11)	9.1766(4)
b (Å)	11.8984(15)	24.707(3)	12.6953(17)	15.1758(18)	27.5266(16)
c (Å)	12.6683(15)	9.3945(8)	14.1956(13)	13.2454(12)	9.5593(5)
α (°)	77.873(14)				
β (°)	85.670(15)	94.007(10)	107.432(10)	91.372(10)	94.747(4)
γ (°)	75.733(14)				
V ($Å^3$)	981.9(2)	1887.3(3)	2337.8(4)	2468.3(4)	2406.4(2)
Z	2	4	4	4	4
T (K)	173(2)	173(2)	173(2)	173(2)	173(2)
D_x (g /cm^3)	1.730	2.016	1.770	1.693	1.974
μ (mm^{-1})	1.097	1.236	0.920	0.953	5.790
Scan range (°)	$2.19 < \theta < 26.01$	$2.17 < \theta < 26.00$	$2.20 < \theta < 26.12$	$2.04 < \theta < 26.09$	$1.48 < \theta < 29.22$
Unique reflections	3112	3497	4401	4809	6505
[I>2σ(I)]	3579	2990	2082	4126	4695
R_{int}	0.0582	0.0351	0.1881	0.0532	0.0678
Final R indices I>2σ(I)]*	0.0329, wR_2 0.0795	0.0242, wR_2 0.0612	0.0551, wR_2 0.1013	0.0320, wR_2 0.0821	0.0737, wR_2 0.1907
R indices (all data)	0.0382, wR_2 0.0826	0.0304, wR_2 0.0648	0.1252, wR_2 0.1176	0.0377, wR_2 0.0838	0.0958, wR_2 0.2012
Goodness-of-fit	1.005	1.052	0.775	1.043	1.077
Max, Min Δρ (e $Å^{-3}$)	0.617, -0.853	0.529, -0.929	0.639, -0.897	1.443, -0.6341	1.432, -4.606

* Structures were refined on F_0^2: $wR_2 = [\Sigma [w(F_0^2 - F_c^2)^2] / \Sigma w(F_0^2)^2]^{1/2}$, where $w^{-1} = [\Sigma (F_0^2) + (aP)^2 + bP]$ and $P = [\max(F_0^2, 0) + 2F_c^2]/3$

Table 4.2: Selected bond lengths and angles for complexes [**1**]Cl.3H_2O, [**2**]PF_6, [**4**]PF_6, [**5**]PF_6 and [**10**]PF_6.

	1 (pyNp)	**2** (tzNp)	**4** (pyNp)	**5** (tzNp)	**10** (pyNp)
			Distances (Å)		
M-Cl	2.4147(8)	2.4045(7)	2.396(2)	2.4080(7)	2.412(3)
M-N1	2.109(3)	2.123(2)	2.112(6)	2.152(2)	2.107(9)
M-N3	2.088(2)	2.091(2)	2.078(6)	2.073(2)	2.136(9)
M-centroid[a]	1.68	1.67	1.69	1.68	1.79
C8-C9	1.478(4)	1.448(4)	1.485(9)	1.444(4)	1.51(2)
			Angles (°)		
N1-M-N3	76.60(9)	76.82(8)	76.9(2)	76.07(9)	74.9(4)
N1-M-Cl	85.75(7)	83.99(6)	83.3(2)	84.76(6)	87.7(3)
N3-M-Cl	85.13(6)	86.12(6)	84.9(2)	86.24(7)	87.4(3)

[a] Calculated centroid of the C_5 or C_6 coordinated aromatic ring.

The distances between the ruthenium atom and the centroid of the C_6 aromatic ring in **1**, **2**, **4** and **5** are comparable (1.67 to 1.69 Å) but quite shorter than the distance between the iridium atom and the C_5 aromatic ring observed in **10** (1.79 Å). The M-N1 bond distances [2.107(9) to 2.152(2) Å] are comparable to those in [(η^6-*p*-^{i}PrC_6H_4Me)RuCl(2,3-bis(2-pyridyl)pyrazine)]BF_4,[44] [(η^6-C_6H_6)RuCl(2-(1-imidazol-2-yl)pyridine)]PF_6,[45] and [(η^5-C_5Me_5)Ir(2-(2'-pyridyl)imidazole)Cl]PF_6.[46]. The Ir-N3 bond distance (2.136(9) Å) in **10** is slightly longer than the corresponding distances in the ruthenium complexes **1**, **2**, **4** and **5** (2.073(2) to 2.091(2) Å), while the M-Cl bond lengths show no significant differences among the five cations. However, a noticeable difference is observed in the distances of the C8-C9 connecting bond (naphthyridine 2-substituted ring C-C bond). In the tzNp derivatives, the C8-C9 distances [1.448(4) in **2** and 1.444(4) Å in **5**] are shorter than those found in the pyNp derivatives **1**, **4** and **10** [1.478(4), 1.485(9) and 1.51(2) Å] respectively.

Complex [**1**]Cl crystallises with three molecules of water per asymmetric unit, forming an intricate hydrogen-bonded network around the chloride atom. It involves the three water molecules and some hydrogen atoms of the pyNp and C_6H_6 ligands (see

Figure 4.8). The O-O and O-C distances of the hydrogen bonds range from 3.12 to 3.77 Å, with O-H···O or C-H···O angles ranging from 137.6 to 177.0°.

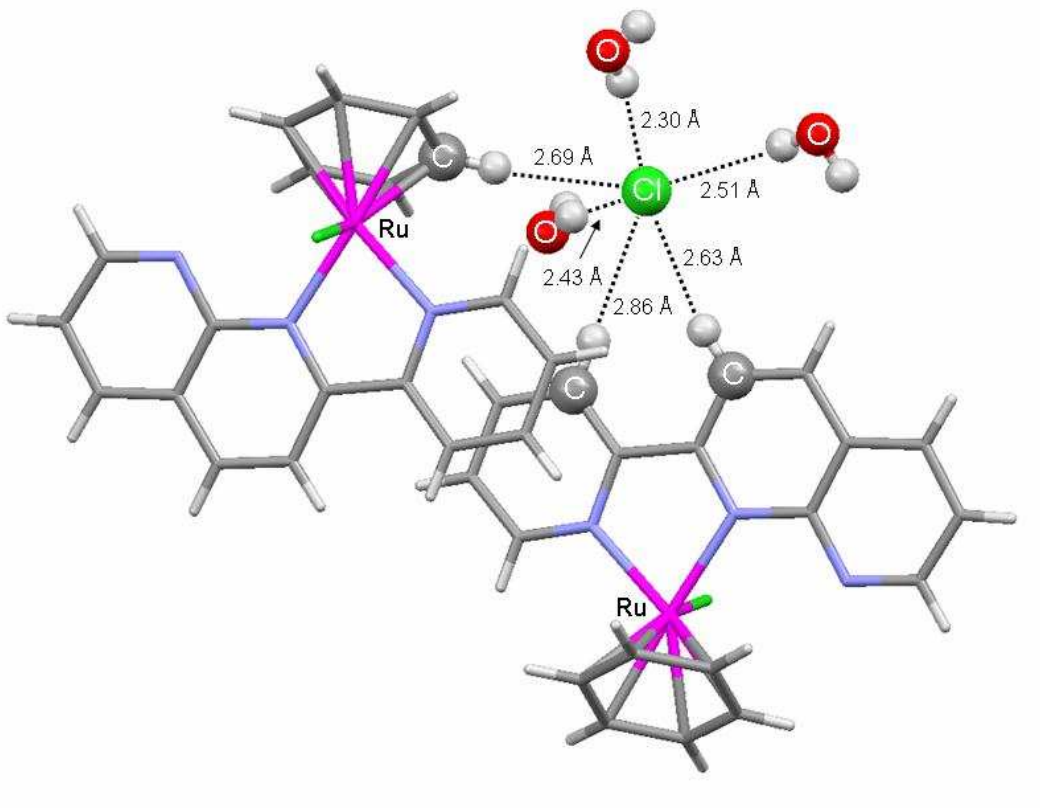

Figure 4.8: Hydrogen-bonded network observed in [**1**]Cl · 3 H_2O with H-Cl distances.

In the crystal packing of [**10**]PF_6, two cationic molecules of **10** form a dimer through π-stacking interactions (see Figure 4.9). The distance observed between the two π-stacking interacting systems (centroid···centroid 3.62 Å) is in good agreement with the theoretical value calculated for a slipped parallel stacking mode.[47]

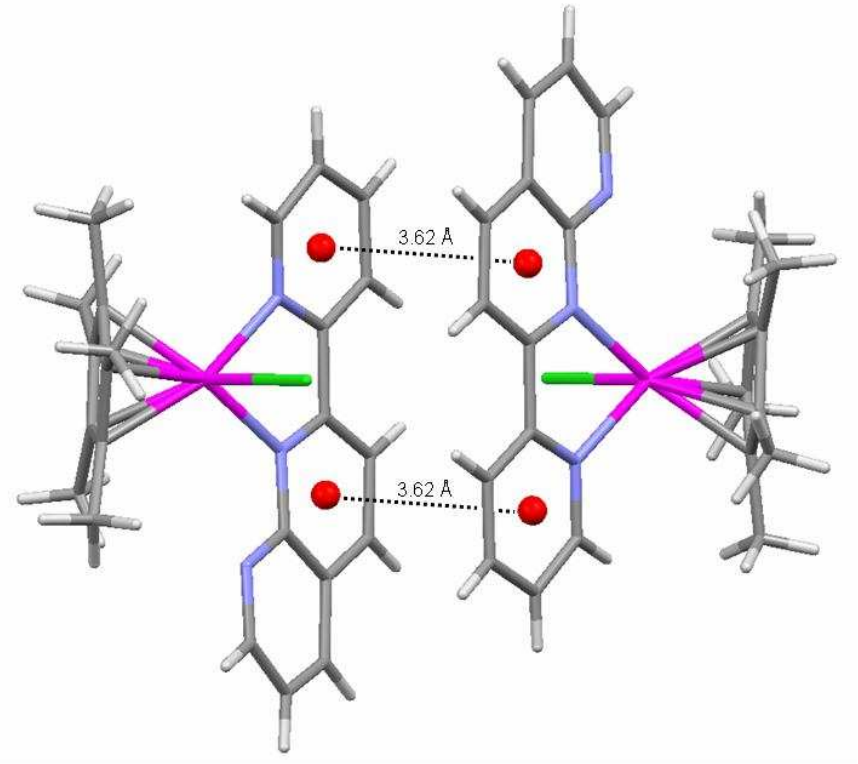

Figure 4.9: Dimeric structure of [**10**]PF_6 showing the separation of the π-stacking system.

4.3.4 UV/Visible spectroscopy

Electronic absorption spectral data of selected complexes at 10^{-5} M concentration in the range 320-520 nm are summarised in Table 4.3. The spectra of these complexes are characterized by two main features, *viz*., an intense ligand–localized or intra-ligand π → π* transition in the ultraviolet region and metal-to-ligand charge transfer (MLCT) dπ(M) → π* (Np-based ligands) bands in the visible region.[48]. Since the low spin d^6 configuration of the mononuclear complexes provides filled orbitals of proper symmetry at the Ru(II), Rh(III) and Ir(III) centres, these can interact with low lying π* orbitals of the ligands. All these complexes show two absorption bands in the region 340-390 nm, while the complexes bearing fuNp ligand (N,O donor) exhibit two absorption bands in blue shift at 330-355 nm, the second being a shoulder of the first band. It shows a series of ligand-centred π – π* transitions with high intensity absorption bands in the UV region. One should therefore expect a band attributable to the metal-to-ligand charge transfer (MLCT) (t_{2g} – π*) transitions in their electronic spectra.[49-52]. All these complexes exhibit a broad absorption band with low intensity and low energy at 420-440 nm, while the complexes bearing fuNp ligand exhibit a very low intensity shoulder in the near visible

region 385 – 390 nm, which originate from dπ (Ru, Rh and Ir) → π* (naphthyridine based ligands) metal-to-ligand charge transfer transitions. Representative spectra of these complexes are presented in Figure 4.10.

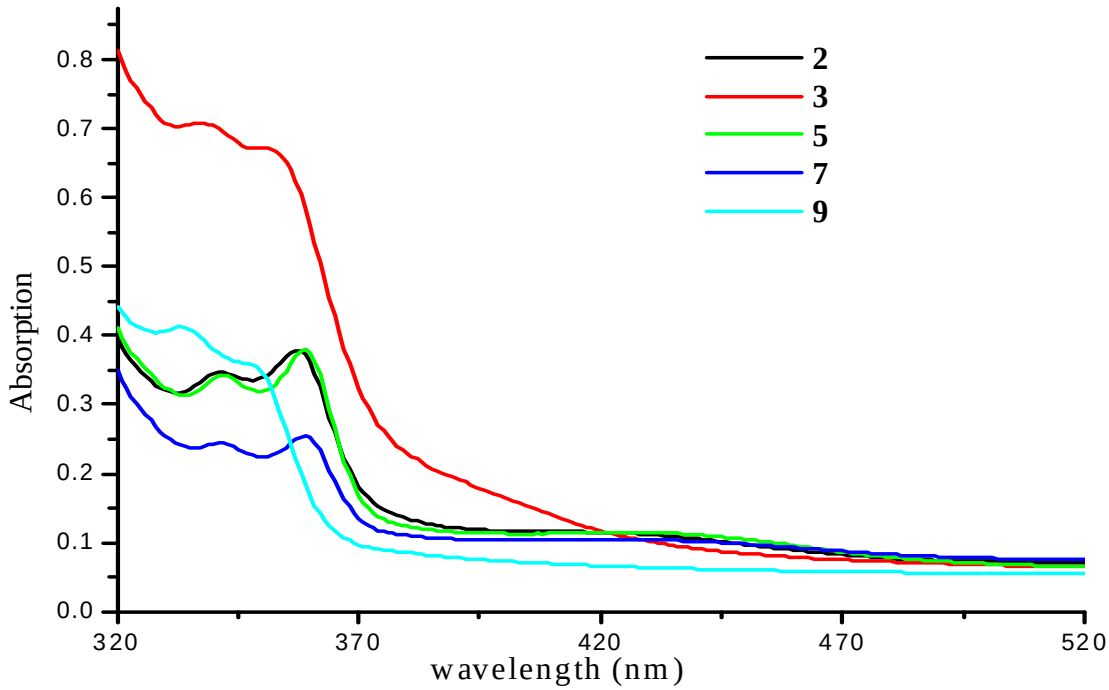

Figure 4.10: Selected UV/Visible electronic spectrum in acetonitrile at 298 K.

Table 4.3: UV/Visible data for selected complexes in acetonitrile at 298 K.

No.	Complex	λ_{max} (nm) / ε 10^{-5} M^{-1} cm^{-1}
2	$[(\eta^6\text{-}C_6H_6)Ru(tzNp)Cl]^+$	342 (0.30) 357 (0.37) 422 (0.12)
3	$[(\eta^6\text{-}C_6H_6)Ru(fuNp)Cl]^+$	338 (0.70) 352 (sh) 385 (sh) (10^{-3} M^{-1} cm^{-1})
5	$[(\eta^6\text{-}p\text{-}^i PrC_6H_4Me)Ru(tzNp)Cl]^+$	342 (0.34) 357 (0.37) 435 (0.11)
7	$[(\eta^5\text{-}C_5Me_5)Rh(pyNp)Cl]^+$	342 (0.24) 385 (0.25) 436 (0.11)
9	$[(\eta^5\text{-}C_5Me_5)Rh(fuNp)Cl]^+$	334 (0.41) 348 (sh) 390 (sh)

4.4 Conclusion

In this work we demonstrated that all metal centres are coordinated to the 2-substituted-1,8-naphthyridine ligand in a five-membered ring chelating fashion involving one nitrogen atom of the naphthyridine moiety and the nitrogen atom of the 2-pyridyl or 2-thiazolyl group and the oxygen atom of the 2-furyl group. The formation of

bridging complexes with the remaining nitrogen atom of the naphthyridine moiety was unsuccessful in our hand.

4.5 Supplementary material

CCDC-**680855** [**1**]Cl 3 H_2O, CCDC-**680856** [**2**]PF_6, CCDC-**680857** [**4**]PF_6, CCDC-**680858** [**5**]PF_6 and CCDC-**680859** [**10**]PF_6 contain the supplementary crystallographic data for this chapter.

References

1 G. Di Marco, A. Bartolotta, V. Ricevuto, S. Campagna, G. Denti, L. Sabatino, G. De Rosa, Inorg. Chem. 30 (1991) 270.

2 V. Balzani, A. Juris, M. Venturi, S. Campagna, S. Serroni, Chem. Rev. 96 (1996) 759.

3 J. F. Endicott, H. B. Schlegel, Md. J. Uddin, D. S. Seniveratne, Coord. Chem. Rev. 229 (2002) 95.

4 W. R. Browne, R. Hage, J. G. Vos, Coord. Chem. Rev. 250 (2006) 1653.

5 M. T. Indelli, C. Chiorboli, F. Scandola, Topics in Current Chemistry. 80 (2007) 215.

6 M. Yanagida, J. Chem. Soc., Dalton Trans. 16 (2000) 2817.

7 Y. Wang, W. Perez, G. Y. Zheng,D. P. Rillema, Inorg. Chem. 37 (1998) 2051.

8 A. C. Lees, B. Evrard, T. E. Keyes, J. G. Vos, C. J. Kleverlaan, M. Alebbi, C. A. Bignozzi, Eur. J. Inorg. Chem. 12 (1999) 2309.

9 C. J. Kleverlaan, M. T. Indelli, C. A. Bignozzi, L. Pavanin, F. Scandola, G. M. Hasselman, G. J. Meyer , J. Am. Chem. Soc. 122 (2000) 2840.

10 T. Ohta, S. Nakahara, Y. Shigemura, K. Hattori, I. Furukawa, Appl. Organometal. Chem. 15 (2001) 699.

11 S. Ogo, K. Uehara, T. Abura, Y. Watanabe, S. Fukuzumi, Organometallics. 23 (2004) 3047.

12 C. A. Sandoval, T. Ohkuma, N. Utsumi, K. Tsutsumi, K. Murata, R. Noyori, Chem. Asian J. 1-2 (2006) 102.

13 R. Noyori, S. Hashigushi, Acc. Chem. Res. 30 (1997) 97, and reference therein.

14 E. P. Kündig, A. Quattropani, M. Inage, A. Ripa, C. Dupre, A. F. J. Cunningham, B. Bourdin, Pure Appl. Chem. 68 (1996) 97.

15 J.W. Faller, M. R. Mazzieri, J. T. Nguyen, J. Parr, M. Tokunaga, Pure Appl. Chem. 66 (1994) 1463.

16 S. G. Davies, Pure Appl. Chem. 60 (1988) 13.

17 C. A. Goss, H. D. Abruna, Inorg. Chem. 24 (1985) 4263.

18 F. Hanasaka, K. -I. Fujita, R. Yamaguchi, Organometallics. 24 (2005) 3422.

19 M. S. El-Shahawi, A. F. Shoair, Spectrochim. Acta A 60 (2004) 121.

20 J.-P. Sauvage, J.-P. Collin, J.-C. Chambron, S. Guillerez, C. Coudret, V. Balzani, F. Barigelletti, L. De Cola, L. Flamigni, Chem. Rev. 94 (1994) 993.

21 Z. Shirin, R. Mukherjee, J. F. Richardson, R. M. Buchanan, J. Chem. Soc., Dalton Trans. (1994) 465.

22 W. Kaim, R. Reinhardt, J. Fiedler, Angew. Chem. Int. Ed. Engl. 36 (1997) 2493.

23 S. Chellamma M. Lieberman, Inorg. Chem. 40 (2001) 3177.

24 T. J. Meyer, M. H. V. Huynh, Inorg. Chem. 42 (2003) 8140.

25 M. Newell, J. A. Thomas, Dalton Trans. (2006) 705.

26 H. Nakajima, H. Nagao, K. Tanaka, J. Chem. Soc., Dalton Trans. (1996) 1405.

27 Y. K. Yan, M. Melchart, A. Hebtemariam, P. J. Sadler, Chem. Commun. (2005) 4764.

28 W. H. Ang, P. J. Dyson, Eur. J. Inorg. Chem. (2006) 4003.

29 M. Auzias, B. Therrien, G. Süss-Fink, P. P. Štěpnička, W. H. Ang, P. J. Dyson, Inorg. Chem. 47 (2008) 578.

30 A. F. A. Peacock, A. Habtemariam, R. Fernandez, V. Walland, F. P. A. Fabbiani, S. Parsons, R. E. Aird, D. I. Jodrell, P. J. Sadler, J. Am. Chem. Soc. 128 (2006) 1739.

31 A.Habtemariam, M. Melchart, R. Fernandez, S. Parsons, I. D. H. Oswald, A. Parkin, F. P. A. Fabbiani, J. E. Davidson, A. Dawson, R. E. Aird, D. I. Jodrell, P. J. Sadler, J. Med. Chem. 49 (2006) 6858.

32 M. Melchart, A. Habtemariam, O. Novakova, S. A. Moggach, F. P. A. Fabbiani, S. Parsons, V. Brabec, P. J. Sadler, Inorg. Chem. 46 (2007) 8950.

33 C. Scolaro, A. Bergamo, L. Brescacin, R. Delfino, M. Cocchietto, G. Laurenczy, T. J. Geldbach, G. Sava, P. J. Dyson, J. Med. Chem. 48 (2005) 4161.

34 M. Abrahamsson, H. C. Becker, L. Hammrstrom, C. Bonnefous, C. Chamchoumis, R. P. Thummel, Inorg. Chem. 46 (2007) 10354.

35 S. K. Patra, N. Sudhukhan, J. K. Bera, Inorg. Chem. 45 (2006) 4007.

36 C. S. Campos-Fernández, L. M. Thomson, J. R. Galán-Mascarós, X. Ouyang, K. R. Dunbar, Inorg. Chem. 41 (2002) 1523.

37 T. Suzuki, Inorg. Chim. Acta 359 (2006) 2431.

38 A. Kukrek, D. Wang, Y. Hou, R. Zong, R. Thummel, Inorg. Chem. 45 (2006) 10131.

39 K. V. Reddy, K. Mogilaiah, B. Srinivasulu, J. Indian Chem. Soc. 63 (1986) 443.

40 R. P. Thummel, F. Lefoulon, D. Cantu, R. J. Mahadevan, J. Org. Chem. 49 (1984) 2208.

41 H. V. D. Poel, G. V. Koten, K. Vrieze, Inorg. Chem. 19 (1980) 1145.

42 P. Govindaswamy, B. Therrien, G. Süss-Fink, P. Štěpnička, Ludvík, J. Organomet. Chem. 692 (2007)1661.

43 R. Lalrempuia, K. M. Rao, P. J. Carroll, Polyhedron, 22 (2003) 605.

44 A. Singh, N. Singh, D. S. Pandey, J. Orgnomet. Chem. 642 (2002) 48.

45 H. Mishra, R. Mukherjee, J. Orgnomet. Chem. 691 (2006) 3545;

46 K. Pachhunga, B. Therrien, K. A. Kreisel, G. P. A. Yap, M. R. Kollipara, Polyhedron. 26 (2007) 3638.

47 S. Tsuzuki, K. Honda, T. Uchimaru, M. Mikami, K. Tanabe, J. Am. Chem. Soc. 124 (2002) 104.

48 E. Binamira-Soriaga, N. L. Keder, W. C. Kaska, Inorg. Chem. 29 (1990) 3167.

49 N. Goswami, R. Alberto, C. L. Barnes, S. S. Jurisson, Inorg. Chem. 35 (1996) 7546.

50 R. Samanta, P. Munshi, B. K. Santra, N. K. Lokanath, M. A. Sridhar, J. S. Prasad, G. K. Lahari, J. Organomet. Chem. 579 (1999) 311.

51 A. K. Ghosh, K. K. Kamar, P. Paul, S.-M. Peng, G.-H. Lee, S. Goswami, Inorg. Chem. 41 (2002) 6343.

52 C. Das, A. K. Ghosh, C.-H. Hung, G.-H. Lee, S.-M. Peng, S. Goswami, Inorg. Chem. 41 (2002) 7125.

Chapter 5

Half-sandwich mono and dinuclear complexes of platinum group metals bearing pyrazolyl-pyridine analogues: Synthesis and spectral characterization

---

The chelating ligands *pp-Cl and bppp* were synthesized and their reactions with arene ruthenium, Cp* rhodium and iridium dimers resulted in the formation of mono and dinuclear complexes. However reactions with the *bppm* ligand which is having Pyrimidine Bridge between pyrazolyl-pyridine units resulted only in the formation of mononuclear complexes.

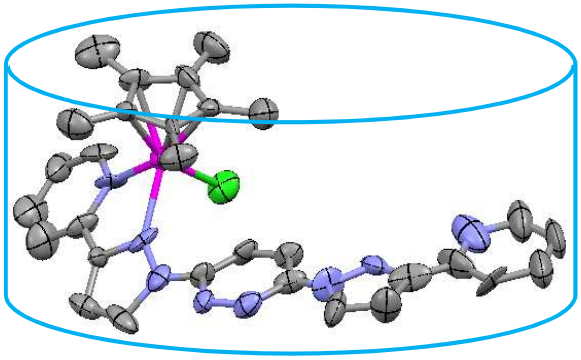

---

*The work presented in this chapter has been published: **K. T. Prasad** and K. Mohan Rao, Polyhedron (communicated).

5.1 Introduction

Mono and binuclear complexes of platinum group metals containing heterocyclic nitrogen based ligands have received considerable attention owing to their catalytic activities[1-8] and very recently as non-linear optical (NLO) materials,[9,10] as well as in the development of new biologically active agents.[11-16] The organometallic complexes of η^6-arene ruthenium,[17,18] and η^5-half-sandwich complexes of rhodium and iridium have attracted considerable interest as potential anticancer agents.[11-16] Another important aspect, especially from the catalytic perspective involves the design of Ru=O functional groups and analogues capable of reversibly accepting multiple electrons and protons within the relative potential range.[19-21] The capacity to modify their environment in order to induce electronic as well as steric effects will allow fabricating tailored catalysis for specific reactions. Inclusion of the pyridazine ring in the backbone of *bppp* ligand results in a more pronounced partitioning of the ligand into distinct bidentate domains than is the case with linear polypyridines. This facilitates the formation of mononuclear and binuclear systems. The former has the potential to behave as metallo-ligands in the development of homo/hetero bimetallic systems.[22-25]

In the present chapter, we have synthesized new nitrogen based ligands such as 3-chloro-6-(3-pyridyl-1-pyrazolyl)pyridazine (*pp-Cl*) and 3,6-bis(3-pyridyl-1-pyrazolyl)-pyridazine (*bppp*) (Chart 5.1) which easily form mono and binuclear complexes with arene ruthenium, Cp* rhodium and Cp* iridium complexes (Cp* = η^5-C_5Me_5). All these new complexes were characterized by elemental analyses, IR, ^{1}H-NMR, UV-Visible and mass spectrometry as well as X-crystallographic analyses for some representative complexes.

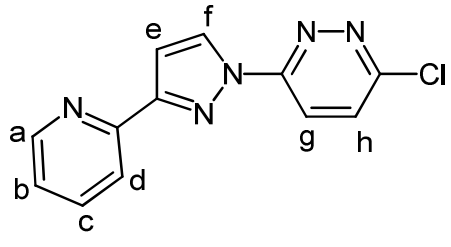

3-chloro-6-(3-pyridyl-1-pyrazolyl)pyr-idazine (*pp-Cl*)

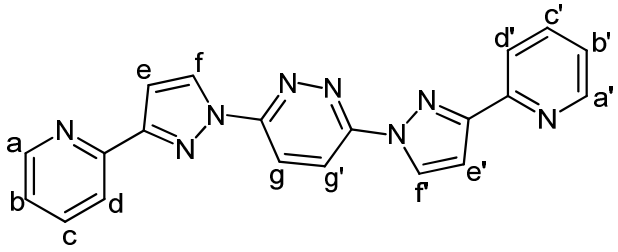

3,6-bis(3-pyridyl-1-pyrazolyl)pyrdazine (*bppp*)

Chart 5.1: Ligands used in this study

5.2 Experimental

5.2.1 Preparations of ligands: pp-Cl and bppp

A mixture of 3,6-dichloropyridazine (500 mg, 3.35 mmol), 3-(2-pyridyl)-1H-pyrazole[31] (1 g, 6.88 mmol), potassium carbonate (1.05 g, 7.59 mmol) and tetrabutyl-ammonium bromide (1.2 g) in 10 ml of acetone was dissolved. It was stirred and refluxed for forty hours and cooled to room temperature. Then the reaction mixture was poured in to 100 ml of water, resulted a whitish precipitate; it was filtered off, washed with excess water and air dried. It was purified by chromatography on silica gel using chloroform as the eluent to give the analytically pure ligand 3-chloro-6-(3-pyridyl-1-pyrazolyl)-pyridazine (*pp-Cl*) (20%) as a pale yellow color powder and the second fraction was eluted with chloroform / methanol (10:1) give the analytically pure ligand 3,6-bis(3-pyridyl-1-pyrazolyl)pyridazine (*bppp*) (80%) as a colorless solid.

5.2.1.1 3-chloro-6-(3-pyridyl-1-pyrazolyl)pyridazine (pp-Cl)

Pale yellow solid, yield 120 mg (13%): ^{1}H NMR (400 MHz, $CDCl_3$, δ): 8.77 (d, 1H, ^{3}J = 2.80 Hz, Ha), 8.68 (d, 1H, 3J = 4.40 Hz, Hf), 8.34 (d, 1H, 3J = 9.20 Hz, Hg), 8.04 (d, 1H, 3J = 8.00 Hz, Hh), 7.77 (dt, 1H, 3J = 1.60 Hz, Hd), 7.63 (d, 1H, 3J = 9.20 Hz, Hc), 7.28 (dt, 1H, 3J = 1.60 Hz, Hb), 7.18 (d, 1H, 3J = 2.40 Hz, He); ESI-MS (m/z): 258.1 (100%) [M+1]; UV–Vis {acetonitrile, λmax nm ($\varepsilon 10^{-5} M^{-1}$ cm^{-1})}: 318 (0.37); Anal. Calc. For $C_{12}H_8ClN_5$ (257.6): C, 55.93; H, 3.13; N, 27.18; Found: C, 54.88; H, 3.15; N, 27.02%.

5.2.1.2 3,6-bis(3-pyridyl-1-pyrazolyl)pyridazine (bppp)

White solid, yield 780 mg (63%): ^{1}H NMR (400 MHz, $CDCl_3$, δ): 8.81 (d, 2H, ^{3}J = 2.40 Hz, Haa′), 8.71 (d, 2H, ^{3}J = 4.40 Hz, Hff′), 8.52 (s, 2H, Hgg′), 8.11 (d, 2H, ^{3}J = 8.00, Hdd′), 7.80 (dt, 2H, ^{3}J = 1.60 Hz, Hcc′), 7.29 (dt, 2H, ^{3}J = 1.60 Hz, Hbb′), 7.21 (d, 2H, ^{3}J = 2.80 Hz, Hee′); ESI-MS (m/z): 367.2 (100%) [M+1]; UV–Vis {acetonitrile, λ_{max} nm ($\varepsilon 10^{-5} M^{-1}$ cm^{-1})}: 316 (0.41), 331 (0.33); Anal. Calc. For $C_{20}H_{14}N_8$ (366.3): C, 65.56; H, 3.85; N, 30.58; Found: C, 65.38; H, 3.89; N, 30.46%

5.2.1.3 4,6-bis(3-pyridyl-1-pyrazolyl)pyrimidine (bppm)[32]

The of bppm ligand was synthesized and isolated in a similar manner described for the synthesis of bppp taking 500 mg (3.35 mmol) of 4,6-dichloropyrimidine, 3-(2-pyridyl)-

1H-pyrazole (1 g, 6.88 mmol), potassium carbonate (1.05 g, 7.59 mmol) and tetrabutyl-ammonium bromide (1.2 g) in 10 ml of acetone was dissolved.

White solid, yield 780 mg (63%): ^{1}H NMR (400 MHz, $CDCl_3$, δ): 8.85 (d, 2H, ^{3}J = 2.40 Hz), 8.73 (s, 1H), 8.70 (d, 2H, ^{3}J = 1.60 Hz), 8.66 (s, 1H), 8.28 (d, 2H, ^{3}J = 7.20), 7.86 – 7.82(dt, 2H, ^{3}J = 1.60 Hz), 7.34 – 7.31 (dt, 2H, ^{3}J = 1.80 Hz), 7.22 (d, 2H, ^{3}J = 2.80 Hz); ESI-MS (m/z): 367.2 (100%) [M+1]; UV–Vis {acetonitrile, λ_{max} nm ($\varepsilon 10^{-5} M^{-1}$ cm^{-1})}: 318 (0.41), 332 (0.33); Anal. Calc. For $C_{20}H_{14}N_8$ (366.3): C, 65.56; H, 3.85; N, 30.58; Found: C, 65.38; H, 3.89; N, 30.46%

5.2.2 General procedure for the preparation of the mononuclear complexes **1** and **2**

A mixture of [(η^6-arene)Ru(μ-Cl)Cl]$_2$ (arene = C_6H_6 and *p*-^{i}PrC_6H_4Me) (0.07 mmol), ligand *pp-Cl* (0.18 mmol) and 2.5 equivalents of NH_4PF_6 in dry methanol (15 ml) was stirred at room temperature for 6 hours. The precipitate was separated by filtration, washed with cold methanol and diethyl ether to remove excess ligand and dried *in vacuo*.

*5.2.2.1 [(η^6-C_6H_6)Ru(pp-Cl)Cl]PF_6 ([**1**]PF_6)*

Orange-yellow solid, yield 75 mg (87%), ^{1}H NMR (400 MHz, CD_3CN, δ): 9.55 (d, 1H, ^{3}J = 5.60 Hz), 8.97 (d, 1H, ^{3}J = 2.80 Hz), 8.72 (d, 1H, ^{3}J = 7.28 Hz), 8.45 (m, 2H), 8.32 (t, 1H, ^{3}J = 7.60 Hz ,7.60 Hz), 7.78 (m, 2H), 5.95 (s, 6H); IR (KBr, cm^{-1}): $\nu_{(P-F)}$ 844s; 1604m, 1408m, 558m; ESI-MS (m/z): 472.1 (100%) $[M-PF_6]^+$; UV–Vis {acetonitrile, λ_{max} nm ($\varepsilon 10^{-5} M^{-1}$ cm^{-1})}: 310 (0.19); Anal. Calc. For $C_{18}H_{14}Cl_2N_5RuP F_6$ (617.2): C, 35.02; H, 2.29; N, 11.35; Found: C, 34.88; H, 2.35; N, 11.28%.

*5.2.2.2 [(η^6-*p*-^{i}PrC_6H_4Me)Ru(pp-Cl)Cl]PF_6 ([**2**]PF_6)*

Dark orange solid, yield 83 mg (90%), ^{1}H NMR (400 MHz, CD_3CN, δ): 9.22 (d, 1H, ^{3}J = 5.60 Hz), 8.75 (d, 1H, ^{3}J = 4.80 Hz), 8.62 (d, 1H, ^{3}J = 3.20 Hz), 8.19 – 8.12 (m, 3H), 7.66 (dd, 1H, ^{3}J = 7.60 Hz ,7.60 Hz), 7.40 (d, 1H, ^{3}J = 3.2 Hz) 5.72 (d, 1H, ^{3}J = 6.40 Hz, Ar_{p-cy}), 5.46 (d, H, ^{3}J = 6.00 Hz, Ar_{p-cy}), 5.30 (d, 1H, ^{3}J = 6.00 Hz, Ar_{p-cy}), 5.18 (d, 1H, ^{3}J = 6.00 Hz, Ar_{p-cy}), 2.37 (sept, 1H, $CH(CH_3)_2$), 2.17 (s, 3H, Ar_{p-cy}-Me), 1.21 (d, 3H, $CH(CH_3)_2$), 1.18 (d, 3H, $CH(CH_3)_2$); IR (KBr, cm^{-1}): $\nu_{(P-F)}$ 844s; 1629m, 1406m, 763m, 558m; ESI-MS (m/z): 527.2 (100%) $[M-PF_6]^+$; UV–Vis {acetonitrile, λ_{max} nm ($\varepsilon 10^{-5} M^{-1}$ cm^{-1})}: 309 (0.28); Anal. Calc. For $C_{22}H_{22}Cl_2N_5RuPF_6$ (673.3): C, 39.24; H, 3.29; N, 10.40; Found: C, 39.11; H, 3.35; N, 10.31%.

5.2.3 General procedure for the preparation of the mononuclear complexes **3** and **4**

A mixture of $[(\eta^5\text{-}C_5Me_5)M(\mu\text{-}Cl)Cl]_2$ (M = Rh, Ir) (0.07 mmol), ligand *pp-Cl* (0.15 mmol) and 2.5 equivalents of ammonium hexafluorophosphate in dry methanol (15 ml) was refluxed for 4 hours. The reaction mixture was cooled over night at room temperature during this time dark yellow color crystalline compound formed. It was separated by filtration, washed with cold methanol and diethyl ether to remove excess ligand and dried in *vacuo.*

*5.2.3.1 $[(\eta^5\text{-}C_5Me_5)Rh(pp\text{-}Cl)Cl]PF_6$ ([**3**]PF_6)*

Dark yellow in color, yield 86 mg (91%), ^{1}H NMR (400 MHz, CD_3CN, δ): 8.91 (d, 1H, ^3J = 5.20 Hz), 8.67 (d, 1H, ^3J = 4.40 Hz), 8.50 (d, 1H, ^3J = 7.60 Hz), 8.36 (m, 3H), 7.44 (dt, 1H, ^3J = 5.20 Hz , 6.80 Hz), 7.22 (d, 1H, ^3J = 2.4 Hz), 2.15 (s, 15H, C_5Me_5); IR (KBr, cm^{-1}): $\nu_{(P\text{-}F)}$ 845s; 1626m, 1458m, 759m, 558m; ESI-MS (m/z): 531.3 (100%) $[M\text{-}PF_6]^+$; UV–Vis {acetonitrile, λ_{max} nm ($\varepsilon 10^{-5}M^{-1}$ cm^{-1})}: 316 (0.27); Anal. Calc. For $C_{22}H_{23}Cl_2N_5RhPF_6$ (676.3): C, 39.07; H, 3.43; N, 10.49; Found: C, 39.01; H, 3.45; N, 10.33%.

*5.2.3.2 $[(\eta^5\text{-}C_5Me_5)Ir(pp\text{-}Cl)Cl]PF_6$ ([**4**]PF_6)*

Dark yellow color, yield 89 mg (88%),^{1}H NMR (400 MHz, CD_3CN, δ): 9.01 (d, 1H, ^3J = 5.60 Hz), 8.71 (d, 1H, ^3J = 4.80 Hz), 8.62 (d, 1H, ^3J = 6.40 Hz), 8.42 (m, 3H), 7.48 (dt, 1H, ^3J = 5.32 Hz , 5.60 Hz), 7.35 (d, 1H, ^3J = 4.80 Hz), 1.88 (s, 15H, C_5Me_5); IR (KBr, cm^{-1}): $\nu_{(P\text{-}F)}$ 845s; 1631m, 1495m, 760m, 558m; ESI-MS (m/z): 620.9 (100%) $[M\text{-}PF_6]^+$; UV–Vis {acetonitrile, λ_{max} nm (ε $10^{-5}M^{-1}$ cm^{-1})}: 318 (0.29); Anal. *Calc*. For $C_{22}H_{23}Cl_2N_5IrPF_6$ (765.4): C, 34.52; H, 3.03; N, 9.05; Found: C, 34.25; H, 3.05; N, 9.00%.

5.2.4 General procedure for the preparation of the mononuclear complexes **5** and **6**

A mixture of $[(\eta^6\text{-arene})Ru(\mu\text{-}Cl)Cl]_2$ (arene = C_6H_6 and *p*-^{i}PrC_6H_4Me) (0.07 mmol), ligand *bppp* (0.15 mmol) and 2.5 equivalents of ammonium hexafluorophosphate in dry methanol (15 ml) was stirred at room temperature for 6 hours. The precipitate was separated by filtration, washed with cold methanol and diethyl ether to remove excess ligand and dried *in vacuo*.

*5.2.4.1 [(η^6-C_6H_6)Ru(bppp)Cl]PF_6 ([**5**]PF_6)*

Brown color; Yield 85 mg (84%), ^{1}H NMR (400 MHz, CD_3CN, δ): 9.48 (d, 1H, ^3J = 5.20 Hz), 8.68 (d, 1H, ^3J = 5.64 Hz), 8.62 (d, 1H, ^3J = 3.20 Hz), 8.32 – 8.28 (m, 5H), 7.76 (dt, 2H), 7.62 (t, 1H, ^3J = 3.32 Hz), 7.43 (d, 1H, ^3J = 3.24 Hz), 7.26 (d, 1H, ^3J = 4.20 Hz), 7.20 (d, 1H, ^3J = 4.00 Hz), 6.01 (s, 6H, C_6H_6); IR (cm^{-1}): 1614m, 1454s, 1437s, 844s, 788s, 558m; ESI-MS: 580.9 [M^+], 545.2 [M - Cl]; UV–Vis {acetonitrile, λ_{max} nm ($\varepsilon 10^{-5} M^{-1}$ cm^{-1})}: 276 (0.57), 314 (0.92), 417 (0.04); Anal. Calc. for $C_{26}H_{20}ClN_8RuPF_6$ (725.9): C, 43.01; H, 2.78; N 15.43. Found: C, 42.89; H, 2.87; N, 15.28%.

*5.2.4.2 [(η^6-p-^{i}PrC_6H_4Me)Ru(bppp)Cl]PF_6 ([**6**]PF_6)*

Orange-yellow solid, Yield 89 mg (83%), ^{1}H NMR (400 MHz, CD_3CN, δ): 9.55 (d, 1H, ^3J = 5.20 Hz), 8.72 (d, 1H, ^3J = 5.64 Hz), 8.68 (d, 1H, ^3J = 3.20 Hz), 8.20 – 8.18 (m, 4H), 7.68 (dt, 2H), 7.42 (t, 1H, ^3J = 3.32 Hz), 7.38 (d, 1H, ^3J = 4.80 Hz), 7.22 (d, 1H, ^3J = 4.20 Hz), 7.18 (d, 2H, ^3J = 5.60 Hz), 5.72 (d, 1H, ^3J = 6.40 Hz, $Ar_{p\text{-}cy}$), 5.42 (d, 1H, ^3J = 6.00 Hz, $Ar_{p\text{-}cy}$), 5.39 (d, 1H, ^3J = 6.00 Hz, $Ar_{p\text{-}cy}$), 5.29 (d, 1H, ^3J = 5.60 Hz, $Ar_{p\text{-}cy}$), 2.70 (sept, 1H, $CH(CH_3)_2$), 2.33 (s, 3H, $Ar_{p\text{-}cy}$-Me), 1.71 (d, 3H, ^3J = 6.20 Hz, $CH(CH_3)_2$), 1.69 (d, 3H, ^3J = 6.80 Hz, $CH(CH_3)_2$); IR (cm^{-1}): 1604m, 1449m, 1437m, 843s, 783m, 558m; ESI-MS: 637.1 [M^+], 602.1 [M - Cl]; UV–Vis {acetonitrile, λ_{max} nm ($\varepsilon 10^{-5} M^{-1}$ cm^{-1})}: 274 (0.57), 313 (0.89), 418 (0.05); Anal. Calc. for $C_{30}H_{28}ClN_8RuPF_6$ (782.1): C, 46.07; H, 3.61; N, 14.33. Found: C, 45.97; H, 3.68; N, 14.17%.

5.2.5 General procedure for the preparation of the mononuclear complexes **7** and **8**

A mixture of [(η^5-C_5Me_5)M(μ-Cl)Cl]$_2$ (M = Rh, Ir) (0.07 mmol), ligand *bppp* (0.15 mmol) and 2.5 equivalents of ammonium hexafluorophosphate in dry methanol (15 ml) was refluxed for 4 hours. The reaction mixture was cooled over night at room temperature during this time dark yellow color crystalline compound formed. It was separated by filtration, washed with cold methanol and diethyl ether to remove excess ligand and dried under vacuum.

*5.2.5.1 [(η^5-C_5Me_5)Rh(bppp)Cl]PF_6 ([**7**]PF_6)*

Dark yellow color, yield 96 mg (84%), ^{1}H NMR (400 MHz, CD_3CN, δ): 9.39 (d, 1H, ^3J = 5.20 Hz), 8.68 (d, 1H, ^3J = 5.40 Hz), 8.54 (d, 1H, ^3J = 3.64 Hz), 8.18 - 8.10 (m, 4H), 7.61 (dt, 2H), 7.48 (d, 1H, ^3J = 3.60 Hz), 7.32 (d, 1H, ^3J = 4.8 Hz), 7.22 (d, 1H, ^3J = 4.20 Hz), 7.16 (d, 2H, ^3J = 3.64 Hz), 2.11 (s, 15H, C_5Me_5); ESI-MS (m/z): 639.2 (100%) [M-PF_6]$^+$;

IR (KBr, cm^{-1}): $\nu_{(P-F)}$ 845s; 1626m, 1458m, 759m, 558m; UV–Vis {acetonitrile, λ_{max} nm ($\varepsilon 10^{-5} M^{-1}$ cm^{-1})}: 276 (0.57), 315 (0.87), 419 (0.04); Anal. Calc. For $C_{30}H_{29}ClN_8RhPF_6$ (784.93): C, 45.91; H, 3.72; N, 14.28; Found: C, 45.93; H, 3.77; N, 14.30%.

*5.2.5.2 [(η^5-C_5Me_5)Ir(bppp)Cl]PF_6 ([**8**]PF_6)*

Dark yellow in color, yield 95 mg (83%): ^{1}H NMR (400 MHz, CD_3CN, δ): 9.40 (d, 1H, ^3J = 5.32 Hz), 8.72 (d, 1H, ^3J = 5.40 Hz), 8.62 (d, 1H, ^3J = 3.64 Hz), 8.20 – 8.14 (m, 4H), 7.65 (dt, 2H), 7.48 (d, 1H, ^3J = 3.60 Hz), 7.31 (d, 1H, ^3J = 4.8 Hz), 7.18 (d, 1H, ^3J = 4.80 Hz), 7.15 (d, 2H, ^3J = 3.60 Hz), 1.98 (s, 15H, C_5Me_5); ESI-MS (m/z): 729.2 (100%) [M-PF_6]$^+$; IR (KBr, cm^{-1}): $\nu_{(P-F)}$ 845s; 1631m, 1495m, 760m, 558m; UV–Vis {acetonitrile, λ_{max} nm ($\varepsilon 10^{-5} M^{-1}$ cm^{-1})}: 277 (0.58), 314 (0.95), 423 (0.04); Anal. Calc. For $C_{30}H_{29}ClN_8IrPF_6$ (874.24): C, 41.22; H, 3.34; N, 12.82; Found: C, 41.19; H, 3.38; N, 12.73%.

5.2.6 General procedure for the syntheses of the dinuclear complexes **9** and **10**

A mixture of [(η^6-arene)Ru(μ-Cl)Cl]$_2$ (arene = C_6H_6 and *p*-^{i}PrC_6H_4Me) (0.10 mmol) and *bppp* (0.10 mmol) was suspended in methanol (20 ml) and stirred at room temperature for 6 hours. Then, ammonium hexafluorophosphate (46 mg, 0.25 mmol) was added to the reaction mixture and further stirred for 3 hours. The precipitate was filtered, washed with methanol and diethylether (3 X 10 ml) and dried *in vacuo*.

*5.2.6.1 [{(η^6-C_6H_6)RuCl}$_2$(μ-bppp)]$(PF_6)_2$ ([**9**]$(PF_6)_2$)*

Orange-yellow solid, Yield 91 mg (85%): ^{1}H NMR (400 MHz, CD_3CN, δ): 9.34 (d, 2H, ^3J = 4.20 Hz), 9.14 (s, 2H), 8.81 (d, 2H, ^3J = 2.40 Hz), 8.24 (d, 2H, ^3J = 6.80 Hz), 7.72 (t, 2H, ^3J = 5.60, 4.80 Hz), 7.50 (d, 2H, ^3J = 2.40 Hz), 7.36 (d, 2H, ^3J = 4.80 Hz), 5.75 (s, 12H, C_6H_6); IR (cm^{-1}): 1614m, 1454m, 1437m, 844s, 788m, 558m; ESI-MS: 940.6[M^{2+}+PF_6^-]$^+$; UV–Vis {acetonitrile, λ_{max} nm ($\varepsilon 10^{-5} M^{-1}$ cm^{-1})}: 278 (0.54), 312 (0.83), 408 (0.04); Anal. Calc. for $C_{32}H_{26}N_8Cl_2RuP_2F_{12}$ (1085.6): C, 35.40; H, 2.41; N 10.32. Found: C, 35.33; H, 2.47; N, 10.18%.

*5.2.6.2 [{(η^6-p-^{i}PrC_6H_4Me)RuCl}$_2$(μ-bppp)]$(PF_6)_2$ ([**10**]$(PF_6)_2$)*

Orange-yellow solid, Yield 99 mg (84%): ^{1}H NMR (400 MHz, CD_3CN, δ): 9.55 (d, 2H, ^3J = 5.60 Hz), 9.37 (s, 2H), 9.14 (d, 2H, ^3J = 2.80 Hz), 8.52 (d, 2H, ^3J = 7.60 Hz), 8.48 (t, 2H, ^3J = 7.20, 7.60 Hz), 8.36 (t, 2H), 7.86 (d, 2H, ^3J = 2.40 Hz), 6.10 (d, 2H, ^3J = 6.00

Hz, $Ar_{p\text{-}cy}$), 5.81 (d, 2H, ^3J = 6.00 Hz, $Ar_{p\text{-}cy}$), 5.69 (d, 2H, ^3J = 6.00 Hz, $Ar_{p\text{-}cy}$), 5.54 (d, 2H, ^3J = 6.00 Hz, $Ar_{p\text{-}cy}$), 2.68 (sept, 2H, $CH(CH_3)_2$), 2.25 (s, 6H, $Ar_{p\text{-}cy}$-Me), 1.18 (d, 3H, ^3J = 6.20 Hz, $CH(CH_3)_2$), 1.12 (d, 3H, ^3J = 3.20 Hz, ^3J = 6.80 Hz, $CH(CH_3)_2$); IR (cm^{-1}): 1604m, 1449s, 1437s, 843s, 783m, 558m; ESI-MS: 1052.6 $[M^{2+}+PF_6^-]^+$; UV–Vis {acetonitrile, λ_{max} nm ($\varepsilon 10^{-5} M^{-1}$ cm^{-1})}: 276 (0.57), 314 (0.91), 410 (0.04); Anal. Calc. for $C_{40}H_{42}N_8Cl_2RuP_2F_{12}$ (1197.8): C, 40.11; H, 3.53; N, 9.36. Found: C, 40.01; H, 3.35; N, 9.27%.

5.2.7 General procedure for the syntheses of the dinuclear complexes **11** and **12**

A mixture of $[(\eta^5\text{-}C_5Me_5)M(\mu\text{-}Cl)Cl]_2$ (M = Rh and Ir) (0.10 mmol) and *bppp* (0.10 mmol) was suspended in methanol (20 ml) and refluxed for 5 hours. Then, ammonium hexafluorophosphate (23 mg, 0.13 mmol) was added to the reaction mixture and further refluxed for an hour. During this time was precipitate was observed. The precipitate was filtered, washed with methanol and diethylether (3 X 10 ml) and dried *in vacuo*.

*5.2.7.1 [{(η^5-C_5Me_5)RhCl}$_2$(μ-bppp)](PF_6)$_2$ ([**11**](PF_6)$_2$)*

Dark yellow color, yield 101 mg (84%): ^{1}H NMR (400 MHz, CD_3CN, δ): 9.38 (d, 2H, ^3J = 5.40 Hz), 9.17 (s, 2H), 8.81 (d, 2H, ^3J = 2.32 Hz), 8.24 (d, 2H, ^3J = 6.80 Hz), 7.75 (t, 2H, ^3J = 5.20, 4.80 Hz), 7.52 (d, 2H, ^3J = 2.32 Hz), 7.37 (d, 2H, ^3J = 4.32 Hz), 2.05 (s, 30H, C_5Me_5); IR (cm^{-1}): 1604m, 1449m, 1437m, 843m, 783m, 558m; ESI-MS: 1058.6 $[M^{2+}+PF_6^-]^+$; UV–Vis {acetonitrile, λ_{max} nm ($\varepsilon 10^{-5} M^{-1}$ cm^{-1})}: 276 (0.39), 314 (0.67), 420 (0.04); Anal. Calc. for $C_{40}H_{44}N_8Cl_2RhP_2F_{12}$ (1203.5): C, 39.92; H, 3.69; N, 9.31. Found: C, 39.21; H, 3.72; N, 9.27%.

*5.2.7.2 [{(η^5-C_5Me_5)IrCl}$_2$(μ-bppp)](PF_6)$_2$ ([**12**](PF_6)$_2$)*

Dark yellow color, yield 105 mg (86%): ^{1}H NMR (400 MHz, CD_3CN, δ): 9.31 (d, 2H, ^3J = 4.36 Hz), 9.14 (s, 2H), 8.78 (d, 2H, ^3J = 2.80 Hz), 8.21 (d, 2H, ^3J = 6.32 Hz), 7.72 (t, 2H, ^3J = 5.60, 4.80 Hz), 7.50 (d, 2H, ^3J = 2.40 Hz), 7.36 (d, 2H, ^3J = 4.80 Hz), 1.99 (s, 15H, C_5Me_5); IR (cm^{-1}): 1604m, 1449m, 1437m, 843s, 783m, 558m; ESI-MS: 1236.2 $[M^{2+}+PF_6^-]^+$; UV–Vis {acetonitrile, λ_{max} nm ($\varepsilon 10^{-5} M^{-1}$ cm^{-1})}: 273 (0.46), 313 (0.71), 418 (0.04); Anal. Calc. for $C_{40}H_{42}N_8Cl_2IrP_2F_{12}$ (1382.1): C, 34.76; H, 3.21; N, 8.11. Found: C, 34.61; H, 3.25; N, 8.01%.

5.2.8 Single crystal X-ray structure analyses

X-ray quality crystals of complexes **2** and **7** were grown by slow diffusion of hexane in dichloromethane / acetonitrile solution of corresponding complexes. The X-ray intensity data were measured at 293(2)° K on a Bruker Apex II CCD area detector employing graphite monochromated using Mo-*K*α radiation (λ = 0.71073 Å). An empirical absorption correction was made by modeling a transmission surface by spherical harmonics employing equivalent reflections with I>2σ(I) using the program SADBAS. The structures were solved by direct methods using the program SHELXS 97 and refined by full matrix least squares base on F_2 using the program SHELXL-97. The weighting scheme used was $W=1/[\sigma 2(F_{02})+0.0311P_2 +3.5016 P]$ where $P = (F_{02}+ 2F_{c2})/3$. Non-hydrogen atoms were refined anisotropically and hydrogen atoms were refined using a "riding" model. Refinement converged at a final R = 0.0423 and 0.0454 (for complexes **2** and **7** respectively, for observed data F_2), and wR2 = 0.0804 and 0.0667 (for complexes **2** and **7** respectively, for unique data F_2). Regarding complex **7** molecular structure, we are encountered two difficulties, they are (i) one is assigning N(8) and C(17), and another one is (ii) occupancy of the solvent molecule acetonitrile. The matter regarding an ambiguity in assigning N(8) and C(17), exchanging the atoms did not improve the refinement. So the labelling was done in analogy with other compounds and represents the most probable orientation of the molecular fragment. The second factor is now explained on the following lines: the central atom of solvent molecule with occupancy of C is 0.5. Since the solvent molecule is acetonitrile, the two heavy peripheral atoms are N and C. It appears that we cannot differentiate between N and C, which can be due to the random orientation of N and C (they exchange the sites). We also could not locate the H atoms associated with the peripheral C atom. This peripheral site was treated as a 50/50 mixture of C and N, which considering the occupancy of this site yields one molecule of acetonitrile (per two molecules of the complex). The distance between the central C atom and peripheral atoms is 1.55 Å. While other solvent molecules may be present, only acetonitrile molecule has been located from the residual density map. Its presence was manifested by a large residual density, and its introduction lowered the R value from 5.55 to 4.43%. Details of crystallographic data collection parameters and refinement are summarized in table 5.1. Selected bond lengths and angles are tabulated in table 5.2.

5.3 Results and discussion

5.3.1 Synthesis of ligands

The ligands 3-chloro-6-(3-pyridyl-1-pyrazolyl)pyridazine (*pp-Cl*) and 3,6-bis(3-pyridyl-1-pyrazolyl)pyridazine were synthesized by the condensation of 3,6-dichloropyridazine and 3-(2-pyridyl)-1H-pyrazole. The reaction was carried out in acetone under refluxing condition in the presence of potassium carbonate and the phase transfer catalyst tetrabutylammonium bromide. The resulting compounds were characterized by spectroscopic methods as detailed in the experimental section.

5.3.2 Synthesis of the mononuclear complexes **1** to **8** as a hexafluorophosphate salts

The mononuclear cationic arene ruthenium and pentamethylcyclopentadienyl rhodium and iridium complexes having 3-chloro-6-(3-pyridyl-1-pyrazolyl)pyridazine (*pp-Cl*) and 3,6-bis(3-pyridyl-1-pyrazolyl)pyridazine (*bppp*) ligands *viz*., $[(\eta^6\text{-}C_6H_6)RuCl(pp\text{-}Cl)]PF_6$ [**1**]PF_6, $[(\eta^6\text{-}p\text{-}^iPrC_6H_4Me)RuCl(pp\text{-}Cl)]PF_6$ [**2**]PF_6, $[(\eta^5\text{-}C_5Me_5)RhCl(pp\text{-}Cl)]PF_6$ [**3**]PF_6 and $[(\eta^5\text{-}C_5Me_5)IrCl(pp\text{-}Cl)]PF_6$ [**4**]PF_6 (Scheme 5.1) and $[(\eta^6\text{-}C_6H_6)RuCl(bppp)]PF_6$ [**5**]PF_6, $[(\eta^6\text{-}p\text{-}^iPrC_6H_4Me)RuCl(bppp)]PF_6$ [**6**]PF_6, $[(\eta^5\text{-}C_5Me_5)RhCl(bppp)]PF_6$ [**7**]PF_6 and $[(\eta^5\text{-}C_5Me_5)IrCl(bppp)]PF_6$ [**8**]PF_6 (Scheme 5.2) have been prepared by the reaction of arene or pentamethylcyclopentadienyl complexes $[(\eta^6\text{-arene})Ru(\mu\text{-}Cl)Cl]_2$ (arene = C_6H_6 and $p\text{-}^iPrC_6H_4Me$) and $[(\eta^5\text{-}C_5Me_5)M(\mu\text{-}Cl)Cl]_2$ (M = Rh and Ir) with 2.1 equivalents of ligand 3-chloro-6-(1-pyridyl-3-pyrazolyl)pyridazine (*pp-Cl*) or 3,6-bis(1-pyridyl-3-pyrazolyl)-pyridazine (*bppp*) in methanol. The complexes **1** to **8** were isolated as hexafluorophosphate salts and exhibit an orange–red color. They are non - hygroscopic, air-stable, shiny crystalline solids sparingly soluble in methanol, dichloromethane and chloroform, but soluble in acetone and acetonitrile. All these metal complexes were fully characterized by IR, NMR and UV-Vis and mass spectrometry.

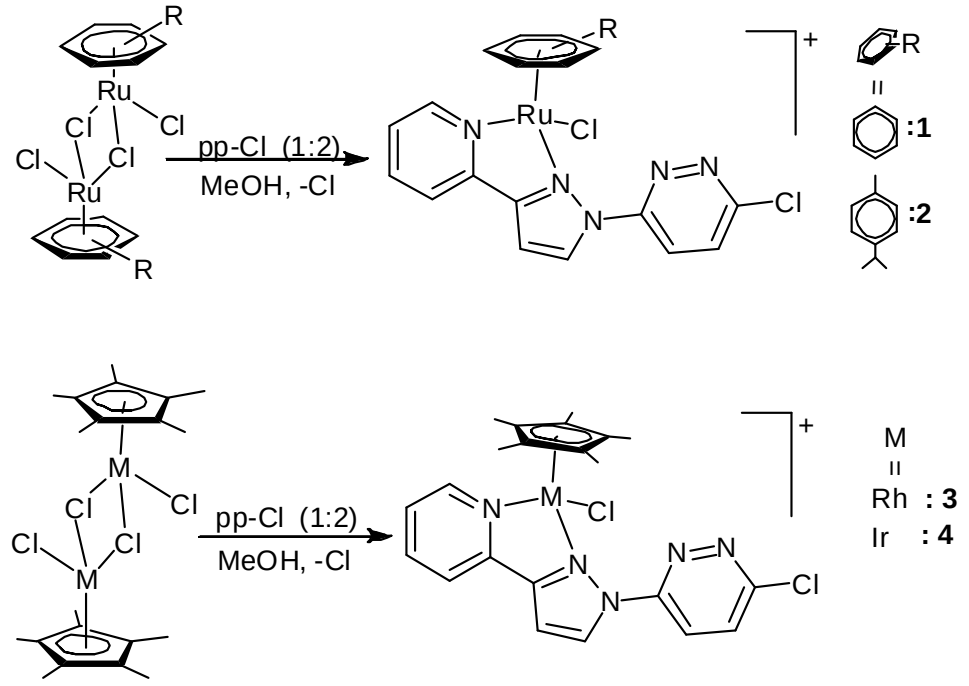

Scheme 5.1

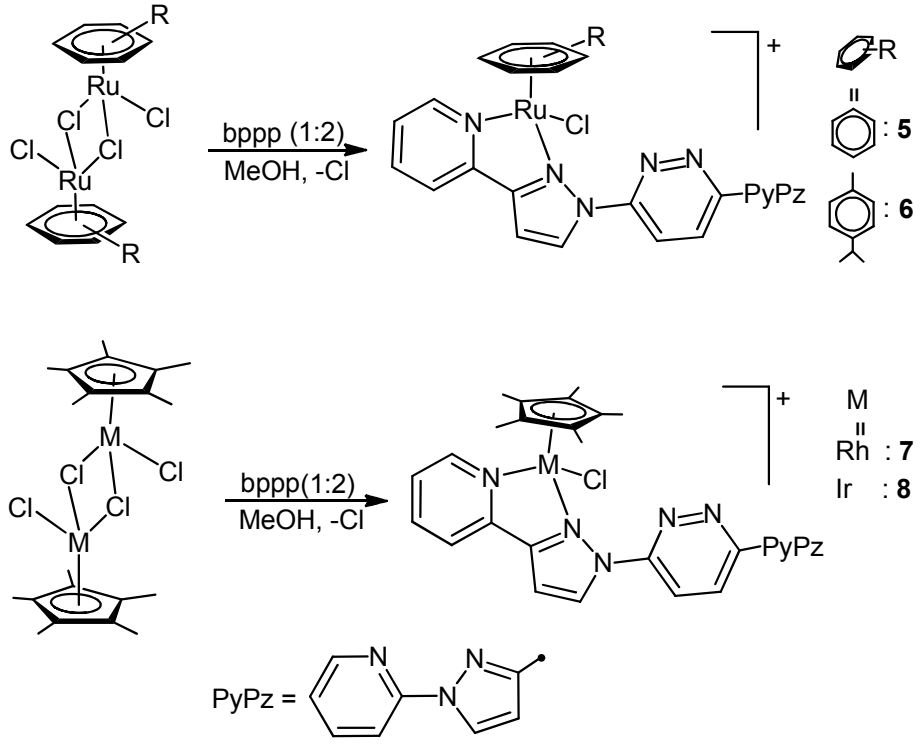

Scheme 5.2

The infrared spectra of the complexes **1** to **8** exhibit a strong band in the region 844-850 cm^{-1}, a typical ν_{P-F} stretching band and for the PF_6 anions as well as peaks

corresponding to phenyl, pyridyl, pyrazolyl and pyridazine (C=C and C=N) rings were observed.

The mass spectra of these compounds exhibited the corresponding molecular ion peaks m/z at 472, 527, 531, 621, 581, 637, 639 and 729. For example the mass spectrum of the complex **2** is depicted in figure 5.1.

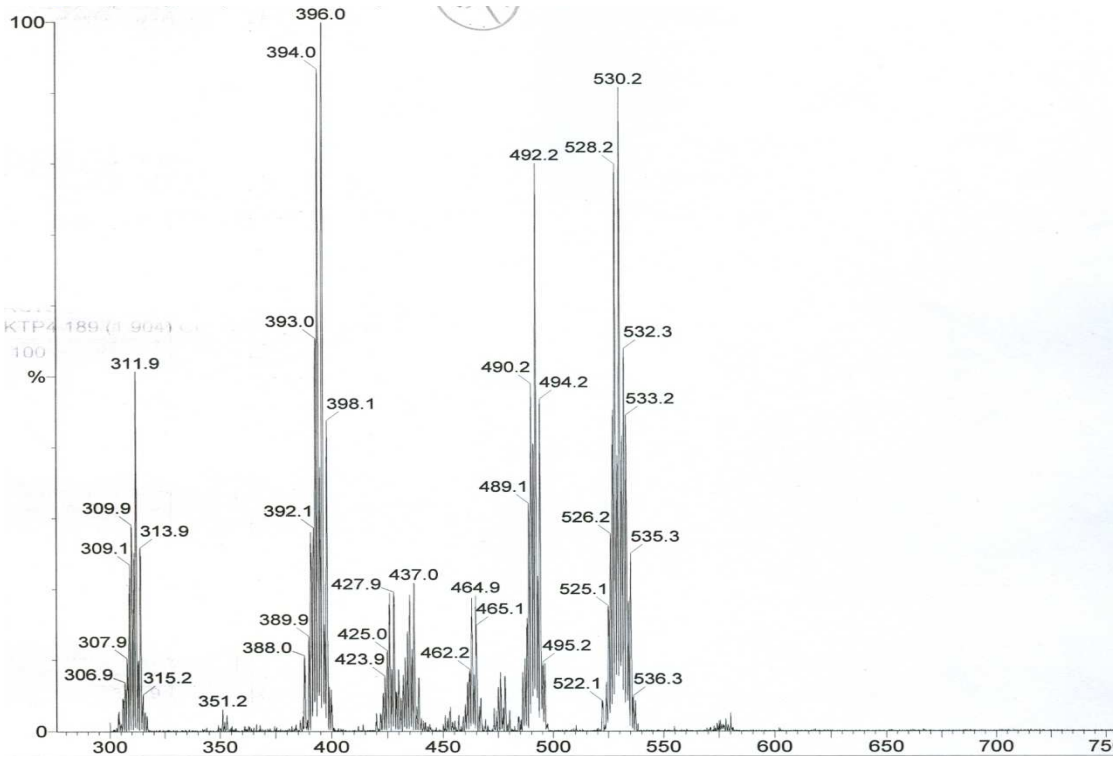

Figure 5.1: Mass spectrum of the complex $[(\eta^6\text{-}p\text{-}^{i}PrC_6H_4Me)Ru(pp\text{-}Cl)Cl]PF_6$ ([**2**]PF_6)

The ^1H NMR spectrum of free ligands 3-chloro-6-(3-pyridyl-1-pyrazolyl)pyridazine (*pp-Cl*) exhibit a characteristic set of eight resonances at 8.77 (d, 1H), 8.68 (d, 1H), 8.34 (d, pyrazolyl, pyridazine and pyridyl ring protons of the 3,6-bis(3-pyridyl-1-pyrazolyl)pyridazine (*bppp*) ligand, indicating formation of mononuclear complexes. Besides these resonances complex **1** and **5** exhibit a singlet at δ = 5.95 and 5.92 respectively for the protons of the benzene ligand. Complexes **2** and **6** exhibits two doublets at δ = 1.71 - 1.69, as well as a septet at δ = 2.70 - 2.32 for the protons of the isopropyl group and a singlet at 2.17 ppm for the methyl protons of *p*-cymene ring. The four doublets observed at 5.59 - 5.39 correspond to the aromatic *p*-cymene ring CH protons. This unusual pattern is due to the diastereotopic methyl protons of the isopropyl group and aromatic protons of the *p*-cymene ligand, since the ruthenium atom is stereogenic due to the coordination of four different ligand atoms and chiral nature of

metal atom.[26-28] Interestingly the chemical shifts of complex **6** shown down field compared to complex **2** of *p*-cymene ligand. Complexes **3**, **4**, **7** and **8** exhibit a strong peak at δ = 2.15, 1.88, 2.11 and 1.98 for pentamethylcyclopentadienyl ligand respectively, which are slightly shifted downfield in comparison to the starting complexes.

5.3.3 Crystal structure analysis of $[(\eta^6\text{-}p\text{-}^{i}PrC_6H_4Me)Ru(pp\text{-}Cl)Cl]PF_6$ ([**2**]PF_6) and $[(\eta^5\text{-}C_5Me_5)Rh(bppp)Cl]PF_6$ ([**7**]PF_6)

The molecular structure of $[(\eta^6\text{-}p\text{-}^{i}PrC_6H_4Me)Ru(\textit{pp-Cl})Cl]PF_6$ ([**2**]PF_6) and $[(\eta^5\text{-}C_5Me_5)Rh(\textit{bppp})Cl]PF_6$ [**7**]PF_6 have been established by single-crystal X-ray structure analysis. Both complexes shown a typical piano-stool geometry with the metal centre coordinated by the aromatic ligand, chloride and a chelating *N*,*N′*-ligand (see figures 5.2 and 5.3). The metal atom is in octahedral arrangement and the *pp-Cl* or *bppp* ligand is found to coordinate through the N1 atom of the pyridine moiety and the N2 atom of the pyrazolyl ring to generate a five-membered ring metallo-cycle (see Figures 5.2 and 5.3). In these complexes, the N atom of pyridazine points away from the metal centre and show no interaction with neighboring cations. Selected bond lengths and angles for complexes **2** and **7** are presented in Table 5.2.

Table 5.1: Crystallographic and structure refinement parameters for compounds [**2**]PF_6 and [**7**]PF_6.

Complex	[**2**]PF_6	[**7**]PF_6
Chemical formula	$C_{22}H_{22}Cl_2F_6N_5PRu$	$C_{30}H_{29}ClF_6N_8PRh.0.5CH_3CN$
Crystal system	Monoclinic	Monoclinic
Formulae weight	673.39	803.96
Wavelength (Å)	0.710	0.710
Space group	C2/c	P 21/n
Crystal color and shape	Plate, yellow	Plate, yellow
Crystal size (mm)	0.28 × 0.15 × 0.09	0.22 × 0.14 × 0.12
a (Å)	10.1768 (8)	8.5156 (17)
b (Å)	22.7250 (16)	19.095 (4)
c (Å)	22.133 (2)	22.334 (5)
α (°)	-	-
β (°)	97.646 (7)	90.46 (3)
γ (°)	-	-
V ($Å^3$)	5073.2 (7)	3631.5 (13)
Z	8	4
T (K)	293 (2)	293 (2)
D_x (g /cm^3)	1.763	1.470
μ (mm^{-1})	0.959	0.65
Scan range (°)	1.79< θ <24.65	2.11< θ <20.00
Unique reflections	4000	3331
Reflections used [I>2σ(I)]	2291	1042
R_{int}	0.0646	0.189
Final R indices [I>2σ(I)]	0.0423, wR_2 0.0803	0.0443, wR_2 0.0626
R indices (all data)	0.0862, wR_2 0.0863	0.1881, wR_2 0.0894
Goodness-of-fit	0.824	0.534
Max, Min Δρ (e $Å^{-3}$)	0.696, -0.718	0.284, -0.261

Table 5.2: Selected bond lengths (Å) and angles (°) for compounds [**1**]PF_6 and [**7**]PF_6.

Complex	[**2**]PF_6		[**7**]PF_6
Interatomic distances			
Ru-N1	2.099(3)	Rh-N1	2.08(1)
Ru-N2	2.089(3)	Rh-N2	2.16(5)
Ru-Cl1	2.406(2)	Rh-Cl1	2.396(4)
Ru-centroid (C_6 ring)	1.683	Rh-centroid (C_5 ring)	1.79
C5-C6	1.351(5)	C5-C6	1.31(1)
N1-C1	1.390(5)	N1-C1	1.39(2)
N2-N3	1.420(5)	N2-N3	1.42(1)
Angles			
N1-Ru-N2	75.50(1)	N1-Rh-N2	73.25 (3)
N1-Ru-Cl1	83.80(1)	N1-Rh-Cl1	86.21(3)
N2-Ru-Cl1	84.52(1)	N2-Rh-Cl1	91.47(2)
Ru1-N1-C5	116.90(2)	Rh1-N1-C5	115.21(8)
Ru1-N2-C6	115.50(2)	Rh1-N2-C6	114.72(4)

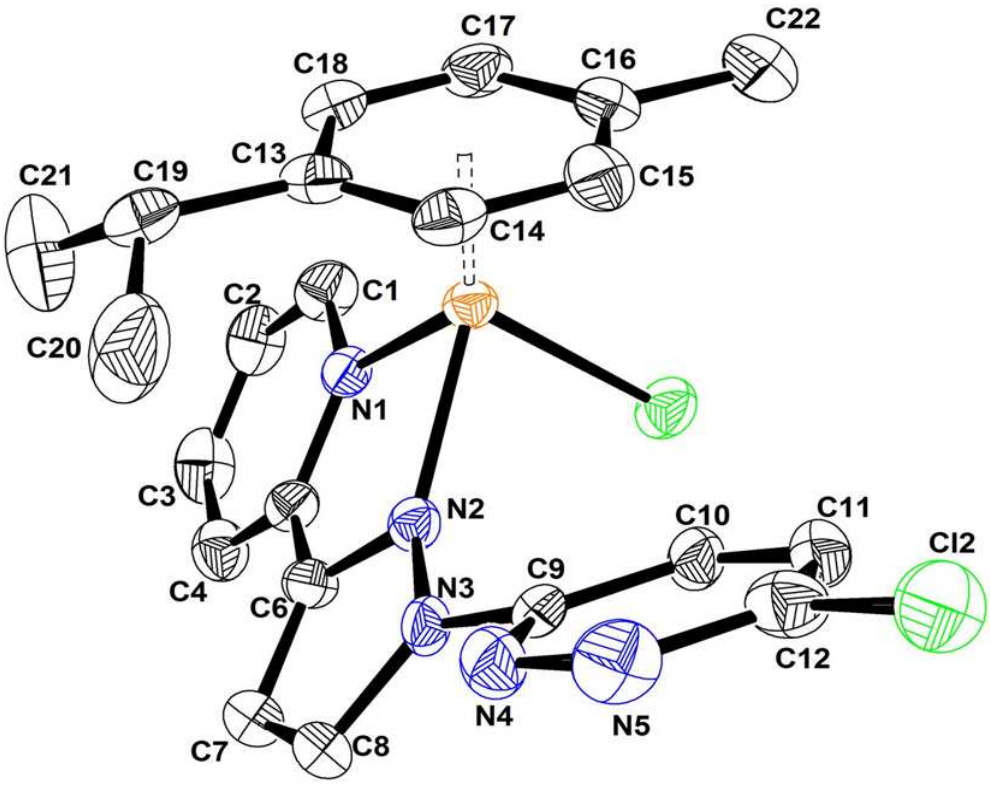

Figure 5.2: Molecular structure of complex [(η^6-*p*-^{i}PrC_6H_4Me)Ru(*pp-Cl*)Cl]PF_6 ([**2**]PF_6).

In the mononuclear complex **2** the N1-metal [2.099(3) Å] distance of the pyridyl ring is slightly longer than the corresponding pyrazolyl, N2-metal distance [2.089(3) Å], in contrast for complex **7** the N1-metal [2.082(1) Å] distance slightly shorter than the corresponding pyrazolyl N2-metal distance [2.161(5) Å], which are comparable to those in $[(\eta^6\text{-}C_6Me_6)RuCl(C_5H_4N\text{-}2\text{-}CH{=}N{=}C_6H_4\text{-}p\text{-}NO_2)]PF_6$,[30] $[Ru(mes)Cl\{C_5H_4N\text{-}2\text{-}C(Me){=}N(CHMePh)\}]BF_4$,[31] $[(\eta^5\text{-}C_5Me_5)RhCl(C_5H_4N\text{-}2\text{-}CH{=}N{=}C_6H_4\text{-}p\text{-}NO_2)]BF_4$,[32] $[(\eta^6\text{-}C_6H_6)Ru(2\text{-}(2\text{-thiazolyl})\text{-}1,8\text{-naphthyridine})Cl]PF_6$,[27] $[(\eta^6\text{-}p\text{-}^iPrC_6H_4Me)RuCl(2,3\text{-bis}(2\text{-pyridyl})pyrazine)]BF_4$.[33] While the M-Cl [2.406(2) and 2.396(4)] bond lengths show no significant differences in all the cations and reported values.[34-37] The N(1)–M(1)–N(2) bond angle in complex **2** and **7** is found to be [75.1(1)°] and [73.2(3)°] respectively, which are similar to those of complexes $[(\eta^6\text{-}p\text{-}^iPrC_6H_4Me)RuCl(2,3\text{-bis}(2\text{-pyridyl})pyrazine)]^+$ [N(1)–Ru(1)–N(2) = 76.5(2)°][33] and $[(\eta^6\text{-}p\text{-}^iPrC_6H_4Me)RuCl(2,3\text{-bis}(2\text{-pyridyl})quinoxaline)]^+$ [37] The distances between the ruthenium atom and the centroid of the $(\eta^6\text{-}p\text{-}^iPrC_6H_4Me)$ ring is 1.683 Å in complex **2**, whereas the distance between the rhodium atom and the centroid of the $\eta^5\text{-}C_5Me_5$ ring is 1.781 Å in complex **7**. These bond distances are comparable to those in the related complex cations $[(\eta^6\text{-}p\text{-}^iPrC_6H_4Me)Ru(pyNp)Cl]PF_6$, $[(\eta^5\text{-}C_5Me_5)Ir(pyNp)Cl]PF_6$ (PyNp=2-(2-pyridyl)-1,8-naphthyridine) (1.79 Å)[27] and $[(\eta^5\text{-}C_5Me_5)Rh(3,6\text{-bis}(2\text{-pyridyl})4\text{-phenylpyridazine})\text{-}Cl]PF_6$ (1.789 Å).

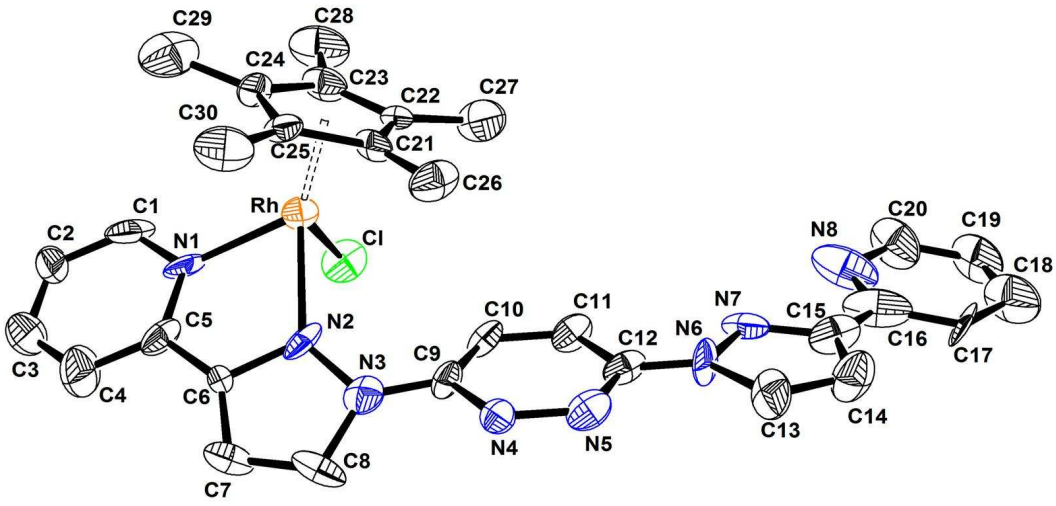

Figure 5.3: Molecular structure of complex $[(\eta^5\text{-}C_5Me_5)Rh(bppp)Cl]PF_6$ [**7**]PF_6. All hydrogen atoms, solvent molecule and anion are omitted for clarity.

5.3.4 Synthesis of the dinuclear complexes **9** to **12** as hexafluorophosphate salts

The reaction of the dimeric chloro complexes $[(\eta^6\text{-arene})Ru(\mu\text{-}Cl)Cl]_2$ (arene = C_6H_6, *p*-$Pr^iC_6H_4Me$) and $[(\eta^5\text{-}C_5Me_5)M(\mu\text{-}Cl)Cl]_2$ (M = Rh, Ir) with 1.5 equiv. of 3,6-bis(3-pyridyl-1-pyrazolyl)pyridazine (*bppp*) in methanol results in the formation of the orange color, air-stable dinuclear dicationic complexes $[\{(\eta^6\text{-}C_6H_6)RuCl\}_2(bppp)]^{2+}$ [**9**]PF_6, $[\{(\eta^6\text{-}p\text{-}^iPrC_6H_4Me)RuCl\}_2(bppp)]^{2+}$ [**10**]PF_6, $[\{(\eta^5\text{-}C_5Me_5)RhCl\}_2((bppp)]^{2+}$ [**11**]PF_6 and $[\{(\eta^5\text{-}C_5Me_5)IrCl\}_2((bppp)]^{2+}$ [**12**]PF_6. All these complexes are isolated as their hexafluorophosphate salts (Scheme 5.3) and they were characterized by IR, Mass, ^{1}H-NMR spectrometry and elemental analyses.

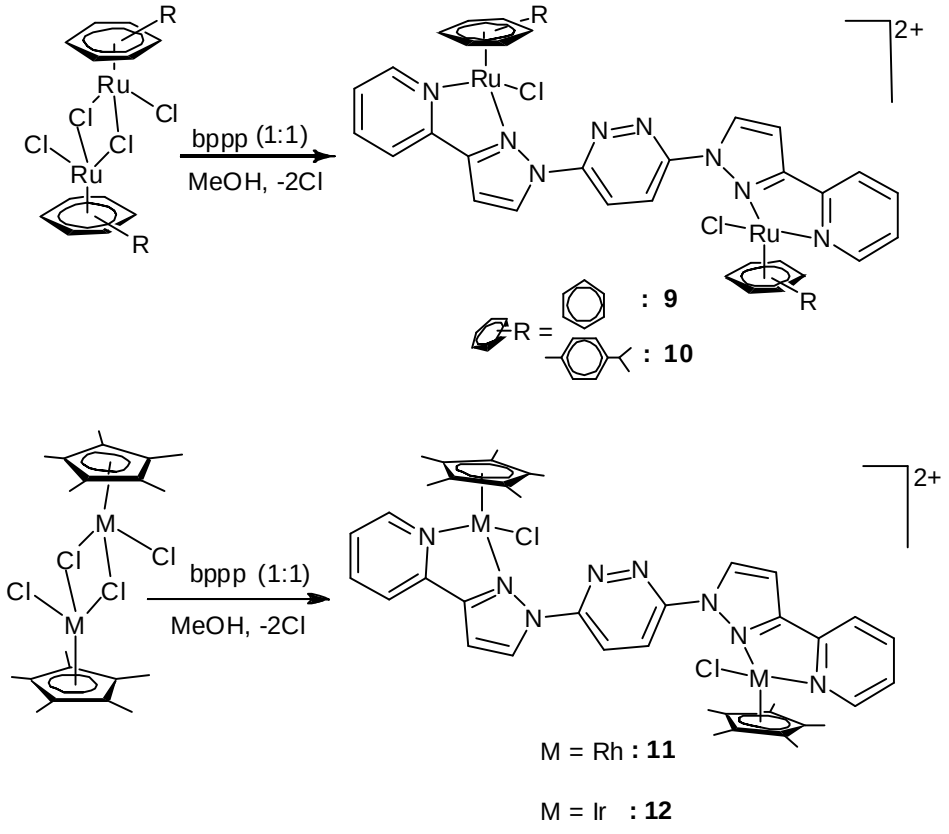

Scheme 5.3

Infrared spectra of these dinuclear complexes **9** to **12**, showed a similar trend to the mononuclear cationic complexes **1** to **8**. In the mass spectra the complexes **7**, **8**, **11** and **12** hexafluorophosphate salts give rise to two main peaks; a minor peak with an approximately 50% intensity attributed to $[M^{2+} + PF_6^-]^+$ at m/z 940, 1052, 1058 and 1236 respectively, and a major peak which corresponds to loss of $[(arene)MCl]^+$ fragment to the formation of mononuclear cations **5- 8** at m/z = 580, 637, 739 and 729 respectively.

The ^{1}H NMR spectra of the dinuclear cationic complexes **9** to **12** exhibit seven distinct resonances at 9.55 (d, 2H), 9.37 (s, 2H), 9.14 (d, 2H), 8.52 (d, 2H), 8.48 (t, 2H), 8.36 (t, 2H), 7.86 (d, 2H) which are assignable to pyridine, pyrazole and pyridazine ring protons of the 3,6-bis(3-pyridyl-1-pyrazolyl)pyridazine (*bppp*) ligand. The chemical shift of the *bppp* ligand protons upon complex formation shifted down field with reference to free ligand. However $H_{ff'}$ protons of metal bounded pyrazoles shifted up field compared to $H_{gg'}$ unbound pyridazine protons of *bppp* ligand up on complexation; this may be due to the metal to ligand charge transfer in all these complexes (Figure 3). Besides these *bppp* ligand resonances complex **9** exhibit a singlet at δ = 5.75 for the two benzene ring and complex **10** exhibits two doublets at δ = 1.18 – 1.12, and septets at δ = 2.68 for the protons of the isopropyl group and a singlet at δ=2.25 for the methyl protons of *p*-cymene ring. The four doublets observed at δ = 6.10 – 5.54 correspond to the aromatic *p*-cymene ring CH protons. Interestingly the chemical shift of these protons as well as methyl protons shifted downfield significantly with reference to starting precursor ranging from δ = 5.20 to 5.42 and mono nuclear complexes (figure 5.4).

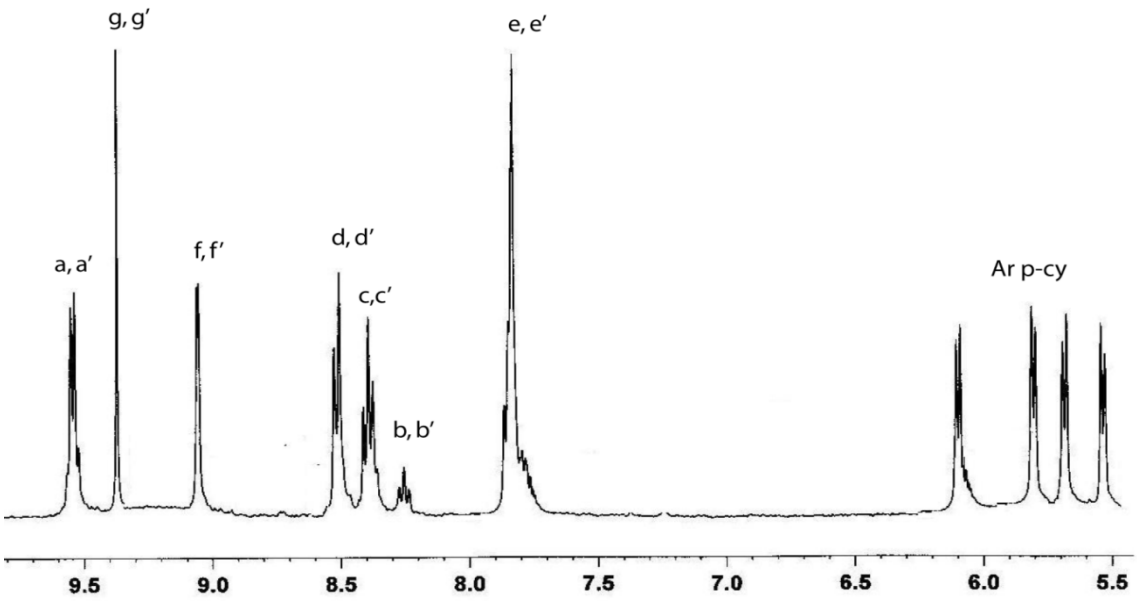

Figure 5.4: ^{1}H-NMR spectrum of compound **18** in $CDCl_3$, represents *bppp* ligand resonances and *p*-cymene ligand aromatic protons.

This could be due to the increased steric nature on the *p*-cymene ring in dinuclear complexes compared to mono nuclear compounds. Complexes **11** and **12** exhibit a strong peak at δ = 2.05 and 1.99 for the protons of pentamethylcyclopentadienyl ligands respectively, which are slightly shifted downfield in comparison to the starting complexes.

5.3.5 UV-Visible spectroscopy

Electronic absorption spectra of compounds *pp-Cl*, *bppp* and complexes **1** to **12** were acquired in acetonitrile, at 10^{-5} M concentration in the range 220-550 nm. The spectral data are well formulated in experimental section. The spectrum of the ligand 3-chloro-6-(3-pyridyl-1-pyrazolyl)pyridazine (*pp-Cl*) exhibit a band at 318 nm, while ligand 3,6-bis(3-pyridyl-1-pyrazolyl)pyridazine (*bppp*) exhibit two bands at 316 nm and 331 nm as a shoulder peak, which are assigned to intra-ligand $\pi \rightarrow \pi^*$ transitions. The electronic spectra of these complexes are characterized by two main features, *viz*., an intense ligand–localized or intra-ligand $\pi \rightarrow \pi^*$ transition in the ultraviolet region and metal-to-ligand charge transfer (MLCT) $d\pi(M) \rightarrow \pi^*$ (L - ligand) bands in the visible region.[38]. Since the low spin d^6 configuration of the mononuclear complexes provides filled orbitals of proper symmetry at the Ru(II), Rh(III) and Ir(III) centers, these can interact with low lying π^* orbitals of the ligands. All the mononuclear complexes **1** to **4** show only an intense band in the region 308-316 nm, while complexes **5** to **8** shown three bands at 276-278 nm, 312 – 314 nm and a broad peak at 417-423 nm. Where as the dinuclear complexes **9** to **12** show three bands, which are almost similar to complexes **5** to **8** at 274 to 276 nm as a shoulder peak at 312-314 nm as a high intense peak and a broad band at 418 - 420 nm. The high intensity band in UV region for both mononuclear and dinuclear complexes is assigned to inter and intra-ligand $\pi - \pi^*$/ $n - \pi^*$ transitions,[39-41] while the low energy absorption band in the visible region for all complexes is assigned to metal-to-ligand charge transfer (MLCT) ($t_{2g} - \pi^*$). Representative spectra of these complexes are represented in figure 5.5.

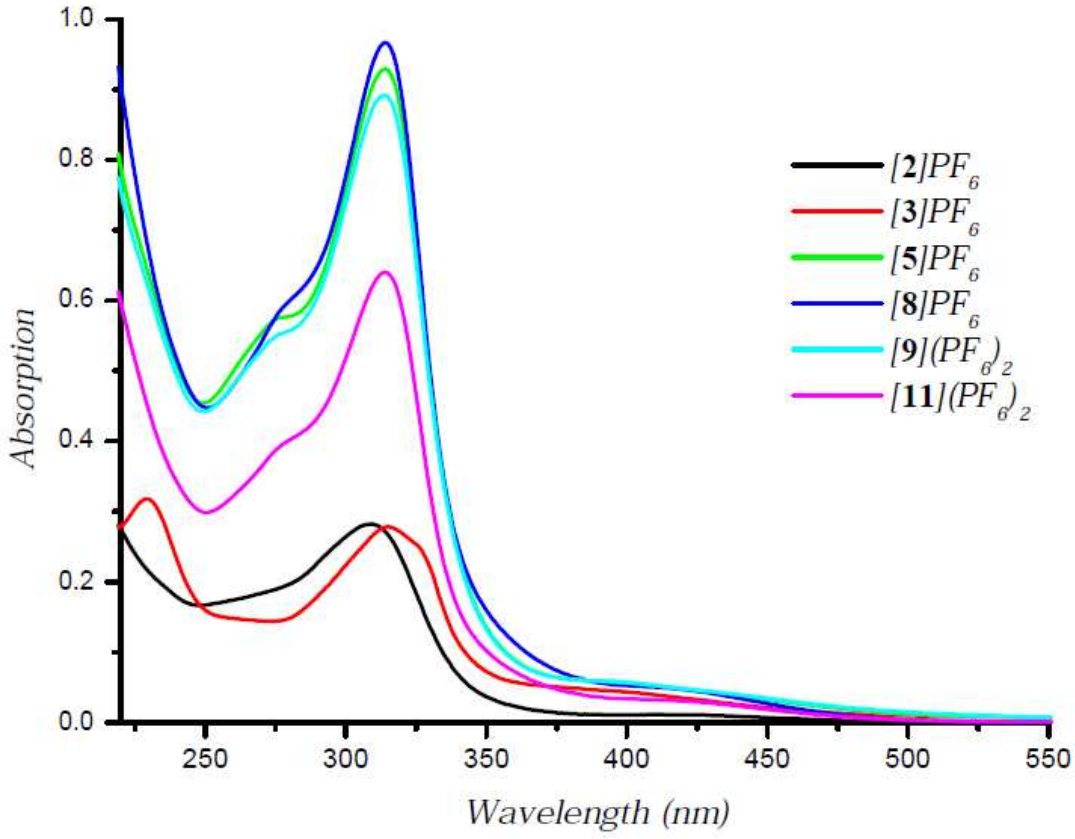

Figure 5.5: UV-Visible electronic spectra of representative complexes in acetonitrile at 298 K.

5.4 Conclusions

In summary, in this work we have prepared two novel chelating ligands 3-chloro-6-(3-pyridyl-1-pyrazolyl)pyridazine (*pp-Cl*) and 3,6-bis(3-pyridyl-1-pyrazolyl)pyridazine (*bppp*). Ligands *pp-Cl* and *bppp* reacted with series of arene ruthenium and Cp* rhodium and iridium complexes giving new series of mononuclear and binuclear complexes. However, we were unable to get single crystals of dinuclear complexes, which were characterized by other spectral techniques.

5.5 Supplementary material

CCDC-**749700** [**2**]PF_6 and CCDC-**749701** [**7**]PF_6 contain the supplementary crystallographic data for this chapter.

References

1 B. M. Trost, Chem. Ber. 129 (1996) 1313.

2 B. M. Trost, M.U. Frederiksen, M. T. Rudd, Angew. Chem. 117 (2005) 6788.

3 B. M. Trost, M. U. Frederiksen, M. T. Rudd, Angew. Chem. Int. Ed. 44 (2005) 6630.

4 F. Hanasaka, K. -I. Fujita, R. Yamaguchi, Organometallics 24 (2005) 3422.

5 M. S. El-Shahawi, A. F. Shoair, Spectrochim. Acta A 60 (2004) 121.

6 R. Noyori, S. Hashigushi, Acc. Chem. Res. 30 (1997) 97, and reference therein.

7 S. –I. Murahashi, H. Takaya, T. Naota, Pure Apply. Chem. 74 (2002) 19.

8 P. Styring, C. Grindon and C. M. Fisher, Catal. Lett., 77 (2001) 219.

9 L. Rigamonti, F. Demartin, A. Forni, S. Righetto and A. Pasini, Inorg. Chem. 45 (2006) 10976.

10 J. Gradinaru, A. Forni, V. Druta, F. Tessore, S. Zecchin, S. Quici and N. Garbalau, Inorg. Chem. 46 (2007) 884.

11 Y. K. Yan, M. Melchart, A. Hebtemariam, P. J. Sadler, Chem. Commun. (2005) 4764.

12 M. Auzias, B. Therrien, G. Süss-Fink, P. P. Štěpnička, W. H. Ang, P. J. Dyson, Inorg. Chem. 47 (2008) 578.

13 A. F. A. Peacock, A. Habtemariam, R. Fernandez, V. Walland, F. P. A. Fabbiani, S. Parsons, R. E. Aird, D. I. Jodrell, P. J. Sadler, J. Am. Chem. Soc. 128 (2006) 1739.

14 A. Habtemariam, M. Melchart, R. Fernandez, S. Parsons, I. D. H. Oswald, A. Parkin, F. P. A. Fabbiani, J. E. Davidson, A. Dawson, R. E. Aird, D. I. Jodrell, P. J. Sadler, J. Med. Chem. 49 (2006) 6858.

15 M. Melchart, A. Habtemariam, O. Novakova, S. A. Moggach, F. P. A. Fabbiani, S. Parsons, V. Brabec, P. J. Sadler, Inorg. Chem. 46 (2007) 8950.

16 C. Scolaro, A. Bergamo, L. Brescacin, R. Delfino, M. Cocchietto, G. Laurenczy, T. J. Geldbach, G. Sava, P. J. Dyson, J. Med. Chem. 48 (2005) 4161.

17 E. Hilllard, A. Vessieres, F. Le Bideau, D. Plazuk, D. Spera, M. Huche, G. Jaouen, Chem. Med. Chem. 1 (2006) 551.

18 M. Auzias, B. Therrien, G. Süss-Fink, P. P. Štěpnička, W. H. Ang, P. J. Dyson, Inorg. Chem. 47 (2008) 578.

19 M. Haga, M. M. Ali, H. Maegawa, K. Nozaki, A. Yoshimura, T. Ohno, Coord. Chem. Rev. 94 (1994) 99.

20 M. Haga, M. M. Ali, R. Arakava, Angew. Chem. Int., Ed. 35 (1996) 76.

21 S. Baitalik, U. Florke, K. Nag, Inorg. Chem. 38 (1999) 3296.

22 R. L. Williams, H. N. Toft, B. Winkel, K. J. Brewer, Inorg. Chem. 42 (2003) 4394.

23 S. M. Scott, K. C. Gordon, A. K. Burrell, J. Chem. Soc., Dalton Trans. (1999) 2669.

24 M. Marcaccio, F. Paolucci, C. Paradisi, S. Roffia, C. Fontanesi, L. J. Yellowlees, S. Serroni, S. Campagna, G. Denti, V. Balzani, J. Am. Chem. Soc. 121 (1999) 10081.

25 J. R. Kirchhoff, K. Kirschbaum, Polyhedron 17 (1998) 4033.

26 A. J. Amoroso, A. M. C. Thompson, J. C. Jeffery, P. L. Jones, J. A. McCleverty, M. D. Ward, J. Chem. Soc., Chem. Com. (1994) 2751.

27 K. T. Prasad, B. Therrien, K. M. Rao, J. Organomet. Chem. 693 (2008) 3049.

28 D. L. Davies, J. Fawcett, R. Krafczyk, D. R. Russell, K. Singh, Dalton Trans. (1998) 2349.

29 D. L. Davies, O. A.-Duaij, J. Fawcett, M. Giardiello, S. T. Hilton, D. R. Russell, Dalton Trans. (2003) 4132.

30 R. Lalrempuia, P. J. Carroll, K. M. Rao, Polyhedron 22 (2003) 605.

31 D. L. Davies, J. Fawcett, R. Krafczyk, D. R. Russell, J. Organomet. Chem. 545-546 (1997) 581.

32 P. Govindaswamy, Y. A. Mozharivskyj, K. M. Rao, Polyhedron 24 (2005) 1710.

33 A. Singh, N. Singh, D. S. Pandey, J. Orgnomet. Chem. 642 (2002) 48.

34 B. Therrien, C. Said-Mohamed, G. Suss-Fink, Inorg. Chim. Acta. 361 (2008) 2601.

35 K. T. Prasad, G. Gupta, A. V. Rao, B. Das, K. M. Rao, Polyhedron 28 (2009) 2649.

36 G. Gupta, K. T. Prasad, B. Das, G. L. P. Yap, K. M. Rao, J. Organomet. Chem. 694 (2009) 2618.

37 R. Lalrempuia, K. M. Rao, Polyhedron 22 (2003) 3155.

38 E. B-Soriaga, N. L. Keder, W. C. Kaska, Inorg. Chem. 29 (1990) 3167.

39 P. Govindaswamy, J. Canivet, B. Therrien, G. Süss-Fink, P. Štěpnička, J. Ludvík, J. Organomet. Chem. 692 (2007) 3664.

40 C. S. Arau´ jo, M. G. B. Drew, V. Félix, L. Jack, J. Madureira, M. Newell, S. Roche, T. M. Santos, J. A. Thomas, L. Yellowlees, Inorg. Chem. 41 (2002) 2250.

41 H. Deng, J. Li, K. C. Zheng, Y. Yang, H. Chao, L. N. Ji, Inorg. Chim. Acta 358 (2005) 3430.

Chapter 6

(Part A)

Mono and dinuclear complexes of half-sandwich platinum group metals (Ru, Rh and Ir) bearing a flexible pyridyl-thiazole multidentate donor ligand

---

In this chapter, we have synthesized new mononuclear and dinuclear complexes with arene ruthenium, rhodium and iridium complexes with polypyridyl ligand as thiazolyl rings backbone. All these new complexes were characterized by elemental analyses, ^{1}H-NMR, UV-Visible and mass spectrometry as well as X-ray crystallographic analyses for some representatives

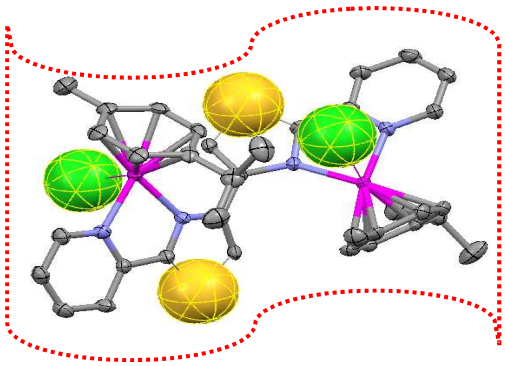

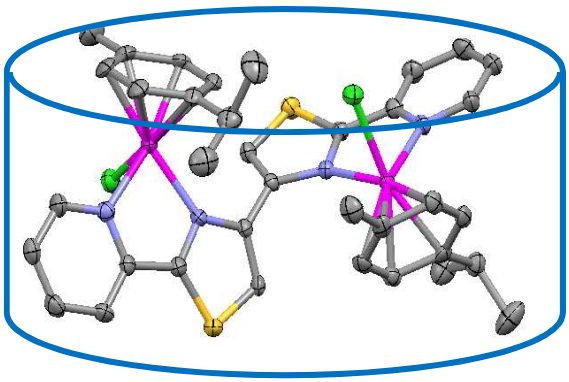

---

*The work presented in this chapter has been published: **K. T. Prasad**, B. Therrien and K. Mohan Rao, J. Organomet. Chem. 695 (2010) 226-234.

6A.1 Introduction

Metal complexes based on polypyridyl ligands constitute versatile components for the construction of multifunctional supramolecular systems in molecular photonics and molecular electronics, sensors, photo-catalysis, solar energy conversion, artificial photosynthesis, non-linear optics, and electrochemo-luminescence amongst others.[1-10] Despite the diversity of these potential applications, relatively little is known about how the properties of electron transfer between a single donor and acceptor is influenced by their inclusion into larger supramolecular assemblies. In this regard, ruthenium complexes bridged by multiple nitrogen donor polypyridyl ligands have received considerable recent attention because of their possible applications in homogeneous catalysis,[11-14] as multi electron storage system[15-16] in the designing of new materials[17-19] and in photophysical and photochemical molecular devices.[20-23] One of the simplest linker used in assembling metals in such arrays is 4,4'-bis(2-pyridyl-4-thiazole) (L). This molecule has been principally explored with Co, Cu and Zn transition metal atoms and has been shown to generate helical structures.[24-25] Besides these helical structures, this molecule acts as a bis-chelating ligand to bridge two metal centers for the formation of dinuclear complexes. Inclusion of the five-membered thiazolyl rings in the backbone results in a more pronounced partitioning of the ligand into distinct bidentate domains than in the case with linear polypyridines. This facilitates the formation of mononuclear and dinuclear systems. The former one has the potential to behave as metallo-ligands in the development of homo/hetero bimetallic systems.[26-28]

Arene ruthenium complexes play an important role in organometallic chemistry. Reactions of the chloro bridged arene ruthenium complexes $[\{(\eta^6\text{-arene})RuCl(\mu\text{-}Cl)\}_2]$ with Lewis bases and a variety of different ligands have been extensively studied. Recently, we have reported a series of mononuclear arene ruthenium complexes of the type $[(\eta^6\text{-arene})RuCl(H\text{-bpp})]^+$ and the dinuclear complexes $[\{(\eta^6\text{-arene})RuCl\}_2(bpp)]^{2+}$ (arene = C_6H_6, *p*-$^{i}PrC_6H_4Me$; bpp = 3,3-bis(2-pyridyl)pyrazole).[29] However, there are no reports dealing with half-sandwich ruthenium / rhodium / iridium complexes with ligands consisting of pyridyl units connected to thiazolyl ring backbone.

In the present contribution, we have synthesized new mononuclear and dinuclear complexes with arene ruthenium, rhodium and iridium complexes with polypyridyl ligand as thiazolyl rings backbone (Chart 6A.1). All these new complexes were characterized by

elemental analyses, ^{1}H-NMR, UV-Visible and mass spectrometry as well as X-ray crystallographic analyses for some representatives.

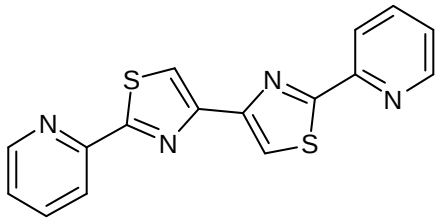

[4,4'-bis(2-pyridyl-4-thiazole)] (**L**)

Chart 6A.1: Ligand used in this study

6A.2 Experimental

6A.2.1 Syntheses of the ligand 4,4'-bis(2-pyridylthiazole) (L)[24]

Preparation of pyridine-2-thioamide: 2-Cyanopyridine (10.0 g, 96.0 mmol) was dissolved in a mixture of Et_3N (2 ml) and ethanol (30 ml). H_2S was slowly bubbled through the solution for 1 h, during which time a yellow precipitate was formed. Collection by filtration gave pure pyridine-2- thioamide as a yellow solid. Yield: 6.63 g, 50%. ESI-MS: *m*/*z* 138 (75%, M^+). ^{1}H NMR [400 MHz, $(CD_3)_2SO$]: δ 10.51 (1H, s, NH), 10.24 (1H, s, NH), 8.70 (1H, d, py), 8.31 (1H, d, py), 8.15 (1H, t, py), 7.68 (1H, t, py).

To a solution of pyridine-2-thioamide (0.30 g, 2.17 mmol) in methanol (15 ml) a solution of 1,4-dibromobutane-2,3- dione (0.26 g, 1.06 mmol) in methanol (15 ml) was added and the solution refluxed for 1 h. After this time the resulting yellow precipitate was filtered, washed with ethanol (5 ml) and diethylether (5 ml) and dried *in vacuo* to give 4,4' bis(2-pyridylthiazole) 2HBr. Yield: 0.41 g, 80%. The free base ligand 4,4' bis(2-pyridylthiazole) 2HBr was prepared from the hydrobromide salt as follows. 4,4' bis(2-pyridylthiazole) 2HBr (0.20 g, 0.41 mmol) was suspended in ammonia (0.88 S.G., 50 ml) and left to stand for 12 h. During this time the suspension changed color from yellow to pink. Filtration and washing with methanol (2 ml) and diethylether (2 ml) gave L as a pale pink solid. Yield: 0.13 g, 100%. ESI-MS: *m*/*z* 322 (75%, M^+). ^{1}H NMR [400 MHz, $(CD_3)_2SO$]: δ 8.68 (2H, d, pyridyl), 8.26 (2H, d, py), 8.24 (2H, s, th), 8.23 (2H, t, py), 7.55 (2H, t, py) L can be recrystallized from MeCN to give colourless plates, but the ligand was generally sufficiently pure to use directly for the complexation reactions.

6A.2.2 Syntheses of the mononuclear complexes 1 – 6

6A.2.2.1 [(η^6-C_6H_6)Ru(L)Cl]PF_6 ([1]PF_6)

A mixture of [(η^6-C_6H_6)Ru(μ-Cl)Cl]$_2$ (50 mg, 0.1 mmol) and **L** [4,4'-bis(2-pyridyl-4-thiazole)] (66 mg, 0.21 mmol) was suspended in methanol (20 ml) and stirred at room temperature for 2 hours. Then, the insoluble materials were filtered through celite and potassium hexafluorophosphate (48 mg, 0.25 mmol) was added to the filtrate. After stirring for 4 hours at room temperature a precipitate was observed. The precipitate was filtered, washed with methanol and diethylether (3 X 10 ml) and dried *in vacuo*.

Yield 85 mg (62%). ^{1}H NMR (400 MHz, CD_3CN) δ = 9.46 (d, 1H, ^3J = 4.76 Hz), 9.15 (s, 1H, tz-H), 8.67 (d, 1H, ^3J = 3.20 Hz), 8.66 (s, 1H, tz-H), 8.36 - 8.08 (dd, 3H), 8.13 (t, 1H, ^3J = 3.32 Hz), 7.63 (t, 2H, ^3J = 2.54 Hz), 5.95 (s, 6H, C_6H_6); IR (cm^{-1}): 1614 (m), 1454 (s), 1437 (s), 844 (s), 788 (s), 558 (s); ESI-MS: 537.1 [M$^+$], 492.2 [M - Cl]; UV–Vis {acetonitrile, λ_{max} nm (ε10^{-5}M^{-1} cm^{-1})}: 338 (0.19); Anal. Calc. for $C_{22}H_{16}N_4S_2RuClPF_6$ (682.01): C, 38.74; H, 2.36; N 8.21. Found: C, 38.53; H, 2.47; N, 8.18%.

*6A.2.2.2 [(η^6-p-^{i}PrC_6H_4Me)Ru(L)Cl]PF_6 ([**2**]PF_6)*

Compound [2]PF_6 was prepared by the same procedure as described above for [1]PF_6 using [(η^6-*p*-^{i}PrC_6H_4Me)Ru(μ-Cl)Cl]$_2$ (60 mg, 0.09 mmol), L [4,4'-bis(2-pyridyl-4-thiazole)] (65 mg, 0.20 mmol) and potassium hexafluorophosphate (36 mg, 0.23 mmol).

Yield 113 mg (78%). ^{1}H NMR (400 MHz, CD_3CN) δ = 9.30 (d, 1H, ^3J = 5.66 Hz), 9.15 (s, 1H,), 9.06 (s, 1H), 8.67 (d, 1H, ^3J = 3.72 Hz), 8.13 (t, 2H, ^3J =7.6 Hz), 8.01 (d, 2H, ^3J = 2.72 Hz), 7.79 (t, 2H, ^3J =6.40 Hz), 5.59 (d, 1H, ^3J = 6.00 Hz, $Ar_{p\text{-}cy}$), 5.52 (d, 1H, ^3J = 6.00 Hz, $Ar_{p\text{-}cy}$), 5.46 (d, 1H, ^3J = 6.00 Hz, $Ar_{p\text{-}cy}$), 5.39 (d, 1H, ^3J = 5.60 Hz, $Ar_{p\text{-}cy}$) 2.70 (sept, 1H, $CH(CH_3)_2$), 2.33 (s, 3H, $Ar_{p\text{-}cy}$-Me), 1.71 (d, 3H, ^3J = 6.20 Hz, $CH(CH_3)_2$), 1.69 (d, 3H, ^3J = 6.80 Hz, $CH(CH_3)_2$); IR (cm^{-1}): 1604(m), 1449(s), 1437(s), 843(s), 783(s), 558(s); ESI-MS: 593.1 [M$^+$], 458.1 [M - Cl]; UV–Vis {acetonitrile, λ_{max} nm (ε10^{-5}M^{-1} cm^{-1})}: 336 (0.20); Anal. Calc. for $C_{26}H_{24}ClF_6N_4PRuS_2$ (738.1): C, 42.31; H, 3.28; N, 7.59. Found: C, 42.27; H, 3.31; N, 7.57%.

*6A.2.2.3 [(η^5-C_5H_5)Ru(L)(PPh_3)]PF_6 ([**3**]PF_6)*

A mixture of [(η^5-C_5H_5)Ru(PPh_3)$_2$Cl] (100 mg, 0.13 mmol), L [4,4'-bis(2-pyridyl-4-thiazole)] (48 mg, 0.15 mmol) and potassium hexafluorophosphate (26 mg, 0.15 mmol) was suspended in methanol (35 ml) and refluxed for 12 hours. Then, the insoluble

materials were filtered through celite and the filtrate was evaporated to dryness. The residue dissolved in dichloromethane and filtered through celite to remove excess potassium hexafluorophosphate and ammonium chloride. The filtrate was reduced to 2 ml on rotary evaporator and excess hexane was added to induce dark red colour precipitate. The precipitate was separated by centrifugation, washed with diethylether (3 X 10 ml) and then dried *in vacuo*.

Yield 70 mg (56%). ^{1}H NMR (400 MHz, CD_3CN) δ = 9.07 (d, 1H, ^{3}J = 4.40 Hz), 9.01 (s, 1H), 8.66 (d, 1H, ^{3}J = 7.60 Hz), 8.16 (s, 1H), 7.82 (t, 1H, ^{3}J=8.00Hz), 7.60 (t, 1H, ^{3}J=6.40 Hz), 7.51 (t, 2H, ^{3}J=7.20 Hz), 7.46 (d, 1H, ^{3}J = 6.42 Hz), 7.28 (d, 1H, ^{3}J = 4.28 Hz), 7.19-7.10 (m, 15H), 4.58 (s, 5H, C_5H_5); ^{31}P {^{1}H} (CD_3CN) δ = 49.34 ppm; IR (cm^{-1}): 1604(m), 1454(s), 1438(s), 844(s), 785(s), 559(s); ESI-MS: 750.8 [M^{+}]; UV–Vis {acetonitrile, λ_{max} nm ($\varepsilon 10^{-5} M^{-1}$ cm^{-1})}: 341 (0.15); Anal. Calc. for $C_{39}H_{30}F_6N_4P_2RuS_2$ (895.82): C, 52.29; H, 3.38; N 6.25. Found: C, 52.11; H, 3.29; N, 6.17%.

*6A.2.2.4 [(η^5-C_5Me_5)Ru(L)(PPh_3)]PF_6 ([**4**]PF_6)*

Compound [**4**]PF_6 was prepared by the same procedure as described above for [**5**]PF_6 using [(η^5-C_5Me_5)Ru(PPh_3)$_2$Cl] (100 mg, 0.12 mmol), L [4,4'-bis(2-pyridyl-4-thiazole)] (44 mg, 0.13 mmol) and potassium hexafluorophosphate (26 mg, 0.15 mmol).

Yield 82 mg (79%). ^{1}H NMR (400 MHz, CD_3CN) δ = 9.17 (d, 1H, ^{3}J = 5.60 Hz), 9.01 (s, 1H), 8.76 (d, 1H, ^{3}J = 4.48 Hz), 8.30 (s, 1H), 7.86 (t, 1H, ^{3}J = 7.60 Hz), 7.72 (t, 1H, ^{3}J = 6.40 Hz), 7.61 (t, 2H, ^{3}J = 6.00 Hz), 7.49 (d, 1H, ^{3}J = 4.20 Hz), 7.22 (d, 1H, ^{3}J = 3.28 Hz), 7.29- 7.10 (m, 15H), 2.01 (s, 15H, C_5Me_5); ^{31}P {^{1}H} (CD_3CN) δ = 51.54 ppm; IR (cm^{-1}): 1624(m), 1458(s), 1437(s), 843(s), 778(s), 557(s); ESI-MS: 820.1 [M^{+}]; UV–Vis {acetonitrile, λ_{max} nm ($\varepsilon 10^{-5} M^{-1}$ cm^{-1})}: 334 (0.55); Anal. Calc. for $C_{44}H_{40}F_6N_4P_2RuS_2$ (965.95): C, 54.71; H, 4.17; N, 5.80. Found: C, 54.59; H, 4.08; N, 5.68%.

*6A.2.2.5 [(η^5-C_5Me_5)Rh(L)Cl]PF_6 ([**5**]PF_6)*

A mixture of [(η^5-C_5Me_5)Rh(μ-Cl)Cl]$_2$ (50 mg, 0.08 mmol) and L [4,4'-bis(2-pyridyl-4-thiazole)] (55 mg, 0.17 mmol) was suspended in methanol (20 ml) and refluxed for 4 hours. Then, the insoluble materials were passed through celite and potassium hexafluorophosphate (36 mg, 0.22 mmol) was added to the filtrate. After refluxing for an hour a precipitate was observed. The precipitate was filtered, washed with methanol and diethylether (3 X 10 ml) and dried *in vacuo*.

Yield: 90 mg (78%). ^{1}H NMR (400 MHz, CD_3CN) δ = 8.95 (d, 1H, ^3J = 5.28 Hz), 8.71 (s, 1H), 8.66 (d, 1H, ^3J = 4.40 Hz), 8.30 (s, 1H), 7.86 (t, 1H, ^3J = 7.40 Hz), 7.62 (t, 1H, ^3J = 6.80 Hz), 7.52 (t, 2H, ^3J = 6.40 Hz), 7.32 (d, 1H, ^3J = 6.44 Hz), 7.22 (d, 1H, ^3J = 6.00 Hz), 2.11 (s, 15H, C_5Me_5); IR (cm^{-1}): 1603(m), 1458(s), 1437(s), 845(s), 785(s), 558(s); ESI-MS: 560.3 [M^+], 525.1 [M - Cl]; UV–Vis {acetonitrile, λ_{max} nm ($\varepsilon 10^{-5} M^{-1}$ cm^{-1})}: 333 (0.72); Anal. Calc. for $C_{26}H_{25}ClF_6N_4PRhS_2$ (705.5): C, 44.26; H, 3.57; N 7.94. Found: C, 44.13; H, 3.43; N, 7.86%.

*6A.2.2.6 [(η^5-C_5Me_5)Ir(L)Cl]PF_6 ([**6**]PF_6)*

Compound [**6**]PF_6 was prepared by the same procedure as described above for [**5**]PF_6 using [(η^5-C_5Me_5)Ir(μ-Cl)Cl]$_2$ (66 mg, 0.08 mmol), L [4,4'-bis(2-pyridyl-4-thiazole)] (57 mg, 0.18 mmol) and potassium hexafluorophosphate (46 mg, 0.25 mmol).
Yield 79 mg (60%). ^{1}H NMR (400 MHz, CD_3CN) δ = 9.01 (d, 1H, ^3J = 5.60 Hz), 8.91 (s, 1H), 8.76 (d, 1H, ^3J = 6.40 Hz), 8.35 (s, 1H), 7.89 (t, 1H, ^3J =7.00 Hz), 7.72 (t, 1H, ^3J =6.80 Hz), 7.52 (t, 2H, ^3J =6.00 Hz), 7.42 (d, 1H, ^3J = 5.60 Hz), 7.28 (d, 1H, ^3J = 6.48 Hz), 1.87 (s, 15H, C_5Me_5); IR (cm^{-1}): 1606(m), 1454(s), 1437(s), 844(s), 785(s), 558(s); ESI-MS: 649.8 [M^+], 614.6 [M - Cl]; UV–Vis {acetonitrile, λ_{max} nm ($\varepsilon 10^{-5} M^{-1}$ cm^{-1})}: 336 (0.74); Anal. Calc. for $C_{26}H_{25}F_6IrN_4PS_2$ (794.8): C, 39.29; H, 3.17; N 7.05. Found: C, 39.13; H, 3.21; N, 6.99%.

6A.2.3 Syntheses of the dinuclear complexes [**7**]$(PF_6)_2$ to [**12**]$(PF_6)_2$

*6A.2.3.1 [{(η^6-C_6H_6)RuCl}$_2$(μ-L)]$(PF_6)_2$ ([**7**]$(PF_6)_2$)*

A mixture of [(η^6-C_6H_6)Ru(μ-Cl)Cl]$_2$ (83 mg, 0.16 mmol) and L [4,4'-bis(2-pyridyl-4-thiazole)] (53 mg, 0.16 mmol) was suspended in methanol (20 ml) and stirred at room temperature for 6 hours. Then, potassium hexafluorophosphate (46 mg, 0.25 mmol) was added to the reaction mixture and further stirred for 3 hours. The precipitate was filtered, washed with methanol and diethylether (3 X 10 ml) and dried *in vacuo*.
Yield 110 mg (60%). ^{1}H NMR (400 MHz, CD_3CN) δ = 9.38 (d, 2H, ^3J = 4.80 Hz), 8.67 (s, 2H, tz-H), 8.22 (d, 2H, ^3J = 8.40 Hz), 8.13 (t, 2H, ^3J =7.20 Hz), 7.43 - 7.51 (m, 2H), 6.01 (s, 6H, C_6H_6), 5.99 (s, 6H, C_6H_6); IR (cm^{-1}): 1604(m), 1449(s), 1437(s), 843(s), 783(s), 558(s); ESI-MS: 891.8 [M^{2+}+PF_6^-]$^+$; UV–Vis {acetonitrile, λ_{max} nm ($\varepsilon 10^{-5} M^{-1}$ cm^{-1})}: 311 (0.35) and 356 (0.31); Anal. Calc. for $C_{28}H_{22}Cl_2F_{12}N_4P_2Ru_2S_2$ (1041.6): C, 32.29; H, 2.13; N 5.38. Found: C, 32.15; H, 2.05; N, 5.28%.

*6A.2.3.2 [{(η^6-p-^{i}PrC$_6$H$_4$Me)RuCl}$_2$(μ-L)](PF$_6$)$_2$ ([**8**](PF$_6$)$_2$)*

Compound [8](PF$_6$)$_2$ was prepared by the same procedure as described above for [7](PF$_6$)$_2$ using [(η^6-*p*-^{i}PrC$_6$H$_4$Me)Ru(μ-Cl)Cl]$_2$ (63 mg, 0.1 mmol), L [4,4'-bis(2-pyridyl-4-thiazole)] (33 mg, 0.1 mmol) and potassium hexafluorophosphate (23 mg, 0.12 mmol). Yield 101 mg (85%). ^{1}H NMR (400 MHz, CD$_3$CN) δ = 9.37 (d, 2H, ^3J = 5.20 Hz), 8.67 (s, 2H, tz-H), 8.26 (d, 2H, ^3J = 5.60 Hz), 8.06 (t, 2H, ^3J =7.00 Hz), 7.57 (t, 2H, ^3J =6.80 Hz), 5.86 (d, 2H, ^3J = 6.00 Hz, Ar$_{p\text{-}cy}$), 5.56 (d, 2H, ^3J = 5.60 Hz, Ar$_{p\text{-}cy}$), 5.47 (d, 2H, ^3J = 6.00 Hz, Ar$_{p\text{-}cy}$), 5.38 (d, 2H, ^3J = 6.40 Hz Ar$_{p\text{-}cy}$), 2.42 (sept, 2H, CH(CH$_3$)$_2$), 2.05 (s, 6H, Ar$_{p\text{-}cy}$-Me), 1.38 (d, 3H, CH(CH$_3$)$_2$); 1.17 (d, 3H, CH(CH$_3$)$_2$), 1.08 (d, 3H, CH(CH$_3$)$_2$), 0.98 (d, 3H, CH(CH$_3$)$_2$); IR (cm^{-1}): 1614(m), 1454(s), 1437(s), 844(s), 788(s), 558(s); ESI-MS: 1008.2 [M^{2+}+PF$_6^-$]$^+$; UV–Vis {acetonitrile, λ_{max} nm (ε10^{-5}M^{-1} cm^{-1})}: 312 (0.56) and 355 (0.35); Anal. Calc. for C$_{36}$H$_{38}$Cl$_2$F$_{12}$N$_4$P$_2$Ru$_2$S$_2$ (1153.7): C, 37.47; H, 3.32; N 4.86. Found: C, 37.33; H, 3.27; N, 4.77%.

*6A.2.3.3 [{(η^5-C$_5$H$_5$)Ru(PPh$_3$)}$_2$(μ-L)](PF$_6$)$_2$ ([**9**](PF$_6$)$_2$)*

A mixture of [(η^5-C$_5$H$_5$)Ru(PPh$_3$)$_2$Cl] (100 mg, 0.13 mmol), L [4,4'-bis(2-pyridyl-4-thiazole)] (22 mg, 0.068 mmol) and ammonium hexafluorophosphate (46 mg, 0.28 mmol) was suspended in methanol (35 ml) and refluxed for 12 hours. Then, the insoluble materials were filtered through celite and filtrate was evaporated to dryness. The residue was dissolved in dichloromethane and filtered through celite to remove ammonium chloride and excess potassium hexafluorophosphate. The filtrate was reduced to 2 ml and excess hexane was added to induce dark red colour precipitate. The precipitate was separated by centrifugation, washed with diethylether (3 X 10 ml) and dried *in vacuo*. Yield 81 mg (80%). ^{1}H NMR (400 MHz, CD$_3$CN) δ = 9.29 (d, 2H, ^3J = 5.60 Hz), 8.67 (s, 2H, tz-H), 8.26 (d, 2H, ^3J = 4.40 Hz), 8.06 (t, 2H, ^3J =7.20 Hz), 7.57 (m, 2H), 7.29-7.02 (m, 30H), 4.86 (s, 10H, C$_5$H$_5$); ^{31}P {^{1}H} (CD$_3$CN) δ = 49.28; IR (cm^{-1}): 1624(m), 1458(s), 1437(s), 843(s), 778(s), 557(s); ESI-MS: 1179 1 [M^{2+}+PF$_6^-$]$^{2+}$; UV–Vis {acetonitrile, λ_{max} nm (ε10^{-5} M^{-1} cm^{-1})}: 314 (0.72) and 356 (0.32); Anal. Calc. for C$_{62}$H$_{50}$F$_{12}$N$_4$P$_4$Ru$_2$S$_2$ (1469.2): C, 50.68; H, 3.43; N 3.81. Found: C, 50.56; H, 3.57; N, 3.77%.

*6A.2.3.4 [{(η^5-C_5Me_5)Ru(PPh_3)}$_2$(μ-L)](PF_6)$_2$ ([**10**](PF_6)$_2$)*

Compound [**10**](PF_6)$_2$ was prepared by the same procedure as described above for [**9**](PF_6)$_2$, using [(η^5-C_5Me_5)Ru(PPh_3)$_2$Cl] (100 mg, 0.12 mmol), L [4,4'-bis(2-pyridyl-4-thiazole)] (20 mg, 0.06 mmol) and potassium hexafluorophosphate (23 mg, 0.12 mmol). Yield: 71 mg, (69%). ^{1}H NMR (400 MHz, CD_3CN) δ = 9.32 (d, 2H, ^3J = 5.20 Hz), 8.78 (s, 2H, tz-H), 8.26 (d, 2H, ^3J = 4.40 Hz), 8.11 (t, 2H, ^3J =7.80 Hz), 7.57 (t, 2H, ^3J =6.40 Hz), 7.29-7.08 (m, 30H), 1.97 (s, 30H); ^{31}P {^{1}H} (CD_3CN) δ = 51.33; IR (cm^{-1}): 1604(m), 1454(s), 1438(s), 844(s), 785(s), 559(s); ESI-MS: 1319.8 [M^{2+}+PF_6^-]$^{2+}$; UV–Vis {acetonitrile, λ_{max} nm ($\varepsilon 10^{-5} M^{-1}cm^{-1}$)}: 310 (0.81) and 358 (0.33); Anal. Calc. for $C_{72}H_{70}F_{12}N_4P_4Ru_2S_2$ (1609.5): C, 53.73; H, 4.38; N, 3.48. Found: C, 53.61; H, 4.27; N, 3.39%.

*6A.2.3.5 [{(η^5-C_5Me_5)RhCl}$_2$(μ-L)](PF_6)$_2$ ([**11**](PF_6)$_2$)*

A mixture of [(η^5-C_5Me_5)Rh(μ-Cl)Cl]$_2$ (75 mg, 0.12 mmol) and L [4,4'-bis(2-pyridyl-4-thiazole)] (39 mg, 0.1 mmol) was suspended in methanol (20 ml) and refluxed for 4 hours. Then, potassium hexafluorophosphate (23 mg, 0.13 mmol) was added to the reaction mixture and further refluxed for an hour. During this time was precipitate was observed. The precipitate was filtered, washed with methanol and diethylether (3 X 10 ml) and dried *in vacuo*.

Yield 118 mg (89%). ^{1}H NMR (400 MHz, CD_3CN) δ = 9.11 (d, 2H, ^3J = 5.20 Hz), 8.72 (s, 2H, tz-H), 8.21 (d, 2H, ^3J = 5.60 Hz), 8.11 (t, 1H, ^3J =7.20 Hz), 7.96 (t, 1H, ^3J =7.24 Hz), 7.57 (t, 2H, ^3J =6.40 Hz), 2.15 (s, 30H, C_5Me_5); IR (cm^{-1}): 1606(m), 1454(s), 1437(s), 844(s), 785(s), 558(s); ESI-MS: 943.6 [M^{2+}+PF_6^-]$^+$; UV–Vis {acetonitrile, λ_{max} nm ($\varepsilon 10^{-5} M^{-1}$ cm^{-1})}: 312 (0.78) and 356 (0.33); Anal. Calc. for $C_{36}H_{40}ClF_{12}N_4P_2Rh_2S_2$ (1088.6): C, 39.72; H, 3.70; N, 5.15. Found: C, 39.53; H, 3.67; N, 5.07%.

*6A.2.3.6 [{(η^5-C_5Me_5)IrCl}$_2$(μ-L)](PF_6)$_2$ ([**12**](PF_6)$_2$)*

Compound [**12**](PF_6)$_2$ was prepared by the same procedure as described above for [**11**](PF_6)$_2$ using [(η^5-C_5Me_5)Ir(μ-Cl)Cl]$_2$ (72 mg, 0.09 mmol), L [4,4'-bis(2-pyridyl-4-thiazole)] (29 mg, 0.09 mmol) and potassium hexafluorophosphate (23 mg, 0.12 mmol). Yield 91 mg (79%). ^{1}H NMR (400 MHz, CD_3CN) δ = 9.44 (d, 2H, ^3J = 5.60 Hz), 8.90 (s, 2H, tz-H), 8.28 (d, 2H, ^3J = 8.00 Hz), 8.15 (t, 1H, ^3J =7.20 Hz), 7.98 (t, 1H, ^3J =6.80 Hz), 7.57 (t, 2H, ^3J =6.44 Hz), 1.54 (s, 30H, C_5Me_5); IR (cm^{-1}): 1603(m), 1458(s), 1437(s),

845(s), 785(s), 558(s); ESI-MS: 1122.5 $[M^{2+}+PF_6^-]^+$; UV–Vis {acetonitrile, λ_{max} nm ($\varepsilon 10^{-5} M^{-1}$ cm^{-1})}: 310 (0.74) and 358 (0.32); Anal. Calc. for $C_{36}H_{40}ClF_{12}Ir_2N_4P_2S_2$ (1267.2): C, 34.12; H, 3.18; N, 4.42. Found: C, 34.02; H, 3.09; N, 4.37%.

6A.2.4 X-ray crystallography

In [**12**]$(PF_6)_2 \cdot CH_2Cl_2$ the max./min. residual density 4.510/-3.120 eÅ^{-3} are located at less than 1 Å from the iridium atoms. Crystallographic details are summarized in table 6A.1 and selected bond lengths and angles are presented in table 6A.2.

6A.3 Results and discussion

6A.3.1 Synthesis of the mononuclear complexes [**1**]PF_6 to [**6**]PF_6 as hexafluorophosphate salts

The mononuclear cationic arene ruthenium as well as cyclopentadienyl and pentamethylcyclopentadienyl ruthenium, rhodium or iridium complexes having 4,4'-bis(2-pyridyl-4-thiazole) (**L**) ligand *viz*., $[(\eta^6\text{-}C_6H_6)RuCl(L)]PF_6$ ([**1**]PF_6), $[(\eta^6\text{-}p\text{-}^iPrC_6H_4Me)RuCl(L)]PF_6$ ([**2**]PF_6), $[(\eta^5\text{-}C_5H_5)Ru(PPh_3)(L)]PF_6$ ([**3**]PF_6), $[(\eta^5\text{-}C_5Me_5)Ru(PPh_3)(L)]PF_6$ ([**4**]PF_6), $[(\eta^5\text{-}C_5Me_5)RhCl(L)]PF_6$ ([**5**]PF_6) and $[(\eta^5\text{-}C_5Me_5)IrCl(L)]PF_6$ ([**6**]PF_6) (Scheme 6A.1) have been prepared by the reaction of arene or cyclopentadienyl or pentamethylcyclopentadienyl complexes $[(\eta^6\text{-arene})Ru(\mu\text{-}Cl)Cl]_2$ (arene = C_6H_6 and *p*-$^iPrC_6H_4Me$), $[(\eta^5\text{-Cp})Ru(PPh_3)_2Cl]$ (Cp = C_5H_5 and C_5Me_5) and $[(\eta^5\text{-}C_5Me_5)M(\mu\text{-Cl})Cl]_2$ (M = Rh and Ir) with appropriate equivalents of ligand **L** [4,4'-bis(2-pyridyl-4-thiazole)] in methanol. These complexes are isolated as hexafluorophosphate salts and complexes [**1**]PF_6 to [**6**]PF_6 are orange–red, resulting as non - hygroscopic, air-stable, shiny crystalline solids. They are sparingly soluble in methanol, dichloromethane and chloroform, but well soluble in acetone and acetonitrile. All these complexes were fully characterized by IR, ^{1}H NMR and electronic spectroscopy. In addition to these complexes 3 and 4 were characterized by ^{31}P NMR also. Analytical data of the complexes conformed well to their respective formulations. Further information about composition of the complexes has also been obtained from mass spectrometry.

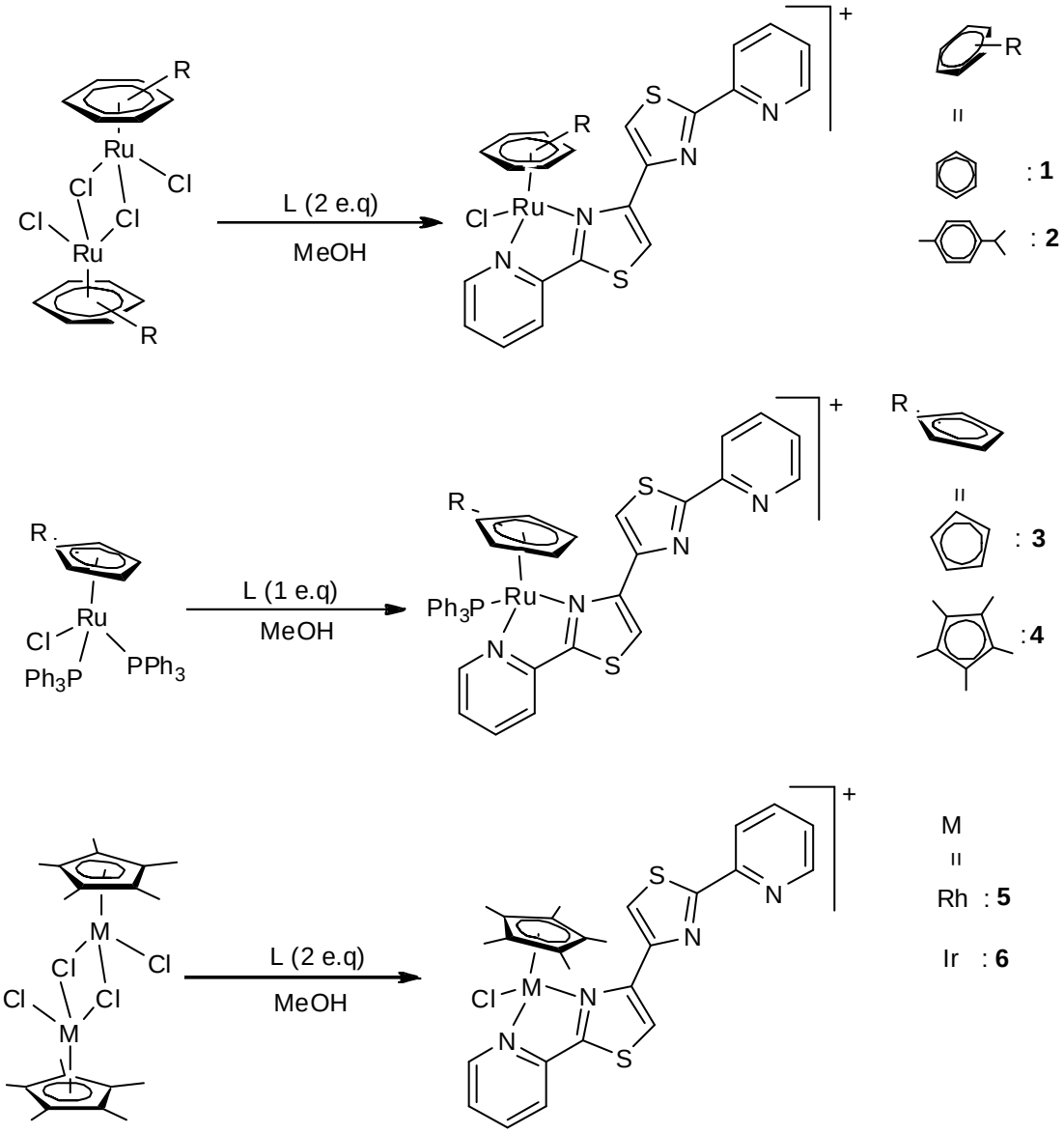

Scheme 6A.1

Infrared spectra of the ligand **L** [4,4'-bis(2-pyridyl-4-thiazole)] display an absorption bands at 1452 cm^{-1} and 1437 cm^{-1} assignable to the stretching frequencies of C=N and C=S bands respectively, consistent with the fact that C=N and C=S stretching frequencies of thiazole appear in the range 1452 cm^{-1} and 1437 cm^{-1}, respectively.[30] Upon coordination with metal atoms, the same bands appeared around 1449-1458 cm^{-1} and 1437 cm^{-1} respectively. The change only in the position of $\nu_{C=N}$ of thiazole suggested that the co-ordination of the metal ion is through nitrogen atom of thiazole not with the sulphur atom. In addition to these bands a strong band in the region 843 cm^{-1} has been

assigned to counter ion PF_6. For instance the IR spectrum of the complex [**2**]PF_6 is depicted in figure 6A.1.

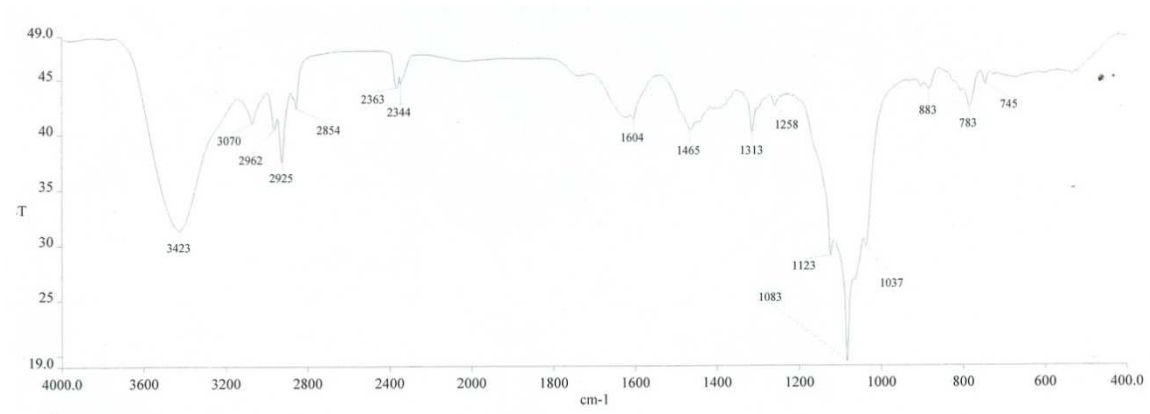

Figure 6A.1: IR spectrum of complex [(η^6-*p*-^{i}PrC_6H_4Me)RuCl(L)]PF_6 [**2**]PF_6

In the mass spectra they give, as expected, rise to the corresponding $[M]^+$ molecular peaks m/z at 537, 593, 750, 820, 560 and 649, respectively. For instance the Mass spectrum of the complex **5** is depicted in figure 6A.2.

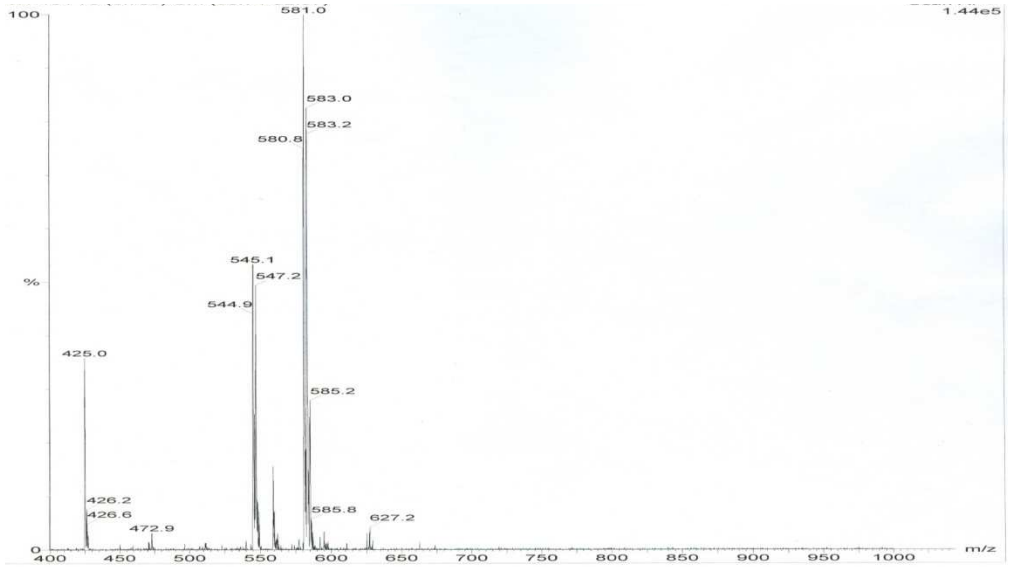

Figure 6A.2: Mass spectrum of complex [(η^5-C_5Me_5)RhCl(L)]PF_6 ([**5**]PF_6)

The ^{1}H NMR spectrum of free ligand L (4,4'-bis(2-pyridyl-4-thiazole)) exhibit a characteristic set of five resonances for the thiazole and pyridyl ring protons. Upon coordination with the metal atom, the mononuclear cationic complexes [**1**]PF_6 to [**6**]PF_6 exhibit between seven and nine distinct resonances assignable to thiazolyl and pyridyl ring protons of the L [4,4'-bis(2-pyridyl-4-thiazole)] ligand indicating formation of

mononuclear complexes, besides these resonances, complex [**1**]PF_6 exhibit a singlet at δ = 5.95 for the protons of the benzene ligand and complex [**2**]PF_6 exhibits two doublets at δ = 1.71 and 1.69, as well as a septet at δ = 2.70 for the protons of the isopropyl group. The two doublets observed at 5.59 and 5.39 ppm correspond to the aromatic *p*-cymene ring CH protons. This unusual pattern is due to the diastereotopic methyl protons of the isopropyl group and aromatic protons of the *p*-cymene ligand, since the ruthenium atom is stereogenic due to the coordination of four different ligand atoms and chiral nature of metal atom.[30] Complex [**3**]PF_6 exhibit a strong peak at δ = 4.58 which is assigned to cyclopentadienyl ligand and complexes [**4**]PF_6 to [**6**]PF_6 exhibit a strong peak at δ = 2.01, 2.11 and 1.84 for the pentamethylcyclopentadienyl ligand respectively, which are slightly shifted downfield in comparison to the starting precursors.

The ^{31}P $\{^1H\}$ NMR spectra of complexes [**3**]PF_6 and [**4**]PF_6 exhibit a strong peak at δ = 49.34 and 51.54 respectively for the triphenylphosphine ligand which is shifted down field as compared to starting neutral precursors δ = 42.00 and 38.50.[33,34]This down field chemical shift of phosphorus nucleus indicates the formation of cationic complexes.

6A.3.2 Crystal structure analysis of [(η^5-C_5H_5)Ru(PPh_3)(L)]PF_6 ([**3**]PF_6) and [(η^5-C_5Me_5)Rh-(L)(Cl)]PF_6 ([**5**]PF_6)

The molecular structure of [(η^5-C_5H_5)Ru(PPh_3)(L)]PF_6 ([**3**]PF_6) and [(η^5-C_5Me_5)Rh(L)(Cl)]PF_6 ([**5**]PF_6) have been established by single-crystal X-ray structure analysis. Both complexes show a typical piano-stool geometry with the metal centre coordinated by the aromatic ligand, a terminal triphenylphosphine or chloride and a chelating *N, N'*-ligand (see Figures 6A.3 and 6A.4). The metal atom is in octahedral arrangement and the L ligand is found to coordinate through the N1 atom of the pyridine moiety and the N2 atom of the thiazolyl ring to generate a five-membered ring metallo-cycle (see Figures 6A.3 and 6A.4). In these complexes, the S atom points away from the metal centre and show no interaction with neighbouring cations. Selected bond lengths and angles for complexes [**3**]PF_6 and [**5**]PF_6 are presented in Table 6A.2. In the mononuclear complexes [**3**]PF_6 and [**5**]PF_6 the metal to nitrogen (N1) bond distance (2.067(8) and 2.100(3) Å) of the pyridine is shorter than the corresponding metal - thiazole nitrogen distance (2.105(8) and 2.146(4) Å), which are comparable to those in [(η^6-C_6Me_6)RuCl(C_5H_4N-2-CH=N=C_6H_4-*p*-NO_2)]PF_6,[35] [Ru(mes)Cl{C_5H_4N-2-C(Me)=N(CHMePh)}]BF_4,[36] [(η^5-C_5Me_5)RhCl(C_5H_4N-2-CH=N=C_6H_4-*p*-NO_2)]BF_4,[37] but unlike in

[(η^6-C_6H_6)Ru(2-(2-thiazolyl)-1,8-naphthyridine)Cl]PF_6,[30] [(η^6-*p*-^{i}PrC_6H_4Me)RuCl(2,3-bis (2-pyridyl)pyrazine)]BF_4[38] [(η^6-C_6H_6)RuCl(2-(1-imidazol-2-yl)-pyridinee)]PF_6[39] and [(η^5-C_5Me_5)Ir(2-(2'-pyridyl)imidazole)Cl]PF_6[40]. Accordingly, there is no significant difference in the M-Cl bond length in **5** [2.407(12) Å] and reported values[41]. The N(1)-M(1)-N(2) bond angle in complex **3** and **5** is found to be [76.40(3)°] and [76.51(1)°] respectively, which are similar to those of complexes [(η^6-*p*-^{i}PrC_6H_4Me)RuCl(2,3-bis(2-pyridyl)pyrazine)]$^+$ [N(1) - Ru(1) - N(2) = 76.5(2)°][36] and [(η^6-*p*-^{i}PrC_6H_4Me)RuCl(2,3-bis(2-pyridyl)quinoxaline)]$^+$ [N(1)-Ru(1)-N(2) = 76.2(2)°][42]. The distances between the ruthenium atom and the centroid of the η^5-C_5H_5 ring is 1.820 Å in complex [**3**]PF_6, whereas the distance between the rhodium atom and the centroid of the η^5-C_5Me_5 ring is 1.785 Å in complex [**5**]PF_6. These bond distances are comparable to those in the related complex cations [Ru(η^5-C_5H_5)(PPh_3)(κ^2-paa)]$^+$, [Ru(η^5-C_5H_5)(κ^1-dppm)(κ^2-paa)]$^+$ [43] and [(η^5-C_5Me_5)Rh(3,6-bis(2-pyridyl)4-phenylpyridazine)-Cl]PF_6 (1.789 Å) and [(η^5-C_5Me_5)Ir(pyNp)Cl]PF_6 (PyNp=2-(2-pyridyl)-1,8-naphthyridine) (1.79 Å).[30]

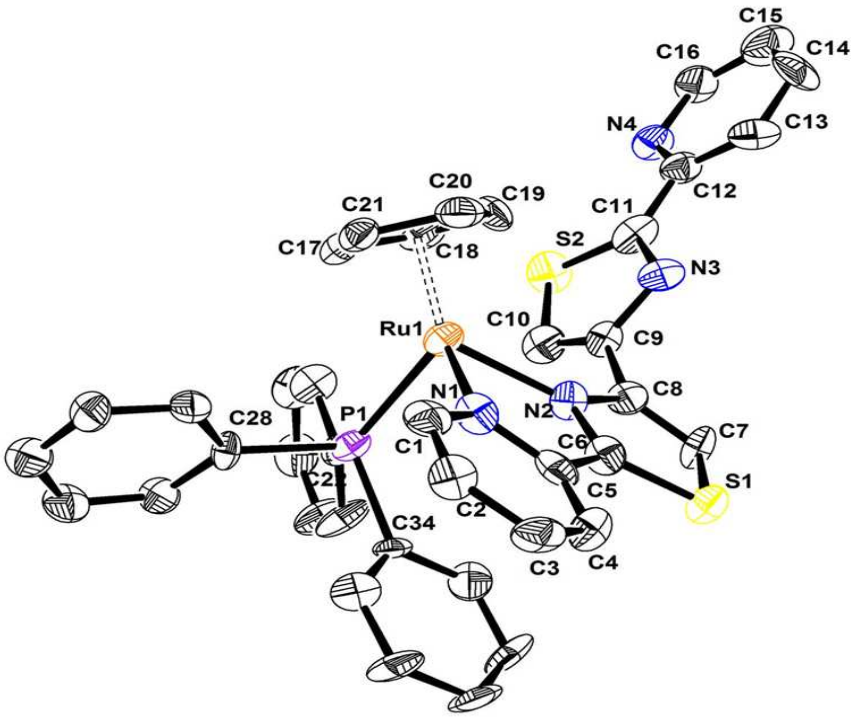

Figure 6A.3: Molecular structure of complex [(η^5-C_5H_5)Ru(PPh_3)(L)]PF_6 [**3**]PF_6 showing ellipsoids at the 50% probability level. Hydrogen atoms, PF_6 anion and solvent molecule are omitted for clarity.

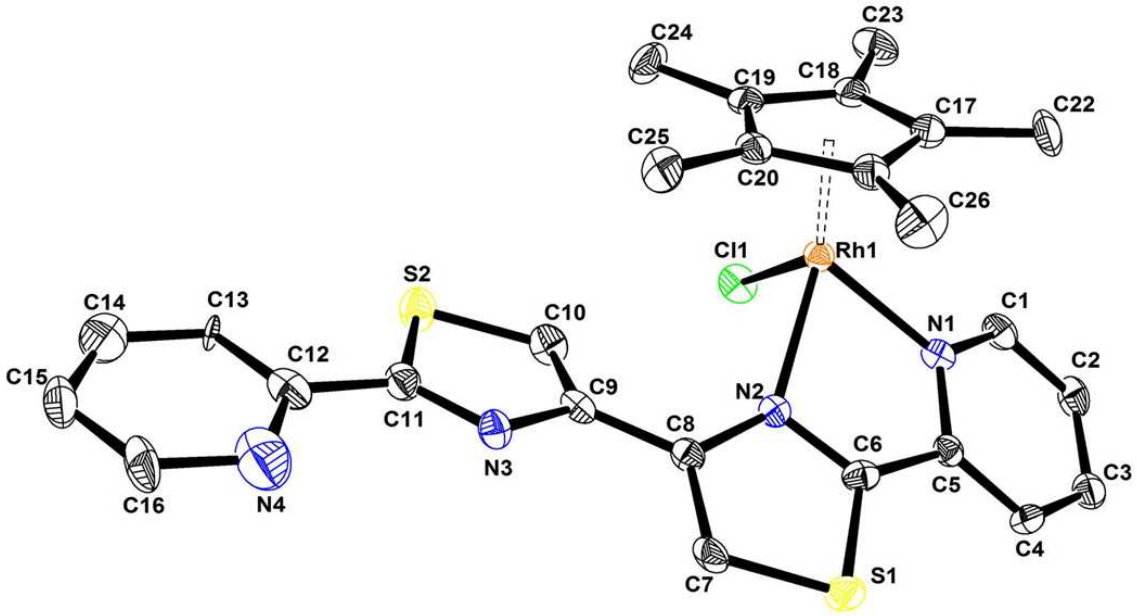

Figure 6A.4: Molecular structure of complex $[(\eta^5\text{-}C_5Me_5)Rh(L)(Cl)]PF_6$ [**5**]PF_6 showing ellipsoids at the 50% probability level. Hydrogen atoms, PF_6 anion and solvent molecule are omitted for clarity.

6A.3.3 Synthesis of the dinuclear complexes [**7**]$(PF_6)_2$–[**12**]$(PF_6)_2$ as hexafluorophosphate salts.

The reaction of the chloro bridged dinuclear complexes $[(\eta^6\text{-arene})Ru(\mu\text{-}Cl)Cl]_2$ (arene = C_6H_6, *p*-$Pr^iC_6H_4Me$); $[(\eta^5\text{-}C_5Me_5)M(\mu\text{-}Cl)Cl]_2$ (M = Rh, Ir) with 1 equiv. of ligand **L** [4,4'-bis(2-pyridyl-4-thiazole)] in methanol results in the formation of the orange color, air-stable dinuclear di-cationic complexes $[\{(\eta^6\text{-}C_6Me_6)RuCl\}_2(L)]^{2+}$ (**7**), $[\{(\eta^6\text{-}p\text{-}^iPrC_6H_4Me)RuCl\}_2(L)]^{2+}$ (**8**), $[\{(\eta^5\text{-}C_5Me_5)RhCl\}_2(L)]^{2+}$ (**11**) and $[\{(\eta^5\text{-}C_5Me_5)IrCl\}_2\text{-}(L)]^{2+}$ (**12**). Similarly reactions of cyclopentadienyl / pentamethylcyclopentadienyl ruthenium triphenylphosphine complexes $[(\eta^5\text{-}Cp)Ru(PPh_3)_2Cl]$ (Cp = C_5H_5 and C_5Me_5) and half equivalent of ligand **L** in methanol at 55 °C leads to the formation of $[\{(\eta^5\text{-}C_5H_5)Ru(PPh_3)\}_2(L)]^{2+}$ (**9**) and $[\{(\eta^5\text{-}C_5Me_5)\ Ru(PPh_3)\}_2(L)]^{2+}$ (**10**). All these complexes are isolated as their hexafluorophosphate salts (Scheme 6A. 2) and they were characterized by mass, ^1H NMR spectrometry, and elemental analysis. In addition to these complexes **9** and **10** were also characterized by ^{31}P NMR spectrometry. On top of these mono and dinuclear complexes we tried to synthesize hetero dinuclear, tri and tetra nuclear complexes by using varieties of transition metals, but results were not fruitful.

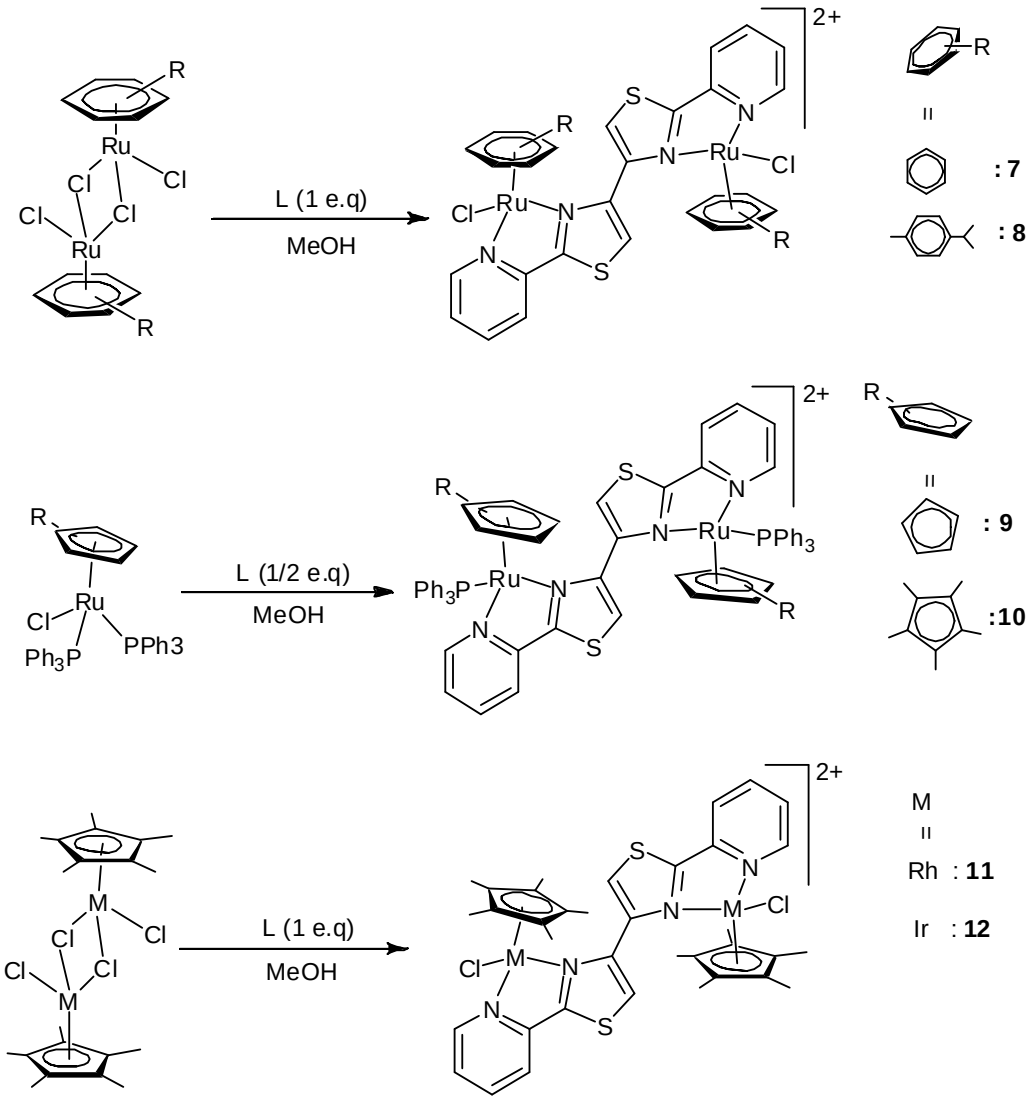

Scheme 6A.2

Infrared spectra of these dinuclear complexes [**7**]$(PF_6)_2$ to [**12**]$(PF_6)_2$, showed a similar trend as the mononuclear cationic complexes [**1**]PF_6 to [**6**]PF_6. In the mass spectra the complexes **7**, **8**, **11** and **12** hexafluorophosphate salts give rise to two main peaks; a minor peak with an approximately 50% intensity attributed to $[M^{2+} + PF_6^-]^+$ at m/z 891, 1008, 943 and 1122, respectively, and a major peak which corresponds to loss of $[(arene)MCl]^+$ fragment to the formation of mononuclear cations **1- 6** at m/z = 537, 593,750, 820, 560 and 649, respectively.

The ^{1}H NMR spectra of the dinuclear cationic complexes [**7**]$(PF_6)_2$ to [**12**]$(PF_6)_2$ exhibit five distinct resonances assignable to thiazolyl ring and pyridyl ring protons of the L ligand indicating formation of dinuclear complexes. Besides these resonances, complex [**7**]$(PF_6)_2$ exhibit two singlets at δ = 6.01 and δ = 5.99 for the protons of the benzene

ligands and complex [**8**]$(PF_6)_2$ exhibits four doublets at δ = 1.38 – 0.98, and septets at δ = 2.42 for the protons of the isopropyl group. The four doublets observed at δ = 5.86 – 5.38 correspond to the aromatic *p*-cymene ring CH protons. Complexes [**9**]$(PF_6)_2$ to [**12**]$(PF_6)_2$ exhibit a strong peak at δ = 4.86 and 1.97, 2.15, 1.54 for the cyclopentadienyl and pentamethylcyclopentadienyl ligands, which are slightly shifted downfield in comparison to the starting complexes. In the dinuclear complexes each arene ligand has exhibited set of individual resonances for each set of protons due to free rotation in solution ([**7**]$(PF_6)_2$ and [**8**]$(PF_6)_2$), where as pentamethylcyclopentadienyl ligand containing complexes ([**11**]$(PF_6)_2$ and [**12**]$(PF_6)_2$) exhibit only one set of resonance for both pentamethylcyclopentadienyl ligands due to centre of inversion in these molecules. For instance the ^{1}H NMR spectrum of the complex **8, 9** and **11** are depicted in figure 6A.5, 6A.6 and 6A.7 respectively.

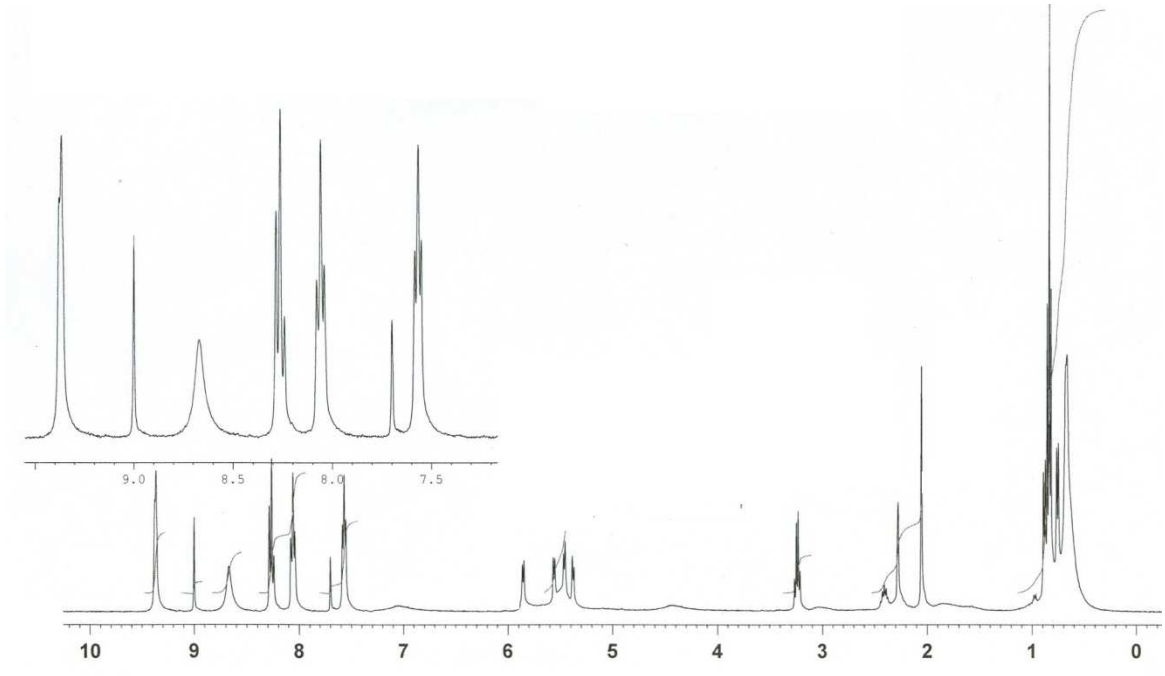

Figure 6A.5: ^{1}H NMR spectrum of complex $[\{(\eta^6\text{-}p\text{-}Pr^iC_6H_4Me)RuCl\}_2(L)]^{2+}$ (**8**) in acetonitrile-d_3.

The ^{31}P NMR spectra of complexes [**9**]$(PF_6)_2$ and [**10**]$(PF_6)_2$ exhibit a strong peak at δ = 49.28 and 51.33 respectively, which are shifted downfield as compared to starting neutral precursors δ = 42.00 and 38.50[45,46] respectively. This down field chemical shift of phosphorus nucleus indicates the formation of cationic complexes.

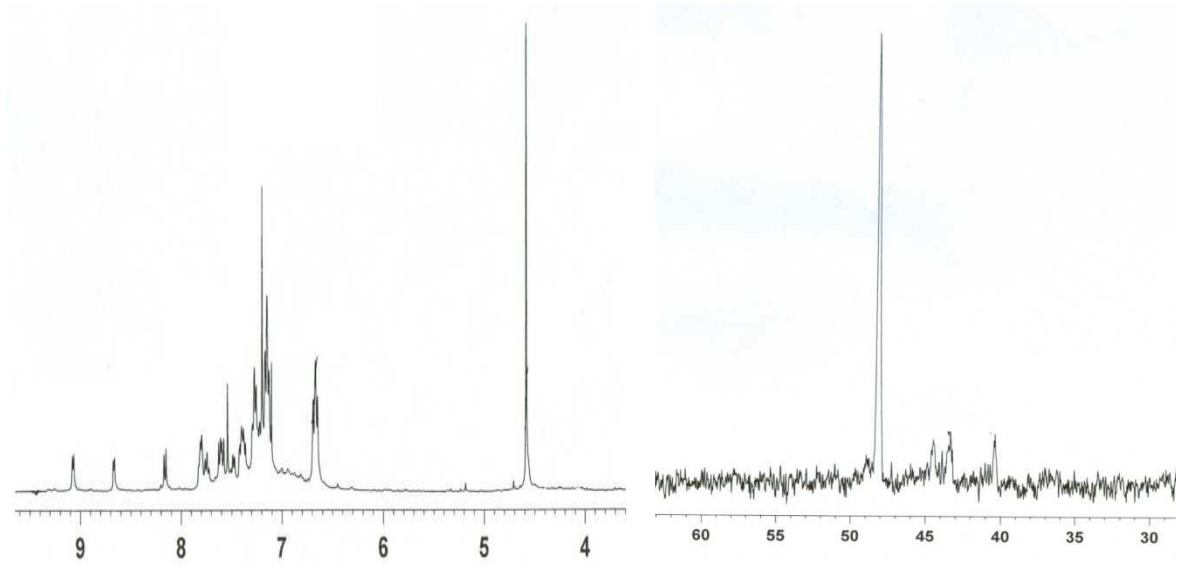

Figure 6A.6: ^{1}H and ^{31}P NMR spectrum of complex $[\{(\eta^5\text{-}C_5H_5)Ru(PPh_3)\}_2(L)]^{2+}$ (**9**) in acetonitrile-d_3.

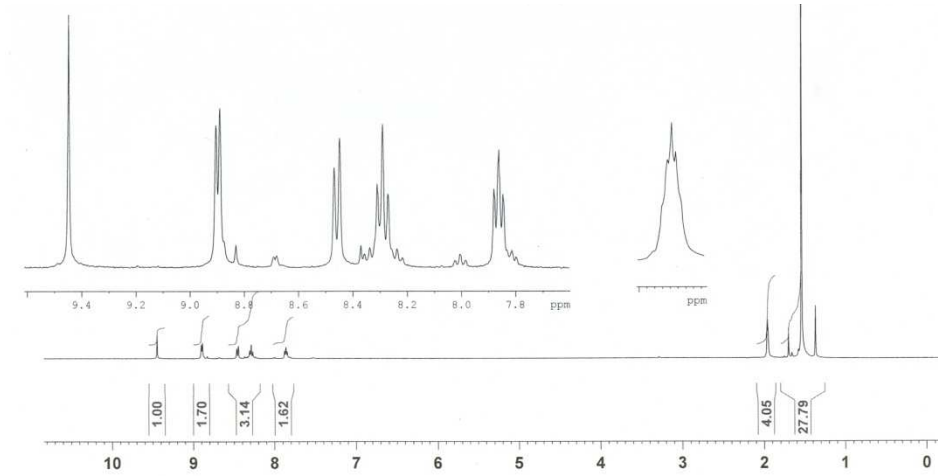

Figure 6A.7: ^{1}H NMR spectrum of complex $[\{(\eta^5\text{-}C_5Me_5)RhCl\}_2(L)]^{2+}$ (**11**) in acetonitrile-d_3.

6A.3.4. Crystal structure analysis of $[\{(\eta^6\text{-}p\text{-}^{i}PrC_6H_4Me)RuCl\}_2(L)]^{2+}$ ([**8**]$(PF_6)_2$) and $[\{(\eta^5\text{-}C_5Me_5)IrCl\}_2(L)]^{2+}$ ([**12**]$(PF_6)_2$)

The molecular structure of $[\{(\eta^6\text{-}p\text{-}^{i}PrC_6H_4Me)RuCl\}_2(L)]^{2+}$ ([**8**]$(PF_6)_2$) and $[\{(\eta^5\text{-}C_5Me_5)IrCl\}_2(L)]^{2+}$ ([**12**]$(PF_6)_2$) have been established by single-crystal X-ray structure analysis. Selected bond lengths and angles for complexes [**8**]$(PF_6)_2$ and [**12**]$(PF_6)_2$ are presented in table 6A.2. In the dinuclear complexes [**8**]$(PF_6)_2$ and [**12**]$(PF_6)_2$, the metal centers are stereogenic. However, while [**8**]$(PF_6)_2$ crystallized as racemic crystals with the

centrosymmetric space group *P*-1, [**12**]$(PF_6)_2$ crystallizes as a racemic mixture of enantiopure crystals with the non-centrosymmetric space group *P* 2_12_12. As well both the complexes show a typical piano-stool geometry with the metal centre coordinated by the aromatic ligand, a terminal chloride and a chelating N,N-ligand (see Figure. 6A.8 and 6A.9). The compounds [**8**]$(PF_6)_2$ and [**12**]$(PF_6)_2$ contain two metal centres (Ru(II) or Ir(III)) bonded to an η^6-*p*-$Pr^iC_6H_4Me$ or η^5-C_5Me_5 ligands, respectively, which are bridged by the L ligand through its nitrogen atoms. Interestingly, the dinuclear dication [**8**]$(PF_6)_2$ reveals a *trans* conformation of the two chloro ligands (see Figure. 6A.8), while the *cis* isomer is observed in the case of [**12**]$(PF_6)_2$ (see Figure 6A.9). The average distances between the metal atom and the carbon atoms of the η^6-*p*-$Pr^iC_6H_4Me$ ring are at 2.20 Å. This bond length is comparable to those in related η^6-*p*-$Pr^iC_6H_4Me$ ruthenium complexes such as [(η^6-*p*-^{i}PrC_6H_4Me)Ru(2-acetylthiazoleazine)Cl]PF_6 [2.10 Å][44] and [(η^6-*p*-^{i}PrC_6H_4Me)Ru(2-(2-thiazolyl)-1,8-naphthyridine)Cl]PF_6 [2.19 Å].[30] The Ru-N bond distances ranging from 2.093(3) to 2.157(3) Å are longer than in the mononuclear complex [**3**]PF_6 [2.067(8) and 2.105(8) Å], while the ruthenium-chlorine bond distances are comparable. In complex [**8**]$(PF_6)_2$, the isopropyl group of the *p*-cymene ligand is located opposite to the halide ligand in order to limit steric interaction. The average distances between the metal atom and the carbon atoms of the η^5-C_5Me_5 ring is at 2.18 Å, which is almost identical to those reported iridium or rhodium complexes such as [(η^5-C_5Me_5)IrCl((S)-1-phenylethylsalicylaldiimine)] [2.17 Å] and [(η^5-C_5Me_5)RhCl((S)-1-phenylethylsalicylaldiimine)] [2.16 Å].[45] The Ir‑Cl bond lengths are 2.406(2) Å [in [**12**]$(PF_6)_2$], which is almost identical to the reported cationic poly-pyridyl iridium complex [{(η^5-C_5Me_5)IrCl}2(2,2'-bipyrimidine)]$^{2+}$ [2.408(8) Å],[46] while Ir‑N bond distances are similar to mononuclear rhodium complex ([**5**]PF_6). The N(1)‑M(1)‑N(2) and N(3)‑M(2)‑N(4) bond angles in complex [**3**]PF_6 and [**5**]PF_6 are found to be [77.13(1)° and 77.03(1)°] and [75.61(9)° and 75.61(9)°], respectively. The distances between the ruthenium atom and the centroid of the η^6-*p*-^{i}PrC_6H_4Me ring is 1.689 Å in complex [**8**]$(PF_6)_2$, whereas the distance between the iridium atom and the centroid of the η^5-C_5Me_5 ring is 1.811 Å in complex [**12**]$(PF_6)_2$. These bond distances are comparable to those in the related complex cations [(η^6-*p*-^{i}PrC_6H_4Me)Ru(2-acetylthiazoleazine)Cl]PF_6[44] and [(η^5-C_5Me_5)Ir(pyNp)Cl]PF_6 (PyNp=2-(2-pyridyl)-1,8-naphthyridine) (1.79 Å).[30]

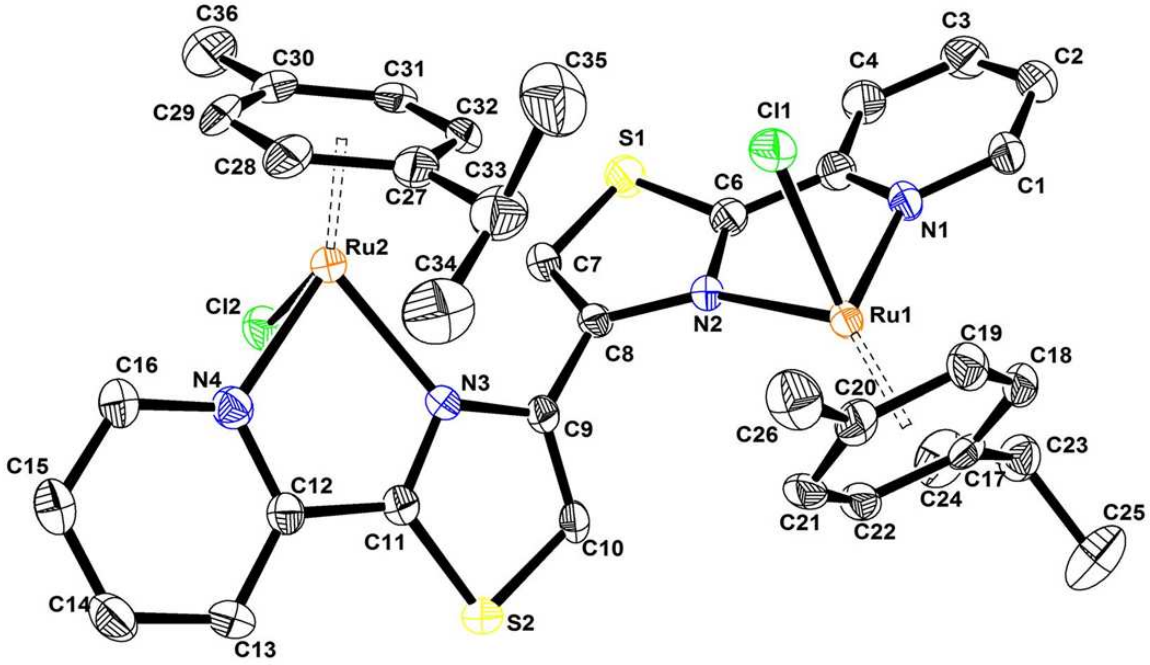

Figure 6A.8: Molecular structure of complex $[\{(\eta^6\text{-}p\text{-}^{i}PrC_6H_4Me)RuCl\}_2(L)]^{2+}$ ([**8**](PF$_6$)$_2$) showing ellipsoids at the 50% probability level. Hydrogen atoms, PF$_6$ anions and solvent molecules are omitted for clarity.

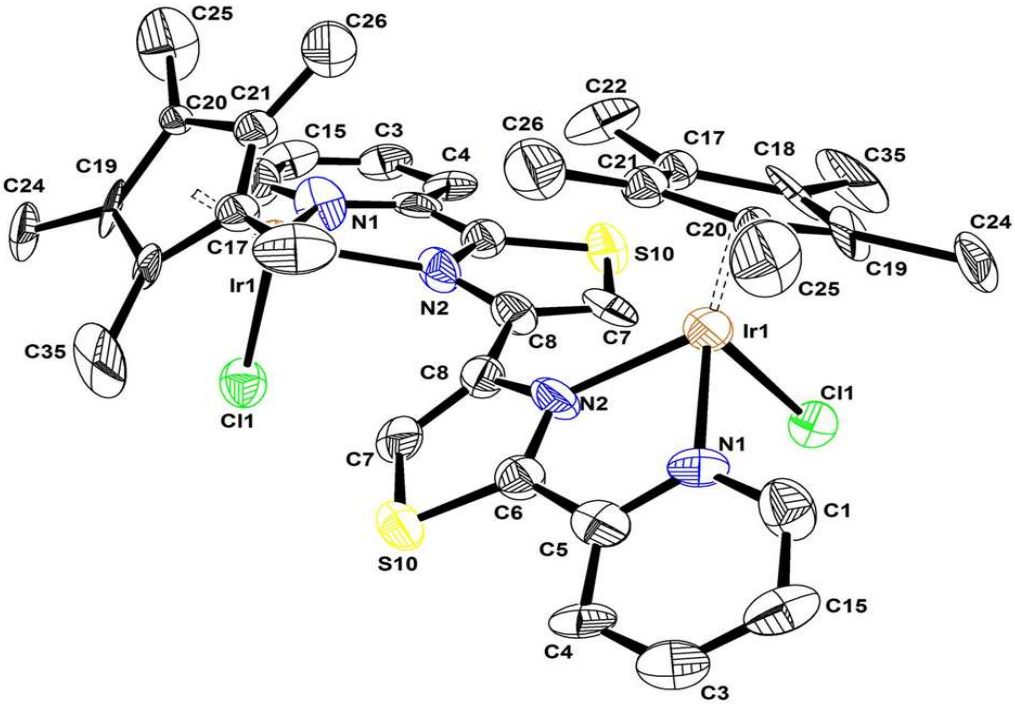

Figure 6A.9: Molecular structure of complex $[\{(\eta^5\text{-}C_5Me_5)IrCl\}_2(L)]^{2+}$ ([**12**](PF$_6$)$_2$) showing ellipsoids at the 50% probability level. Hydrogen atoms, PF$_6$ anions and solvent molecule are omitted for clarity.

Table 6A.1: Crystallographic and structure refinement parameters for complexes [**3**]$PF_6 \cdot (CH_3)_2CO$, [**5**]$PF_6 \cdot (CH_3)_2CO$, [**8**]$(PF_6)_2 \cdot CH_3CN$ and [**12**]$(PF_6)_2 \cdot CH_2Cl_2$.

	[**3**]$PF_6 \cdot (CH_3)_2CO$	[**5**]$PF_6 \cdot (CH_3)_2CO$	[**8**]$(PF_6)_2 \cdot CH_3CN$	[**12**]$(PF_6)_2 \cdot CH_2Cl_2$
Chemical formula	$C_{42}H_{36}F_6N_4OP_2RuS_2$	$C_{29}H_{31}ClF_6N_4OPRhS_2$	$C_{38}H_{41}Cl_2F_{12}N_5P_2Ru_2S_2$	$C_{37}H_{42}Cl_4F_{12}Ir_2N_4P_2S_2$
Formula weight	953.88	799.03	1194.86	1423.01
Crystal system	Triclinic	Triclinic	Triclinic	Orthorhombic
Space group	*P* -1 (no. 2)	*P* -1 (no. 2)	*P* -1 (no. 2)	$P2_12_12$ (no. 18)
Crystal color and shape	orange block	orange rod	orange block	orange rod
Crystal size	0.23 x 0.17 x 0.16	0.28 x 0.23 x 0.18	0.35 x 0.26 x 0.21	0.27 x 0.19 x 0.16
a (Å)	9.995(1)	8.588(2)	12.0713(12)	11.809(2)
b (Å)	13.505(2)	11.802(2)	13.3379(13)	25.787(5)
c (Å)	15.294(2)	16.802(3)	15.1076(16)	7.588(2)
α (°)	98.163(17)	70.68(3)	67.863(11)	90
β (°)	91.233(16)	89.32(3)	80.764(12)	90
γ (°)	96.897(15)	80.92(3)	88.372(12)	90
V (Å^3)	2027.2(5)	1585.4(5)	2222.5(4)	2310.7(9)
Z	2	2	2	2
T (K)	173(2)	173(2)	173(2)	173(2)
D_c (g.cm^{-3})	1.563	1.674	1.785	2.045
μ (mm^{-1})	0.636	0.872	1.053	6.227
Scan range (°)	$2.18 < \theta < 26.21$	$2.40 < \theta < 26.10$	$2.07 < \theta < 26.13$	$2.34 < \theta < 26.03$
Unique reflections	7491	5827	8164	4541
Reflections used [I>2σ(I)]	1896	3376	5144	2982
R_{int}	0.1776	0.0484	0.0441	0.2056
Flack parameter	-	-	-	0.38(3)
Final R indices [I>2σ(I)]*	0.0479, *w*R_2 0.0895	0.0348, *w*R_2 0.0620	0.0335, *w*R_2 0.0675	0.0922, *w*R_2 0.2146
R indices (all data)	0.2140, *w*R_2 0.1243	0.0797, *w*R_2 0.0685	0.0669, *w*R_2 0.0750	0.1300, *w*R_2 0.2394
Goodness-of-fit	0.531	0.752	0.831	0.986
Max, Min Δρ/e (Å^{-3})	0.428, -0.829	0.654, -1.051	0.757, -0.899	4.272, -3.043

*Structures were refined on F_0^2: $wR_2 = [\Sigma[w(F_0^2 - F_c^2)^2] / \Sigma w(F_0^2)^2]^{1/2}$, where $w^{-1} = [\Sigma(F_0^2) + (aP)^2 + bP]$ and $P = [\max(F_0^2, 0) + 2F_c^2]/3$

Table 6A.2: Selected bond lengths (Å) and angles (º) for complexes [**3**]PF_6, [**5**]PF_6, [**8**]$(PF_6)_2$.and [**12**]$(PF_6)_2$.

	[**3**]PF_6	[**5**]PF_6	[**8**]$(PF_6)_2$	[**12**]$(PF_6)_2$
Distances (Å)				
M-N1	2.067(8)	2.100(3)	2.094(3)	2.06(2)
M-N2	2.105(7)	2.146(3)	2.156(3)	2.193(15)
M-N3	-	-	2.112(3)	2.06(2)^{i}
M-N4	-	-	2.111(3)	2.193(15)^{i}
M-P1	2.322(2)	-	-	-
M-Cl1	-	2.4068(12)	2.3789(10)	2.402(6)
M-Cl2	-	-	2.4004(12)	2.402(6)^{i}
M-centroid 1	1.820	1.785	1.689	1.818
M-centroid 1	-	-	1.690	1.818
M1 – M2	-	-	6.073(1)	6.558(2)^{i}
		Angles (º)		
N1-M-N2	76.3(3)	76.51(13)	77.12(12)	75.5(8)
N3-M-N4	-	-	77.04(11)	75.5(8)^{i}
N1-M-P1	89.1(2)			
N2-M-P1	91.69(19)			
N1-M-Cl1	-	87.36(9)	82.43(9)	84.2(6)
N2-M-Cl1	-	94.54(9)	83.90(8)	89.7(8)
N3-M-Cl2	-	-	82.54(10)	84.2(6)^{i}
N4-M-Cl2	-	-	85.19(10)	89.7(8)^{i}

i = 1-x, -y, z

6A.3.5 UV-Visible spectroscopy

Electronic absorption spectra of complexes [**1**]PF_6 to [**12**]$(PF_6)_2$ were acquired in acetonitrile, at 10^{-5} M concentration in the range 250-550 nm. The spectral data of these complexes conformed well to their respective formulations. The spectra of these complexes are characterized by two main features, *viz*., an intense ligand–localized or intra-ligand $\pi \rightarrow \pi^*$ transition in the ultraviolet region and metal-to-ligand charge transfer (MLCT) $d\pi(M) \rightarrow \pi^*$ (**L** - ligand) bands in the visible region.[47] Since the low spin d^6

configuration of the mononuclear complexes provides filled orbitals of proper symmetry at the Ru(II), Rh(III) and Ir(III) centers, these can interact with low lying π* orbitals of the ligands. All the mononuclear complexes [**1**]PF_6 to [**6**]PF_6 show only an intense band in the region 333-341 nm while all dinuclear complexes [**7**]$(PF_6)_2$ to [**12**]$(PF_6)_2$ show two bands, one at 310 to 312 nm with high intensity as well as a second one at 355- 358 nm observed as a shoulder peak (see Figure 6A.10). The high intensity band in UV region for both mononuclear and dinuclear complexes is assigned to inter and intra-ligand π – π*/ n – π* transitions[46,30,48] while the low energy absorption band in the visible region for dinuclear complexes is assigned to metal-to-ligand charge transfer (MLCT) (t_{2g} – π*). Representative spectra of these complexes are represented in figure 6A.10.

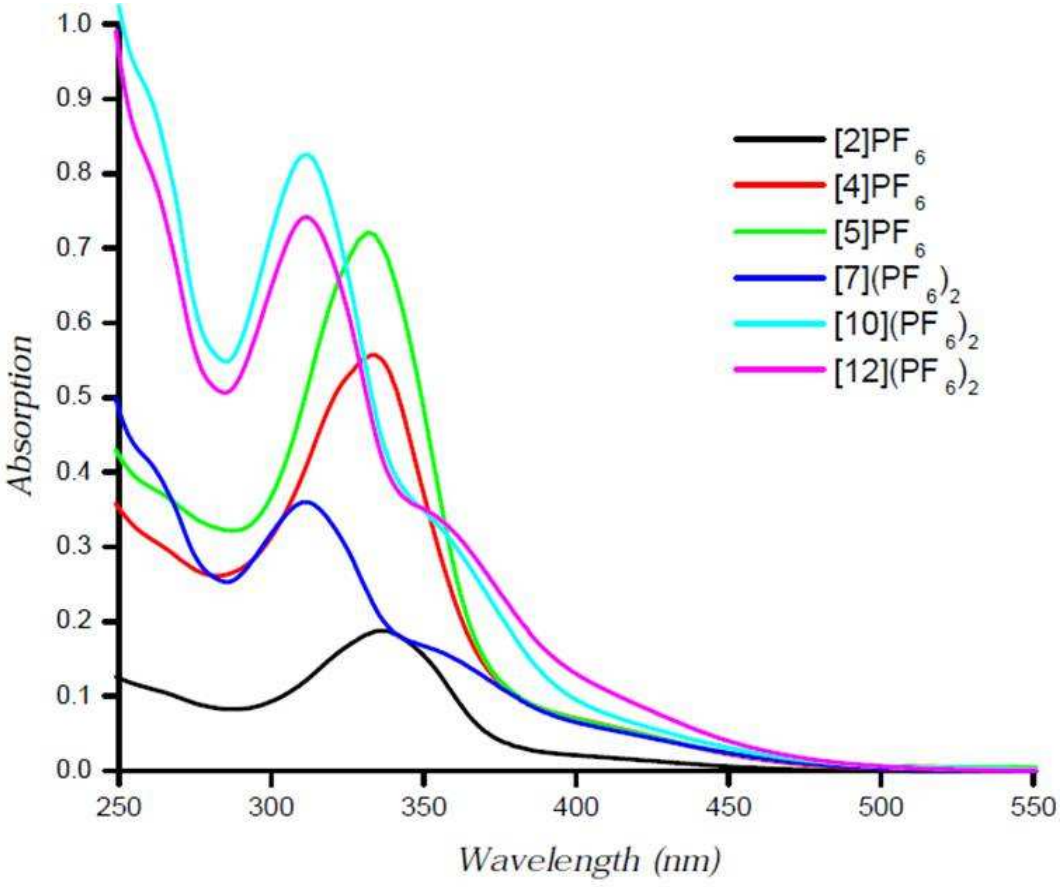

Figure 6A.10: UV-Visible electronic spectra of representative complexes in acetonitrile at 298 K.

6A.4 Conclusions

In summary in this work ligand L [4,4'-bis(2-pyridyl-4-thiazole)] reacted with series of arene and cyclopentadienyl ruthenium, rhodium and iridium complexes yielded

novel series of mononuclear complexes [**1**]PF_6 to [**6**]PF_6 as well as dinuclear complexes [**7**]$(PF_6)_2$ to [**12**]$(PF_6)_2$ in good yield, which are remarkably stable in air as well as in solution. In all these, both mono and dinuclear complexes, the metal atom is bonded with the major coordinated sites N1 and N2 or N3 and N4 and not with the other possible coordinated sites N1 and S1 or N3 and S2. But our effort to make hetero-nuclear complexes by using other binding site sulphur was unsuccessful.

6A.5 Supplementary material

CCDC **745007**, **745008**, **745009** and **745010** contains the supplementary crystallographic data for [**3**]$PF_6.(CH_3)_2CO$, [**5**]$PF_6.(CH_3)_2CO$, [**8**]$(PF_6)_2.CH_3CN$ and [**12**]$(PF_6)_2.CH_2Cl_2$.

References

1 B. J. Coe and N. R. M. Curati, Comments. Inorg. Chem. 25 (2004) 147.

2 W. R. Browne, N. M. O-Boyle, J. J. McGarvey, J. G. Vos, Chem. Soc. Rev. 34 (2005) 641.

3 G. De Ruiter, T. Gupta, M. E. V. D. Boom, J. Am. Chem. Soc. 130 (2008) 2744.

4 M. A. Ischay, M. E. Anzovino, J. Du, T. P. Yoon, J. Am. Chem. Soc. 130 (2008) 12886.

5 F. Gao, Y. Wang, D. Shi, J. Zhang, M. Wang, X. Jing, R. H. -Baker, P. Wang, S. M. Zakeeruddin, M. Graetzel, J. Am. Chem. Soc. 130 (2008) 10720.

6 M. Graetzel, Nature 414 (2001) 338.

7 E. Baranoff, J. P. Collin, L. Flamigni, J. P. Sauvage, Chem. Soc. Rev. 33 (2004) 147.

8 C. Feuvrie, O. Maury, H. Le Bozec, I. Ledoux, J. P. Morrall, G. T. Dalton, M. Samoc, M. G. Humprey, J. Phys. Chem. A, 111 (2007) 8980.

9 B. A. Gorman, P. S. Francis, N. W. Barnett, Analyst 131 (2006) 616.

10 V. Balzani and A. Juris, Coord. Chem. Rev. 211 (2001) 97.

11 F. Hanasaka, K. -I. Fujita, R. Yamaguchi, Organometallics 24 (2005) 3422.

12 R. Noyori, S. Hashigushi, Acc. Chem. Res. 30 (1997) 97, and reference therein.

13 S. –I. Murahashi, H. Takaya, T. Naota, Pure Apply. Chem. 74 (2002) 19.

14 C. A. Sandoval, T. Ohkuma, N. Utsumi, K. Tsutsumi, K. Murata, R. Noyori, Chem. Asian J. 1-2 (2006) 102.

15 J. J. Hopfield, J. N. Onuchic, D. N. Beratan, Science 241 (1988) 817.

16 J.-P. Sauvage, J.-P. Collin, J.-C. Chambron, S. Guillerez, C. Coudret, V. Balzani, F. Barigelletti, L. Decola, L. Flamigni, Chem. Rev. 94 (1994) 993.

17 S. Campagna, S. Serroni, F. Puntoriero, C. Di Pietro, V. Ricevuto, in: V. Balzani (Ed.), Electron Transfer in Chemistry, vol. 5, VCH-Wiley, Weinheim, 2001, p. 186.

18 D. P. Funeriu, J.-M. Lehn, K. M. Fromm, D. Fenske, Chem. Eur. J. 6 (2000) 2103.

19 F. Loiseau, C. Di Pietro, S. Serroni, S. Campagna, A. Licciardello, A. Manfredi, G. Pozzi, S. Quici, Inorg. Chem. 40 (2001) 6901.

20 W. R. Browne, N. M. O-Boyle, W. Henry, A. L. Guckian, S. Horn, T. Fett, C. M. O-Connor, M. Duati, L. De Cola, C. G. Coates, K. L. Ronayne, J. J. McGarvey, J. G. Vos, J. Am. Chem. Soc. 127 (2005) 1229.

21 M. -J. Kim, R. Konduri, H. Ye, F. M. MacDonnell, F. Puntoriero, S. Serroni, S. Campagna, T. Holder, G. Kinsel, K. Rajeshwar, Inorg. Chem. 41 (2002) 2471.

22 D. M. Dattelbaum, C. M. Hartshorn, T. J. Meyer, J. Am. Chem. Soc. 124 (2002) 4938.

23 H. Masui, A. L. Freda, M. C. Zerner, A. B. P. Lever, Inorg. Chem. 39 (2000) 141.

24 C. R. Rice, S. Wörl, J. C. Jeffery, R. L. Paul, M. D. Ward, J. Chem. Soc., Dalton trans. (2001) 550.

25 C-S. Tsang, H-L. Yeung, W-T. Wong, H-L. Kwong, Chem. Commun. (2009) 1999.

26 R. L. Williams, H. N. Toft, B. Winkel, K. J. Brewer, Inorg. Chem. 42 (2003) 4394.

27 M. Marcaccio, F. Paolucci, C. Paradisi, S. Roffia, C. Fontanesi, L. J. Yellowlees, S. Serroni, S. Campagna, G. Denti, V. Balzani, J. Am. Chem. Soc. 121 (1999) 10081.

28 J. R. Kirchhoff, K. Kirschbaum, Polyhedron 17 (1998) 4033.

29 G. Gupta, G. P. A. Yap, B. Therrien, K. M. Rao, Polyhedron 28 (2009) 844.

30 K. T. Prasad, B. Therrien, K. M. Rao, J. Organomet. Chem. 693 (2008) 3049.

31 D. L. Davies, J. Fawcett, R. Krafczyk, D. R. Russell, K. Singh, Dalton Trans. (1998) 2349.

32 D. L. Davies, O. A.-Duaij, J. Fawcett, M. Giardiello, S. T. Hilton, D. R. Russell, Dalton Trans. (2003) 4132.

33 K. S. Singh, P. J. Carroll, K. M. Rao, Polyhedron 24 (2005) 391.

34 P. Govindaswamy, Y. A. Mozharivskyj, K. M. Rao, Polyhedron 23 (2004) 1567.

35 R. Lalrempuia, P. J. Carroll, K. M. Rao, Polyhedron 22 (2003) 605.

36 D. L. Davies, J. Fawcett, R. Krafczyk, D. R. Russell, J. Organomet. Chem. 545-546 (1997) 581.

37 P. Govindaswamy, Y. A. Mozharivskyj, K. M. Rao, Polyhedron 24 (2005) 1710.

38 A. Singh, N. Singh, D. S. Pandey, J. Orgnomet. Chem. 642 (2002) 48.

39 H. Mishra, R. Mukherjee, J. Orgnomet. Chem. 691 (2006) 3545

40 K. Pachhunga, B. Therrien, K. A. Kreisel, G. P. A. Yap, K. M. Rao, Polyhedron 26 (2007) 3638.

41 G. Gupta, K.T. Prasad, B. Das, G. L. P. Yap, K. M. Rao, J. Organomet. Chem. 694 (2009) 2618.

42 R. Lalrempuia, K. M. Rao, Polyhedron 22 (2003) 3155.

43 K. Pachhunga, B. Therrien, K. A. Kreisel, G. P. A. Yap, K. M. Rao, Polyhedron 26 (2007) 3638.

44 K. T. Prasad, G. Gupta, A. V. Rao, B. Das, K. M. Rao, Polyhedron 28 (2009) 2649.

45 H. Brunner, A. KÖllnberger, T. Burgemeister, M. Zabel, Polyhedron 19 (2000) 1519.

46 P. Govindaswamy, J. Canivet, B. Therrien, G. Süss-Fink, P. Štěpnička, J. Ludvík, J. Organomet. Chem. 692 (2007) 3664.

47 E. Binamira-Soriaga, N. L. Keder, W. C. Kaska, Inorg. Chem. 29 (1990) 3167.

48 C. S. Arau´ jo, M. G. B. Drew, V. Félix, L. Jack, J. Madureira, M. Newell, S. Roche, T. M. Santos, J. A. Thomas, L. Yellowlees, Inorg. Chem. 41 (2002) 2250.

Chapter 6

(Part B)

New series of platinum group metal complexes bearing η^5- and η^6-Cyclichydrocarbons and Schiff base derived from 2-acetylthiazole: syntheses and structural studies

---

In this chapter we focus on the synthetic methodology applied for the development of homogeneous and immobilized half- sandwich ruthenium, rhodium and iridium complexes bearing Schiff base (*ata*) as a specific N, N-bidentate bridging ligand has shown below.

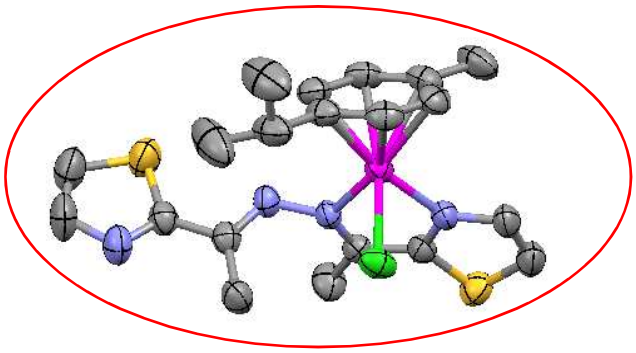

---

*The work presented in this chapter has been published: **K. T. Prasad**, G. Gupta, A. V. Rao, B. Das and K. Mohan Rao, Polyhedron 28 (2009) 2864.

6B.1 Introduction

Recent interest in half- sandwich platinum group metal complexes with symmetrical Schiff bases come from the fact they can serve as synthetic models related to biological systems,[1-7] as homogeneous catalysts in systems like,[8-17] and supported chemical processes[18,19] and very recently as non-linear optical (NLO) materials.[20,21] Their attractiveness does also come from their preparative accessibility, their structural variability in addition to many of these novel ruthenium complexes combine an appropriate balance between the electronic and steric environment around the metal core.

Moreover, some of the nitrogen-donor ligands impart to the catalyst for good tolerance towards various organic functionalities, air, and moisture, thus widening the scope and limit's of their application. Of the above mentioned ligands, Schiff bases are of a great interest for creating new active and selective ruthenium catalytic systems.[22,23] There are few reports of half-sandwich Ru(II), Rh(III) and Ir (III) complexes with N,N-donor polypyridyl azine Schiff base ligands,[24,25] but there are no reports with thiazole azine ligand in the literature. Complexes imparting other than pyridyl azine ligands are yet to be explored, in view of the fact that ring size and the substituents in the heterocyclic ring system significantly modifies the acidity and regulate the physical and chemical properties of the complexes.[26-27] The arene and cyclopentadienyl platinum group metal complexes containing thiazole azine ligand is being reported for the first time.

In the present communication we focus on the synthetic methodology applied for the development of homogeneous and immobilized half- sandwich ruthenium, rhodium and iridium complexes bearing Schiff base (*ata*) as a specific N, N-bidentate bridging ligand has shown below.

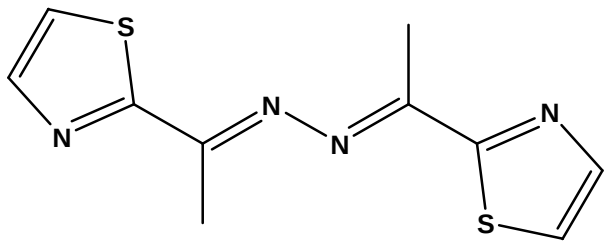

2-acetylthiazole azine *(ata)*

6B.2 Experimental

6B.2.1 Preparation ligand 2-acetylthiazole azine (ata)

2-acetylthiazole (2.50 g, 20 mmol) was added to a dichloromethane solution (30 ml) containing formic acid (0.2 ml). This mixture was added to hydrazine (35 wt% solution in H_2O) (0.916 ml, 10 mmol) solution (in 30 ml ethanol). The resulting solution was stirred for 4h at room temperature. The brownish yellow solid which precipitated out from the reaction mixture, was filtered and washed with hexane (25 ml × 2) and dried under vacuum to give a yellow solid of 2-acetylthiazole azine (*ata*).

Yield: 97%, M. P.: 152-154 ºC: $C_{10}H_{10}N_4S_2$ (250.34) Calc.: C 47.98, H 4.03, N 22.38; Found: C 48.01, H 4.06, N 22.28; ^{1}H NMR ($CDCl_3$, δ): 7.91 (d, 2H, J_{H-H} = 3.20 Hz), 7.44 (d, 2H, J_{H-H} = 3.20 Hz), 2.58 (s, 6H, tz-Me); ESI-MS (m/z): 250.12; IR (KBr, cm^{-1}): 1606, 1490, 1417, 1063,750.

6B.2.2 General Procedure for the preparation of the mononuclear complexes [**1**]PF_6 – [**3**]PF_6

A mixture of [(η^6-arene)Ru(μ-Cl)Cl]$_2$ (arene = C_6H_6, *p*-^{i}PrC_6H_4Me and C_6Me_6) (0.07 mmol), ligand *ata* (0.18 mmol) and 2.5 equivalents of NH_4PF_6 in dry methanol (15 ml) was stirred at room temperature for 6 hours. The precipitate was separated by filtration, washed with cold methanol and diethyl ether to remove excess ligand and dried under vacuum.

6B.2.2.1 [(η^6-C_6H_6)Ru(ata)Cl]PF_6 ([1]PF_6)

Orange-yellow solid, yield 70 mg (79%): $C_{16}H_{21}ClN_4S_2RuPF_6$ (609.5) Calc.: C 34.89, H 3.84, N 10.17; Found: C 34.68, H 3.98, N 10.28: ^{1}H NMR (CD_3CN, δ): 8.75 (d, 1H, J_{H-H} = 2.98 Hz), 8.52 (d, 1H, J_{H-H} = 3.20 Hz), 7.98 (d, 1H, J_{H-H} = 3.20 Hz), 7.62 (d, 1H, J_{H-H} = 3.2 Hz), 6. 50 (s, 6H), 2.56 (s, 3H, tz-Me), 2.47 (s, 3H, tz-Me); ESI-MS (m/z): 525.1 (100%) [M-PF_6]$^+$; IR (KBr, cm^{-1}): $\nu_{(P-F)}$ 844s; 1604, 1408, 558.

*6B.2.2.2 [(η^6-p-^{i}PrC_6H_4Me)Ru(ata)Cl]PF_6 ([**2**]PF_6)*

Dark orange solid, yield 86 mg (89%): $C_{20}H_{24}ClS_2N_4RuPF_6$ (651.5) Calc.: C 36.07, H 3.63, N 8.41; Found: C 36.18, H 3.68, N 8.35: ^{1}H NMR ($CDCl_3$, δ): 8.55 (d, 1H, J_{H-H} = 2.88 Hz), 8.06 (d, 1H, J_{H-H} = 3.20 Hz), 7.98 (d, 1H, J_{H-H} = 3.2 Hz), 7.71 (d, 1H, J_{H-H} = 2.80 Hz), 5.90 (d, 1H, J_{H-H} = 2.8 Hz, Ar_{p-cy}), 5.87 (d, H, J_{H-H} = 2.4 Hz, Ar_{p-cy}), 5.72 (d, 1H,

J_{H-H} = 4 Hz, Ar_{p-cy}), 5.68 (d, 1H, J_{H-H} = 2.8 Hz, Ar_{p-cy}), 2.93 (sept, 1H, J_{H-H} = 4.4 Hz, $CH(CH_3)_2$), 2.56 (s, 3H, tz-Me), 2.47 (s, 3H, tz-Me), 2.28 (s, 3H, Ar_{p-cy}-Me), 1.26 (d, 3H, $CH(CH_3)_2$), 1.18 (d, 3H, $CH(CH_3)_2$) ; ESI-MS (m/z): 525.1 (100%) $[M-PF_6]^+$; IR (KBr, cm^{-1}): $\nu_{(P-F)}$ 844s; 1629, 1406, 763, 558.

*6B.2.2.3 [(η^6-C_6Me_6)Ru(ata)Cl]PF_6 ([**3**]PF_6)*

Orange-yellow solid, yield 85 mg (88%): $C_{22}H_{28}ClN_4S_2RuPF_6$ (694.1) Calc.: C 38.07, H 4.07, N 8.07; Found: C 38.11, H 4.18, N 8.02: ^{1}H NMR ($CDCl_3$, δ): 8.75 (d, 1H, J_{H-H} = 2.98 Hz), 8.52 (d, 1H, J_{H-H} = 3.20 Hz), 7.98 (d, 1H, J_{H-H} = 3.20 Hz), 7.62 (d, 1H, J_{H-H} = 3.2 Hz), 2.56 (s, 3H, tz-Me), 2.47 (s, 3H, tz-Me), 2.28 (s, 18H),; ESI-MS (m/z): 549.14 (100%) $[M-PF_6]^+$; IR (KBr, cm^{-1}): $\nu_{(P-F)}$ 844s; 1624, 1437, 1409, 769, 558.

6B.2.3 General Procedure for the preparation of the mononuclear complexes [**4**]PF_6 and [**5**]PF_6

A mixture of [(η^5-C_5Me_5)M(μ-Cl)Cl]$_2$ (M = Rh, Ir) (0.07 mmol), ligand *ata* (0.15 mmol) and 2.5 equivalents of NH_4PF_6 in dry methanol (15 ml) was refluxed for 4 hours. The reaction mixture was cooled over night at room temperature, during this time dark yellow colour crystalline compound was formed. It was separated by filtration, washed with cold methanol and diethyl ether to remove excess ligand and dried under vacuum.

*6B.2.3.1 [(η^5-C_5Me_5)Rh(ata)Cl]PF_6 ([**4**]PF_6)*

Dark yellow color, yield 86 mg (85%): $C_{20}H_{25}ClN_4S_2RhPF_6$ (668.89) Calc.: C 35.91, H 3.77, N 8.38; Found: C 36.00, H 3.89, N 8.29: ^{1}H NMR (CD_3CN, δ): 8.33 (d, 1H, J_{H-H} = 5.58 Hz), 8.05 (d, 1H, J_{H-H} = 3.2 Hz), 7.82 (d, 1H, J_{H-H} = 2.8 Hz), 7.68 (d, 1H, J_{H-H} = 3.2 Hz), 2.57 (s, 3H, tz-Me), 2.50 (s, 3H, tz-Me), 1.77 (s, 15H, C_5Me_5); ESI-MS (m/z): 523.1 (100%) $[M-PF_6]^+$; IR (KBr, cm^{-1}): $\nu_{(P-F)}$ 845s; 1626, 1458, 759, 558.

*6B.2.3.2 [(η^5-C_5Me_5)Ir(ata)Cl]PF_6 ([**5**]PF_6)*

Dark yellow color, yield 95 mg (84%): $C_{20}H_{25}ClN_4S_2IrPF_6$ (818.21) Calc.: C 31.68, H 3.32, N 7.39; Found: C 31.70, H 3.48, N 7.48: ^{1}H NMR (CD_3CN, δ): 8.58 (d, 1H, J_{H-H} = 3.28 Hz), 8.26 (d, 1H, J_{H-H} = 3.26 Hz), 7.88 (d, 1H, J_{H-H} = 2.88 Hz), 7.68 (d, 1H, J_{H-H} = 3.24 Hz), 2.57 (s, 3H, tz-Me), 2.40 (s, 3H, tz-Me), 1.99 (s, 15H, C_5Me_5); ESI-MS (m/z): 613.18 (100%) $[M-PF_6]^+$; IR (KBr, cm^{-1}): $\nu_{(P-F)}$ 845s; 1631, 1495, 760, 558.

6B.2.4 General Procedure for the preparation of the mononuclear complexes [**6**]PF_6 - [**8**]PF_6

A mixture of [(η^5-Cp)Ru(PPh_3)$_2$Cl] (η^5-Cp = η^5-C_5H_5, η^5-C_5Me_5, η^5-C_9H_7) (0.1 mmol), ligand *ata* (0.12 mmol) and 1.5 equivalents of NH_4PF_6 in dry ethanol (15 ml) was refluxed for 10 hours. It was changed to dark red color from dark yellow color. The solvent was evaporated on rotary evaporator and residue was dissolved in dichloromethane and filtered to remove ammonium chloride and filtrate was evaporated to 2 ml and excess hexane was added to induce dark color precipitate.

*6B.2.4.1 [(η^5-C_5H_5)Ru(ata)(PPh_3)]PF_6 ([**6**]PF_6)*

Orange color, yield 60 mg (73%): $C_{33}H_{30}N_4S_2RuP_2F_6$ (823.75) Calc.: C 48.12, H 3.67, N 6.80; Found: C 48.11, H 3.73, N 6.75: ^{1}H NMR ($CDCl_3$, δ) 8.52 (d, 1H, J_{H-H} = 2.80 Hz), 8.12 (d, 1H, J_{H-H} = 3.2 Hz), 7.77 (d, 1H, J_{H-H} = 3.2 Hz), 7.68 (d, 1H, J_{H-H} = 3.2 Hz), 7.46-7.23 (m, 15H), 4.57 (s, 5H, C_5H_5), 2.57 (s, 3H, tz-Me), 2.50 (s, 3H, tz-Me); ESI-MS (m/z): 678.78 (100%) [M-PF_6]$^+$; IR (KBr, cm^{-1}): $\nu_{(P-F)}$ 845s; 1626, 1458, 766, 558: ^{31}P {^{1}H} ($CDCl_3$): 49.34 ppm.

*6B.2.4.2 [(η^5-C_5Me_5)Ru(ata)(PPh_3)]PF_6 ([**7**]PF_6)*

Orange color, yield 68mg (76%): $C_{38}H_{40}N_4S_2RuP_2F_6$ (893.88) Calc.: C 51.06, H 4.51, N 6.27; Found: C 51.10, H 4.62, N 6.24: ^{1}H NMR ($CDCl_3$, δ) 8.87 (d, 1H, J_{H-H} = 2.80 Hz), 8.52 (d, 1H, J_{H-H} = 3.2 Hz), 7.87 (d, 1H, J_{H-H} = 3.2 Hz), 7.79 (d, 1H, J_{H-H} = 3.2 Hz), 7.46-7.23 (m, 15H), 2.57 (s, 3H, tz-Me), 2.50 (s, 3H, tz-Me), 2.19 (s, 15H, C_5Me_5); ESI-MS (m/z): 748.88 (100%) [M-PF_6]$^+$; IR (KBr, cm^{-1}): ν(P-F) 845s; 1621, 1479, 749, 558: ^{31}P {^{1}H} ($CDCl_3$): 48.54 ppm.

*6B.2.4.3 [(η^5-C_9H_7)Ru(ata)(PPh_3)]PF_6 ([**8**]PF_6)*

Yellowish brown colour, yield 66 mg (76%): $C_{37}H_{35}N_4S_2RuP_2F_6$ (876.83) Calc.: C 50.68, H 4.02, N 6.39; Found: C 50.61, H 4.19, N 6.34: ^{1}H NMR ($CDCl_3$, δ) 8.52 (d, 1H, J_{H-H} = 2.80 Hz), 8.12 (d, 1H, J_{H-H} = 3.2 Hz), 7.77 (d, 1H, J_{H-H} = 3.2 Hz), 7.68 (d, 1H, J_{H-H} = 3.2 Hz), 7.46-7.23 (m, 20H), 4.87(t, 1H), 4.71 (d, 2H); 2.57 (s, 3H, tz-Me), 2.50 (s, 3H, tz-Me); ESI-MS (m/z): 731.87 (100%) [M-PF_6]$^+$; IR (KBr, cm^{-1}): ν(P-F) 845s; 1629, 1468, 763, 558: ^{31}P {^{1}H} ($CDCl_3$): 54.42 ppm.

*6B.2.5 Procedure for the preparation of complex ([**9**]PF_6)*

The complex [**4**]PF_6 (50 mg, 0.074 mmol) was dissolved in 20 ml of dichloromethane in a small diameter test tube and layered with diethylether and it was sealed and kept at room temperature. Dark orange crystalline compound was observed after three days. The crystalline compound was separated by filtration and washed with diethyl ether and dried at room temperature.

6B.2.5.1 [(η^5-C_5Me_5)Rh(ata)Cl]PF_6 ([**9**]PF_6)*

$C_{15}H_{22}ClF_6N_3PRhS$ (559.73) Calc.: C 32.19, H 3.96, N 7.51; Found: C 32.00, H 3.99, N 7.29: ^{1}H NMR (CD_3CN, δ): 8.23 (d, 1H, J_{H-H} = 5.58 Hz), 7.89(d, 1H, J_{H-H} = 2.8 Hz), 4.78 (s, 2H, NH_2), 2.61 (s, 3H, tz-Me), (s, 15H, C_5Me_5); ESI-MS (m/z): 415.72 (100%) [M-PF_6]$^+$; IR (KBr, cm^{-1}): $\nu_{(P-F)}$ 845s; 759, 558, 1626, 1458, 2891.

6B.2.6 Single crystal X-ray structure analyses

Crystals suitable for X-ray diffraction study for compound [**2**]PF_6 and [**4**]PF_6 were grown by slow diffusion of diethylether into dichloromethane solution of complexes [**2**]PF_6 and [**4**]PF_6, respectively. The bright orange crystals of compound [**2**]PF_6 , the red color crystal of [**4**]PF_6 were mounted on a Stoe-Image Plate Diffraction system equipped with a ϕ circle goniometer, using Mo-Kα graphite monochromated radiation (λ = 0.71073 Å) with ϕ range 0-200°, increment of 1.2°, D_{max}-D_{min} = 12.45-0.81 Å. X-ray intensity data were collected with Mo-Kα graphite monochromatic radiation at 296 (2)K, with 0.3°ω scan mode and 10 second per frame. The intensity data were corrected for Lorentz and polarization effects. The H-atoms were included in calculated positions and treated as riding atoms using the SHELXL default parameters. The non-H atoms were refined anisotropically, using weighted full-matrix least-squares on F^2. The data collection parameters and bond lengths and angles are presented in table 1 and 2 respectively.

6B.3 Results and discussion

6B.3.1 Syntheses of ligand and complexes

Mononuclear cationic arene ruthenium complexes having *ata* ligand *viz*., [(η^6-C_6H_6)Ru(*ata*)Cl]PF_6 ([**1**]PF_6), [(η^6-*p*-^{i}PrC_6H_4Me)Ru(*ata*)Cl]PF_6 ([**2**]PF_6) and [(η^6-C_6Me_6)Ru(*ata*)Cl]PF_6 ([**3**]PF_6) (Scheme 6B.1) have been expediently prepared by the reaction of arene ruthenium dimers [(η^6-arene)Ru(μ-Cl)Cl]$_2$ (arene = C_6H_6, *p*-^{i}PrC_6H_4Me,

C_6Me_6) and two equivalents of 2-acetylthiazole azine (*ata*) in methanol at room temperature in the presence of NH_4PF_6. These complexes are isolated as hexafluorophosphate salts.

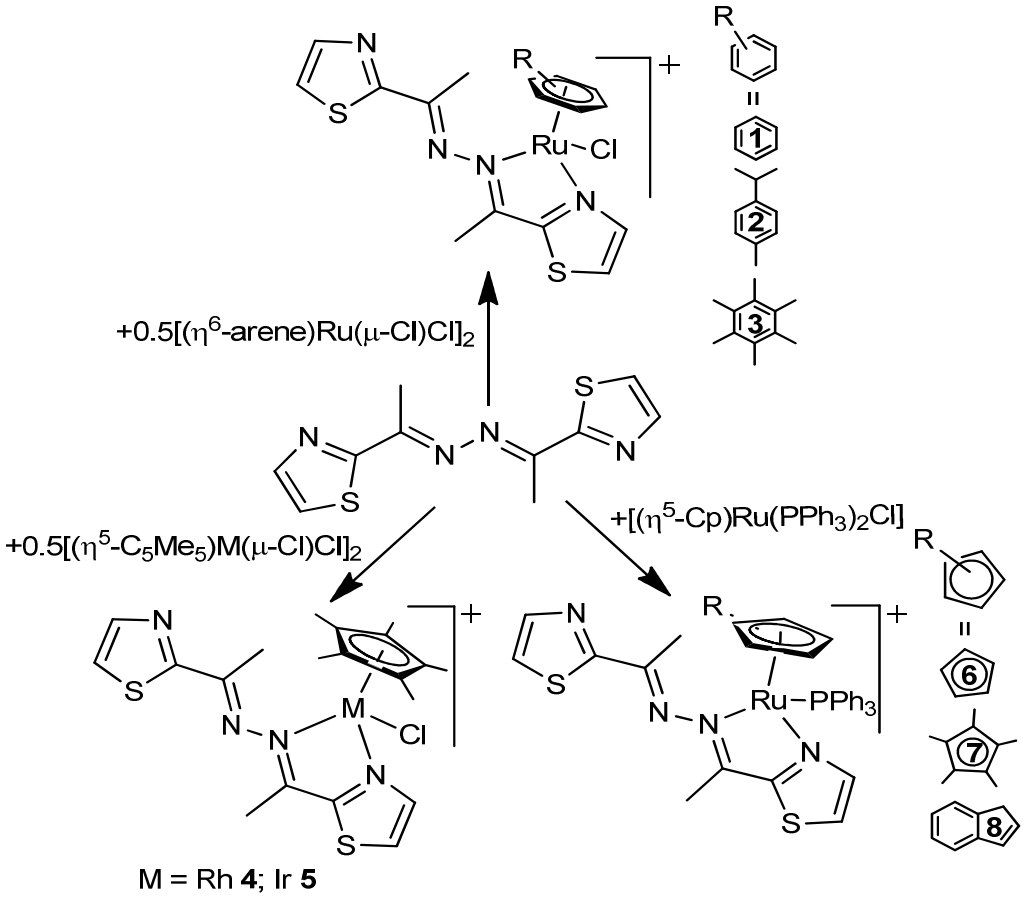

Scheme 6B.1

Similarly, the pentamethylcyclopentadienyl Rh and Ir dimers $[(\eta^5\text{-}C_5Me_5)M(\mu\text{-}Cl)Cl]_2$ (M = Rh, Ir) with the 2-acetylthiazole azine (*ata*) ligand at 50 °C leads to the formation of the mononuclear cationic complexes $[(\eta^5\text{-}C_5Me_5)Rh(ata)Cl]PF_6$ ([**4**]PF_6) and $[(\eta^5\text{-}C_5Me_5)Ir(ata)Cl]PF_6$ ([**5**]PF_6) (Scheme 6B.1) which are isolated as their hexafluorophosphate salts.

The cyclopentadienyl ruthenium triphenylphosphine complexes $[(\eta^5\text{-}C_5H_5)Ru(PPh_3)_2Cl]$, $[(\eta^5\text{-}C_5Me_5)Ru(PPh_3)_2Cl]$ and $[(\eta^5\text{-}C_9H_7)Ru(PPh_3)_2Cl]$ with the 2-acetylthiazole azine (*ata*) ligand in methanol at 70 °C leads to the formation of the mononuclear cationic complexes $[(\eta^5\text{-}C_5H_5)Ru(ata)PPh_3]PF_6$ ([**6**]PF_6, $[(\eta^5\text{-}C_5Me_5)Ru(ata)PPh_3]PF_6$ ([**7**]PF_6) and $[(\eta^5\text{-}C_9H_7)Ru(ata)PPh_3]PF_6$ ([**8**]PF_6) (Scheme 6B.1) by replacement of one triphenylphosphine and chloride which are isolated as their hexafluorophosphate salts.

In order to prepare the dinuclear complexes we have used two fold metal to ligand or one fold metal to mononuclear complexes concentration, but we were not successful in either of the cases. This could be due to the steric strain from arene or pentamethylcyclopentadienyl ligands already present on metal atoms.

6B.3.2 Characterization

The mononuclear complexes were fully characterized by IR, NMR (^{1}H and ^{31}P), and electronic spectroscopy. Analytical data of the complexes conformed well to their respective formulations. Further information about composition of the complexes has also been obtained from Mass spectrometry.

Infrared spectra of the ligand display an absorption band at 1606 cm^{-1} (ata) assignable to the C=N bond, consistent with the fact that C=N stretching frequencies of Schiff bases appear in the range 1680-1603 cm^{-1} [28-29] and complexes display the same band at higher wave numbers and appeared around 1626 cm^{-1}. The bands associated with thiazole ring such as C=N and C=S appeared at about 1430 and 1406 cm^{-1}, these values are showing less wave numbers as compared to free ligand (1490 and 1417 cm^{-1}) respectively. The shift in the position of $\nu_{C=N}$ of both azine and thiazole suggested that the co-ordination of the metal ion is through thiazole and azine of nitrogen and not through the thiazole sulphur. Strong band in the region 844 cm^{-1} have been assigned to counter ion PF_6. For instance the IR spectrum of the complex **2** is depicted in figure 6B.1 and Mass spectrum of the complexes **1** and **6** are depicted in figure 6B.2 and 6B.3 respectively.

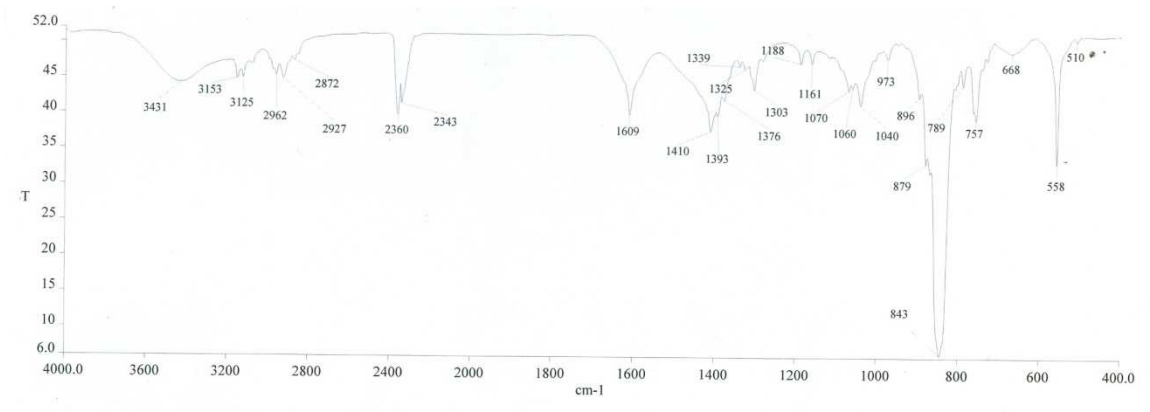

Figure 6B.1: IR spectrum of complex $[(\eta^6\text{-}p\text{-}^{i}PrC_6H_4Me)Ru(ata)Cl]PF_6$ ([**2**]PF_6)

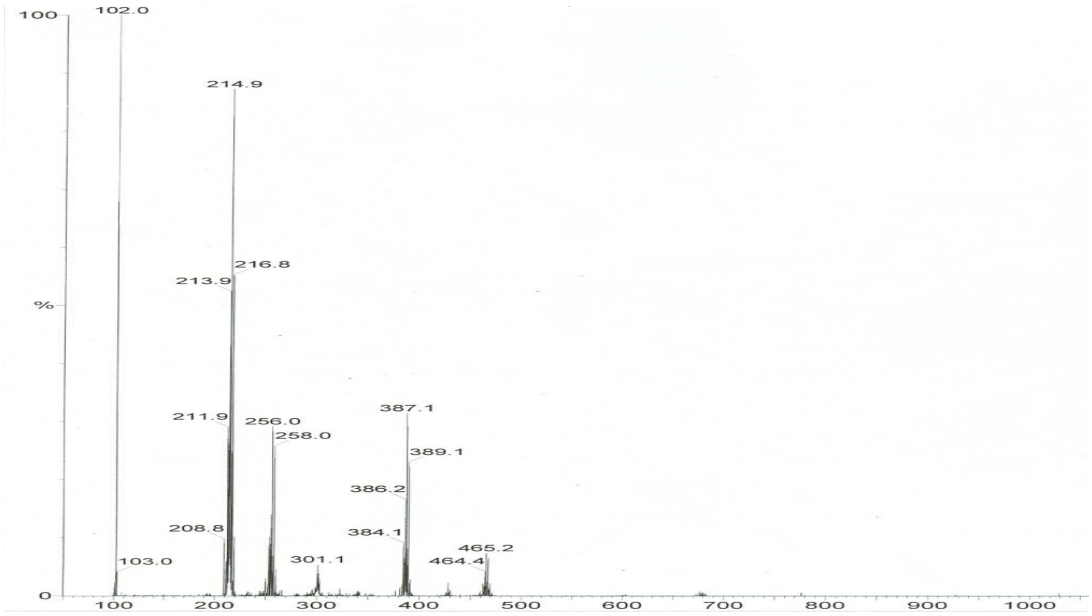

Figure 6B.2: Mass spectrum of complex $[(\eta^6\text{-}C_6H_6)Ru(ata)Cl]PF_6$ ([**1**]PF_6)

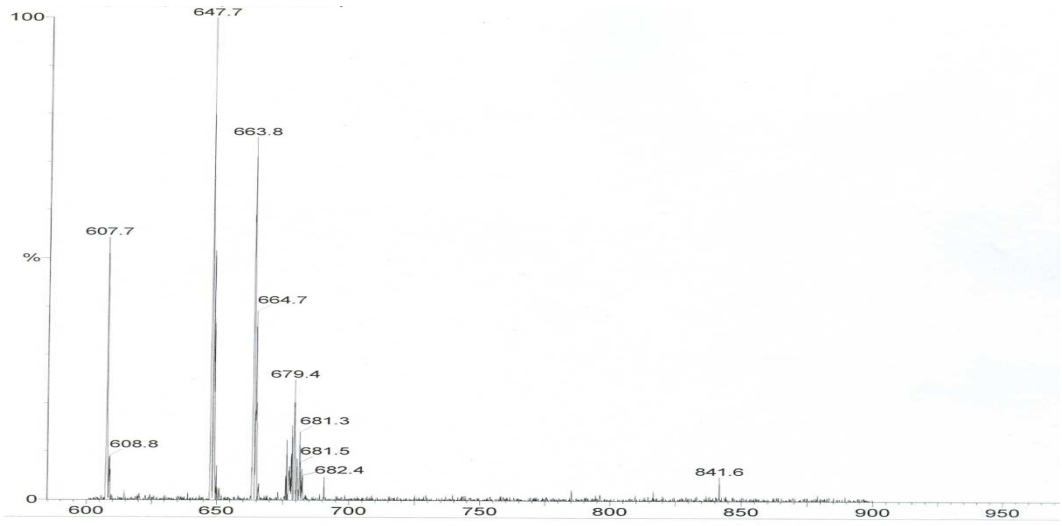

Figure 6B.3: Mass spectrum of complex $[(\eta^5\text{-}C_5H_5)Ru(ata)(PPh_3)]PF_6$ ([**6**]PF_6)

The ^{1}H NMR spectrum of free ligand (*ata)* exhibit a characteristic set of three resonances for the thiazole ring protons and methyl protons of N=C-CH_3 group. Upon coordination with the metal atom, the mononuclear cationic complexes [**1**]PF_6 to [**5**]PF_6 exhibit six distinct resonances assignable to thiazolyl ring and N=C-CH_3 protons of the *ata* ligand indicating formation of mononuclear complexes. Besides these signals complexes [**1**]PF_6 and [**3**]PF_6 exhibit a singlet for the protons of the benzene ring and

protons of the hexamethylbenzene at δ 6.50 and 2.28 respectively. Complex **2** exhibit a singlet at δ=2.28 for methyl protons, a septet at δ=2.82 for the CH proton of the isopropyl group. Interestingly we observe an unusual pattern for the diastereotopic methyl protons of the isopropyl group and diastereotopic CH protons of the *p*-cymene ligand showing two doublets at δ= 1.26 to 1.18, and four doublets in the range δ= 5.90 to 5.68 instead of one doublet and two doublets respectively with reference to the starting precursor. This unusual pattern is due to the diastereotopic methyl protons of the isopropyl group and aromatic protons of the *p*-cymene ligand, since the ruthenium atom is stereogenic due to the coordination of four different ligand atoms and chiral nature of metal atom.[31,32,38]

Complexes [**4]PF$_6$** and [**5]PF$_6$** exhibit a singlet for the methyl protons of the pentamethylcyclopentadienyl ligand at δ 1.77 and 1.99 ppm. Complexes [**6]PF$_6$** and **[7]PF$_6$** exhibit a singlet at δ 4.57 and 2.19 for the protons of cyclopentadienyl ligand and methyl protons of pentamethylcyclopentadienyl ligands respectively. Complex [**8]PF$_6$** exhibits a characteristic three sets of signals such as multiplet, triplet and doublet, for the protons of the indenyl ligand in the range of 7.46, 4.81 and 4.71 respectively. The protons of the triphenylphosphine ligand exhibit a multiplet at δ=7.22 to 7.55. For instance the ^{1}H NMR spectrum of the complex **2** is depicted in figure 6B.4 and spectrum of complex 6 is depicted in figure 6B.5.

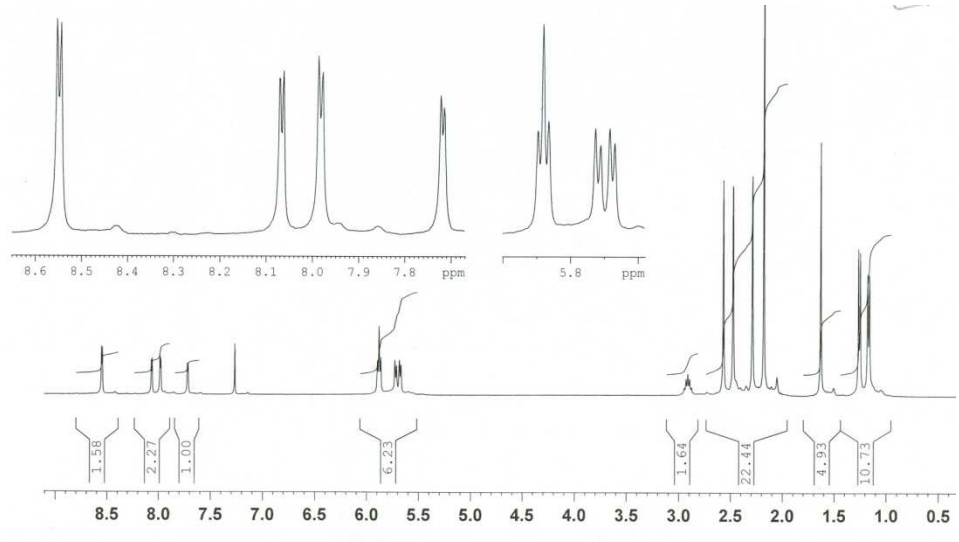

Figure 6B.4: ^{1}H NMR spectrum of complex [(η^6-*p*-^{i}PrC$_6$H$_4$Me)Ru(*ata*)Cl]PF$_6$ ([**2**]PF$_6$) in acetonitrile-d_3.

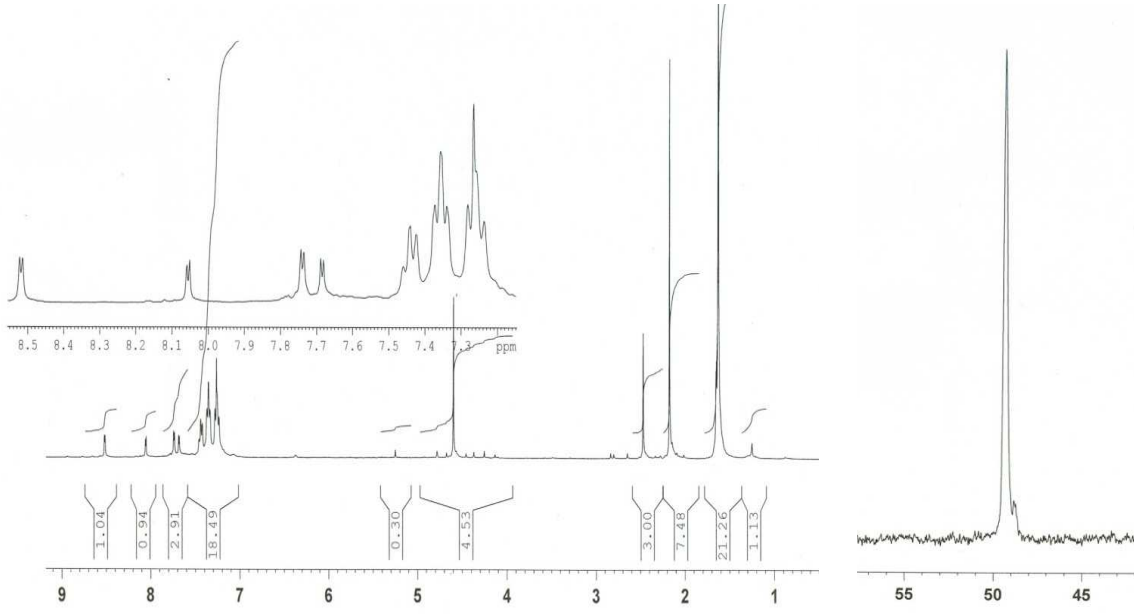

Figure 6B.5: ^{1}H and ^{31}P NMR spectrum of complex $[(\eta^5\text{-}C_5H_5)Ru(ata)(PPh_3)]PF_6$ ([**6**]PF_6) in Chloroform-d_1.

The ^{31}P NMR spectra of complexes [**6**]PF_6, [**7**]PF_6, and [**8**]PF_6 showing down field shift compared to starting precursors *viz.* δ 49.34, 48.54, and 54.42 ppm respectively. This down field chemical shift of phosphorus nucleus indicates the formation of cationic complexes.

6B.3.3 Molecular structure presentation

The molecular structures of $[(\eta^6\text{-}p\text{-}^{i}PrC_6H_4Me)Ru(ata)Cl]^+$ (**2**) and $[(\eta^5\text{-}C_5Me_5)Rh(ata^*)Cl]^+$ (**9**) (ata*= hydrolysed product of ata) ($N(CH_2CH_2SCC(CH_3))N\text{-}NH_2$) have been established by single-crystal X-ray analysis of their hexafluorophosphate salts. All the cationic complexes show a typical piano-stool geometry with the metal centre being coordinated by the arene/pentamethylcyclopentadienyl ligand, a terminal chloride and the chelating *ata/ ata** ligand. The metal atom is in octahedral arrangement with two cis-nitrogen atoms of the ata/ata* ligand acting as a bidentate chelating ligand through two neighboring thiazole and azine nitrogen atoms. The molecular structures of complexes [**2**]PF_6 and [**9**]PF_6 are shown in figure 6B.6 and figure 6B.7, respectively, and bond lengths and angles are presented in table 2.

In the mononuclear complexes [**2**]PF_6 and [**9**]PF_6 the metal to nitrogen bond distance (2.087(3), and 2.097(4) Å) of the thiazole is shorter than the corresponding azine

N-metal distance (2.104(2) and 2.136(5) Å) which are comparable to those in [(η^6-C_6Me_6)RuCl-(C_5H_4N-2-CH=N=C_6H_4-p-NO_2)]PF_6,[33] [Ru(mes)Cl{C_5H_4N-2-C(Me)=N(CHMePh)}]BF_4,[34] [(η^5-C_5Me_5)RhCl(C_5H_4N-2-CH=N=C_6H_4-p-NO_2)]BF_4.[35] The Rh-N bond distance (2.097(4) and 2.136(5) Å) in [**9**]PF_6 is slightly longer than the corresponding distances of ruthenium complex **2** (2.104(3) Å), while the M-Cl [2.406(8) and 2.396(15)] bond lengths show no significant differences in both the cations and other reported values.[36] The N-M-N bond angles [75.58(10) in **2** and 75.88(17)° in **9**] are similar to those in other reported complexes [(η^5-C_5Me_5)Ru(PPh_3)(C_5H_4N-CH=N-N=CH-C_5H_4N)]BF_4 and [(η^5-C_9H_7)Ru-(PPh_3)(C_5H_4N-2-CH=N=C_6H_4-p-NO_2)]PF_6 [75.90(2) and 75.53(8)°].[37]

The distances between the ruthenium atom and centroid of η^6-*p*-^{i}PrC_6H_4Me ring is 1.692 Å in complex [**2**]PF_6, whereas the distance between the rhodium atom and the centroid of the η^5-C_5Me_5 ring is 1.782 Å in complex [**9**]PF_6**.** These bond distances are comparable to those in the related complex cations [(η^6-*p*-^{i}PrC_6H_4Me)Ru(pyNp)Cl]PF_6 and [(η^5-C_5Me_5)Ir(pyNp)Cl]PF_6 (PyNp=2-(2-pyridyl)-1,8-naphthyridine) (1.68 and 1.79 Å).[38] The solid state molecular structures of representative complexes have been presented in figure 6B.6 and 6B.7 respectively.

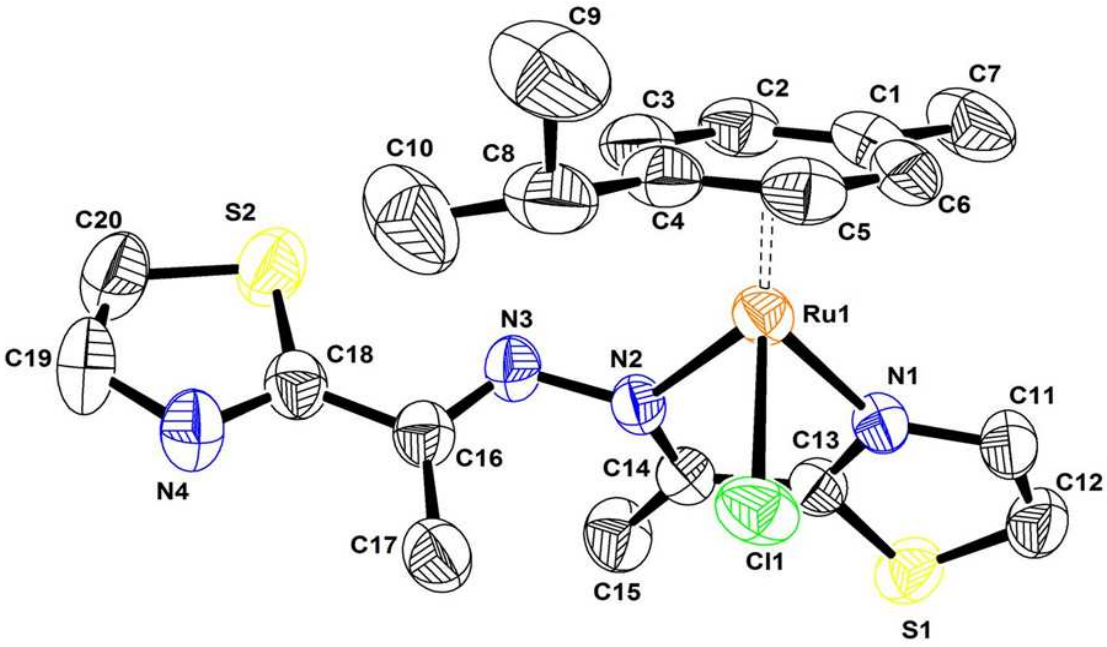

Figure 6B.6: Molecular structure of [(η^6-*p*-^{i}PrC_6H_4Me)Ru(ata)Cl]PF_6 ([**2**]PF_6) at 50% probability level. Hydrogen atoms and hexafluorophosphate anion have been omitted for clarity

Table 6B.1: Crystallographic and structure refinement parameters for complexes

Complex	[2]PF_6	[9]PF_6
Chemical formula	$C_{20}H_{24}ClF_6N_4PRuS_2$	$C_{15}H_{22}ClF_6N_3PRhS$
Crystal system	Triclinic	Triclinic
Space group	*P*-1	*P*-1
Crystal color and shape	Plates, yellow	Plates, redish yellow
Crystal size	0.45X0.30X0.18	0.36X0.28X0.18
a (Å)	7.8486 (4)	8.2601 (9)
b (Å)	12.9523 (7)	11.6219 (12)
c (Å)	13.4155 (8)	12.1958 (14)
α (°)	99.008 (3)	76.593 (7)°
β (°)	90.073 (3)	77.719 (7)°
γ (°)	98.780 (3)	78.838 (7)°
V ($Å^3$)	1330.74 (13)	1099.9 (2)
Z	2	2
T (K)	296 (2)	296 (2)
D_x (g /cm^3)	1.662	1.690
μ (mm^{-1})	0.97	1.12
Scan range (°)	1.54< θ <28.38	1.74< θ <28.08
Unique reflections	6542	4390
Reflections used [I>2σ(I)]	5109	3402
Rint	0.037	0.043
Final R indices [I>2σ(I)]	0.0406, *w*R_2 0.0943	0.0556, *w*R_2 0.1439
R indices (all data)	0.0563, *w*R_2 0.1013	0.0742, *w*R_2 0.1556
Goodness-of-fit	1.022	1.098
Max, Min Δρ (e $Å^{-3}$)	0.62 -0.62	0.76 -0.72

Table 6B.2: Selected bond lengths (Å) and angles (º) for complexes [**1**]PF_6.and [**9**]PF_6.

[**1**]PF_6	Interatomoic distances	[**9**]PF_6	
Ru-N1	2.087(3)	Rh-N1	2.097(4)
Ru-N2	2.104(2)	Rh-N2	2.136(5)
Ru-Cl1	2.406(8)	Rh-Cl1	2.396(15)
Ru-centroid (arene)	1.692	Rh-centroid (C_5 ring)	1.782
N2-N3	1.398(3)	N2-N3	1.369(6)
N1-C13	1.326(4)	N1-C13	1.318(7)
N2-C14	1.299(4)	N2-C11	1.292(7)
C13-C14	1.439(4)	C11-C13	1.458(8)
	Angles		
N1-Ru-N2	75.58(10)	N2-Rh-N3	75.88 (17)
N1-Ru-Cl1	83.80(7)	N4-Rh-Cl1	84.25(13)
N2-Ru-Cl1	88.24(7)	N3-Rh-Cl1	87.88(13)
Ru1-N2-C14	119.10(2)	Rh1-N1-C13	114.13(4)
Ru1-N1-C13	114.39(2)	Rh1-N2-C11	117.59(4)

Calculated centroid of the C_6 or C_5 coordinated aromatic ring.

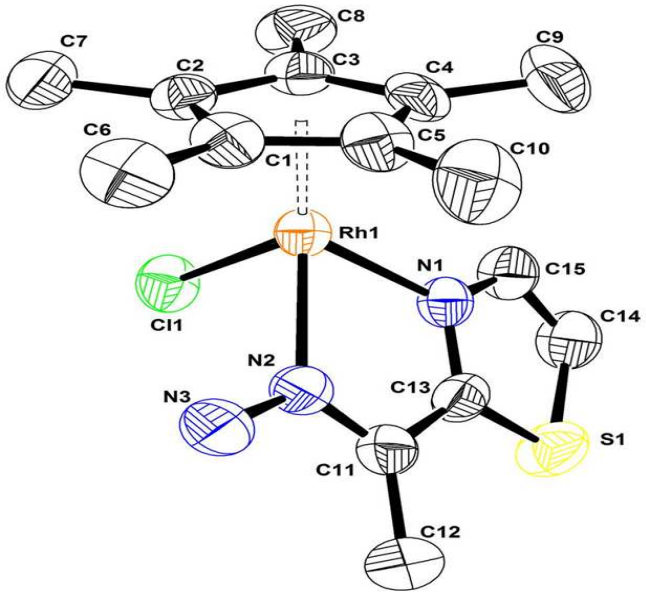

Figure 6B.7: Molecular structure of [Cp*Rh(ata*)Cl]PF_6 [**9**]PF_6 at 50% probability level. Hydrogen atoms and hexafluorophosphate anion have been omitted for clarity

6B.3.4 UV-visible spectroscopy

Electronic absorption spectra of complexes [**1**]PF_6 to [**4**]PF_6 and [**6**]PF_6 and [**7**]PF_6 were acquired in acetonitrile, at 10^{-5} M concentration in the range 250-550 nm and spectral data are summarized in Table 3. The spectra of these complexes are characterized by two main features, *viz*., an intense ligand–localized or intra-ligand $\pi \rightarrow \pi^*$ transition in the ultraviolet region and metal-to-ligand charge transfer (MLCT) $d\pi(M) \rightarrow \pi^*$ (ata - ligand) bands in the visible region.[39] Since the low spin d^6 configuration of the mononuclear complexes provides filled orbitals of proper symmetry at the Ru(II), Rh(III) and Ir(III) centers, these can interact with low lying π^* orbitals of the ligands. All these complexes show an intense band in the region 310-320 nm and a low energy absorption band in the visible region 407 – 425 nm. The high intensity band in UV region is assigned to inter and intra-ligand $\pi - \pi^*$ transitions,[40,41] while the low energy absorption band in the visible region is assigned to metal-to-ligand charge transfer (MLCT) ($t_{2g} - \pi^*$). Electronic Spectra of these complexes are presented in Figure 6B.8.

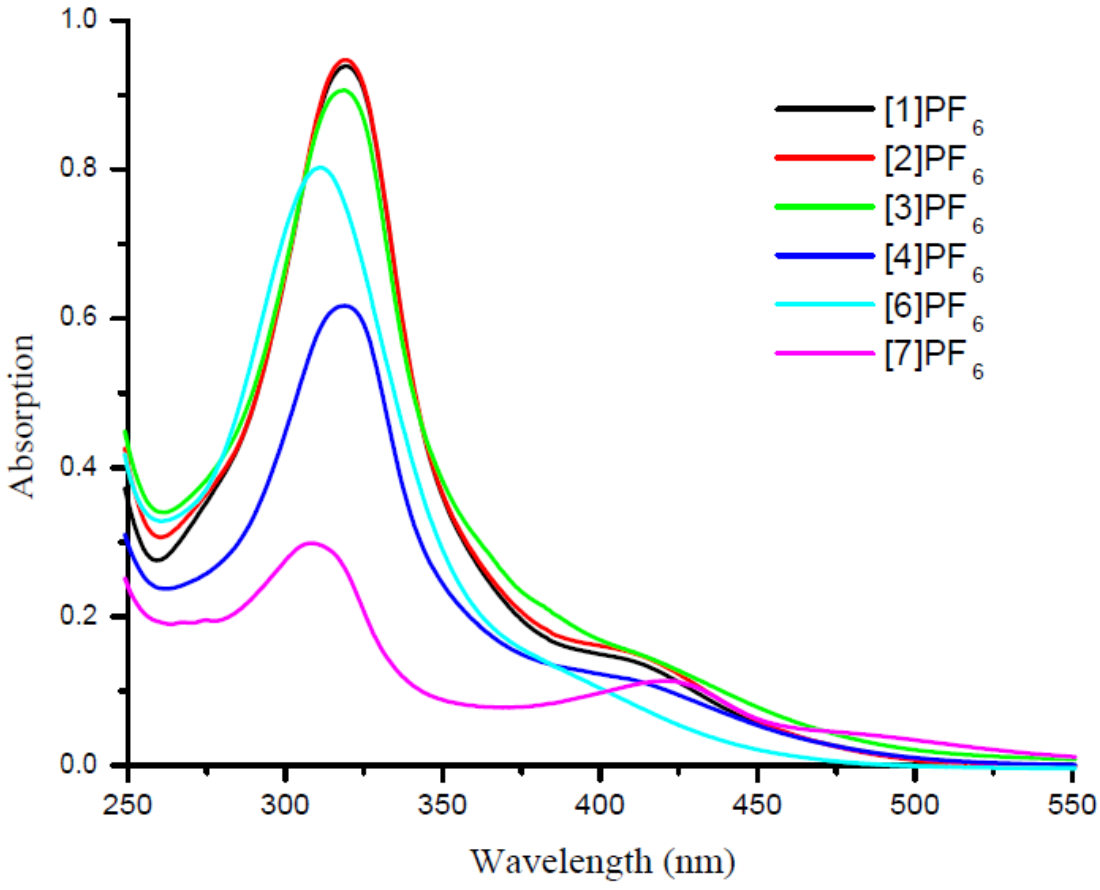

Figure 6B.8: UV-visible electronic spectra of complexes in acetonitrile at 298 K.

Table 6B.3. UV-visible spectral data for selected complexes in acetonitrile at 298 K.

Sl. No.	Complex	λ_{max} (nm) / ε 10^{-5} M^{-1} cm^{-1}
1	$[(\eta^6\text{-}p\text{-}^{i}PrC_6H_4Me)Ru(ata)Cl]^+$	320 (0.93) 412
2	$[(\eta^6\text{-}C_6H_6)Ru(ata)Cl]^+$	319(0.95) 415
3	$[(\eta^6\text{-}C_6Me_6)Ru(ata)Cl]^+$	319 (0.90) 420
4	$[(\eta^5\text{-}C_5Me_5)Rh(ata)Cl]^+$	310 (0.80) 413
6	$[(\eta^5\text{-}C_5H_5)Ru(ata)PPh_3]^+$	320 (0.61) 407
7	$[(\eta^5\text{-}C_5Me_5)Ru(ata)PPh_3]^+$	310 (0.29) 425

6B.4 Conclusions

In summary, in this work ligand *ata* reacted with series of arene and cyclopentadienyl ruthenium, rhodium and iridium complexes giving novel series of mononuclear complexes [**1**]PF_6 to [**8**] PF_6 in good yield, which are remarkably stable in air as well as in solution. In all these complexes, the metal is bonded with the major coordinated sites N1 and N2 and not with the other possible coordinated sites N1 and S1, where as our effort to make binuclear complexes by using other binding sites i.e., N3 and N4 or N3 and S2 was not fruitful.

6B.5 Supplementary material

CCDC-727807 [**2**]PF_6 and CCDC-727808 [**9**]PF_6 contain the supplementary crystallographic data for this chapter.

References

1 M. Calligaris and L. Randaccio, in Comprehensive Coordination Chemistry, ed. G. Wilkinson, R. D. Gillard and J. A. McCleverty, Pergamon Press, Oxford, 1987, p. 715.

2 Y. -G. Li, D. -H. Shi, H. -L. Zhu, H. Yan and S. W. Ng, Inorg. Chim. Acta, 2007, 360, 2881.

3 I. Rousso, N. Friedman, M. Sheves and M. Ottolenghi, Biochemistry, 1995, 34, 12059.

4 T. Baasov and M. Sheves, Biochemistry, 1986, 25, 5249.

5 A. J. Davenport, D. L. Davis, J. Fawcett, S. A. Garratt, D. R. Russell, J. Chem. Soc., Dalton Trans. (2000) 4432.

6 J. W. Faller, J. Parr, Organometallics 19 (2000) 1829.

7 H. Chen, J. A. Parkinson, S. Parsons, R.A. Coxall, R.O. Gould, P.J. Sadler, J. Am. Chem. Soc. 124 (2002) 3064.

8 H. Chen, P. J. Sadler, D. I. Jodrell, Brit. J. Cancer 86 (2002) 1652.

9 I. Ojima, Catalytic Asymetric Syntheses, VCH Publishers, New York, 1993.

10 D. M. Boghaei and S. Mohebi, Tetrahedron, 58 (2002) 5357.

11 C. R. K. Rao, H. Aneetha, B. Srinivas, P. S. Zacharias and A. Ramachandraiah, Polyhedron, 13 (1994) 2659.

12 B. De Clercq, F. Verpoort, Macromolecules 35 (2002) 8943.

13 T. Opstal, F. Verpoort, Angew. Chem., Int. Ed. 42 (2003) 2876.

14 T. Opstal, F. Verpoort, Synlett 6 (2002) 935.

15 S. N. Pal, S. Pal, Inorg. Chem. 40 (2001) 4807.

16 B. De Clercq, F. Verpoort, Adv. Synth. Catal. 34 (2002) 639.

17 B. De Clercq, F. Lefebvre, F. Verpoort, Appl. Catal. A 247 (2003) 345.

18 N. T. S. Phan, D. H. Brown, H. Adams, S. E. Spey and P. Styring, Dalton Trans., (2004) 1348.

19 P. Styring, C. Grindon and C. M. Fisher, Catal. Lett., 77 (2001) 219.

20 L. Rigamonti, F. Demartin, A. Forni, S. Righetto and A. Pasini, Inorg. Chem. 45 (2006) 10976.

21 J. Gradinaru, A. Forni, V. Druta, F. Tessore, S. Zecchin, S. Quici and N. Garbalau, Inorg. Chem. 46 (2007) 884.

22 K. C. Gupta, A. K. Sutar, Coord. Chem. Rev. 252 (2008) 1420.

23 P. A. Vigato and S. Tamburini, Coord. Chem. Rev., 248, (2004) 1717.

24 S. K. Singh, M. Chandra, D. S. Pandey, M. C. Puerta, P. Valerga, J. Organomet. Chem. 689 (2004) 3612.

25 B. Mondal, V. G. Puranik, and G.K. Lahiri, Inorg. Chem. 41 (2002) 5831.

26 E. C. Constable. Coord. Chem. Rev., 93 (1989) 205.

27 T. Yamamoto, Z. Zhou, T. Kanbara, M. Shimura, K. Kizu, T. Maruyama, T. Takamura, T. Fukuida, B. Lee, N. Ooba, S. Tomaru, T. Kurihara, T. Kaino, K. Kubota, S. Sasaki. J. Am. Chem. Soc. 118 (1996) 10389.

28 M. Calligaris, L. Randaccio, Schiff Bases as Acyclic Polydentate Ligands in Comprehensive Coordination Chemistry; G. Wilkinson, R. D. Gillard, J. A. McCleverty, Eds.; Pergamon Press: New York, 2 (1987) 715.

29 P. A. Vigato, S. Tanburini, Coord. Chem. Rev. 248 (2004) 1717.

30 R. H. -Molina, A. Mederos, Acyclic and Macrocyclic Schiff Base Ligands in Comprehensive Coordination Chemistry II; J. A. McCleverty, T. J. Meyer, Eds.; Pergamon Press: New York, 2 (2004) 411.

31 D. L. Davies, J. Fawcett, R. Krafczyk, D. R. Russell, K. Singh, Dalton Trans. (1998) 2349.

32 D. L. Davies, O. A.-Duaij, J. Fawcett, M. Giardiello, S. T. Hilton, D. R. Russell, Dalton Trans. (2003) 4132.

33 R. Lalrempuia, K. M. Rao, P. J. Carroll, Polyhedron 22 (2003) 605.

34 D.L. Davies, J. Fawcett, R. Krafczyk, D. R. Russell, J. Organomet. Chem. 545-546 (1997) 581.

35 P. Govindaswamy, Y. A. Mozharivskyj, K. M. Rao, Polyhedron, 24 (2005) 1710.

36 A. Singh, M. Chandra, A. N. Sahay, D. S. Pandey, K. K. Pandey, S. M. Mobin, M. C. Puerta, P. Valerga. J. Organomet. Chem. 689 (2004) 1821.

37 K. S. Singh, Y. A. Mozharivskyj, C. ThÖne, K. M. Rao, J. Organomet. Chem. 690 (2005) 3720.

38 K. T. Prasad, B. Therrien, K. M. Rao, J. Organomet. Chem. 693 (2008) 3049.

39 E. Binamira-Soriaga, N. L. Keder, W. C. Kaska, Inorg. Chem. 29 (1990) 3167.

40 C.S. Arau´ jo, M. G. B. Drew, V. Fe´lix, L. Jack, J. Madureira, M.Newell, S. Roche, T.M. Santos, J.A. Thomas, L. Yellowlees, Inorg. Chem. 41 (2002) 2250.

41 H. Deng, J. Li, K. C. Zheng, Y. Yang, H. Chao, L. N. Ji, Inorg. Chim. Acta 358 (2005) 3430.

Chapter 7

Syntheses and characterization of mono and dinuclear complexes of platinum group metals bearing benzene-linked bis(pyrazolyl)methane ligands

---

In this chapter, we have synthesized homogeneous and immobilized half-sandwich rhodium, iridium and ruthenium complexes bearing bis(pyrazolyl)methanes bridged by benzene-linker, as bidentate or tetradentate bridging ligands (L). The Cp* rhodium and iridium complexes with ligands L give both mono and dinuclear complexes, while only dinuclear complexes are obtained with arene ruthenium complexes.

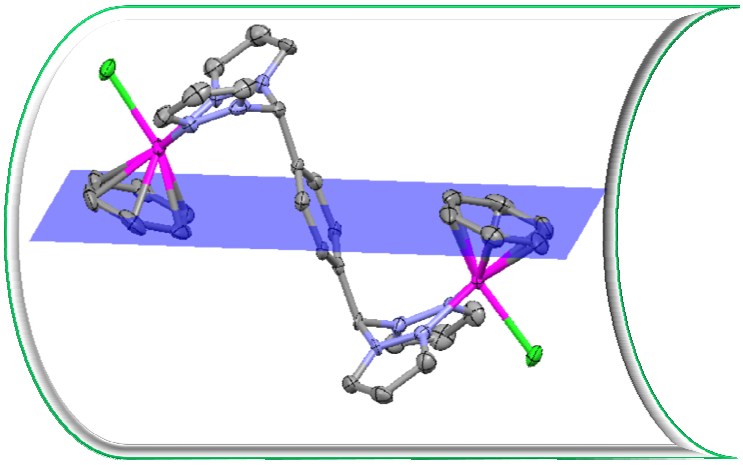

---

*The work presented in this chapter has been published: K. T. Prasad, B. Therrien and K. Mohan Rao, J. Organomet. Chem. 695 (2010) XXXX.

7.1 Introduction

The coordination chemistry of poly(pyrazolyl)borate and methane ligands has revealed an impressive number of compounds with interesting structural, catalytic, and electronic properties.[1-6] The chemistry of poly(pyrazolyl)methane ligands is less extensive than that of their borate analogues due to the fact that convenient synthetic routes of functionalized neutral methane species have only recently been developed.[7-10] By functionalizing the pyrazolyl groups in the original poly(pyrazolyl)borate and -methane compounds, a multitude of "second-generation" ligands have been prepared.[1-6] More recently, functionalization of the borate or methane backbone has yielded a variety of "third-generation" ligands[11] as bis- and tris(pyrazolyl)methane compounds where two or more of the methane units are linked through organic spacers of varying degrees of flexibility, resulting in multitopic ligands.

The chemistry of "second generation" bis(pyrazolyl)methane complexes of rhodium, iridium and ruthenium is relatively less studied as compared to borate complexes of rhodium and iridium.[11-13] Indeed, the chemistry of arene ruthenium and pentamethylcyclopentadienyl (Cp*) rhodium and iridium complexes of bis(pyrazolyl)-methane ligands bridged by a benzene-linker (third-generation) has yet to be explored. Arene ruthenium, rhodium and iridium complexes of bis(pyrazolyl)methanes have attracted attention due to their catalytic ability in reactions such as the alcoholysis of ketones and silanes, hydroformylation and hydroaminomethylation of alkenes and hydroamination.[14-16] Besides these, nitrogen donor ligands with platinum group metals have been shown to be effective catalysts for oxidation reactions[17] and for ring-opening metathesis polymerization[18] and recent studies of arene ruthenium complexes have shown that they are found to inhibit cancer cell growth.[19,20]

In recent years, we have been carrying out arene ruthenium and Cp* rhodium and iridium complexation reactions with a variety of nitrogen-based ligands[21-27] including pyrazolyl-pyrimidine, pyrazolyl-pyridazine and pyridyl-pyridazine ligands. All of these ligands after coordination with metal have given five membered chelating complexes; this is the first time that isolated six membered chelating complexes with 1,4-bis{bis(pyrazolyl)-methyl}benzene (L1) or 1,4-bis{bis(3-methylpyrazolyl)methyl}benz-ene (L2) (Chart 7.1) ligands have been isolated with these metal complexes.

In the present chapter, we have synthesized homogeneous and immobilized half-sandwich rhodium, iridium and ruthenium complexes bearing bis(pyrazolyl)methanes

bridged by benzene-linker, as bidentate or tetradentate bridging ligands (L). The Cp* rhodium and iridium complexes with ligands L give both mono and dinuclear complexes, while only dinuclear complexes are obtained with arene ruthenium complexes. All these complexes are characterized by IR, NMR, mass spectrometry and UV/Visible spectroscopy. The molecular structures of three representative complexes are presented as well.

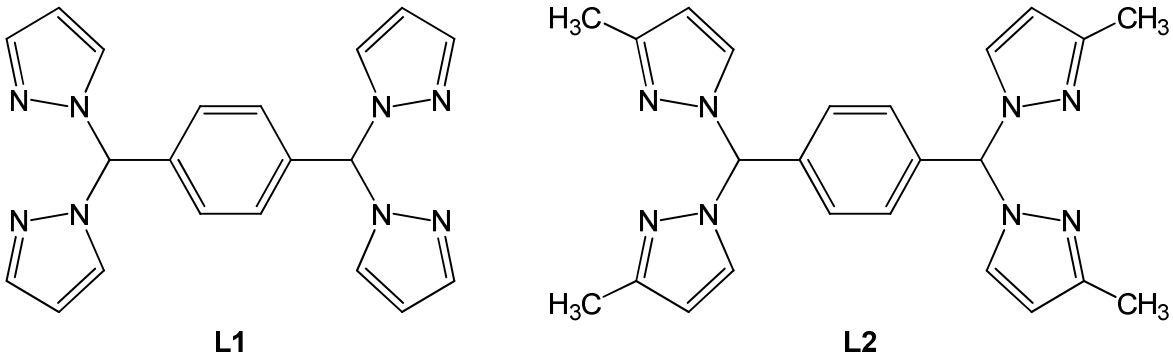

Chart 7.1: Ligands used in present study

7.2 Experimental

7.2.1 General procedure for the syntheses of ligands **L1** and **L2**

Sodium hydride (4.29 g, 0.179 mol) was suspended in 200 ml of THF and cooled in an ice-water bath for 30 min. Pyrazole (12.2 g, 0.179 mol) was added over 15 min, and the resulting solution was stirred at 0 °C for 30 min. Thionyl chloride (6.53 ml, 89.4 mmol) was added dropwise over 10 min at 0 °C, and the resulting pale yellow suspension was allowed to reach room temperature while stirring for 40 min. Terephthaldicarboxaldehyde (3.00 g, 22.4 mmol) and anhydrous cobalt chloride (0.29 g, 2.24 mmol) were added to this suspension at once, and the system was heated at reflux for 24 h. After cooling to room temperature, 160 ml of water was added and the system stirred for 30 min. The organic and aqueous layers were separated, and the aqueous layer was extracted with CH_2Cl_2 (2 - 100 ml). The combined organic extracts were washed with water (100 mL), dried over MgSO4, and stripped, leaving a pale yellow solid that was recrystallized from absolute ethanol to afford 7.33 g (89%) of **L1** that was pure by melting point (166-168 °C) and by NMR. Similar procedure was applied for the preparation of L2.

7.2.2 General procedure for the syntheses of the mononuclear complexes **1** to **4**

A mixture of $[(\eta^5\text{-}C_5Me_5)M(\mu\text{-}Cl)Cl]_2$ (M = Rh, Ir) (0.08 mmol), ligand L (L1 or L2) (0.17 mmol) and 2.5 equivalents of NH_4PF_6 in dry methanol (20 ml) was refluxed at 50°C for 6 to 8 hours, after which an orange precipitate was observed. The precipitate was separated by filtration, washed with cold methanol, diethyl ether and dried *in vacuo*.

7.2.2.1 $[(\eta^5\text{-}C_5Me_5)Rh(L1)Cl]PF_6$ ($[\mathbf{1}]PF_6$)

Yield: 90 mg (72%). ^{1}H NMR (400 MHz, CD_3CN) δ = 8.29 (s, 1H, $CH(pz)_2$), 8.05 (d, 2H, *J* = 1.80 Hz, pz-5H), 7.91 (d, 2H, *J* = 2.40 Hz, pz-3H), 7.78 (s, 1H, $CH(pz)_2$), 7.64 (d, 2H, *J* = 1.2 Hz, pz-5H), 7.58 (d, 2H, *J* = 2.40 Hz, pz-3H), 7.05 (d, 2H, *J* = 7.2 Hz, C_6H_4), 6.75 (d, 2H, *J* = 6.8 Hz, C_6H_4), 6.41-6.38 (m, 4H, pz-4H), 1.54 (s, 15H, C_5Me_5); IR (KBr, cm^{-1}): 3441(w), 3134(m), 1629(m), 1447(m), 1399(m), 1296(m), 1103(m), 845(s), 760(m), 558(m); ESI-MS: 643.8 [M^+], 608.5 [M - Cl]; UV–Vis {acetonitrile, λ_{max} nm (ε $10^{-5}\cdot M^{-1}\cdot cm^{-1}$)}: 223 (0.59), 341 (0.04); Anal. Calc. for $C_{30}H_{33}F_6N_8PRhCl$ (788.9): C, 45.67; H, 4.22; N 14.20. Found: C, 45.53; H, 4.23; N, 14.13%.

7.2.2.2 $[(\eta^5\text{-}C_5Me_5)Rh(L2)Cl]PF_6$ ($[\mathbf{2}]PF_6$)

Yield 99 mg (74%). ^{1}H NMR (400 MHz, CD_3CN) δ = 8.31 (s, 1H, $CH(pz)_2$), 8.01 (d, 2H, *J* = 1.80 Hz, pz-5H), 7.81 (s, 1H, $CH(pz)_2$), 7.62 (d, 2H, *J* = 1.2 Hz, pz-5H), 7.07 (d, 2H, *J* = 7.2 Hz, C_6H_4), 6.76 (d, 2H, *J* = 6.8 Hz, C_6H_4), 6.41-6.37 (m, 4H, pz-4H), 2.61 (bs, 6H, Pz-3Me), 2.38 (bs, 6H, Pz-3Me), 1.58 (s, 15H, C_5Me_5); IR (KBr, cm^{-1}): 3441(w), 3134(m), 1629(m), 1447(m), 1399(m), 1296(m), 1103(m), 845(s), 760(m), 558(m); ESI-MS: 700.6 [M^+], 675.6 [M - Cl]; UV–Vis {acetonitrile, λ_{max} nm (ε $10^{-5}\cdot M^{-1}\cdot cm^{-1}$)}: 229 (0.43), 394 (0.22); Anal. Calc. for $C_{34}H_{41}F_6RhN_8PCl$ (845.6): C, 48.32; H, 4.89; N, 13.26. Found: C, 48.23; H, 4.91; N, 13.18%.

7.2.2.3 $[(\eta^5\text{-}C_5Me_5)Ir(L1)Cl]PF_6$ ($[\mathbf{3}]PF_6$)

Yield: 90 mg (64%). ^{1}H NMR (400 MHz, CD_3CN) δ = 8.26 (s, 1H, $CH(pz)_2$), 7.99 (d, 2H, *J* = 1.80 Hz, pz-5H), 7.87 (d, 2H, *J* = 2.40 Hz, pz-3H), 7.78 (s, 1H, $CH(pz)_2$), 7.61 (d, 2H, *J* = 1.2 Hz, pz-5H), 7.50 (d, 2H, *J* = 2.40 Hz, pz-3H), 7.05 (d, 2H, *J* = 7.2 Hz, C_6H_4), 6.75 (d, 2H, *J* = 6.8 Hz, C_6H_4), 6.39-6.36 (m, 4H, pz-4H), 1.52 (s, 15H, C_5Me_5); IR (KBr, cm^{-1}): 3448(w), 3134(m), 1627(m), 1446(m), 1399(m), 1296(m), 1103(m), 843(s), 760(m), 558(m); ESI-MS: 733.3 [M^+], 698.1 [M - Cl]; UV–Vis {acetonitrile, λ_{max}

nm (ε $10^{-5}\cdot M^{-1}\cdot cm^{-1}$)}: 225(0.73), 352 (0.038); Anal. Calc. for $C_{30}H_{33}F_6N_8PIrCl$ (878.5): C, 41.03; H, 3.79; N, 12.76. Found: C, 43.93; H, 3.73; N, 12.65%.

*7.2.2.4 [(η^5-C_5Me_5)Ir(L2)Cl]PF_6 ([**4**]PF_6)*

Yield 89 mg (60%). ^{1}H NMR (400 MHz, CD_3CN) δ = 8.27 (s, 1H, $CH(pz)_2$), 8.02 (d, 2H, *J* = 1.80 Hz, pz-5H), 7.76 (s, 1H, $CH(pz)_2$), 7.62 (d, 2H, *J* = 1.2 Hz, pz-5H), 7.09 (d, 2H, *J* = 7.2 Hz. C_6H_4), 6.78 (d, 2H, *J* = 6.8 Hz, C_6H_4), 6.42-6.36 (m, 4H, pz-4H), 2.63 (s, 6H, Pz-3Me), 2.37 (s, 6H, Me_3-Pz), 1.55 (s, 15H, C_5Me_5); IR (KBr, cm^{-1}): 3441(w), 3134(m), 1629(m), 1447(m), 1399(m), 1296(m), 1103(m), 845(s), 760(m), 558(m); ESI-MS: 789.4 [M^+], 754.2 [M - Cl]; UV–Vis {acetonitrile, λ_{max} nm (ε $10^{-5}\cdot M^{-1}\cdot cm^{-1}$)}: 228 (0.51), 485 (0.02); Anal. Calc. for $C_{34}H_{41}F_6IrN_8PCl$ (934.8): C, 43.70; H, 4.42; N, 11.99. Found: C, 43.67; H, 4.49; N, 11.86%.

7.2.3 General procedure for the syntheses of the dinuclear complexes **5** to **8**

A mixture of $[(Cp^*)M(\mu\text{-}Cl)Cl]_2$ (M = Rh, Ir) (0.08 mmol), ligand L (L1 or L2) (0.08 mmol) and 2.5 equivalents of NH_4PF_6 in dry methanol (20 ml) was refluxed at 50^{o}C for 12 hours, after which a dark orange precipitate was formed. The precipitate was separated by filtration, washed with cold methanol, diethyl ether and dried *in vacuo*.

*7.2.3.1 [{(η^5-C_5Me_5)RhCl}$_2$(μ-L1)]$(PF_6)_2$ ([**5**]$(PF_6)_2$)*

Yield 80 mg (84%). ^{1}H NMR (400 MHz, CD_3CN) δ = 8.31 (s, 2H, $CH(pz)_2$), 8.09 (d, 4H, *J* = 1.60 Hz, pz-5H), 7.95 (d, 4H, *J* = 2.11 Hz, pz-3H), 6.76 (s, 4H, C_6H_4), 6.41 (dd, 4H, *J* =1.20 Hz, pz-4H), 1.48 (s, 30H, C_5Me_5); IR (KBr, cm^{-1}): 3446(w), 3134(m), 1629(m), 1446(m), 1401(m), 1295(m), 1103(m), 843(s), 760(m), 555(m); ESI-MS: 1062.6 [M^{2+} + PF_6^-]$^+$; UV–Vis {acetonitrile, λ_{max} nm (ε $10^{-5}\cdot M^{-1}\cdot cm^{-1}$)}: 224 (0.54), 307 (0.05) and 437 (0.01); Anal. Calc. for $C_{40}H_{48}F_{12}N_8P_2Rh_2Cl_2$ (1207.6): C, 39.79; H, 4.01; N, 9.28. Found: C, 39.53; H, 4.06; N, 9.19%.

7.2.3.2 [{(η^5-Cp)RhCl}$_2$(μ-L2)]$(PF_6)_2$ ([**6**]$(PF_6)_2$)*

Yield 80 mg (84%). ^{1}H NMR (400 MHz, CD_3CN) 8.33 (s, 2H, $CH(pz)_2$), 8.07 (d, 4H, *J* = 1.64 Hz, pz-5H), 6.78 (s, 4H, C_6H_4), 6.39 (dd, 4H, *J* =1.20 Hz, pz-4H), 2.76 (s, 12H, pz-3Me), 1.49 (s, 30H, C_5Me_5); IR (KBr, cm^{-1}): 3446(b), 3131(m), 1627(m), 1446(m), 1408(m), 1296(m), 1103(m), 845(s), 761(m), 585(m); ESI-MS: 1118.6 [M^{2+} + PF_6^-]$^+$; UV–Vis {acetonitrile, λ_{max} nm (ε $10^{-5}\cdot M^{-1}\cdot cm^{-1}$)}: 228 (0.59), 310 (0.04) and 430 (0.02);

Anal. Calc. for $C_{44}H_{56}Cl_2F_{12}N_4P_2Rh_2$ (1263.6): C, 41.82; H, 4.47; N, 8.87. Found: C, 41.71; H, 4.55; N, 8.65%.

*7.2.3.3 [{(η^5-C_5Me_5)IrCl}$_2$(μ-L1)](PF$_6$)$_2$ ([**7**](PF$_6$)$_2$)*

Yield 91 mg (77%). ^{1}H NMR (400 MHz, CD_3CN) δ = 8.32 (s, 2H, $CH(pz)_2$), 8.06 (d, 4H, *J* = 1.62 Hz, pz-5H), 8.01 (d, 4H, *J* = 2.16 Hz, pz-3H), 6.78 (s, 4H, C_6H_4), 6.44 (dd, 4H, *J* = 1.22 Hz, pz-4H), 1.51 (s, 30H, C_5Me_5); IR (KBr, cm^{-1}): 3441(b), 3134(m), 1629(m), 1447(m), 1399(m), 1296(m), 1103(m), 845(s), 760(m), 558(m); ESI-MS: 1241.5 [M^{2+}+PF_6^-]$^+$; UV–Vis {acetonitrile, λ_{max} nm (ε $10^{-5}\cdot M^{-1}\cdot cm^{-1}$)}: 225 (0.58), 312 (0.04) and 391 (0.03); Anal. Calc. for $C_{40}H_{48}Cl_2F_{12}Ir_2N_8P_2$ (1386.2): C, 34.66; H, 3.49; N, 8.08. Found: C, 34.42; H, 3.52; N, 8.01%.

*7.2.3.4 [{(η^5-C_5Me_5)IrCl}$_2$(μ-L2)](PF$_6$)$_2$ ([**8**](PF$_6$)$_2$)*

Yield 81 mg (65%). ^{1}H NMR (400 MHz, CD_3CN) δ = 8.33 (s, 2H, $CH(pz)_2$), 8.09 (d, 4H, *J* = 1.60 Hz, pz-5H), 6.74 (s, 4H, C_6H_4), 6.44 (dd, 4H, *J* =1.20 Hz, pz-4H), 2.76-2.80 (s, 12H, pz-3Me), 1.48 (s, 30H, C_5Me_5); IR (KBr, cm^{-1}): 3446(b), 3134(m), 1629(m), 1446(m), 1401(m), 1295(m), 1103(m), 843(s), 760(m), 558(m); ESI-MS: 1297.5 [M^{2+} + PF_6^-]$^+$; UV–Vis {acetonitrile, λ_{max} nm (ε $10^{-5}\cdot M^{-1}\cdot cm^{-1}$)}: 228 (0.71), 316 (0.04) and 397 (0.02); Anal. Calc. for $C_{44}H_{56}Cl_2F_{12}Ir_2N_8P_2$ (1442.2): C, 36.64; H, 3.91; N, 7.77. Found: C, 36.62; H, 3.99; N, 7.65%.

7.2.4 General procedure for the synthesis of the dinuclear complexes **9** to**14**

A mixture of [(η^6-arene)Ru(μ-Cl)Cl]$_2$ (arene = C_6H_6, *p*-^{i}PrC_6H_4Me or C_6Me_6) (0.1 mmol), ligand L (L1 or L2) (0.1 mmol) and 2.5 equivalents of NH_4PF_6 in dry methanol (15 ml) was stirred at room temperature for 10 hours, after which an orange precipitate was observed. The precipitate was filtered, washed with cold methanol, diethyl ether and dried *in vacuo*.

*7.2.4.1 [{(η^6-C_6H_6)RuCl}$_2$(μ-L1)](PF$_6$)$_2$ ([**9**](PF$_6$)$_2$)*

Yield 80 mg (72%). ^{1}H NMR (400 MHz, CD_3CN) δ = 8.26 (s, 2H, $CH(pz)_2$), 8.07 (d, 4H, *J* = 1.40 Hz, pz-5H), 7.95 (d, 4H, *J* = 2.00 Hz, pz-3H), 6.75 (s, 4H, C_6H_4), 6.41 (dd, 4H, *J* = 1.24 Hz, pz-4H), 5.40 (s, 12H, C_6H_6); IR (KBr, cm^{-1}): 3441(b), 3134(m), 1629(m), 1447(m), 1399(m), 1296(m), 1103(m), 845(s), 760(m), 558(m); ESI-MS: 944.8 [M^{2+} + PF_6^-]$^+$; UV–Vis {acetonitrile, λ_{max} nm (ε $10^{-5}\cdot M^{-1}\cdot cm^{-1}$)}: 226 (0.73), 307 (0.05) and 428

(0.01); Anal. Calc. for $C_{32}H_{30}Cl_2F_{12}N_8P_2Ru_2$ (1089.6): C, 35.27; H, 2.78; N, 10.28. Found: C, 35.15; H, 2.81; N, 10.18%.

*7.2.4.2 [{(η^6-C_6H_6)RuCl}$_2$(μ-L2)](PF$_6$)$_2$ ([**10**](PF$_6$)$_2$)*

Yield 76 mg (66%). ^{1}H NMR (400 MHz, CD_3CN) δ = 8.31 (s, 2H, $CH(pz)_2$), 8.07 (d, 4H, *J* = 1.40 Hz, pz-5H), 6.78 (s, 4H, C_6H_4), 6.46 (dd, 4H, *J* = 1.24 Hz, pz-4H), 5.48 (s, 12H, C_6H_6), 2.86 (s, 12H, pz-3Me); IR (KBr, cm^{-1}): 3448(b), 3134(m), 1627(m), 1446(m), 1399(m), 1296(m), 1103(m), 843(s), 760(m), 558(m); ESI-MS: 1000.2 $[M^{2+} + PF_6^-]^+$; UV–Vis {acetonitrile, λ_{max} nm (ε $10^{-5}\cdot M^{-1}\cdot cm^{-1}$)}: 229 (0.65), 316 (0.05) and 430 (0.02); Anal. Calc. for $C_{36}H_{38}Cl_2F_{12}N_8P_2Ru_2$ (1145.7): C, 37.74; H, 3.34; N, 9.78. Found: C, 37.65; H, 3.35; N, 9.65%.

*7.2.4.3 [{(η^6-p-^{i}PrC$_6$H$_4$Me)RuCl}$_2$(μ-L1)](PF$_6$)$_2$ ([**11**](PF$_6$)$_2$)*

Yield 91 mg (81%). ^{1}H NMR (400 MHz, CD_3CN) δ = 8.32 (s, 2H, $CH(pz)_2$), 8.04 (d, 4H, *J* = 1.40 Hz, pz-5H), 7.95 (d, 4H, *J* = 2.04 Hz, pz-3H), 6.76 (s, 4H, C_6H_4), 6.41 (dd, 4H, *J* = 1.28 Hz, pz-4H), 5.57 (d, 4H, *J* = 5.60 Hz, $Ar_{p\text{-}cy}$), 5.38 (d, 4H, *J* = 5.80 Hz, $Ar_{p\text{-}cy}$), 2.84 (sept, 2H, $CH(CH_3)_2$), 2.17 (s, 6H, $Ar_{p\text{-}cy}$-Me), 1.25 (d, 6H, $CH(CH_3)_2$); 1.21 (d, 6H, $CH(CH_3)_2$); IR (KBr, cm^{-1}): 3441(b), 3134(m), 1629(m), 1447(m), 1399(m), 1296(m), 1103(m), 845(s), 760(m), 558(m); ESI-MS: 1056.2 $[M^{2+} + PF_6^-]^+$; UV–Vis {acetonitrile, λ_{max} nm (ε $10^{-5}\cdot M^{-1}\cdot cm^{-1}$)}: 224 (0.65), 316 (0.05) and 431 (0.02); Anal. Calc. for $C_{40}H_{46}Cl_2F_{12}N_8P_2Ru_2$ (1201.8): C, 39.97; H, 3.86; N, 9.32. Found: C, 39.78; H, 3.97; N, 9.27%.

*7.2.4.4 [{(η^6-p-^{i}PrC$_6$H$_4$Me)RuCl}$_2$(μ-L2)](PF$_6$)$_2$ ([**12**](PF$_6$)$_2$)*

Yield 79 mg (63%). ^{1}H NMR (400 MHz, CD_3CN) δ = 8.34 (s, 2H, $CH(pz)_2$), 8.03 (d, 4H, *J* = 1.40 Hz, pz-5H), 6.76 (s, 4H, C_6H_4), 6.41 (d, 4H, *J* = 3.20 Hz, pz-4H), 5.55 (d, 4H, *J* = 5.60 Hz, $Ar_{p\text{-}cy}$), 5.39 (d, 4H, *J* = 5.80 Hz, $Ar_{p\text{-}cy}$), 2.87 (s, 12H, pz-3Me), 2.79 (sept, 2H, $CH(CH_3)_2$), 2.16 (s, 6H, $Ar_{p\text{-}cy}$-Me), 1.26 (d, 6H, $CH(CH_3)_2$); 1.21 (d, 6H, $CH(CH_3)_2$); IR (KBr, cm^{-1}): 3446(b), 3134(m), 1627(m), 1448(m), 1399(m), 1296(m), 1105(m), 843(s), 762(m), 558(m); ESI-MS: 1112.2 $[M^{2+} + PF_6^-]^+$; UV–Vis {acetonitrile, λ_{max} nm (ε $10^{-5}\cdot M^{-1}\cdot cm^{-1}$)}: 229 (0.56), 307 (0.05) and 437 (0.02); Anal. Calc. for $C_{44}H_{54}Cl_2F_{12}N_4P_2Ru_2$ (1257.9): C, 42.01; H, 4.33; N, 8.91. Found: C, 41.93; H, 4.36; N, 8.87%.

*7.2.4.5 [{(η^6-C_6Me_6)RuCl}$_2$(μ-L1)](PF$_6$)$_2$ ([**13**](PF$_6$)$_2$)*

Yield 101 mg (80%). ^{1}H NMR (400 MHz, CD_3CN) δ = 8.35 (s, 2H, $CH(pz)_2$), 8.07 (d, 4H, *J* = 1.40 Hz, pz-5H), 7.97 (d, 4H, *J* = 2.00 Hz, pz-3H), 6.75 (s, 4H, C_6H_4), 6.44 (dd, 4H, *J* = 1.24 Hz, pz-4H), 2.28 (s, 36H, C_6Me_6); IR (KBr, cm^{-1}): 3441(b), 3134(m), 1629(m), 1447(m), 1399(m), 1296(m), 1103(m), 845(s), 760(m), 558(m); ESI-MS: 1112.8 [M^{2+} + PF_6^-]$^+$; UV–Vis {acetonitrile, λ_{max} nm (ε $10^{-5}\cdot M^{-1}\cdot cm^{-1}$)}: 228 (0.68), 312 (0.05) and 427 (0.02); Anal. Calc. for $C_{44}H_{54}Cl_2F_{12}N_8P_2Ru_2$ (1257.9): C, 42.01; H, 4.33; N, 8.91. Found: C, 42.05; H, 4.41; N, 8.88%.

*7.2.4.6 [{(η^6-C_6Me_6)RuCl}$_2$(μ-L2)](PF$_6$)$_2$ ([**14**](PF$_6$)$_2$)*

Yield 86 mg (65%). ^{1}H NMR (400 MHz, CD_3CN) δ = 8.36 (s, 2H, $CH(pz)_2$), 8.07 (d, 4H, *J* = 1.40 Hz, pz-5H), 6.78 (s, 4H, C_6H_4), 6.46 (d, 4H, *J*= 2.24 Hz, pz-4H), 2.85 (s, 12H, pz-3Me), 2.26 (s, 36H, C_6Me_6); IR (KBr, cm^{-1}): 3446(b), 3135(m), 1626(m), 1446(m), 1402(m), 1296(m), 1103(m), 844(s), 760(m), 558(m); ESI-MS: 1169.8 [M^{2+} + PF_6^-]$^+$; UV–Vis {acetonitrile, λ_{max} nm (ε $10^{-5}\cdot M^{-1}\cdot cm^{-1}$)}: 229 (0.71), 317 (0.04) and 397 (0.03); Anal. Calc. for $C_{48}H_{62}Cl_2F_{12}N_8P_2Ru_2$ (1314.1): C, 43.87; H, 4.76; N, 8.53. Found: C, 43.75; H, 4.75; N, 8.52%.

7.2.5 Single crystal X-ray structure analyses

In [**7**](PF$_6$)$_2$·2 CH_3CN, the residual electron densities greater than 1 eÅ^{-3} are all located at less than 1 Å from the iridium atoms. Crystallographic details are summarized in Table 7.1 and selected bond lengths and angles are presented in Table 7.2. Figures 7.6 to 7.8 were drawn with ORTEP–32

7.3 Results and discussion

7.3.1 Synthesis of the mononuclear complexes **1** to **4** as hexafluorophosphate salts

The mononuclear cationic pentamethylcyclopentadienyl rhodium and iridium complexes having 1,4-bis{bis(pyrazolyl)-methyl}benzene (L1) and 1,4-bis{bis(3-methylpyrazolyl)methyl}benzene (L2) ligands *viz*., [(η^5-C_5Me_5)RhCl(L)]$^+$ {L = L1 (**1**), L2 (**2**)}, [(η^5-C_5Me_5)IrCl(L)]$^+$ {L = L1 (**3**), L2 (**4**)} (Scheme 7.1), have been prepared by the reaction of pentamethylcyclopentadienyl complexes [(η^5-C_5Me_5)M(μ-Cl)Cl]$_2$ (M = Rh, Ir) with two equivalents of ligands L1 or L2 in methanol. These complexes are isolated as their hexafluorophosphate salts and complexes **1** to **4** are orange/red, non-

hygroscopic, and air-stable, shiny crystalline solids. They are sparingly soluble in methanol, dichloromethane, chloroform and acetone, but well soluble in acetonitrile and dimethylsulphoxide.

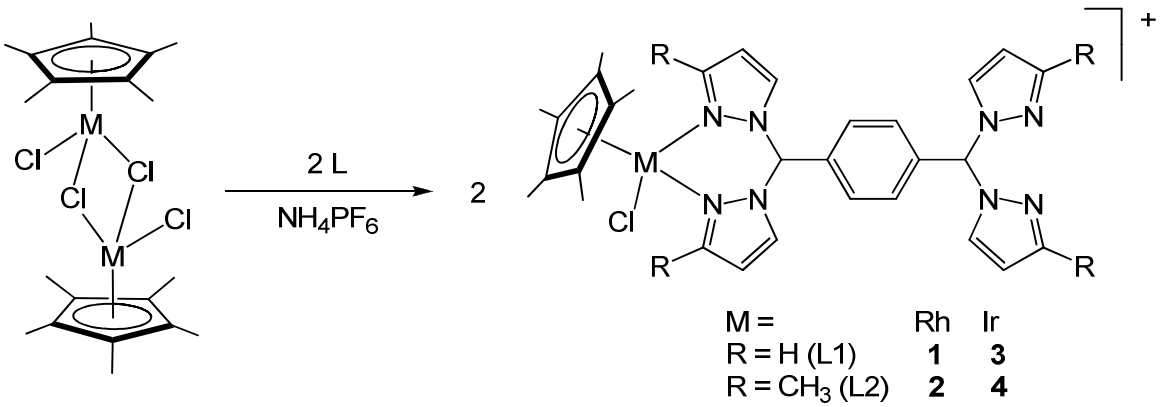

Scheme 7.1

7.3.2 Characterization of the mononuclear complexes **1** to **4**

All these mononuclear complexes were characterized by IR, ^{1}H NMR, mass and elemental analysis. The infrared spectra of the complexes **1** – **4** exhibit a strong band in the region 844-850 cm^{-1} for a typical $\nu_{P\text{-}F}$ stretching band and a medium band in the region 555-558 cm^{-1} $\delta_{P\text{-}F}$ for the PF_6 anion. Moreover, all complexes show absorption bands around 1620-1631, 1446-1458, 1270-1296 and 1103-1058 cm^{-1} corresponding to $\nu_{C=N}$ vibrations of pyrazoles.[29,30] Besides these absorptions, two absorption bands at 2990-3050 cm^{-1} and 3400-3450 cm^{-1} were also observed for N-H vibrations. The mass spectra of these complexes **1**-**4** exhibit the corresponding molecular ion peaks at *m/z* = 643, 700, 733 and 789. For instance the mass spectra of the complexes **1** and **3** were presented in figure 7.1 and 7.2 respectively.

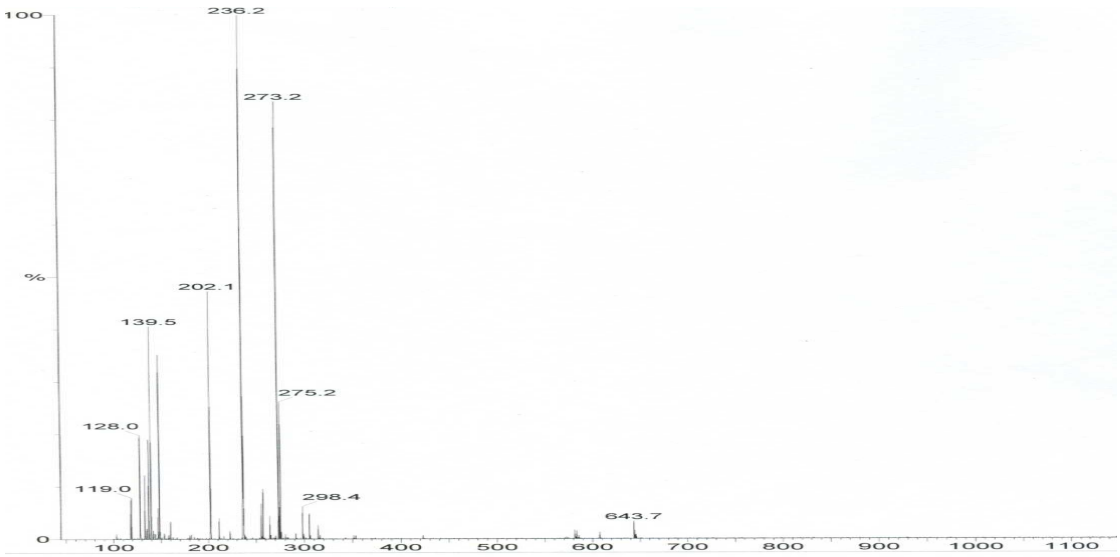

Figure 7.1: Mass spectrum of complex $[(\eta^5\text{-}C_5Me_5)Rh(L1)Cl]PF_6$ ([**1**]PF_6)

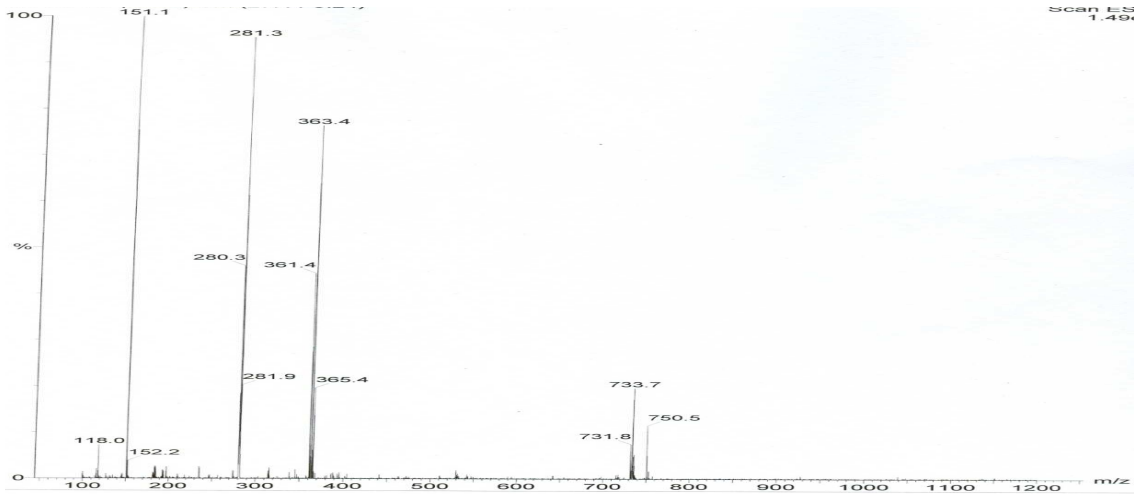

Figure 7.2: Mass spectrum of complex $[(\eta^5\text{-}C_5Me_5)Ir(L1)Cl]PF_6$ ([**3**]PF_6)

The ^{1}H NMR spectra of free ligand (L1 or L2) exhibit a characteristic set of five resonances for the pyrazole, methyl and benzene ring protons. Upon coordination with the metal atom, the mononuclear cationic complexes **1** to **4** show ten distinct resonances assignable to pyrazole or methyl-pyrazole and benzene ring protons of the (L1 or L2) ligand indicating formation of mononuclear complexes. The methylic proton {-C***H***$(Pz)_2$-} of ligand has shown two singlets at δ= 8.29 and 7.78 corresponding to coordinated and uncoordinated to the metal complex indicating formation of mono nuclear compounds. Besides these resonances complexes **1** to **4** exhibit a singlet at $\delta \approx 1.5$ for the protons of the pentamethylcyclopentadienyl ligand.

7.3.3 Synthesis of dinuclear complexes **5** to **14** as hexafluorophosphate salts

The reaction of the chloro bridged dinuclear complexes $[(\eta^5\text{-}C_5Me_5)M(\mu\text{-}Cl)Cl]_2$ (M = Rh, Ir); $[(\eta^6\text{-arene})Ru(\mu\text{-}Cl)Cl]_2$ (arene = C_6H_6, *p*-$^{i}PrC_6H_4Me$ and C_6Me_6) with 1 equiv. of 1,4-bis{bis(pyrazolyl)-methyl}benzene (L1) or 1,4-bis{bis(3-methylpyrazolyl)-methyl}benzene (L2) in methanol results in the formation of orange, air-stable, dinuclear dicationic complexes $[\{(\eta^5\text{-}C_5Me_5)RhCl\}_2(\mu\text{-}L)]^{2+}$ {L = L1 (**5**); Lp2 (**6**)}, $[\{(\eta^5\text{-}C_5Me_5)IrCl\}_2(\mu\text{-}L)]^{2+}$ {L = L1 (**7**); L2 (**8**)}, $[\{(\eta^6\text{-}C_6H_6)RuCl\}_2(\mu\text{-}L)]^{2+}$ {L=L1 (**9**); L2 (**10**)}, $[\{(\eta^6\text{-}p\text{-}^{i}PrC_6H_4Me)RuCl\}_2(\mu\text{-}L)]^{2+}$ {L = L1 (**11**); L2 (**12**)} and $[\{(\eta^6\text{-}C_6H_6)RuCl\}_2(\mu\text{-}L)]^{2+}$ {L = L1 (**13**); L2 (**14**)}. All complexes are isolated as their hexafluorophosphate salts (Scheme 7.2) and they are characterized by IR, mass, ^{1}H NMR spectrometry, UV-visible spectroscopy, and elemental analysis.

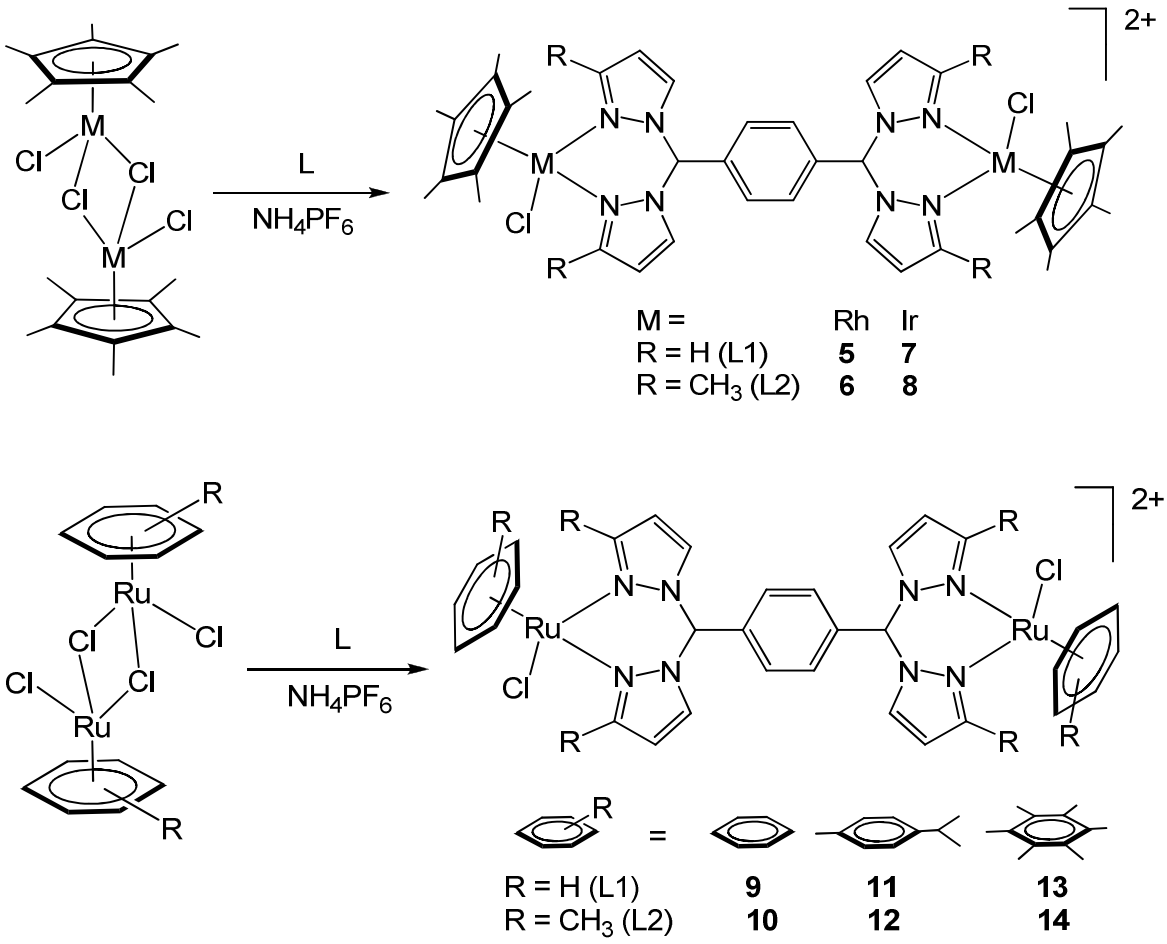

Scheme 7.2

7.3.4 Characterization of the dinuclear complexes **5** to **14**

Infrared spectra of the dinuclear complexes **5** to **14** show a similar trend as the mononuclear cationic complexes **1** to **4**. The mass spectra of the complexes **5** to **14** give rise to two main peaks; a minor peak with an approximately 50% intensity attributed to $[M^{2+} + PF_6^-]^+$ at m/z 1062, 1118, 1241, 1297, 944, 1000, 1056, 1112, 1112 and 1169, respectively, and a major peak, which corresponds to loss of $[(Cp^*/arene)MCl]^+$ fragment and the formation of mononuclear cations **1** to **6** at m/z = 643, 700, 733, 789, 585, 641, 641, 697, 669 and 725, respectively. For instance the mass spectrum of the complex 6 is presented in figure 7.3.

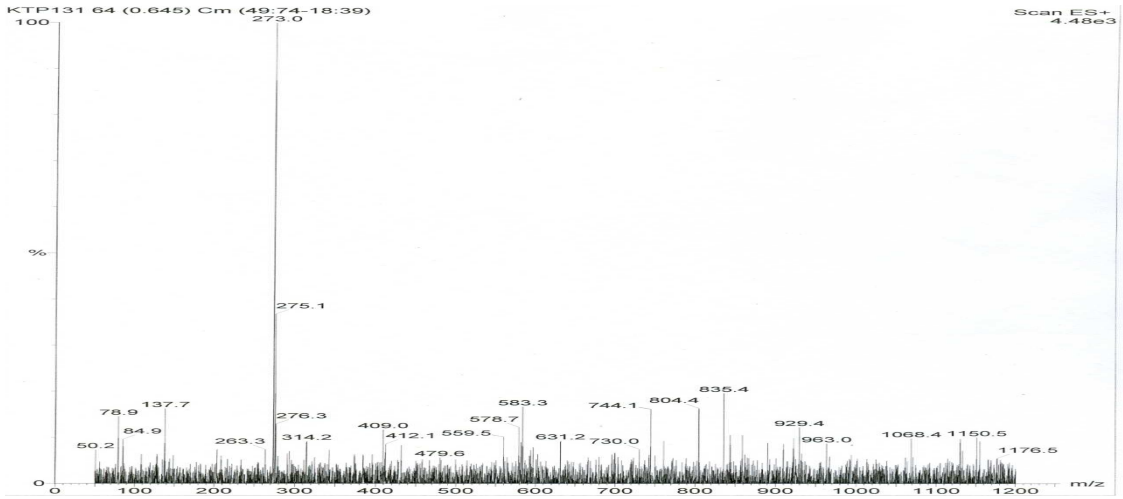

Figure 7.3: Mass spectrum of the complex $[\{(\eta^5\text{-}Cp^*)RhCl\}_2(\mu\text{-}L2)](PF_6)_2$ ([**6**]$(PF_6)_2$)

The ^{1}H NMR spectra of the dinuclear dicationic complexes **5** to **14** exhibited five distinct resonances assignable to pyrazole rings, methyl and benzene ring protons of the ligands (L1 or L2) indicating formation of dinuclear complexes. For instance the ^{1}H NMR spectra of the complexes **9** and **11** are presented in figure 7.4 and 7.5 respectively. The methylic proton {-C***H***$(Pz)_2$-} of ligand has exhibited a singlet at δ = 8.36 to 8.33 indicating formation of dinuclear compounds. Besides these resonances, complexes **5** to **8** exhibit a singlet at $\delta \approx 1.5$ for the protons of the pentamethylcyclopentadienyl ligands. Interestingly, in these complexes, the chemical shift of the protons of the pentamethylcyclopentadienyl ligands does not show downfield shift as like with other nitrogen based ligands.[21-27] Complexes **9** and **10** exhibit a singlet at δ = 5.40 and 5.48 for protons of benzene ligands, complexes **11** and **12** exhibits a doublet at δ = 1.21 for the

protons of the isopropyl methyl groups, a singlet at δ = 1.26 for the methyl protons, a septet at δ = 2.79 for the proton of the isopropyl group. The two doublets centered at δ ≈ 5.55 and 5.38 correspond to the CH aromatic protons of the *p*-cymene rings. Complexes **13** to **14** exhibit a strong peak at δ = 2.25 for the methyl protons of hexamethylbenzene ligand. In similar case with the Cp* analogues the arene ruthenium complexes also the chemical shifts of the arene ligands of ruthenium does not shifted down filed as compared to other N-based ligands, this could be due to the geometrical orientation of arene ligands to the benzene-linker.[24-27]

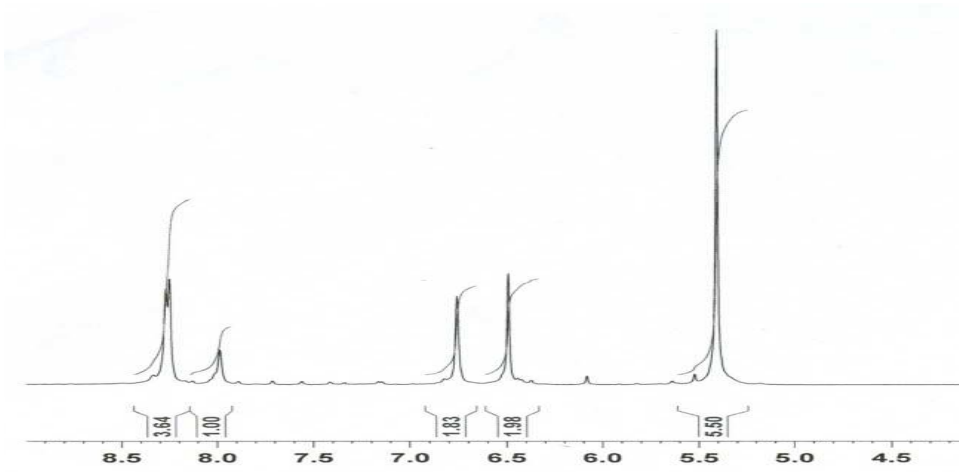

Figure 7.4: ^{1}H NMR spectrum of complex [{(η^6-C_6H_6)RuCl}$_2$(μ-L1)](PF_6)$_2$ ([**9**](PF_6)$_2$)

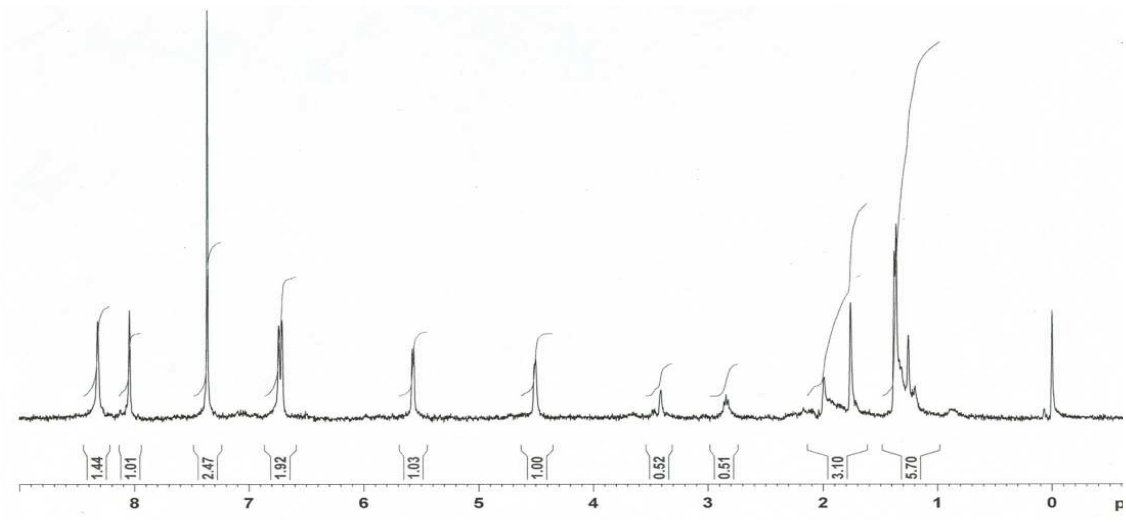

Figure 7.5: ^{1}H NMR spectrum of complex [{(η^6-*p*-^{i}PrC$_6$H$_4$Me)RuCl}$_2$(μ-L1)](PF_6)$_2$ ([**11**](PF_6)$_2$)

7.3.5 Crystal structure analysis of ([**7**](PF$_6$)$_2$), ([**9**](PF$_6$)$_2$) and ([**11**](PF$_6$)$_2$)

The molecular structure of complexes [{(η^5-C$_5$Me$_5$)IrCl}$_2$(μ-L1)]$^{2+}$ ([**7**](PF$_6$)$_2$), [{(η^6-C$_6$H$_6$)RuCl}$_2$(μ-L1)]$^{2+}$ ([**9**](PF$_6$)$_2$) and [{(η^6-*p*-^{i}PrC$_6$H$_4$Me)RuCl}$_2$(μ-L1)]$^{2+}$ ([**11**]-(PF$_6$)$_2$) were determined by single crystal X-ray diffraction analysis. The crystallographic data are gathered in Table 7.1 and the selected bond lengths and angles for complexes [**7**](PF$_6$)$_2$, [**9**](PF$_6$)$_2$ and [**11**](PF$_6$)$_2$ are presented in Table 7.2. The corresponding ORTEP drawings are shown in Figures 7.6, 7.7 and 7.8, respectively. All complexes show typical piano-stool geometry and have a half-sandwich structure consisting of coordinated pentamethylcyclopentadienyl or arene; a chloride and the ligand through nitrogens (see Figures 7.6 to 7.8).

The distance of the iridium atoms and the corresponding centroids of η^5-C$_5$Me$_5$ rings is 1.79 Å in complex **7**. The distance between the ruthenium atoms and the centroid of the C$_6$H$_6$ and η^6-*p*-^{i}PrC$_6$H$_4$Me rings in complexes **9** and **11** are almost equivalent at 1.67 Å. These distances are comparable to those in the related complex cations [(η^6-*p*-^{i}PrC$_6$H$_4$Me)Ru(2-acetylthiazoleazine)Cl]$^+$ and [{(η^6-*p*-Pr^{i}C$_6$H$_4$Me)RuCl}$_2$(4,6-bis(3,5-dimethylpyrazolyl)-pyrimidine)]$^{2+}$.[24,31] The average Ir-C distances of complex **7** is slightly shorter (2.16 Å) than the corresponding Ru-C distances. Indeed the average Ru-C distances of complex **9** are slightly shorter (2.17 Å) than the complex **11**, which contain *p*-cymene ligand (2.19 Å), which are almost identical to those reported iridium or rhodium complexes such as [(η^5-C$_5$Me$_5$)IrCl((S)-1-phenylethylsalicylaldiimine)] [2.17 Å][32] and [(η^6-*p*-^{i}PrC$_6$H$_4$Me)Ru(2-(2-thiazolyl)-1,8-naphthyridine)Cl]PF$_6$ [2.19 Å].[26]

The Ir-N bond distances of complex **7** at 2.110(6) and 2.093(6) Å are slightly longer than the Ru-N bond distances of complex **9** which are ranging from 2.081(4) to 2.089(5) Å, but are comparable to those found in **11** [2.102(4) and 2.098(4) Å]. All metal-chlorido bond distances are comparable, ranging from 2.391(1) to 2.395(2) Å, and are almost identical to other reported values.[24,26] In all complexes the η^5-C$_5$Me$_5$, η^6-C$_6$H$_6$ or η^6-*p*-^{i}PrC$_6$H$_4$Me rings are positioned opposite to each other to the benzene-linker and chlorine atoms of the two metal atoms are located at the periphery of the complexes. The N1–Ir1–N3 bond angle in complex **7** is found to be 86.0(2)° and in complexes **9** and **11** are found to be 84.3(2), 83.8(2)° and 85.1(2)°, respectively.

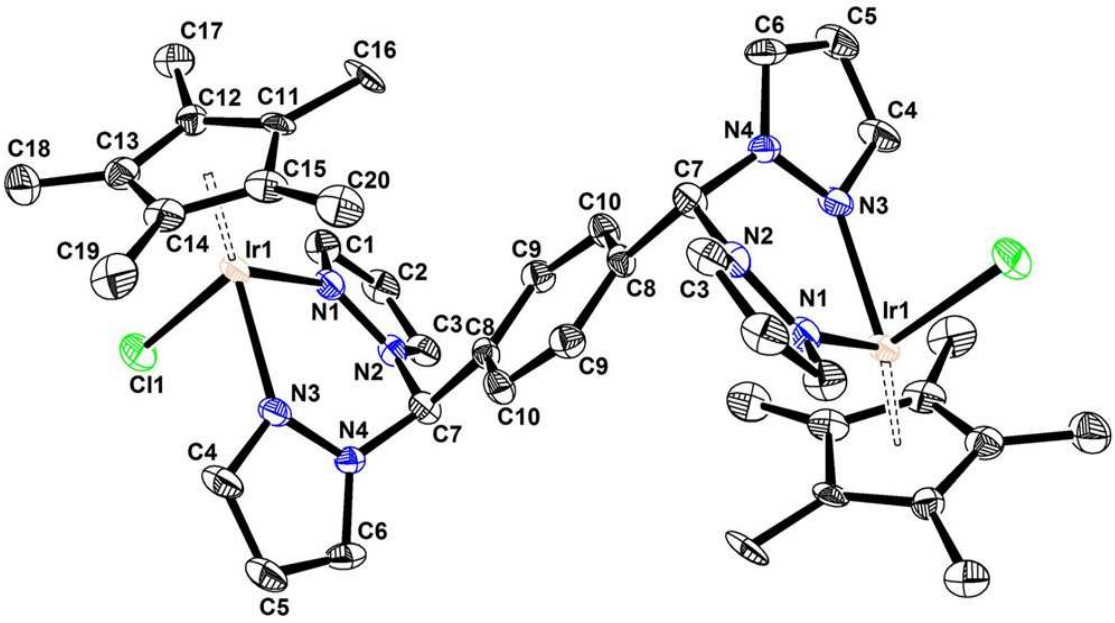

Figure 7.6: ORTEP diagram with labelling scheme for [**7**]$(PF_6)_2$ · 2 CH_3CN, at 50% probability level, PF_6 anions and acetonitrile molecules omitted for clarity (symmetry code: i = 2-x, 2-y, -z).

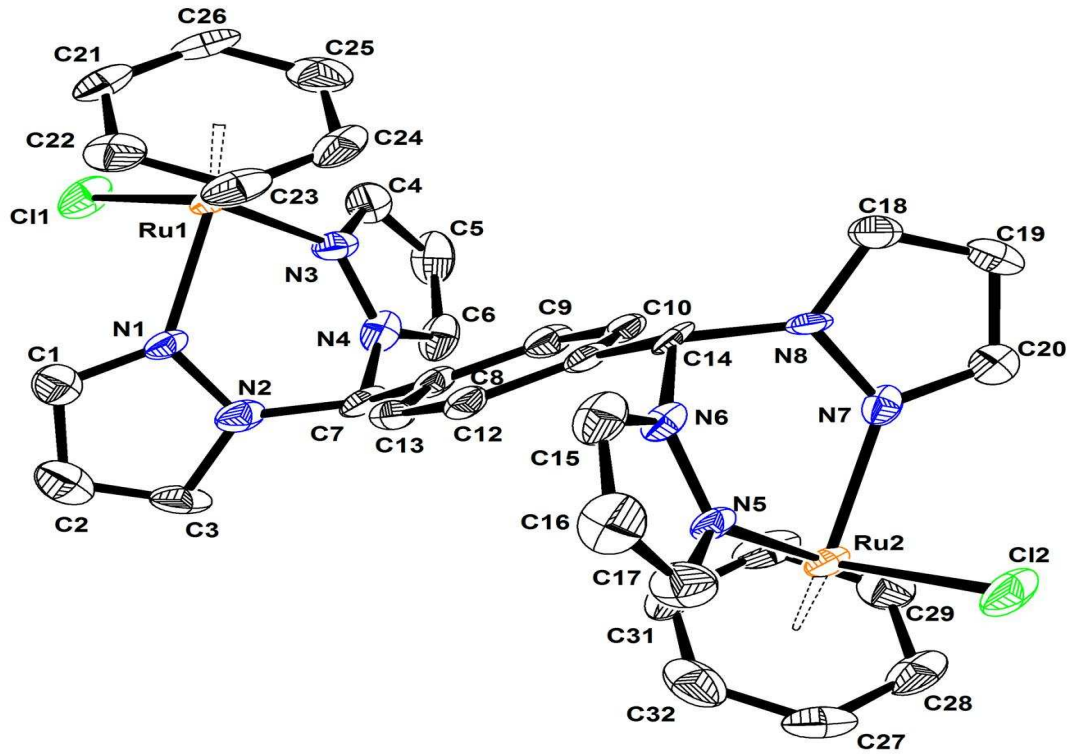

Figure 7.7: ORTEP diagram with labelling scheme for [**9**]$(PF_6)_2$ · CH_3CN, at 50% probability level, PF_6 anions and acetonitrile molecules omitted for clarity.

Table 7.1: Crystallographic and structure refinement parameters for complexes [**7**]$(PF_6)_2 \cdot 2\ CH_3CN$, [**9**]$(PF_6)_2 \cdot CH_3CN$ and [**11**]$(PF_6)_2 \cdot 2\ CH_3CN$.

Complex	[**7**]$(PF_6)_2$	[**9**]$(PF_6)_2$	[**11**]$(PF_6)_2$
Chemical formula	$C_{44}H_{54}Cl_2F_{12}Ir_2N_{10}P_2$	$C_{34}H_{33}Cl_2F_{12}N_{10}P_2Ru_2$	$C_{44}H_{52}Cl_2F_{12}N_{10}P_2Ru_2$
Formula weight	1468.21	1130.67	1130.67
Crystal system	monoclinic	Monoclinic	monoclinic
Space group	*P* $2_1/n$ (no. 14)	*P* $2_1/n$ (no. 14)	*P* $2_1/c$ (no. 14)
Crystal color and shape	orange block	orange block	orange block
Crystal size (mm^3)	0.27 x 0.24 x 0.22	0.25 x 0.22 x 0.18	0.25 x 0.22 x 0.18
a (Å)	13.6968(13)	15.3761(9)	9.4659(7)
b (Å)	14.0285(9)	13.9492(10)	25.737(2)
c (Å)	14.5963(14)	19.9223(13)	11.0998(9)
α (°)			
β (°)	114.169(10)	105.567(7)	110.868(9)
γ (°)			
V ($Å^3$)	2558.8(4)	4116.3(5)	2526.8(3)
Z	2	4	2
T (K)	173(2)	173(2)	173(2)
D_x (g /cm^3)	1.906	1.824	1.688
μ (mm^{-1})	5.540	1.036	0.855
Scan range (°)	$2.11 < \theta < 26.18$	$2.09 < \theta < 26.04$	$2.12 < \theta < 26.04$
Unique reflections	5045	8055	4849
Reflections used [I>2σ(I)]	3675	4212	3295
R_{int}	0.0745	0.0944	0.0591
Final R indices [I>2σ(I)]*	0.0415, wR_2 0.1038	0.0428, wR_2 0.0789	0.0463, $wR_2$0.1189
R indices (all data)	0.0616, wR_2 0.1103	0.0982, wR_2 0. 0872	0.0704, $wR_2$0.1269
Goodness-of-fit	0.927	0.797	0.961
Max, Min Δρ (e $Å^{-3}$)	3.086, -2.055	0.952, -0.929	1.538, -0.792

* Structures were refined on F_0^2: $wR_2 = [\Sigma[w(F_0^2 - F_c^2)^2] / \Sigma w(F_0^2)^2]^{1/2}$, where $w^{-1} = [\Sigma(F_0^2) + (aP)^2 + bP]$ and $P = [\max(F_0^2, 0) + 2F_c^2]/3$.

Table 7.2: Selected bond lengths and angles for complexes [**7**]$(PF_6)_2 \cdot 2\ CH_3CN$, [**9**]$(PF_6)_2 \cdot CH_3CN$ and [**11**]$(PF_6)_2 \cdot 2\ CH_3CN$.

	[**7**]$(PF_6)_2$	[**9**]$(PF_6)_2$	[**11**]$(PF_6)_2$
Inter atomic distances (Å)			
M-M	9.4781(9)	8.8236(8)	8.8285(13)
M-N1	2.110(6)	2.086(4)	2.102(4)
M-N3	2.093(6)	2.089(5)	2.098(4)
M-N5		2.081(4)	
M-N7		2.085(5)	
M-Cl1	2.394(2)	2.395(2)	2.391(1)
M-Cl2		2.392(2)	
M-centroid*	1.788	1.668	1.673
N1-N2	1.345(8)	1.352(6)	1.351(6)
N3-N4	1.372(8)	1.358(7)	1.350(6)
N5-N6		1.366(6)	
N7-N8		1.366(6)	
Angles (°)			
N1-M-N3	86.0(2)	84.31(17)	85.08(16)
N5-M-N7		83.82(17)	
N1-M-Cl1	84.01(17)	84.42(13)	85.20(11)
N3-M-Cl1	83.36(18)	84.80(13)	83.15(11)
N5-M-Cl2		84.54(12)	
N7-M-Cl2		84.77(13)	
M-N1-N2	125.4(5)	124.6(3)	126.2(3)
M-N3-N4	125.9(5)	125.4(3)	125.2(3)
M-N5-N6		125.4(3)	
M-N7-N8		125.5(3)	

*Calculated centroid-to-metal distances (η^6-C_6 or η^5-C_5 coordinated aromatic ring)

These bond angles are comparable to those in the related complex cations [(η^6-C_6H_6)Ru(bpzmArOCH_3)]BPh_4 and [(η^6-*p*-^{i}PrC_6H_4Me)Ru(bpzmArNO_2]BPh_4.[13] All compounds crystallise with acetonitrile molecules, which surprisingly interact strongly with neither the cation nor the anions. However, all hydrogen atoms of the tertiary

carbons (C7 as well as C14 in **9**) are involved in C-H···F or C-H···Cl interactions in the crystal packing. In [**7**]$(PF_6)_2 \cdot 2\ CH_3CN$ and [**11**]$(PF_6)_2 \cdot 2\ CH_3CN$, the C···F separations are ranging from 3.31 to 3.58 Å with C-H···F angles ranging from 131.3 to 163.1°, while in [**9**]$(PF_6)_2 \cdot CH_3CN$, the C···Cl distances are 3.40 and 3.43 Å with C-H···Cl angles of 153.2 and 142.8°, respectively.

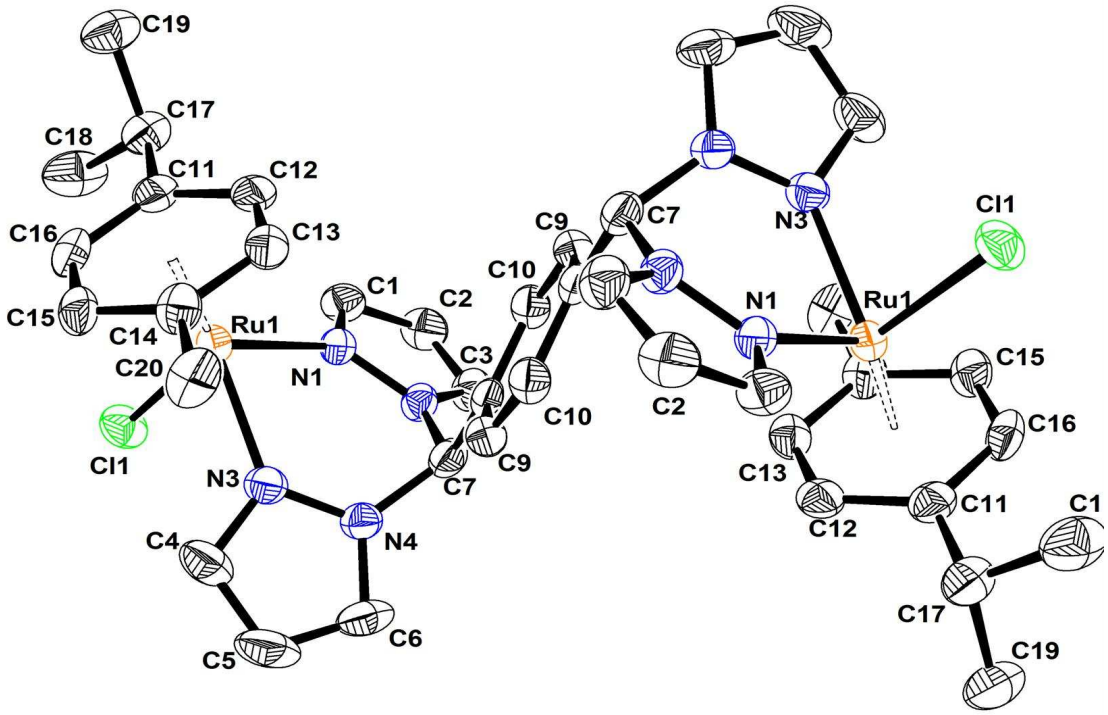

Figure 7.8: ORTEP diagram with labelling scheme for [**11**]$(PF_6)_2 \cdot 2\ CH_3CN$, at 50% probability level, PF_6 anions and acetonitrile molecules omitted for clarity (symmetry code: i = -x, 1-y, -z).

7.3.6 UV-Visible spectroscopy

Electronic absorption spectra of the mononuclear compounds [**1**]PF_6 – [**4**]PF_6 as well as the dinuclear compounds [**5**]$(PF_6)_2$ – [**14**]$(PF_6)_2$ were acquired in acetonitrile, at 10^{-5} M concentration in the range 200-600 nm. Electronic spectra of representative complexes are depicted in Figure 7.9 without showing the strong absorption at 224-229 nm. The spectra of these complexes are characterized by two main features, *viz*., an intense ligand–localized or intra-ligand $\pi \rightarrow \pi^*$ transition in the ultraviolet region and metal-to-ligand charge transfer (MLCT) $d\pi(M) \rightarrow \pi^*$ (L1 - ligand) bands in the visible region.[33] Since the low spin d^6 configuration of the mononuclear complexes provides filled orbitals of suitable symmetry at the Ru(II), Rh(III) and Ir(III) centers, these can

interact with low lying π* orbitals of the ligands. All mononuclear compounds [**1**]PF_6 – [**4**]PF_6 show a high intensity band in the region 224 -230 nm and a medium intensity band in the region 341-394 nm in UV region, these two bands are attributed to the ligand–localized or intra-ligand π → π* transitions. Whereas the dinuclear complexes [**5**]$(PF_6)_2$ – [**14**]$(PF_6)_2$ show three bands, for instance a high intensity band in the region 224-230 nm, a medium intensity band in the region 307-317 nm and a second medium intensity low energy absorption band in the visible region 394 – 437 nm. The medium intensity bands in the UV region is assigned to π → π*, the high intensity band in the UV region is assigned to inter and intra-ligand π → π*/ n → π* transitions,[24,27] while the low energy absorption band in the visible region is assigned to metal-to-ligand charge transfer (MLCT) (t_{2g} – π*).

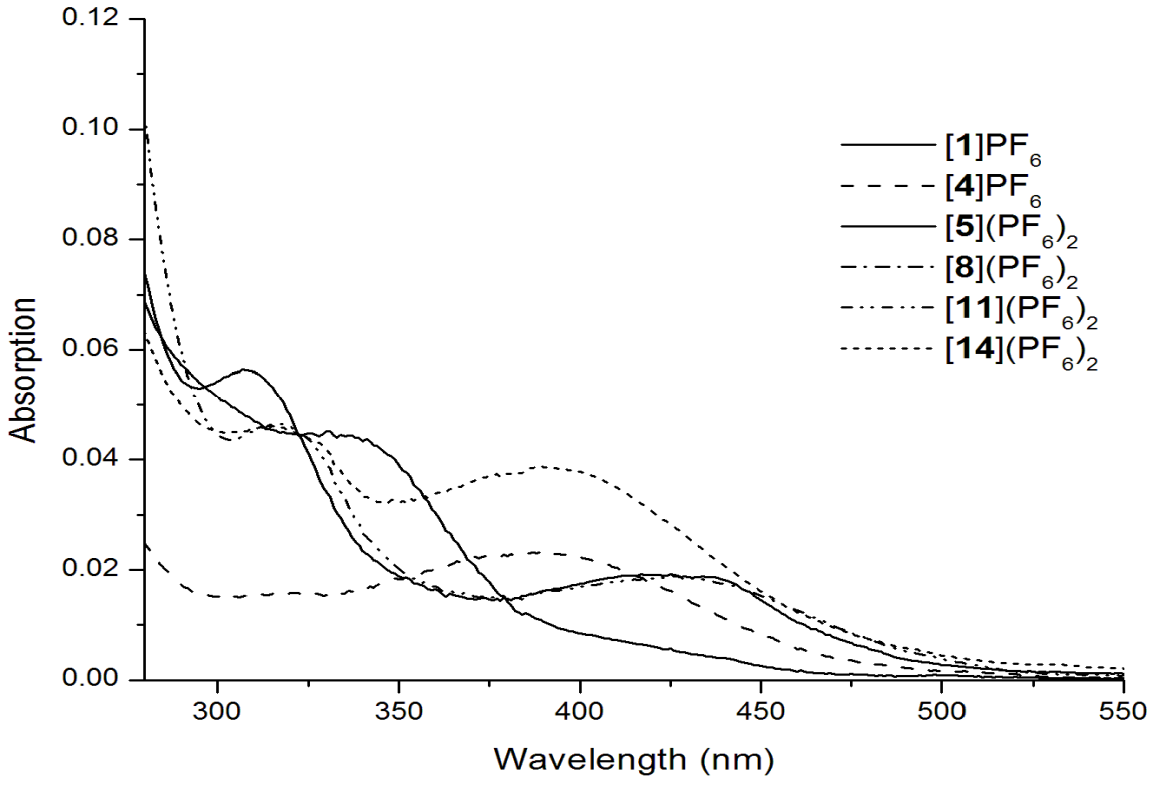

Figure 7.9: UV-visible electronic spectra of selected complexes (acetonitrile, 10^{-5} M, 298 K).

7.4 Conclusions

In this work, we have showed that ligand L reacts with arene ruthenium and pentamethylcyclopentadienyl rhodium and iridium complexes to yield a series of mono and dinuclear complexes in good yield, which are remarkably stable in air as well as in

solution. The Cp* derivatives yielded both mono and dinuclear complexes, while only dinuclear complexes are obtained with the arene ruthenium analogues, despite different molar ratio of ligands. In all these, both mono and dinuclear complexes the metal atom is bonded to the coordinated sites N1 and N3 or N4 and N6.

7.5 Supplementary material

CCDC-**757062** ([**7**]$PF_6 \cdot 2\ CH_3CN$), **757063** ([**9**]$(PF_6)_2 \cdot CH_3CN$) and **757064** ([**11**]$(PF_6)_2$ 2 CH_3CN) contain the supplementary crystallographic data for this chapter.

References

1 S. Trofimenko, Scorpionates: The Coordination Chemistry of Polypyrazolylborate Ligands; Imperial College: London, 1999.

2 S. Trofimenko, Chem. Rev. 93 (1993) 943.

3 C. Pettinari, C. Santini, Compr. Coord. Chem. II 1 (2004) 159.

4 D. L. Reger, Comments Inorg. Chem. 21 (1999) 1.

5 H. R. Bigmore, S. C. Lawrence, P. Mountford, C. S. Tredget, Dalton Trans. (2005) 635.

6 G. J. Long, F. Grandjean, D. L. Reger, Top. Curr. Chem. 233 (2004) 91.

7 C. Pettinari, R. Pettinari, Coord. Chem. Rev. 249 (2005) 525.

8 C. Pettinari, R. Pettinari, Coord. Chem. Rev. 249 (2005) 663.

9 D. L. Reger, T. C. Grattan, K. J. Brown, C. A. Little, J. J. S. Lamba, L. Rheingold, R. D. Sommer, J. Organomet. Chem. 607 (2000) 120.

10 S. Juliá, J. M. del Mazo, L. Avila, J. Elguero, Org. Prep. Proc. Int. 16 (1984) 299.

11 D. L. Reger, R. P. Watson, M. D. Smith, P. J. Pellechia, Organometallics 25 (2006) 743-755 and references there in;

12 D. L. Reger, E. A. Foley, M. D. Smith, Inorg. Chem. 49 (2010) 234-242

13 M. C. Carrión, F. Sepúlveda, F. A. Jalón, B. R. Manzano, Organometallics 28 (2009) 3822-3833 and references there in.

14 C. Slugovc, I. Padilla-Martínez, S. Sirol, E. Carmona, Coord. Chem. Rev., 213 (2001) 129.

15 L. D. Field, B. A. Messerle, M. Rehr, L. P. Soler and T. W. Hambley, Organometallics 22 (2003) 2387.

16 E. Teuma, M. Loy, C. Le Berre, M. Etienne, J.-C. Daran, P. Kalck, Organometallics 22 (2003) 5261.

17 S. Burling, L. D. Field, B. A. Messerle, S. L. Rumble, Organometallics 26 (2007) 4335.

18 A. W. Stumpf, E. Saive, A. Demonceau, A. F. Noels, J. Chem. Soc., Chem. Commun. (1995) 1127

19 B. Therrien, G. Süss-Fink, P. Govindaswamy, A. K. Renfrew, P. J. Dyson, Angew. Chem. Int. Ed. 47 (2008) 3773.

20 Y.-K. Yan, M. Melchart, A. Habtemariam, P. J. Sadler, Chem. Commun. (2005) 4764, and references therein.

21 K. S. Singh, Y. A. Mozharivskyj, K. M. Rao, Z. Anorg. Allg. Chem. 632 (2005) 172.

22 P. Govindaswamy, P. J. Carroll, Y. A. Mozharivskyj, K. M. Rao, J. Organomet. Chem. 690 (2005) 885.

23 G. Gupta, G. P. A. Yap, B. Therrien, K. M. Rao, Polyhedron, 28 (2009) 844.

24 K. T. Prasad, B. Therrien, S. Geib, K. M. Rao, J. Organomet. Chem. 696 (2010) 495.

25 G. Gupta, K. T. Prasad, B. Das, G. P. A. Yap and K. M. Rao, J. Organomet. Chem. 694 (2009) 2618.

26 K. T. Prasad, B. Therrien, K. M. Rao, J. Organomet. Chem. 693 (2008) 3049.

27 K. T. Prasad, B. Therrien, K. M. Rao, J. Organomet. Chem. 695 (2010) 226.

28 E. A. Nudnova, A. S. Potapov, A. I. Khlebnikov, V. D. Ogorodnikov, Russ. J. Org. Chem. 43 (2007) 1698-1702.

29 A. S. Potapov, G. A. Domina, A. I. Khlebnikov, V. D. Ogorodnikov, Eur. J. Org. Chem. (2007) 5112.

30 H. van der Poel, G. van Koten, K. Vrieze, Inorg. Chem. 19 (1980) 1145.

31 K. T. Prasad, G. Gupta, A. V. Rao, B. Das, K. M. Rao, Polyhedron 28 (2009) 2649.

32 H. Brunner, A. Köllnberger, T. Burgemeister, M. Zabel, Polyhedron 19 (2000) 1519.

33 E. Binamira-Soriaga, N. L. Keder, W. C. Kaska, Inorg. Chem. 29 (1990) 3167.

Curriculum Vitae

Personal profile

Name: K. Thirumala Prasad

Date of Birth: 14th May 1982

Permanent Address: Komarole Village, P O & Mandal
Prakasam Distict
Andhra Pradesh
India-523373
Ph. No. 09441747389
E Mail- kthirumalaprasad@gmail.com

Education

2004 Master of Science in chemistry (Inorganic Chemistry) (72%), Acharya Nagarjuna University, University College, Guntur, Andhra Pradesh, India.

2002 Bachelor of Science (Chemistry, Mathematics and Physics) (83%), Acharya Nagarjuna University, Andhra Loyola College, Vijayawada, Andhra Pradesh, India.

1999 Intermediate (Chemistry, Physics and Mathematics) (72%), Board of Intermediate, Umamaheswara Junior College, Ongole, Andhra Pradesh, India.

1997 Class 10th (General Science and Social studies) (61%), Secondary School of Certificate, Vignan High School, Komarole, Andhra Pradesh, India.

Research publications and communications

1 "Cationic half-sandwich complexes (Rh, Ir, Ru) containing 2-substituted-1,8-naphthyridine chelating ligands: Syntheses, X-ray structure analyses and spectroscopic studies" **K. Thirumala Prasad**, B. Therrien, K. Mohan Rao, J. Orgnomet. Chem. 693 (2008) 3049.

2 "New series of platinum group metal complexes bearing η^5- and η^6 - Cyclichydrocarbons and Schiff base derived from 2-acetylthiazole: syntheses and structural studies" **K. Thirumala Prasad**, G. Gupta, A. V. Rao, B. Das and K. Mohan Rao, Polyhedron 28 (2009) 2864.

3 "Ruthenium half-sandwich complexes with tautomerized pyrazolyl-pyridazine ligands: Synthesis, spectroscopic and molecular structural studies" G. Gupta, **K. Thirumala Prasad**, B. Das, G. P. A. Yap and K. Mohan Rao, J. Organomet. Chem. 694 (2009) 2618.

4 "Mono and dinuclear complexes of half-sandwich platinum group metals (Ru, Rh and Ir) bearing flexible pyridiyl-thiazole multidentate donor ligand" **K. Thirumala Prasad**, B. Therrien, K. Mohan Rao, J. Organomet. Chem. 695 (2010) 226-234.

5 "Mono and dinuclear half-sandwich platinum group metal complexes bearing pyrazolyl-pyrimidine ligands: Syntheses and structural studies". **K. Thirumala Prasad**, B. Therrien, S. Geib and K. Mohan Rao, J. Organomet. Chem. 696 (2010) 495-504.

6 "Spectral, structural and DFT studies of platinum group metal 3,6-bis(2-pyridyl)-4-phenylpyridazine complexes and their ligand bonding modes" **K. Thirumala Prasad**, G. Gupta, A. K. Chandra, M. P. Pavan, K. Mohan Rao, J. Organomet. Chem. 695 (2010) 707-716.

7 "Study of half-sandwich platinum group metal complexes bearing dpt-NH2 ligand" G. Gupta, **K. Thirumala Prasad**, B. Das, and K. Mohan Rao, Polyhedron 29 (2010) 904-910

8 "Novel mononuclear η^5-pentamethyl-cyclopentadienyl complexes of platinum group metals bearing pyrazolylpyridazine ligands: Syntheses and spectral studies" G. Gupta, **K. Thirumala Prasad**, A. V. Rao, S. J. Geib, B. Das and K. Mohan Rao, Inorg. Chim. Acta (2010) (In press)

9 “Syntheses and characterization of mono and dinuclear complexes of platinum group metals bearing benzene-linked bis(pyrazolyl)methane ligands” **K. Thirumala Prasad**, B. Therrein, K. Mohan Rao, J. Organomet. Chem. 695 (2010) (in press).

10 “Half-sandwich mono and dinuclear complexes of platinum group metals bearing pyrazolyl-pyridine analogues: Synthesis and spectral characterization" **K. Thirumala Prasad**, Y Mozharivskyj, Peng Wang, K. Mohan Rao, Polyhedron (Submitted)

11 **“**Synthesis, characterization and structural studies of half - sandwich platinum group metal complexes with pyrimidine bridged pyrazolyl-pyridine ligand” **K. Thirumala Prasad**, Yurij Mozharivskyj, Peng Wang, K. Mohan Rao, Polyhedron (Submitted)

12 **“**Syntheses, characterization and structural studies of mononuclear half-sandwich platinum group metal complexes containing pyridazine bridged ligands” **K. Thirumala Prasad**, B.Therrein, K. Mohan Rao, (Under preparation)

13 “Half sandwich arene ruthenium dinuclear complexes bearing rigid pyridiyl-thiazole multidentate donor ligand” **K. Thirumala Prasad**, B. Therrien, K. Mohan Rao (Under preparation)